Tanins condensés pour mousses rigides et nouvelles réactions de réticulations des matériaux polyphénoliques

Francisco José Santiago-Medina

THÈSE

Présentée et soutenue publiquement pour l'obtention du grade de

DOCTEUR DE L'UNIVERSITÉ DE LORRAINE

Spécialité : Sciences du Bois et des Fibres

par

Francisco José SANTIAGO-MEDINA

TANINS CONDENSES POUR MOUSSES RIGIDES ET NOUVELLES REACTIONS DE RETICULATIONS DES MATÉRIAUX POLYPHÉNOLIQUES

Sous la direction d'**Antonio PIZZI**

À Épinal, le 8 décembre 2017

Rapporteurs :

Pr. Bertrand CHARRIER	Professeur, Université de Pau et du Pays de l'Adour
Pr. Frédéric PICHELIN	Professeur, Bern University of Applied Sciences

Examinateurs:

Pr. Christine GERARDIN	Professeur, Université de Lorraine
Pr. Marie-Pierre LABORIE	Professeur, Albert-Ludwigs University of Freiburg

Directeur de Thèse :

Pr. Antonio PIZZI	Professeur, Université de Lorraine

ENSTIB, 27 Rue Philippe Séguin – BP 21042 – 88051 Épinal Cedex 9

REMERCIEMENTS

Quiero comenzar agradeciendo a mi tutor Pr. Antonio PIZZI. È molto facile lavorare con una persona come te, sempre pieno di positivismo. Voglio ringraziarti per la vostra fiducia in me in questi tre anni, per i vostri consigli e la vostra esperienza infinita. Tony, per me è stato un grande piacere di aver lavorato con uno scienziato como te.

Remercier également les rapporteurs pour avoir accepté de corriger ce travail et les examinateurs pour leurs observations et propositions.

Sincèrement, je veux montrer ma gratitude à tout le personnel de l'atelier et aux composantes du laboratoire LERMAB pour leur aide pendant toutes ces années. Surtout, à Linda BOSSER pour faciliter la vie des doctorants, toujours avec une sourire et une solution pour chacun des problèmes administratifs. Un grand merci pour ta joie, ton affection et pour ta bonne humeur.

Remercier à toutes et à tous les doctorant(e)s et étudient(e)s avec lesquels j'ai partagé tous ces grand moments pendant ces trois dernières années. Personas entre los que he encontrado grandes amigos procedentes de todos los rincones del planeta (Argentina, China, Chile, Italia, Brasil, Irán, Sudan, Argelia, Macedonia, Túnez, Líbano, México,…). Os recordaré siempre y os llevaré en un hueco de mi corazón. Habéis pasado muchos y no me gustaría olvidarme de ninguno de vosotros: mis compañeros/as de oficina Quentin, Marie-Christine, Thouraya, Xeudong (the happiest person), Saman (the Strongman) e Imane. César Segovia, Cyril y Oussama por tantas tardes y domingos de fútbol, llenas de goles y 'petit-ponts'. Clément, Romain y Damien, componentes del equipo con el que obtuvimos por dos años consecutivos el torneo de Vaudéville. La bonita pareja formada por Benoit y Perrine por todas esas 'soirées' en vuestra casa. Y como no, mi pareja de mexicanitos favoritos, Jimena (lo más bonito de México) y D. César. Los compañeros de laboratorio durante estos tres años Siham y Cecilia. Y al resto de compañeros/as que han ido pasando por el ENSTIB durante estos años: Giuseppe, Ángela, Víctor y la jefa Judith, Amalia, Zélie, Diem, Seb, Blagoj, Radouan, Merlin,…

En el ENSTIB he podido conocer a muchas personas pero me gustaría agradecer especialmente a César Segovia y a su familia, por acogerme desde el primer momento y por todos esos viajes hacía los partidos los domingos por la mañana. A Cyril DEHARBE por toda su ayuda prestada durante estos años en la preparación de cualquier 'manip' y para la utilización de cualquier máquina. A Maxime por todas esas conversaciones junto a Clara durante esos largos paseos por los bosques de Les Vosges. A Imane, aunque llegó y revolucionó la oficina porque no se calla ni debajo del agua y sea "majnouné", me he reído mucho con ella en la oficina. Y a Clément L'HOSTIS, un amigo que gano para siempre, una grandísima persona siempre dispuesto a ayudar y a sacar una sonrisa con sus 'tours de magie'. Gracias por los buenos momentos pasados durante estos años, te espero en tierras españolas y ahora ya soy un seguidor más del Stade Rennes, un fuerte abrazo pequeño gorrión.

Agradecer a la Prof. Zeinab OSMAN por su invitación a Sudan, e igualmente a todos sus estudiantes y a su grupo de laboratorio que tan bien me acogieron y me trataron durante mi estancia en Khartoum. Especialmente a Mohammed y a Nahla.

Me gustaría dedicar unas líneas a la familia de Lutins Malins por todos esos viernes jugando a las magics después de salir de la universidad.

Tampoco puedo olvidarme de los que me han ayudado a llegar hasta aquí, no puedo olvidarme de mis compañeros de Ingeniería Química. Los que después de los años siguen siendo como mis hermanos, Antonio y Manuel (mi compi). A Sergio, un tío increíble y mejor persona, siempre atento y con el que siempre se puede contar. A mi Julito, la primera persona que conocí cuando llegué a la Universidad. Y a otros también indispensables durante mi estancia por la Universidad de Huelva como son Carlos, Pablo, Almu, Ana, Adri, Iván, Fran, Juanito,…

Es obligatorio acordarme de los amigos de toda la vida, los del pueblo, con los que me reúno cada vez que vuelvo al pueblo y comparto tantas tardes y tantas risas. Especialmente quiero acordarme de Txema y de Julio y Alejandro, y por supuesto, de mi compadre Sergio, con quien he compartido tantísimos momentos desde mi infancia.

Quiero agradecer el apoyo recibido durante estos años por mi familia. Muy especialmente a mi madre, quien me dio la vida y no hay cosa más grande que te puedan dar en este mundo, siempre me has apoyado en todo lo que me he propuesto hacer y de ti he aprendido una de las cosas más importantes de mi vida, "lo que se empieza se acaba". Y a mi hermano, del cual admiro la constancia que pone en cada pedalada y en cada objetivo que se propone. Sigue así hermano, porque sin duda con tu carisma y tu perseverancia podrás hacer cualquier cosa que te propongas en la vida y ahí estará tu hermano para apoyarte y ayudarte en lo que te haga falta.

Quiero dedicar este último párrafo antes de terminar a quien lo ha sido todo en mi vida durante estos últimos años. A la persona por la que llegue a Épinal y la persona por la que no me fui en los momentos que existieron más dudas. A la persona junto a la cual mejor me lo paso y me gusta compartir mí tiempo, y junto a la cual he vivido tantísimos momentos inolvidables. A mi mitad. Gracias Clara, gracias mi Cielo.

...llegué hace diez años sin nada,

y diez años después me voy de tus brazos como

doctor de una de tus universidades.

Gracias Francia y gracias Épinal

“Y así viajé por toda la tierra y fui un peregrino
durante toda mi vida, solo, un extranjero en tierra
extraña. Después Tú hiciste crecer en mí Tu
arte por debajo del hálito de la terrible tormenta
que ruge en mi interior”.

A mi madre y a mi hermano

SOMMAIRE

Liste des figures

Liste des tableaux

Introduction

Dans les dernières décennies, l'épuisement des ressources pétrolières s'est accéléré, entraînant l'augmentation du prix du pétrole et de ses dérivés. Le pétrole, le gaz et le charbon constituent les principales ressources primaires exploitées pour les besoins énergétiques mondiaux. Le secteur énergétique est le plus consommateur de ressources fossiles, juste devant celui des transports. Ainsi, afin de limiter les consommations d'énergie, les matériaux d'isolation se doivent d'être, de nos jours, de plus en plus performants pour éviter, ou au moins limiter, les pertes d'énergies inutiles. Les matériaux isolants sont un exemple de produits issus de l'industrie pétrochimique présents dans notre environnement quotidien.

Actuellement, il y a une plus grande prise de conscience de la société dans la nécessité de préserver de l'environnement, et de l'impact fort des secteurs industriels, de leurs processus technologiques et leurs produits sur l'écosystème. Ces circonstances ont amené la communauté scientifique à concentrer ses efforts sur l'utilisation des ressources naturelles pour développer de nouveaux produits qui ont traditionnellement été obtenus à partir de produits pétroliers ou d'autres matières premières non renouvelables. Parmi les industries concernées sont les industries de matériaux isolantes, les lubrifiants, les adhésifs, les revêtements, des peintures ou des produits d'étanchéité, qui incorporent dans leurs formulations des huiles et/ou solvants organiques, des tensioactifs et des matériaux polymères de natures différentes provenant directement de l'industrie pétrochimique. Les huiles minérales, par exemple, peuvent contaminer les eaux souterraines pendant plus de 100 ans, même de petites quantités peuvent inhiber la croissance des arbres et peuvent être toxiques pour la vie aquatique. Pour minimiser les dommages causés par la pollution des produits pétroliers, à nombre croissant de produits respectueux de l'environnement est actuellement développé.

Dans les années 90, une innovation technologique a été réalisée par le Laboratoire d'Etude et de Recherche sur le Matériau Bois (LERMAB) dans le contexte des produits naturels pour remplacer les produits pétrochimiques existants. À partir de produits biosourcés à plus de 90%, un nouveau procédé a permis de synthétiser de nouveaux isolants très performants : des mousses solides, constituées à plus de 60% en masse de tanins condensés, obtenues par polymérisation des extractibles issus d'écorce de bois.

Les travaux de cette thèse sont réalisés dans le cadre du projet « BRIIO » (BiosouRced InsulatIOn). Ce projet est une collaboration regroupant deux laboratoires de l'Université de Lorraine et deux entreprises. L'objectif du projet est la valorisation des extraits naturels tels que les tanins ou la lignine, pour la fabrication de mousse solides projetables pour l'isolation des bâtiments, ainsi que l'étude de la fiabilité technique, économique et l'impact environnemental du produit résultant. Cela a conduit à la fois à l'étude du processus d'extraction du tanin, comme des réactions possibles de celui-ci ou de lignine pour application ultérieure à des mousses solides ou à d'autres fins.

Cette thèse s'organise en trois parties :

- Une première partie d'étude bibliographique en présentant les composants de la mousse solide, ainsi comme les généralités sur la lignine et sur les panneaux de particules.
- Une seconde partie présentant les résultats obtenus au cours de cette thèse, sous forme de publications parues et /ou acceptées dans différent journaux scientifiques.
- Une dernière partie en présentant les conclusions générales et les perspectives qui en découlent.

Première partie :
Étude bibliographique

Étude Bibliographique

1 Les tanins

1.1 Rôle naturel

Les tanins sont des composants polyphénoliques présents naturellement dans les végétaux. Après la cellulose, les hémicelluloses et la lignine, les tanins sont le quatrième composant de la biomasse (Hernes and Hedges, 2000). Ils jouent un rôle de défense contre les insectes et les champignons, car leur forte caractéristique d'astringence rend la plante difficilement assimilable par ces organismes (Robbins et al., 1987). Les tanins se trouvent dans toutes les plantes en différents proportions. Les écorces des arbres en général en contiennent la quantité la plus significative, mais le tanin est présent dans tout le cytoplasme de toutes les cellules végétales (Haslam, 1989).

Les différents bois stockent les tanins dans différentes zones de la plante :

- Le pin (*Pinus radiata*), le chêne (*Quercus robur*) et le mimosa (*Acacia mearnsii* ou *mollissima*) contiennent la majorité de leurs tanins dans l'écorce.
- Le gambier (*Uncaria gambir*) dans les feuilles.
- Le pecan (*Carya illinoensis*) dans les noix de moelle.
- Le châtaignier (*Castanea sativa*) et le quebracho (*Schinopsis balansae*) stockent leurs tanins dans toute la structure.

1.2 Propriétés

Les tanins végétaux peuvent se combiner aux protéines pour donner des complexes solubles ou insolubles. Ils possèdent malgré les différences de leurs constitutions un ensemble de caractères communs :

- Ils précipitent les protéines de leur solution, en particulier la gélatine.
- Ils donnent avec les sels des métaux lourds des laques de couleurs variées ; en particulier avec les sels de fer, on obtient des laques de couleur bleue-noire.
- Ils précipitent avec les matières colorantes cationiques.

- Ils sont plus ou moins solubles dans l'eau, leurs solutions sont toujours acides. En raison de la taille de leurs molécules et de leur tendance à se polymériser par oxydation, les solutions aqueuses de tanins se comportent comme des dispersions colloïdales.
- Ils sont amorphes et sans point de fusion précis.
- Ils sont capables de se fixer sur la substance dermique de la peau en tripe et de la transformer en cuir.

1.3 Procédé d'extraction

L'extrait tannant est le résultat de la concentration par évaporation de l'eau de la solution obtenue par lessivage méthodique de la matière tannante naturelle.

L'extrait obtenu peut être liquide, c'est alors une solution concentrée contenant 50 % de matières sèches. Il est aujourd'hui le plus souvent solide, en poudre et renferme 90 à 96 % de matières sèches. Les opérations nécessaires pour préparer un extrait tannant sont sensiblement les mêmes quelle que soit la matière tannante concernée. Pour décrire ces opérations, on prendra comme exemple la fabrication de l'extrait de bois de châtaignier.

1.3.1 Fabrication de l'extrait de bois de châtaignier

La fabrication comprend cinq opérations principales :

- Découpe du bois.
- Extraction du tannin.
- Préconcentration et décantation des bouillons.
- Concentration des bouillons.
- Obtention de l'extrait solide

1.3.1.1 Découpage du bois

Tableau 1: Extrait de tanin en fonction de la taille des copeaux.

Epaisseur des copeaux en mm	18	15	10	5
Tanin extrait en 4 heures (en % de la teneur totale en tannin)	47	50	60	62

Le bois est découpé en copeaux taillés perpendiculairement à l'axe longitudinal de la bûche. Comme le montre le tableau suivant, l'épaisseur des copeaux a une grande influence sur la vitesse de diffusion de l'eau et par conséquent sur la vitesse d'extraction des produits solubles. En général, l'épaisseur des copeaux est comprise entre 5 et 10 mm.

Pour cette opération, on utilise une découpeuse à tambour représentée sur la figure 1. Elle comprend un tambour (A) constitué par deux cônes tronqués en acier assemblés par leur petite base. Il porte des lames (B) en acier, inclinées par rapport au rayon du tambour et dépassant celui-ci de l'épaisseur désirée pour les copeaux.

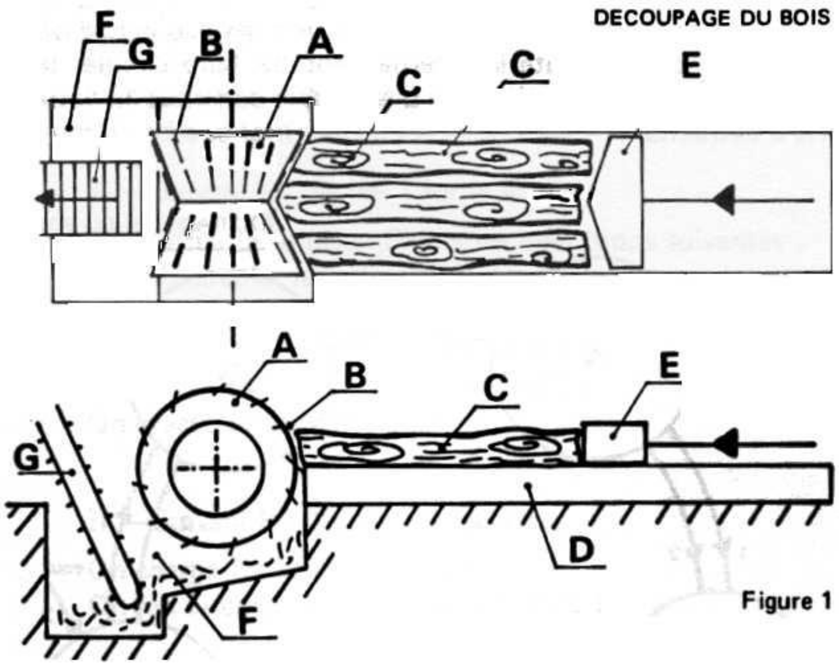

Figure 1: Découpe du bois pour l'extraction du tanin.

Devant le tambour, on trouve un couloir (D) dans lequel sont placées les bûches à découper (C). Ces bûches sont poussées contre le tambour jusqu'à découpage complet par le poussoir (E). Les copeaux tombent dans une fosse (F) de laquelle ils sont transportés au-dessus de la batterie d'extraction par un élévateur (G).

1.3.1.2 Extraction

L'extraction est conduite méthodiquement selon le principe du contre-courant, de façon à extraire le maximum de tannin et à obtenir des solutions les plus concentrées possibles. Pour cela, les conditions de l'extraction sont telles que le bois le plus épuisé soit en contact avec la solution la moins concentrée et que le bois le plus riche soit en contact avec la solution la plus concentrée. L'opération est réalisée dans une série d’autoclaves reliés par une tuyauterie permettant de faire circuler les solutions de l’une à l’autre. L’ensemble constitue la batterie d’extraction.

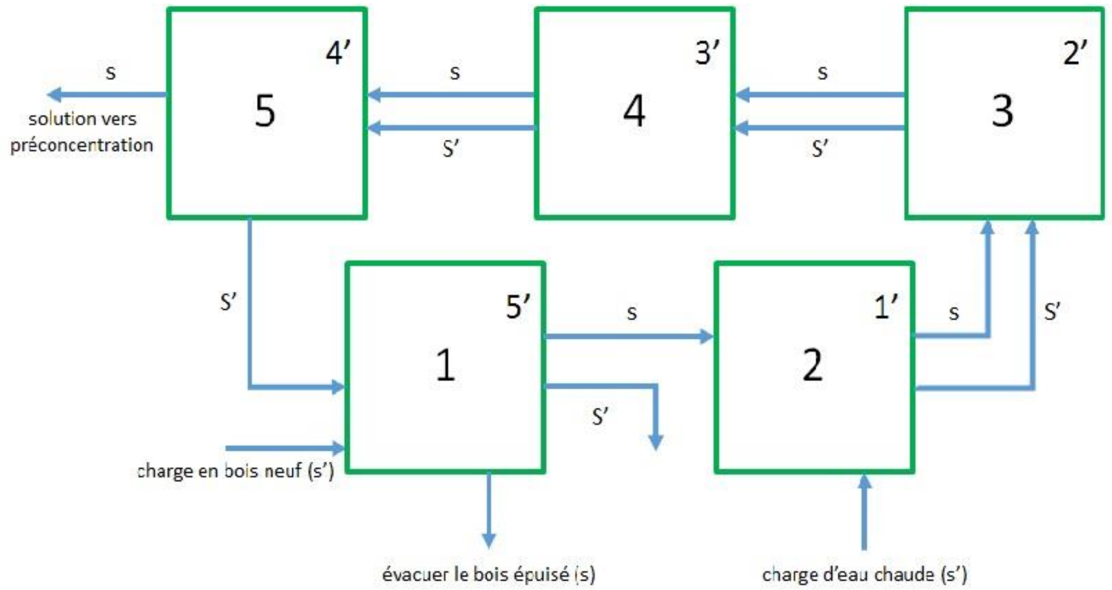

Figure 2: Schéma d’une série d’extracteurs en contre-courant.

La température varie au cours de l’opération de 110 à 90°C et elle est maintenue par réchauffage par injection de vapeur. Considérons une batterie de 5 autoclaves représentée schématiquement sur la figure 2.

Tableau 2: Des cellules ombre bleu indiquent les mouvements de la solution dans les autoclaves et les mouvements du bois sont indiquées pour les cellules brun.

	Phase 1	
	De…	à…
Bois le plus riche	5	Opération suivant
	4	5
	3	4
	2	3
	1	2
	1	Évacuer le bois épuisé
	Charge de bois neuf	1

	Renumérotation		
	De…	à…	
	1	5’	
	2	1’	
	3	2’	
	4	3’	
	5	4’	
	Phase 2		
Bois le plus riche	De…	à…	
	Charger de l’eau chaude	2 ou 1’	L’eau le plus diluée et le bois le plus épuisé

Au cours du procédé, l'autoclave n° 5 renferme le bois le plus riche et la solution la plus concentrée. En 4-3-2 se trouve du bois de plus en plus appauvri en tanins au contact de solutions de plus en plus diluées. En 1 se trouve le bois en contenant le moins avec la solution la plus diluée.

La circulation des solutions, le déchargement et chargement du bois se font en deux phases comme indiqué dans le tableau 2.

Après 1 à 2 heures de contact, on recommence les mêmes circulations des solutions, déchargement et chargement du bois. En 24 heures, 18 cycles peuvent être effectués.

1.3.1.3 Pré-concentration et décantation

A la sortie de la batterie d'extraction, la solution récoltée, appelée bouillon, a une densité de 3° Baumé (Bé) environ ce qui correspond sensiblement à une concentration de 5 à 6 % de matières sèches. La température du bouillon est de 90°C. Cette solution est à peu près limpide. Par refroidissement, cette solution se trouble et laisse décanter les molécules insolubles.

Si on poursuit les opérations, c'est à dire la concentration, on obtiendra un extrait qui, mis en solution par le tanneur, donnera des solutions riches en insolubles. Ces insolubles occasionneront quelques difficultés au moment du tannage. Il est donc nécessaire d'éliminer ces insolubles. La quantité d'insolubles décantables varie avec la concentration et la température. Ainsi, pour obtenir l'élimination convenable des insolubles il faut amener la concentration des bouillons de 5-6 % à 10-12 %, refroidir les bouillons ainsi pré-concentrés à 15-18°C, et décanter et éliminer les insolubles formés.

À fin d'atteindre cet objectif, la solution provenant de l'extraction traverse un échangeur dans lequel elle est refroidie par la solution décantée circulant en sens inverse. Ainsi, la solution pré-concentrée se refroidit de 80 à 40°C, inversement la solution décantée se réchauffe de 15 à 40°C. La solution décantée passe ensuite dans un réchauffeur d'où elle sort à 80-85°C pour être envoyée à la concentration. Tandis que la solution pré-concentrée traverse ensuite un réfrigérant d'où elle sort vers 15-18°C. Elle est alors envoyée dans des cuves où elle reste au repos 24 heures. Les insolubles tombent au fond sous forme de boue. Lorsque la solution limpide est renvoyée dans le circuit, la boue est pompée pour être introduite dans la batterie d'extraction au niveau de l'autoclave renfermant le bois le moins concentré en tanins. Ainsi les insolubles sont retenus par les copeaux, les produits solubles passent dans les bouillons de la batterie d'extraction. La figure 3 montre un schéma de ce processus.

La solution sortant de la pré-concentration a une teneur de 10-12 % de matières sèches et une température de 80-85°C.

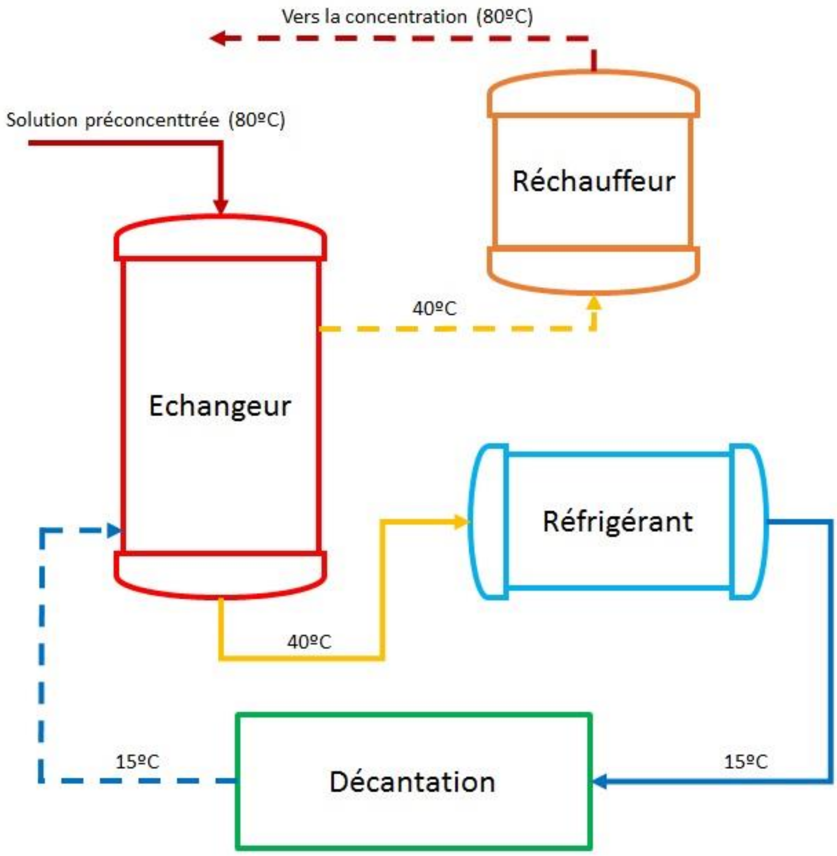

Figure 3: Schéma de décantation de la solution pré-concentrée.

1.3.1.4 Concentration :

La concentration des solutions consiste à faire évaporer l'eau pour augmenter la teneur en matières sèches de la solution. Généralement en deux phases. Dans une première phase, on atteint une concentration de l'ordre de 50% de matières sèches (25° Bé). Dans cette phase, on obtient un extrait liquide, qui pendant longtemps fût livrés directement à la tannerie. Après, dans une deuxième phase, on passe de l'extrait liquide à l'extrait sec, généralement en poudre, renfermant moins de 10 % d'eau.

L'évaporation de l'eau est conduite sous pression réduite et par conséquent à une température relativement basse (inférieure à 100°C) afin d'éviter l'hydrolyse et l'oxydation du tannin. Deux types d'appareils peuvent être utilisés pour cette opération : les évaporateurs à caisse verticale et les évaporateurs Kestner.

L'évaporateur à caisse verticale est composé essentiellement d'une cuve cylindrique surmonté d'un dôme également cylindrique. Dans la moitié inférieure de la cuve se trouve un faisceau tubulaire dans lequel est envoyée de la vapeur pour chauffer le liquide contenu dans l'appareil. Dans le dôme sont disposées des chicanes (brise mousse) pour empêcher les mousses formées par l'ébullition du liquide d'être entraînées dans le circuit vapeur.

Les appareils sont groupés par séries de 3 ou 4. L'ensemble prend le nom de triple effet ou quadruple effet. Pour décrire le principe de fonctionnement de ces appareils, on étudiera le cas triple effet représenté sur la figure 4.

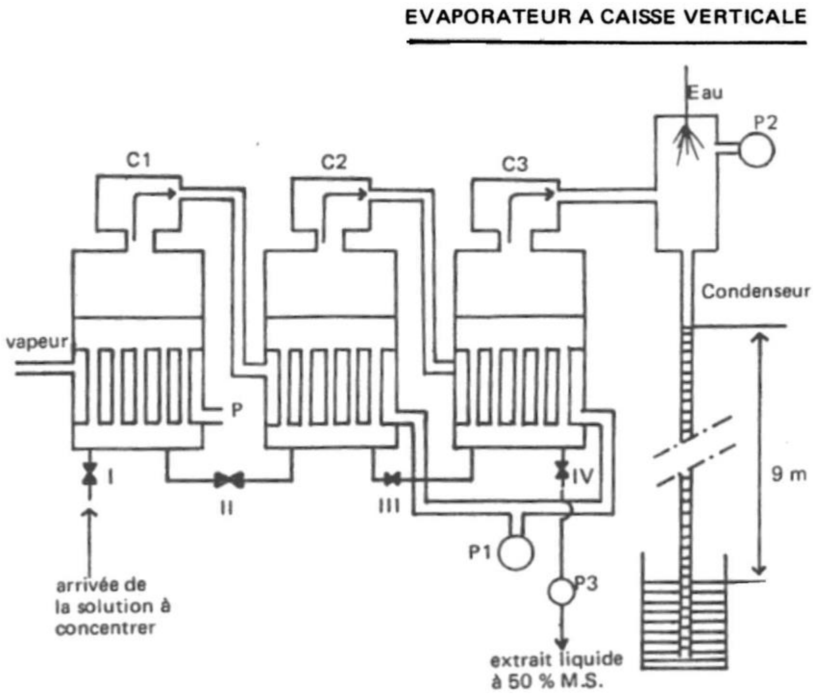

Figure 4: Schéma d'un évaporateur à caisse verticale.

Lors du fonctionnement, les caisses renferment des solutions de plus en plus concentrées de C1 à C3. Dans cette dernière on obtiendra l'extrait liquide à environ 50 % de matières sèches, soit environ 25° Bé.

Suivant le parcours suivi par la vapeur, le faisceau tubulaire de C1 est alimenté par de la vapeur basse pression provenant de la source de vapeur de l'usine. En chauffant la solution contenue dans C1, la vapeur se condense et l'eau condensée est évacuée en P dans le circuit général de purge. La solution entre en ébullition, la vapeur formée passe dans le faisceau tubulaire de C2. En chauffant la solution contenue dans C2, qui entre en ébullition, et en condensant la vapeur, qui provoque une dépression en C1. L'eau condensée dans le faisceau tubulaire de C2 est extraite par la pompe P1 et la vapeur formée dans C2 passe dans le faisceau tubulaire de C3. En chauffant la solution contenue dans C3, qui entre en ébullition. La vapeur se condense provoquant une dépression en C2 et l'eau condensée dans le faisceau tubulaire de C3 est extraite aussi par la pompe P1. La vapeur formée dans C3 arrive dans le condenseur barométrique où elle se condense provoquant ainsi une dépression en C3. La pompe P2 est une pompe à vide qui maintient la dépression en éliminant les incondensables. Ainsi s'établit un équilibre des conditions d'ébullition dans chaque appareil qui sont approximativement les suivantes :

- C1 : température d'ébullition 84°C, pression 0.56 bar.
- C2 : température d'ébullition 70°C, pression 0.30 bar.
- C3 : température d'ébullition 54°C, pression 0.15 bar.

Suivant le chemin de la solution à concentrer, elle arrive dans C1 par la vanne I. Après, elle passe en C2 par la vanne II, en C3 par la vanne III et en IV on extrait la solution concentrée (extrait liquide à 50 % de matières sèches) au moyen d'une pompe P3, car il faut vaincre la dépression qui règne en C3. Cette circulation se fait en continu, pour cela on règle l'ouverture des vannes I, II, III et IV afin de maintenir le niveau de liquide à peu près constant dans les trois appareils.

L'évaporateur Kestner est très différent de la caisse verticale et son fonctionnement est basé sur le phénomène d'ascension des liquides. Prenons un tube fermé à la partie inférieure, de faible diamètre et très long, enfermé dans une housse chauffante. On remplit ce tube jusqu'au tiers de sa hauteur environ avec la solution à concentrer. En chauffant, le liquide entre en ébullition et la vapeur d'eau formée s'élève à très grande vitesse. Elle entraîne le liquide dans un mouvement ascendant, le plaquant en une mince pellicule contre la paroi du tube. Au fur et à mesure de l'ascension contre la paroi chaude, l'eau s'évapore et la solution qui arrive au sommet du tube est beaucoup plus concentrée que la solution de départ. Toute cette action se passe à grande vitesse et le rendement de l'évaporation est très élevé.

Un évaporateur Kestner est constitué d'un faisceau tubulaire de 7 mètres de hauteur enfermé dans une enceinte chauffée. La solution à concentrer est introduite à la base du faisceau. La vapeur arrive dans la partie supérieure du faisceau à grande vitesse, entraînant la solution concentrée. Pour séparer liquide et vapeur, le mélange passe dans un séparateur tangentiel pourvu à l'intérieur d'une chicane centrifuge. Le liquide est projeté sur la paroi et se rassemble au fond du séparateur, la vapeur s'échappe au centre par la partie supérieure. Ces appareils peuvent être groupés en multiples effets (voir figure 5). L'ensemble fonctionne alors dans les mêmes conditions de température et de pression que les multiples effets à caisses verticales décrits précédemment.

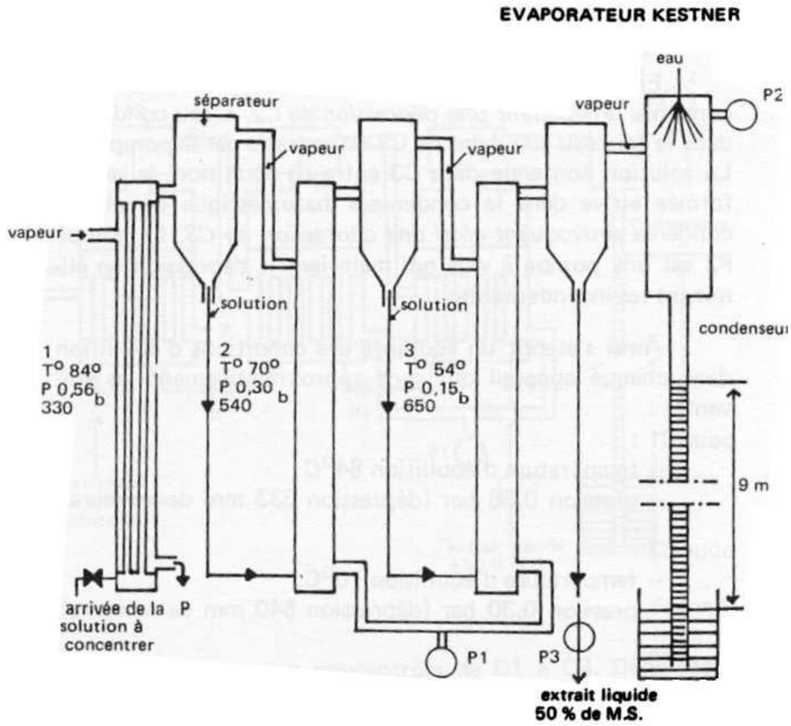

Figure 5: Evaporateur de type Kestner.

1.3.1.5 Obtention de l'extrait solide (poudre) :

Les extraits tannants ne sont que rarement livrés à l'état liquide mais le plus généralement à l'état d'extraits solides en poudre. Il s'agit donc de déshydrater l'extrait liquide obtenu précédemment. Le moyen le plus répandu aujourd'hui est l'atomiseur. L'opération consiste à pulvériser l'extrait liquide par un dispositif mécanique sous forme de très fines gouttelettes (d'un brouillard) dans une enceinte traversée par un courant d'air chaud à 120ºC. L'eau s'évapore presque instantanément et les gouttelettes se transforment en poussière. Une petite partie de ces particules se rassemblent au fond de l'atomiseur, mais la plus grande partie est entraînée par l'air et la vapeur d'eau. Il suffit ensuite de séparer ces particules solides de l'air et de la vapeur. Pour cela, le mélange passe dans les séparateurs tangentiels, généralement deux ou trois à la suite. Les particules solides projetées contre la paroi tombent au fond des appareils, l'air et la vapeur d'eau s'échappent par la partie centrale vers le séparateur suivant, puis dans l'atmosphère. La poudre est alors évacuée vers l'ensachage. La figure 6 montre un schéma de l'équipement de pulvérisation.

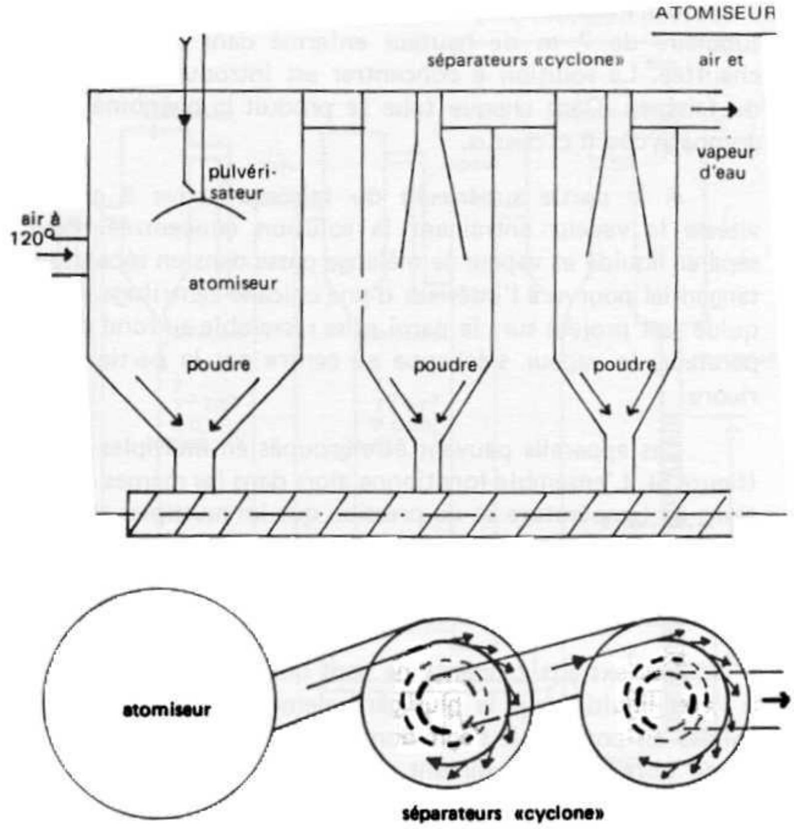

Figure 6: Atomiseur.

1.3.2 Fabrication de l'extrait de bois de quebracho :

L'extrait de quebracho est préparé à partir du bois du même arbre. La technique de séparation de l'extrait est sensiblement la même que celle décrite pour l'extrait de châtaignier. Cependant, pour le quebracho, il n'y a pas la phase de décantation. L'extrait obtenu après évaporation à sec présente une propriété particulière : il n'est pas soluble dans l'eau froide (température ambiante). Il se dissout dans l'eau chaude à 80-100°C et par refroidissement la solution se trouble et après filtration on peut constater que le filtrat ne renferme qu'une faible quantité de tannin. Cet extrait s'appelle extrait de quebracho brut soluble à chaud. Sous cette forme, ce produit est difficilement utilisable dans les méthodes de tannage classiques où l'on opère à température ambiante ou au maximum à 30°C. Il est donc nécessaire de solubiliser l'extrait brut. C'est en 1897 que Lepetit, Dolfus et Gansser ont breveté un procédé dit de sulfitation permettant d'atteindre ce but. On traite une solution concentrée (50 % de matières sèches) d'extrait de quebracho brut par de l'hydrogénosulfite de sodium (bisulfite de sodium $NaHSO_3$) à chaud sous pression en autoclave. Après ce traitement on obtient un produit parfaitement soluble dans l'eau froide. Après évaporation à sec, on se trouve en présence de l'extrait de quebracho sulfité soluble à froid.

L'extrait de quebracho sulfité est un tannin doux. Il pénètre rapidement dans la peau en tripe, le cuir obtenu n'a pas un indice de tannage élevé, il est souple, de couleur claire. En modérant le traitement de sulfitation, généralement en diminuant la proportion d'hydrogénosulfite de sodium, on n'obtient qu'une solubilisation partielle. On prépare ainsi l'extrait de quebracho mi-soluble dont les solutions, troubles à froid, renferment un fort pourcentage de tannin soluble. Ce genre de produit est utilisé en particulier pour le retannage de certains cuirs au chrome pour lesquels on recherche un effet de remplissage important.

1.4 Classification des tanins

Du point de vue de la composition chimique, on distingue deux grandes familles de tanins : les tanins hydrolysables et les tanins condensés. Le type de tanins ne dépend que du végétal duquel ils sont extraits.

1.4.1 Les tanins hydrolysables

Les tanins hydrolysables sont constitués de produits phénoliques simples comme l'acide gallique, l'acide digallique, l'acide ellagique et de monosaccharides, surtout le glucose. Ils tirent leur nom de leur facilité à s'hydrolyser en présence d'un acide ou d'une base (Carretero, 2000). Ils sont divisés en gallotanin et en ellagotanins (Jurd, 1962).

Les tanins hydrolysables sont disponibles en grande quantité mais peu valorisés. Néanmoins, leur faible réactivité avec le formaldéhyde limite leur utilisation dans le domaine des colles. Industriellement, on utilise principalement les tanins de châtaignier et de tara pour le tannage du cuir (Pizzi, 1994).

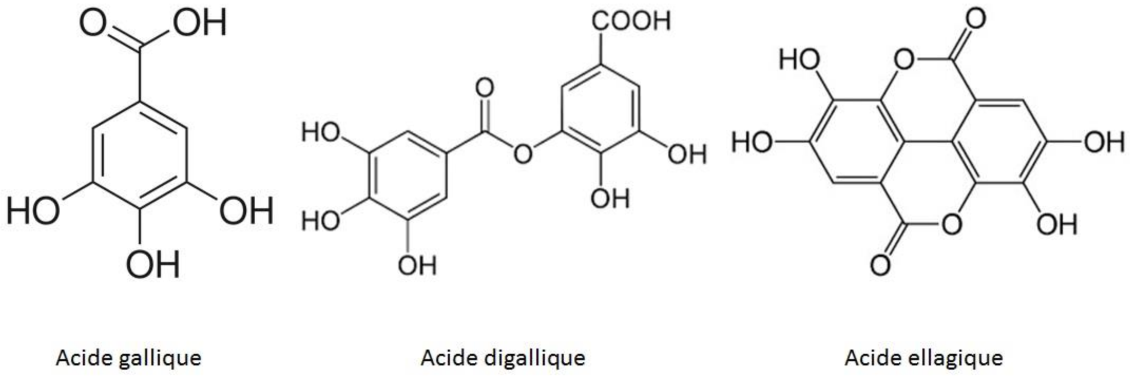

Figure 7: Types de tanins hydrolysables.

Ces dernières années, certaines études ont permis de les utiliser comme copolymères avec du phénol et du formaldéhyde pour la préparation de résines dans la fabrication de colles à bois phénoliques (Spina et al., 2013a, 2013b). D'autres études ont montré qu'ils peuvent se substituer aux isocyanates dans la fabrication de mousses polyuréthanes (Thébault et al., 2014) ou comme précurseur dans les résines époxy (Aouf et al., 2014).

1.4.2 Tanin condensés

Les tannins condensés sont constitués d'unités flavonoïdes. Présentant différents degrés de polymérisation, ils sont associés à leurs précurseurs : catéchines (flavanes-3-ols), leucoanthocyanes (flavanes-3,4-diols) (Drewes and Roux, 1963; Roux and Paulus, 1961) et à des carbohydrates dont la plus ou moins grande proportion influence la viscosité et la réactivité du tannin.

Comme le montre le schéma en figure 8, il est possible d'obtenir deux types d'anneau A et deux types d'anneau B :

- Anneau A porte un seul groupe hydroxyle en C7 : anneau résorcinol.
- Anneau A porte deux groupes hydroxyles en C5 et C7 : anneau phloroglucinol.
- Anneau B porte deux groupes hydroxyles en C3' et C4' : anneau catéchol.
- Anneau B porte trois groupes hydroxyles en C3', C4' et C5' : anneau pyrogallol.

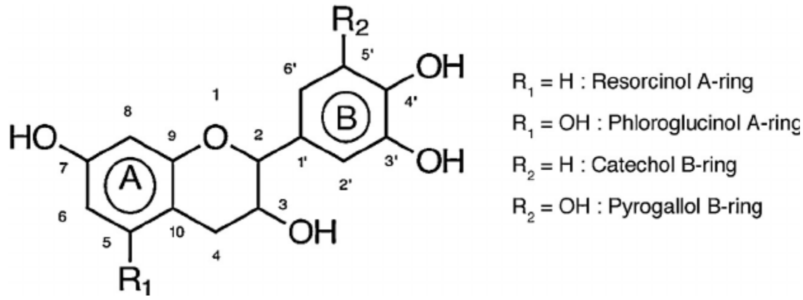

Figure 8: Schéma d'un flavonoïde et sa numérotation.

Une nomenclature des polyflavonoïdes a été définie à partir de ces différents types d'anneaux (Porter, 1988) (Tableau 3) :

Tableau 3: Nomenclature des flavonoïdes.

Type de l'anneau A	Type de l'anneau B	Flavonoïde	Polyflavonoïde
Phloroglucinol	Pyrogallol	Gallocatéchine	Prodelphinidine
Phloroglucinol	Catéchol	Catéchine	Procyanidine
Résorcinol	Pyrogallol	Robinetinidol	Prorobinetinidine
Résorcinol	Catéchol	Fisetinidol	Profisetinidine

Les tannins condensés sont toujours constitués d'un mélange aux proportions diverses des quatre types de polyflavonoïdes définis ci-dessus. Ainsi pour le type d'anneau A, la proportion de phloroglucinol par rapport au résorcinol permet de déterminer la réactivité du tannin vis à vis des aldéhydes et de présager de la qualité du réseau d'enchevêtrement. Pour l'anneau B, la proportion de noyaux de type pyrogallol par rapport aux noyaux de type catéchol influe sur l'ouverture de l'hétérocycle pyranique et détermine le type de réarrangement à envisager pour la structure suivant les conditions de pH (Pizzi and Stephanou, 1994a, 1994b).

La technique d'analyse C^{13} RMN des tannins condensés a permis de mettre en évidence les types de polyflavonoïdes rencontrés pour un tannin déterminé. Néanmoins cette méthode ne permet pas de différencier les prodelphinidines des procyanidines, ni les prorobinetinidines des profisetinidines (Thompson and Pizzi, 1995).

D'après Roux et al. (1975), seuls les flavonoïdes de type flavan-3-ol et flavan-3,4-diol participent à la formation des tannins condensés. En effet, le groupe carboxyle en position 4 des autres types de flavonoïde réduit le caractère nucléophile et occupe une des positions de condensation. La substitution méta de l'anneau A de type résorcinol des flavan-3,4-diols par les groupes hydroxyles et l'oxygène de l'hétérocycle crée une très forte nucléophilie pour les positions C6 et C8. Ainsi, les unités des tannins condensés sont principalement liées par des liaisons C4-C6 et C4-C8. La première étape de réaction de condensation est la formation de proanthocyanidines dimères appelés aussi biflavonoïdes. On parle réellement de tannins condensés pour une répétition de 3 à 8 unités de flavonoïdes (Pizzi, 1980; Roux, 1972; Roux et al., 1975, 1976).

Il est possible de faire une classification des principaux extraits de tanins condensés en fonction de la nature du polyflavonoïde majoritaire, du type d'enchaînement et du degré de polymérisation (Tableau 4).

Tableau 4: Classification des différents types de tanins condensés.

Aspect			
Extraits	Mimosa (*Acacia mearnsii* ou *mollissima*)	Quebracho (*Schinopsis balansae*)	Pine (*Pinus radiata*)
Types des flavonoïdes	Prorobinetinidine	Profisetinidine	Procyanidine
Enchaînement	4-6	4-6	4-8
Degré de polymérisation	Elevé	Elevé	Très elevé

Aspect		
Extraits	Pecan (*Carya illinoensis*)	Gambier (*Uncaria gambir*)
Types des flavonoïdes	Procyanidine	Procyanidine
Enchaînement	4-8	4-8
Degré de polymérisation	Très elevé	Bas

1.4.2.1 Techniques d'analyses

Différentes techniques peuvent être utilisées pour la caractérisation de tanins. Certaines d'entre elles sont décrites ci-dessous.

1.4.2.1.1 Spectroscopie de résonance magnétique nucléaire (RMN ^{13}C)

Méthode utile pour déterminer la structure de tanins. La spectroscopie de résonance magnétique nucléaire permet de préciser la formule développée, la stéréochimie et la conformation du composé étudié (Breitmaier and Voelter, 1990; Mansouri et al., 2007; Mansouri and Pizzi, 2006).

Les essais, qui peuvent être effectués en phase liquide ou solide, donnent lieu à des spectres RMN correspondant à l'absorption par certains atomes présents dans l'échantillon, de certaines fréquences électromagnétiques. L'interprétation de ces signaux (position, aspect et intensité) conduit à un ensemble d'information d'où l'on déduit des détails de structure concernant l'échantillon.

1.4.2.1.2 Spectrométrie de masse MALDI-ToF

La spectrométrie de masse « Matrix Assisted-Laser Desorption/Ionization-Time of Flight » (MALDI-ToF) permet d'évaluer le poids moléculaire des fragments polymères. Cette technique douce d'ionisation est combinée avec les analyseurs de masse à temps de vol (ToF). Elle présente l'avantage de fournir un spectre de masses complet, pour une gamme de masses pratiquement illimitée, à partir de peu d'échantillon.

L'introduction de cette technique dans l'investigation des tanins (Pasch et al., 2001) a permis une meilleure connaissance des enchaînements des flavonoïdes dans les polymères tanniques.

1.4.2.1.3 Analyse thermomécanique (TMA)

Un analyseur thermomécanique permet de déterminer les variations dimensionnelles d'un échantillon placé dans un environnement thermiquement contrôlé. Selon la méthode adoptée (compression, flexion, traction pu pénétration) et la charge appliquée (statique ou dynamique), il est possible de suivre et de déduire les comportements relatifs à la variation dimensionnelle. Celle-ci peut traduire le coefficient d'expansion thermique, la température de transition vitreuse ou le ramollissement et indirectement le module de Young.

L'analyse thermomécanique en flexion trois points a permis de quantifier l'enchevêtrement du réseau par détermination du nombre moyen de degré de liberté des segments de polymères au cours de l'autocondensation des tannins (Garcia and Pizzi, 1998a). Dans l'analyse des thermogrammes obtenus, l'augmentation du module d'Young est liée à deux phénomènes : la progression de la réaction d'autocondensation du tannin par paliers successifs correspondant aux différences de réactivités des sites disponibles sur l'anneau A et l'anneau B mais aussi l'autocondensation à basse température initiale qui conduit à la formation de polymères linéaires dont la longueur augmente jusqu'à une valeur limite qui dépend de la température et de la concentration, longueur critique à partir de laquelle se forme un réseau d'enchevêtrement de ces polymères linéaires qui correspond à un autre palier sur la courbe du Module d'Young (Garcia and Pizzi, 1998b).

1.4.2.1.4 Autres techniques de caractérisation

D'autres techniques d'analyse ont également permis d'isoler et d'identifier les molécules que constituant les tanins ainsi que leur degré de polymérisation. Comme la chromatographie liquide haute performance (Cheynier et al., 1999), la chromatographie à perméation de gel (Cadahía et al., 1996). La spectroscopie d'absorption de l'ultraviolet (Muralidharan, 1997) permet d'identifier globalement la famille d'un tannin alors que la spectroscopie infrarouge à transformée de Fourier permet de définir un tannin donné (Nakagawa and Sugita, 1999). La spectroscopie du proche infrarouge a également aidé à analyser un extrait de tannin, en déterminant la part d'extractibles, de tannins et de non tannins pour une espèce de tannin donnée (Donkin and Pearce, 1995).

1.4.2.2 Réactivité des tanins condensés

La relative accessibilité et/ou réactivité des flavonoïdes a été étudiée grâce à la bromation sélective dans la pyridine de modèles des familles du phloroglucinol et du résorcinol. On peut alors observer la bromation préférentielle de la (+)-tétra-O-méthylcatéchine en C8 (Roux et al., 1975), et c'est uniquement lorsque ce site est occupé que la substitution commence en C6. Le noyau B n'est pas réactif à moins qu'il n'y ait un excès de réactif de bromation : on observe alors un faible degré de substitution en C6'. La séquence de bromation de la (+)-tétra-O-méthylcatéchine (8>6>>6') est présentée sur la figure 9A. Cependant, pour le résorcinol équivalent, la (-)-tri-O-méthylfustine, la séquence de substitution devient 6>8>>6' comme montre la figure 9B.

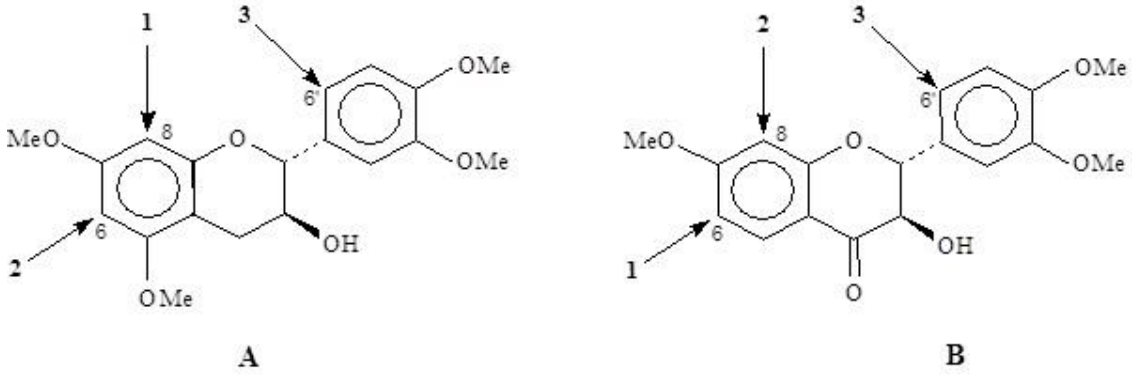

Figure 9: Représentation des sites réactifs des flavonoïdes par bromation.

La substitution préférentielle des flavonoïdes de type phloroglucinol en C8 et de type résorcinol en C6 doit vraisemblablement être liée à la plus grande accessibilité de ces sites. En utilisant le résorcinol comme modèle simplifié, il apparaît que les di-,tri- et tétramères formés lors de la réaction (en milieu acide ou alcalin) de celui-ci avec le formaldéhyde, ne privilégient pas la position en ortho des deux groupements hydroxydes. Cette substitution préférentielle qui semble être respectée dans la structure des biflavonoïdes, et confirmée par les réactions de modèles phénoliques, n'est cependant pas respectée à un degré de réticulation supérieur.

1.4.2.2.1 Autocondensation des tanins

Les flavonoïdes sont capables de réagir entre eux via des réactions radicalaires d'autocondensation conduisant à la formation et au durcissement d'un réseau d'enchevêtrement en présence de bases ou d'acides faibles de Lewis (Masson et al., 1996a, 1996b, 1997; Meikleham et al., 1994; Merlin and Pizzi, 1996; Pizzi et al., 1995b; Pizzi and Meikleham, 1995). L'analyse thermomécanique en flexion trois points a permis de quantifier l'enchevêtrement du réseau par détermination du nombre moyen de degré de liberté des segments de polymères au cours de l'autocondensation des tannins [Garcia et Pizzi, 1998, (1)] et a permis de conclure qu'il se forme, au début, un polymère linéaire jusqu'à un seuil critique à partir duquel un réseau enchevêtré se forme. En présence d'acides minéraux forts et avec un apport de chaleur, les tanins sont susceptibles de réagir de deux manières différentes. La première étant la dégradation des polymères et la formation de catéchine et d'anthocyanidines comme l'illustre le biflavanoïde typique de la Figure 10.

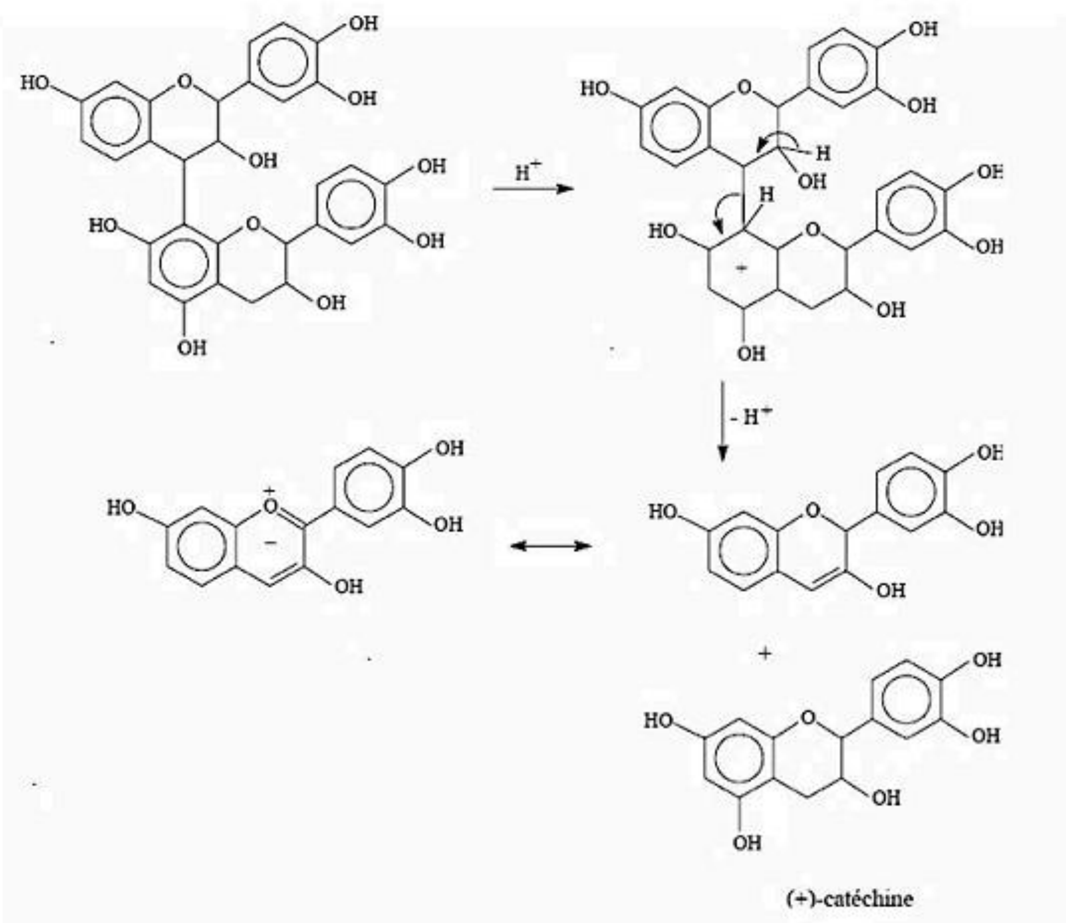

Figure 10: Dégradation des tanins en catéchine et anthocyanidine (Pizzi, 1983).

La deuxième réaction est une condensation résultant de l'hydolyse des hétérocycles (liaisons p-hydroxybenzyléther). Les ions p-hydroxybenzy carbonium (Figure 11) créés se condensent alors avec les sites nucléophiles, C6 et C8, d'autres unités de tanin pour former les phlobaphènes (Meikleham et al., 1994; Pizzi and Meikleham, 1995; Roux et al., 1975).

En milieu basique, les tanins peuvent également réagir de deux façons différentes. La première réaction est la rupture de la liaison interflavonoïde C4-C8. Cette réaction est particulièrement présente dans les tanins de pin et de noix, mais beaucoup plus rarement dans les tanins de mimosa (Pizzi et al., 1993). Ainsi, cette rupture de liaison mène à la formation d'un carbocation en C4 qui peut ensuite entraîner une recondensation basique en C6 ou C8 (Figure 12).

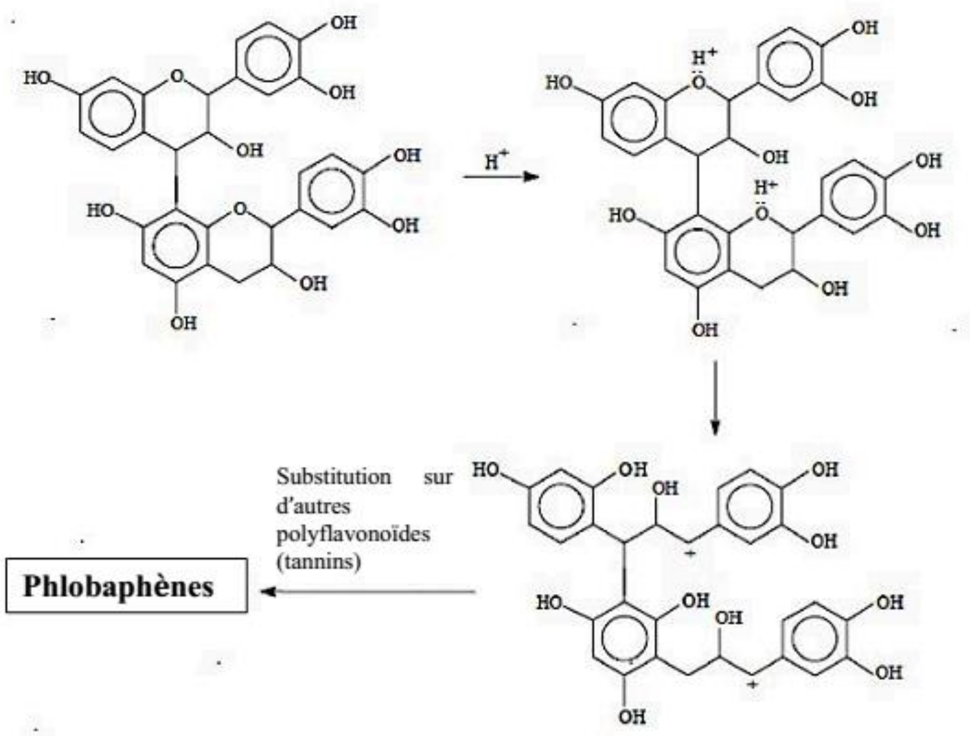

Figure 11: Autocondensation acide par hydrolyse des hétérocycles.

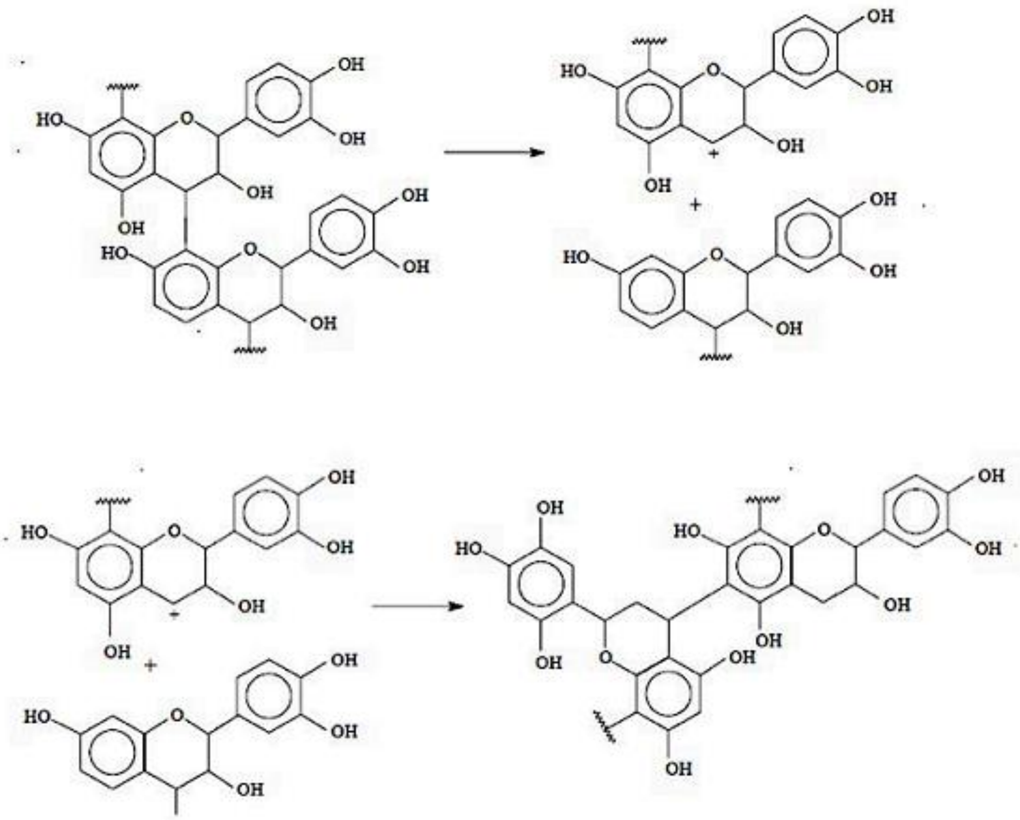

Figure 12: Autocondensation basique, rupture des liasons interflavonoïdes puis aotuocondensation. Examples pour les tanins de pin et de noix de pecan (Pizzi, 1983).

La seconde réaction (Figure 13) est une autocondensation partielle. Cette autocondensation est due à l'augmentation de réactivité liée à l'ouverture de l'hétérocycle (Navarrete, 2011). Ceci étant très nettement visible lors des études menées sur la catéchine monomère.

Ces réactions d'autocondensation des tanins condensés ont été utilisées pour la fabrication de panneaux de particules et ceci sans emploi d'aldéhydes comme durcisseurs (Meikleham et al., 1994; Pizzi et al., 1995a). L'ajout de certains durcisseurs peut perturber les réactions d'autocondensation (Garcia et al., 1997).

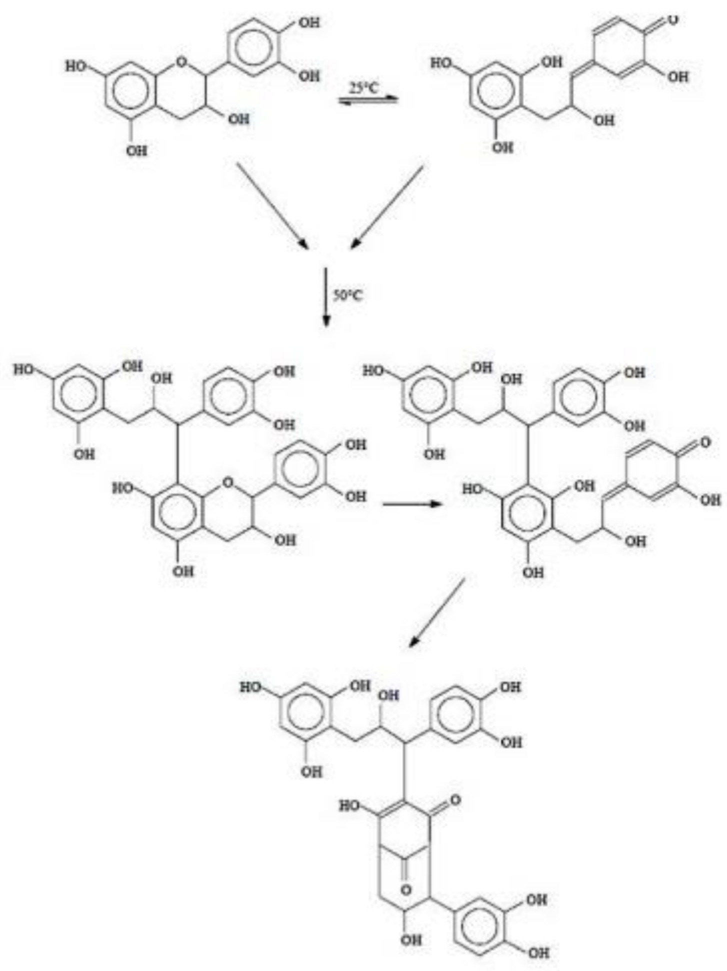

Figure 13: Réarrangement catéchinique (Navarrete, 2011).

Les différences dans les cinétiques de réaction dépendent des types de tanins (Masson et al., 1997). L'autocondensation des tanins induit une augmentation de a viscosité de la résine mais il n'y a pas de gélification (Pizzi and Stephanou, 1993) sauf en présence d'un catalyseur comme la silice ou présence de matériaux lignocellulosiques (Pizzi, 1994).

Quelques coréactifs, tel que le paraformaldéhyde, semblent renforcer l'autocondensation des tanins en contribuant à la réticulation finale (Garcia and Pizzi, 1998a). Ainsi, d'autres coréactifs, comme l'héxamine semblent amplifier la formation du réseau final par synergie entre les deux mécanismes de condensation pour les tanins qui réagissent lentement. Au contraire, pour les tanins qui réagissent plus rapidement comme les tanins de type procyanidine, l'héxamine ne montre pas d'interférence avec le mécanisme d'autocondensation.

1.4.2.2.2 Réaction avec les aldéhydes

Les polyflavonoïdes étant de nature polyphénolique, ils réagissent de la même manière que les phénols, aussi bien en milieu acide qu'en milieu basique. L'augmentation de l'alcalinité du milieu augmente la nucléophilie du phénol, tout particulièrement vers pH 8 où des ions phénates sont formés. Concernant les réactivités des noyaux A et B, les sites nucléophiles de l'anneau A sont plus réactifs que ceux de l'anneau B, pour n'importe quel type de tanins. L'explication réside dans la présence de groupements hydroxyles vicinaux qui provoquent l'activation de la globalité du noyau B sans localisation de la réactivité comme cela se produit sur le noyau A.

Pour les tanins condensés, il subsiste seulement un site hautement réactif, l'autre étant engagé dans une liaison interflavonoïde. Les flavonoïdes qui ont un noyaux A de type résorcinol montrent une réactivité vis-à-vis du formaldéhyde comparable, quoique légèrement inférieure, à celle du résorcinol (Pizzi, 1978; Rossouw et al., 1980). Les noyaux B de type pyrogallol ou catéchol ne sont donc pas réactifs, sauf lorsqu'il y a formation d'anions à des pH relativement élevés (environ pH 10) (Roux et al., 1975). Parfois, les noyaux B de type catéchol sont réactifs à température plus élevée (Osman and Pizzi, 2002).

En pratique, seuls les noyaux A interviennent dans la formation du réseau tridimensionnel. Cependant, certaines recherches suggèrent que dans des milieux légèrement acides ou basiques et avec un excès de résorcinol, les noyaux B de type pyrogallol sont capables de réagir avec le formaldéhyde (Pizzi, 1977). Des molécules modèles ont été étudiées à température ambiante, qu'ils ont permis observer la formation de dimères pyrogallol-formaldéhyde, ainsi que de dimères et de trimères résorcinol-formaldéhyde. Ceci indique qu'en dépit d'une participation limitée des noyaux B dans la formation d'un réseau tridimensionnel tanin-formaldéhyde, un tel réseau reste toujours faible.

Afin de résoudre ce problème, des agents de réticulation comme des résines phénoliques ou aminoplastiques peuvent être utilisées. Elles permettent l'établissement de liaisons entre des sites trop distants pour être reliés par un pont de type méthylène (Pizzi and Roux, 1978; Pizzi and Scharfetter, 1978).

1.4.2.2.3 Réaction avec le formaldéhyde

Le formaldéhyde réagit avec des tanins pour amorcer la polymérisation à travers des ponts méthylène dans les sites actifs des molécules de flavonoïdes, principalement les noyaux A (Pizzi and Mittal, 2003).

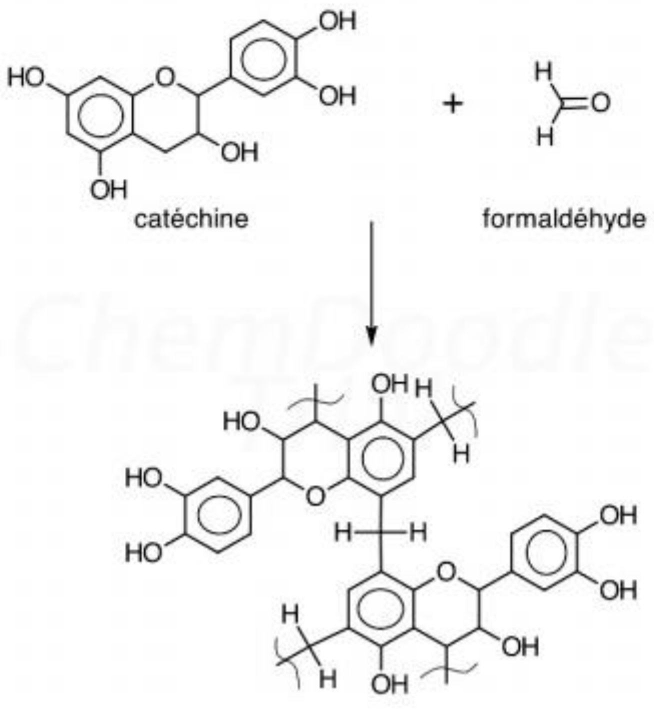

Figure 14: Réaction entre les flavonoïdes et le formaldéhyde.

Il existe une dépendance entre la réaction tanins-formaldéhyde et le pH de la réaction. Il a été observé que la réaction des tanins de mimosa avec le formaldéhyde est plus lente entre 4.0 et 4.5. Ainsi, la quantité de formaldéhyde réagissant avec des tanins dans ces domaines de pH, est la plus faible (Plomley, 1966). A pH neutre, le formaldéhyde réagit rapidement avec les flavonoïdes en C6 et C8. Cependant, le catéchol et les noyaux B de type catéchol ne réagissent pas avec le formaldéhyde à des pH inférieurs à 10, mais l'addition d'acétate de zinc permet aux noyaux B de type catéchol de réagir avec le formaldéhyde à ces pH. La gamme optimale de pH étant de pH 4.5 à 5.5, comme le montre la plus grande quantité de formaldéhyde consommée (Hillis and Urbach, 1959). Ainsi, l'utilisation d'une petite quantité d'acétate de zinc (5 à 10% par rapport à la résine solide) permet un haut degré de réticulation ne conférant cependant pas au réseau une force comparable à celle obtenue grâce à l'addition de résines synthétiques (Osman and Pizzi, 2002).

Le formaldéhyde est l'aldéhyde généralement utilisé lors de la préparation et du durcissement d'adhésifs à base de tanins. Il est normalement additionné aux tanins en solution, au pH désiré, sous la forme de formaline liquide ou sous la forme du para-formaldéhyde polymère, capable de se dépolymériser rapidement en milieu alcalin. Il suffit d'un faible degré de condensation avec le formaldéhyde pour que la taille et la configuration des molécules de tanins leur imposent l'immobilité. Ceci à un point tel que les sites réactifs sont alors trop éloignés pour que puisse s'établir un pont de type méthylène (Roux et al., 1975). Le résultat en est une polymérisation incomplète, d'où faiblesses et fragilisations souvent caractéristiques des adhésifs tanins-formaldéhyde.

Pendant la réaction des tanins avec le formaldéhyde, deux réactions compétitives peuvent se produire : la réaction de l'aldéhyde avec les tanins condensés à proprement parler et la formation d'un nombre important de ponts de type méthylène-éther instables à partir du formaldéhyde non réagi. Ces ponts sont aisément réarrangés pour former des ponts méthylène avec libération de formaldéhyde (Pizzi and Mittal, 2003).

Malheureusement la réactivité des noyaux A vis-à-vis du formaldéhyde est alors tellement élevée que la trop faible durée de conservation des résols tanins-formaldéhyde les rend industriellement inutilisables (Pizzi, 1978). Cependant, la réaction du formaldéhyde avec les tanins peut être contrôlée par addition d'alcool, une partie du formaldéhyde est alors stabilisée par formation d'hémiacétals (Pizzi and Scharfetter, 1978). Lorsque l'adhésif est durci (en augmentant la température), l'alcool est libéré à vitesse constante et le formaldéhyde, progressivement reformé à partir des hémiacétals, s'évapore moins qu'en absence d'alcool. La présence de celui-ci permet donc de rendre le formaldéhyde non réactif, ce qui a pour conséquence d'augmenter la durée de vie en pot de tels adhésifs, mais uniquement à température ambiante.

La forte toxicité du formaldéhyde pousse les recherches scientifiques à trouver de nouvelles formulations pour diminuer ou éliminer ses émissions. Deux axes principaux a été développé en la fabrication de adhésives : l'emploi de durcisseurs qui n'émettent pas de formaldéhyde, comme autres aldéhydes, et l'autocondensation des tanins.

Figure 15: Réction entre le formaldéhyde et un alcool. Formation d'un hémiacétal.

1.4.2.2.4 Réactivité avec d'autres aldéhydes

Les cinétiques de réaction de divers aldéhydes avec les tanins condensés de type résorcinol et phloroglucinol ont été étudiées (Rossouw, 1979). Des différences notables ont été observées dans les vitesses de réaction des tanins de type résorcinol et phloroglucinol avec certains aldéhydes. Dans le cas des tanins de type phloroglucinol, les vitesses de réaction se classent ainsi :

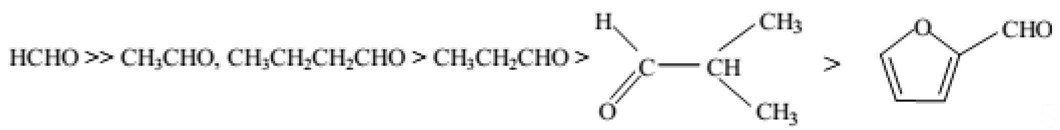

Figure 16: Vitesses de réaction pour les tanins de type phloroglucinol.

La figure 17 ci-dessous, représente l'échelle de réactivité pour les tanins de type résorcinol.

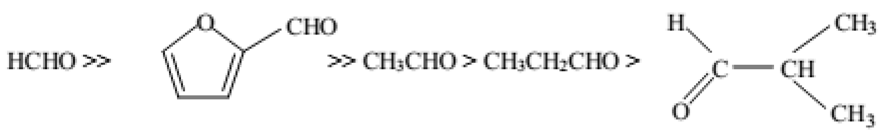

Figure 17: Vitesses de réaction pour les tanins de type résorcinol.

La plus grande différence, entre ces deux échelles de réactivité, est la position du furaldéhyde. Si sa réactivité vis-à-vis des réactifs phénoliques et des flavonoïdes possédant un noyau A de type résorcinol est importante, elle est fortement limitée par des problèmes d'encombrement stérique dans le cas des flavonoïdes ayant un noyau A de type phloroglucinol (Rossouw, 1979). Dans le cas des flavonoïdes de type résorcinol, l'attaque de l'aldéhyde a lieu en C8, site considérablement moins encombré stériquement que le site C6 des flavonoïdes de type phloroglucinol.

Les sites réactifs sont parfois trop éloignés les uns des autres pour permettre l'établissement de ponts de type méthylène, et ainsi la création d'un réseau optimum. D'autres aldéhydes à caractère bifonctionnel peuvent être utilisés comme substituts du formaldéhyde. Certains de ces aldéhydes sont :

- Glutaraldéhyde, qui est généralement utilisé comme désinfectant. Il est un composé toxique et irritant. Bien qu'il réagit dans une moindre mesure que le formaldéhyde avec les tanins, il a été utilisé pour la fabrication de colles tanins-résorcine-glutaraldéhyde (Sauget et al., 2014).
- Le glyoxal est un intermédiaire de réaction couramment utilisé en chimie et il est disponible en grande quantité. Il possède plusieurs avantages : il est très peu nocif, il ne présente que peu de risques pour l'homme et est classé parmi les composés non-toxiques par les organismes de santé. Il est aussi biodégradable et n'est pas volatil. Son principal défaut est sa réactivité moindre par rapport au formaldéhyde avec les flavonoïdes. Mais les travaux de Ballerini et al. (2005) ont montré que des résines à base de tanins de pin radiata pour colle à bois peuvent être réalisées en utilisant le glyoxal comme durcisseur.
- Le furfural est un efficace agent de réticulation et un excellent plastifiant, lors de son utilisation dans les adhésifs à base de tanins (Pizzi, 1978), même s'il réagit lentement avec les composés phénoliques (Plomley, 1966). Cependant, il est toxique et irritant. Mais, sa réactivité est quasiment identique à celle du formaldéhyde avec les flavonoïdes qui possèdent un anneau A de type résorcinol (Rossouw et al., 1980).

2 L'alcool furfurylique

2.1 Caractéristiques physico-chimiques

L'alcool furfurylique est un produit liquide à température ambiante, transparent et incolore ou jaune clair selon l'état de conservation du produit. Ce produit est considéré nocif par inhalation, ingestion et contact avec la peau selon la directive européenne 2001/60/CEE.

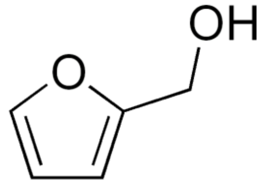

Figure 18: Molécule d'alcool furfurilyque.

Ce composé organique présente des caractéristiques aromatiques et alcooliques. Les caractéristiques physico-chimiques les plus importantes de l'alcool furfurylique sont sa forte solubilité dans l'eau et dans les alcools de bas poids moléculaire et sa grande réactivité chimique dans le cadre d'oxydations et de polymérisations. Il est utilisé principalement dans la chimie des résines, des peintures, des matériaux synthétiques et surtout dans les fonderies.

2.2 Production de l'alcool furfurylique

Ce produit chimique est considéré comme un produit naturel, parce qu'il est obtenu à partir des hémicelluloses de différents types de produits agricoles comme la sciure, le blé ou le maïs. Il est obtenu principalement à partir de deux réactions:

1) Hydrolyse des pentosanes des hémicelluloses.

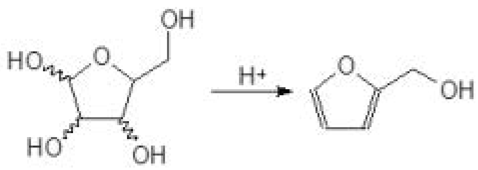

2) Hydrogénation catalytique à haute pression du furfural.

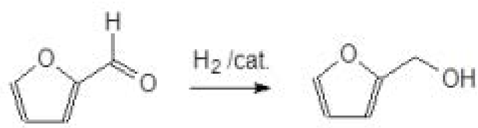

Les catalyseurs sont constitués généralement par des métaux. Des études récentes ont montré l'efficacité des mélanges Co-Mo et B (Chen et al., 2002) et Cu-MgO (Nagaraja et al., 2003).

2.3 Réactivité de l'alcool furfurylique.

L'alcool furfurylique peut être transformé en 2,5-bis(hydroxymethyl)furan par réaction avec le formaldéhyde (Gandini, 1997) :

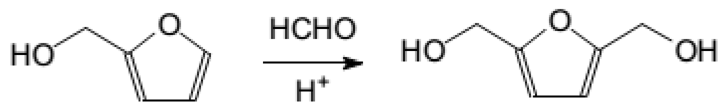

Figure 19: Réaction de l'alcool furfurylique avec le formaldéhyde.

Cette réaction avec le formaldéhyde permet de générer un composé qui peut être un intermédiaire très efficace dans la polymérisation mixte avec les tanins condensés.

L'alcool furfurylique est aussi bien connu pour subir une réaction d'auto-condensation très exothermique en milieu acide selon le chemin suivant.

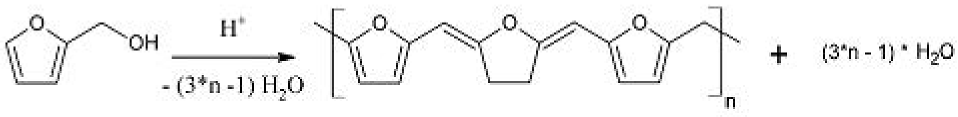

Figure 20: Autocondensation de l'alcool furfurylique en milieu acide.

Une fois que l'énergie d'activation de cette réaction est atteinte, le processus s'auto-entretient et tout l'alcool furfurylique est rapidement transformé en poly-alcool furfurylique. La réaction de polycondensation conduit à des polymères linéaires, ramifiés et même à des structures tridimensionnelles selon les conditions de catalyse appliquées.

Beaucoup d'études ont été menées sur ces matériaux afin d'évaluer leur résistance à la chaleur et à la corrosion, et leur fort caractère ininflammable. En raison de ces caractéristiques, ces produits sont largement utilisés dans l'industrie des fonderies et des vernis anti-corrosifs.

2.3.1 Réactivité de l'alcool furfurylique avec les tanins

Des études de base sur la réactivité de l'alcool furfurylique ont été conduites avec des molécules modèles de tanins (Foo and Hemingway, 1985). Ainsi la catéchine a été amenée à réagir sur l'alcool furfurylique en milieu acide. Deux flavonoïdes distincts substitués en positions C8 et C6 par des groupements furanyles ont été obtenus avec un rendement de 4% et 1,5% respectivement. La plus grande réactivité de la position C8 par rapport à la position C6 était prévisible et cela sera d'autant plus vérifiable avec des substituants de fort encombrement stérique.

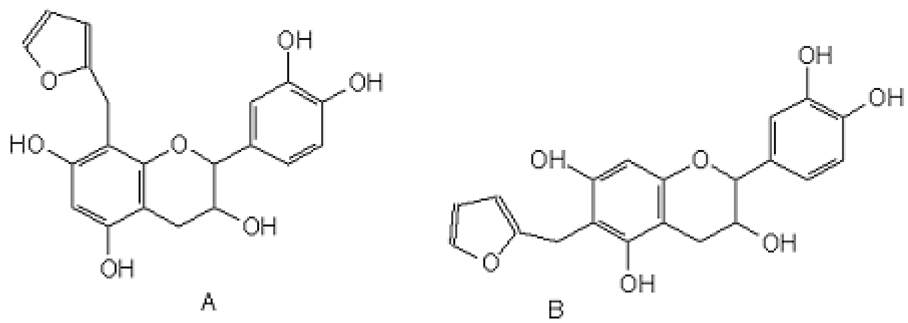

Figure 21: Produits de réaction de l'alcool furfurylique sur la catéchine:A-4% et B-1,5% rendement.

D'autres études ont été menées pour avoir des informations plus précises sur la réactivité de l'alcool furfurylique avec le tannin de mimosa.

3 Les tensioactifs

Les molécules tensioactives sont aussi appelées agents de surface ou encore surfactants. Ils peuvent être originaires de substances naturelles ou synthétiques. Ces molécules sont amphiphiles car elles sont constituées d'une partie hydrophile qui présente une affinité pour les solvants polaires, et une partie hydrophobe qui aura une meilleure affinité pour les solvants apolaires (Larpent, 1995). La partie hydrophile est aussi appelée tête polaire. Tandis que la zone apolaire, le plus souvent hydrocarbonée, est désignée par le terme de queue hydrophobe.

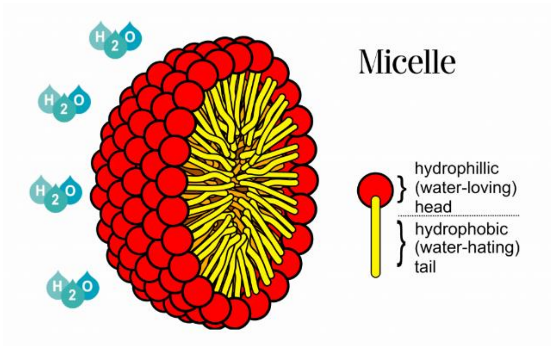

Figure 22: Tensioactifs. Micelle.

Du fait de cette double affinité, ces molécules vont s'adsorber aux interfaces liquide-gaz, liquide-solide ou liquide-liquide, pour former un film interfacial (liquide-

liquide) ou superficiel (liquide/gaz). Ceci va entraîner l'abaissement de la tension superficielle.

Ils sont largement utilisés dans l'industrie pour leurs multiples propriétés. Ils peuvent être mis à profit dans la teinture des filtres ou la polymérisation en émulsion avec leur pouvoir solubilisant (Sobisch, 1994). Ils sont utilisés pour leur pouvoir moussant (Jakobs et al., 2005) à cause de la capacité de certains tensioactifs pour former rapidement des couches interfaciales et superficielles résistantes. Mais ils peuvent aussi être anti-moussants (Wang et al., 2006). Leur pouvoir émulsionnat qui leur permet de disperser et de maintenir en suspension un liquide dans un autre liquide non miscible (Lorinc, 1974). Mais ils ont aussi beaucoup d'autres propriétés, ce qui explique son utilisation dans une grande variété de secteurs de l'industrie chimique (Koumbi Mounanga, 2008).

3.1 Classification des tensioactifs

Les tensioactifs peuvent être classés suivant la nature de leur tête polaire. Ils sont ainsi distingués :

- Les tensioactifs anioniques qui s'ionisent dans l'eau pour donner un anion organique. Ce sont les plus utilisés. Ils correspondent la plupart du temps à des carboxylates, à des sulfonates ou à des sulfates. Leur activité est limitée aux milieux basiques (Wu and Schork, 2001).
- Les tensioactifs cationiques qui s'ionisent dans l'eau pour donner un cation organique. Ils peuvent présenter des propriétés anti-microbiennes. Ils sont généralement des sels d'ammoniums quaternaires, très souvent associés à un chlorure (Le Perchec, 1994).
- Les tensioactifs zwittérioniques qui possèdent à la fois une charge négative et une charge positive. Ils sont compatibles avec tous les autre tensioactifs et s'utilisent à tous les pH (Larpent, 1995).
- Les tensioactfs non ioniques qui ne présentent aucune charge lorsqu'ils sont dans un solvant polaire, et ce, quelque pH. Ils sont compatibles avec les autres types de tensioactifs et sont donc souvent utilisés en association (Hellsten, 1986; Host and Rocher, 2001).

Les tensioactifs peuvent également être classés par rapport à leur partie hydrophobe. Ils sont ainsi distingués : les tensioactifs hydrogénés, les surfactants lipidiques, les composés mésogènes, les tensioactifs perfluorés et les tensioactifs siliconés.

4 Les mousses

Une mousse se définit comme la dispersion d'un gaz dans une phase condensée liquide ou solidifiée. La formation des mousses est un processus que l'on observe régulièrement dans la nature quand un gaz est mélangé mécaniquement dans un liquide, comme la formation d'écume à la surface des vagues, un exemple de mousse liquide. Puis, les mousses solides sont plus difficiles à trouver dans la nature. En général, elles sont produites à partir du dégagement d'un gaz dans un milieu liquide à haute viscosité qui durcit pendant que le gaz s'échappe. On trouve d'exemples dans la vie quotidienne comme le pain ou la majorité des gâteaux.

Figure 23: Des exemples de mousses que sont dans la vie quotidienne.

4.1 Définition

Au sens strict, le terme de mousse désigne la dispersion d'un gaz dans un liquide. Si elle est dispersée dans un solide, on parle de mousse solide. La mousse solide est un cas particulier de solide cellulaire. Ce qui distingue une mousse solide d'un solide cellulaire, réside dans la formation du matériau. Pour avoir une mousse solide, il faut d'abord obtenir une mousse liquide, qui donnera une morphologie imposé par la minimisation de l'énergie de surface. Par contre, les solides cellulaires ne sont pas nécessairement fait à partir d'un état liquide, et peuvent donc avoir tout type de morphologie. Il est possible fabriquer un mousse métallique par frittage d'une poudre (Banhart, 2001). Également, selon Gibson and Ashby (1997), une mousse doit avoir une masse volumique inférieure à 0.3 g cm^{-3} pour être qualifiée de mousse.

4.2 Etapes de formation des mousses rigides

Afin d'obtenir une mousse solide, il doit y avoir un optimum entre l'expansion et le durcissement. La majeure difficulté réside dans le réglage des cinétiques du dégazage et de la polymérisation pour obtenir cet optimum (Figure 24). Si le gaz s'évapore trop vite, la structure collapse avant de durcir. Dans le cas contraire, si le durcissement est trop rapide, il n'y a pas de formation de cellules et on obtient une résine solide. Pour obtenir une mousse rigide quatre étapes se distinguent : l'induction, l'expansion, la polymérisation et le mûrissement.

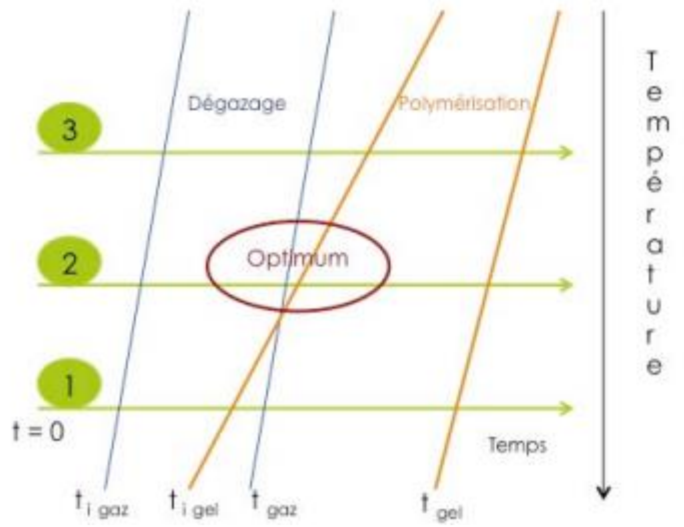

Figure 24: Représentation schématique des étapes successives d'évaporation et de polymérisation lors de la formation d'une mousse cellulaire.

Après le temps d'induction, le seuil d'activation est passé et le dégagement d'une proportion significative de gaz forme de nombreuses bulles. Cela implique l'expansion verticale de la mousse. La résine est encore liquide. Puis, les chaînes macromoléculaires réticulent pour former un réseau tridimensionnel autour des bulles. Cette étape est critique pour la stabilité de la mousse rigide future. Cette étape est déterminée par la vitesse de réticulation et le dégazage. Un optimum pour ces mécanismes est souhaitable qu'ils soient concomitants (Figure 24). Une fois la mousse formée et stabilisée mécaniquement, le point de gélification de la résine est passé mais la polymérisation n'est pas totalement finie. Le gaz va continuer de s'échapper à travers la mousse et celle-ci va sécher. Il est possible que certains bulles plus fines s'assemblent pour former de plus grandes bulles, plus stables. Ce phénomène se nomme le mûrissement d'Oswald.

Lors de la fabrication des mousses solides, plusieurs paramètres sont à prende en compte. Comme la gravité, la température, la pression, la viscosité, la rhéologie interfaciale, etc. Les temps de réactions dépendent de la pression, de la température, et des énergies d'activation des constituants (Bikard, 2009). Mais les moules utilisés sont également importants. Le type de moule peut affecter certaines caractéristiques de la mousse. Comme l'expansion et l'épaisseur de la peau de la mousse.

4.3 Organisation structurelle des cellules

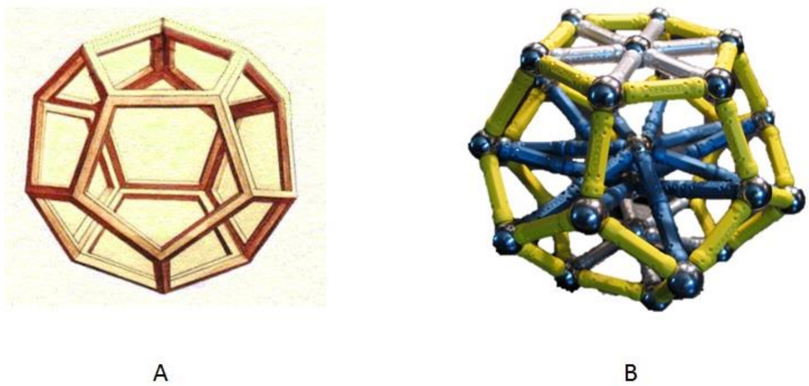

Figure 25: A. Dodécaèdre pentagonale. B. Tétrakaidécaèdre.

L'intérêt de modéliser ce type de système cellulaire est né au XIXème siècle. Un mathématicien belge, Joseph Plateau en 1873, fut l'un des pionniers dans l'impulsion de nombreuses études sur les mousses liquides. Il a identifié la forme des cellules comme rhombic dodecahedron et a permis décrire quatre principes fondamentaux. Mais études sur la distribution et la forme des différentes cellules dans une structure mousseuse statique ont été menées dans les années 90 (Weaire and Phelan, 1996). Ces études ont permis de comprendre que les cellules s'organisent selon une structure constituée par deux types de polyèdres : 2 dodecahedron pentagonal et 6 tétrakaidécaèdre (polyèdre formé par 12 pentagones et 2 hexagones).

Les conditions de Plateau s'énoncent :

1. Les bulles sont formés de surfaces lisses continues.
2. La courbure moyenne de chaque portion de paroi est constante
3. Les bulles s'intersectent en un point triple et forment un angle de 120ºC, cette intersection s'appelle « bord de Plateau ».
4. Quatre bords de Plateau se coupent sous un angle de 109.47º.

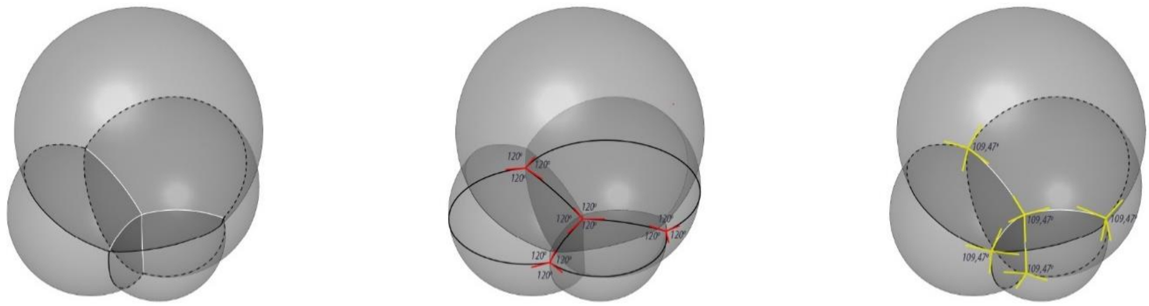

Figure 26: À gauche, premier et deuxième énoncé de Plateau. Au centre, troisième énoncé de Plateau. À droite, quatrième énoncé de Plateau.

Les configurations qui ne respectent pas les conditions de Plateau ne sont pas stables et tendent rapidement à se réarranger selon une configuration de Plateau.

4.4 Les mousses de tanins

Dans les années 90, Meikleham and Pizzi (1994) ont développé la mousse de tanin à travers de l'utilisation d'une résine tannin-formaldéhyde. Le moussage physique est assuré par la chaleur provenant de l'autocondensation de l'alcool furfurylique. Cette chaleur permet l'évaporation de l'éther diéthylique, un solvant à faible température d'ébullition. Suite à ces premières recherches, les mousses à base de tanins ont été et encore sont un sujet de recherche intéressant d'un point de vue écologique (Lacoste et al., 2014a, 2014b; Tondi and Pizzi, 2009).

Les mousses de tanins sont généralement développées suivant un processus de moussage physique. Diffèrentes réactions simultanées rentrent en jeu. L'autocondensation exothermique de l'alcool furfurylique permet l'augmentation de la température, qui permet l'évaporation de l'agent moussant. L'autocondensation des tanins intervient également avec la réaction entre le tanin et l'alcool furfurylique. L'ajout du formaldéhyde permet le durcissement du polymère en formation lors du moussage, augmentant la résistance mécanique de la mousse.

Depuis la formulation initiale, d'autres formulations de mousses de tanins ont été développées. Diffèrent types de tanins condensés ont été utilisé, comme le mimosa (*Acacia mearnsii*) (Tondi et al., 2009b), le quebracho (*Schinopsis lorentzii* et *balansae*) (Basso et al., 2015; Martinez de Yuso et al., 2014), et le pin (*Pinus radiata* (Lacoste et al., 2013a) et *Pinus pinaster* (Lacoste et al., 2014b)). Aussi, les mousses à base de tanins ont été préparés en utilisant différents types de moussage comme le moussage chimique (Basso et al., 2014b), le moussage physique (Basso et al., 2015; Li et al., 2013), les deux ensembles (Li et al., 2012b, 2012a) ou même des formulations sans agent de moussage (Basso et al., 2013a). De plus, des matériaux cellulaires ont également été obtenus par une méthode mécanique (Szczurek et al., 2014). Ensuite, pour améliorer les propriétés des mousses, différents agents de réticulation ont été étudiés dans des conditions acides, telles que le formaldéhyde (Tondi et al., 2009b), d'autres aldéhydes (Lacoste et al., 2013b) ou sans aucun d'entre eux (Basso et al., 2011). Des mousses dans des conditions alcalines ont également été développées (Basso et al., 2014a; Meikleham and Pizzi, 1994).

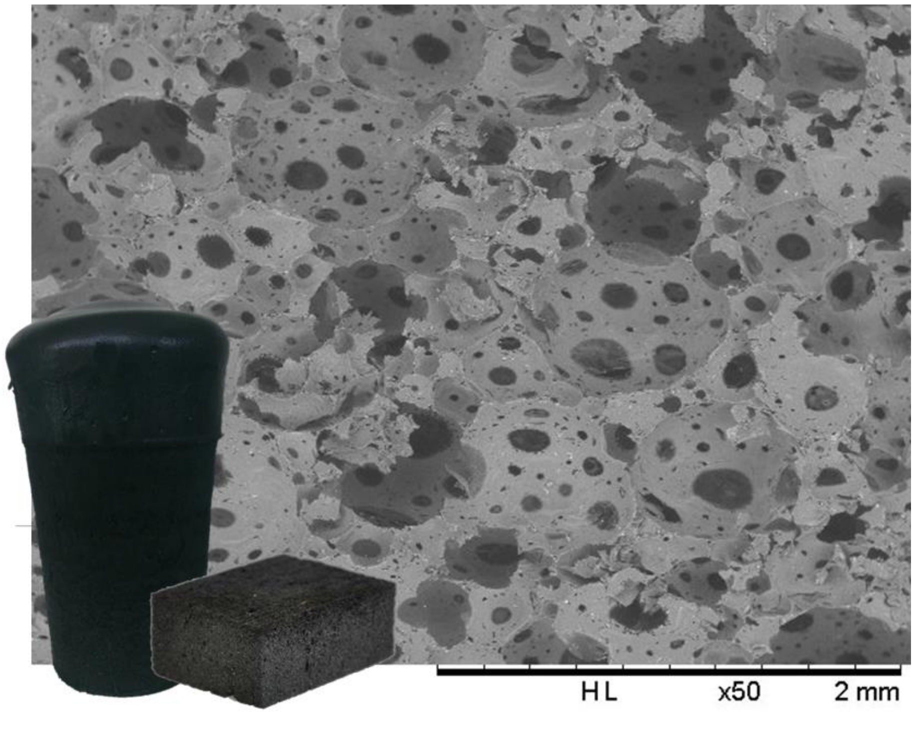

Figure 27: Mousses rigides à base de tanin.

4.4.1 Propriétés et applications

L'avantage majeur des mousses de tanins, en dehors du fait qu'elles soient d'origine biosourcée, est leur résistance exceptionnelle au feu (Meikleham and Pizzi, 1994). Les mousses de tanins ont des performances supérieures aux phénoliques, et cela sans ajout des retardateurs de flamme (Celzard et al., 2011). Le temps d'ignition est extrêmement long dans les mousses de tanins. Tondi et al. (2009b) ont mesuré que par un flux da chaleur de 50 $kW \cdot m^{-2}$, correspondant au flux dégagé lors d'un violent incendie, le temps d'ignition est supérieur à 100s pour les mousses de tanins. A titre comparatif, le temps d'extinction de mousses phénoliques commerciales a été estimé à 6s (Auad et al., 2007).

Les mousses de tanins sont considérés comme d'excellents isolants. Elles peuvent être employées directement à l'intérieur de panneaux en bois pour la construction sans que leur caractère acide affecte le bois (Tondi et al., 2008). Elles possèdent de très faibles conductivités thermiques, qui dépendent bien évidement des formulations mais qui peuvent descendre de 0.035 à 0.040 $W \cdot m^{-1} \cdot K^{-1}$ (Lacoste et al., 2013a; Li et al., 2013) et qui sont comparables aux mousses d'origine synthétique, et de possèdent de bonnes propriétés mécaniques. De plus, leurs bonnes performances acoustiques les placent comme des potentiels absorbants biosourcés, comparables à ceux disponibles actuellement sur le marché (Lacoste et al., 2015a).

En outre, les mousses à base de tanins peuvent être utilisées afin de dépolluer les eaux usées car ce sont de matériaux poreux qui sont capables d'absorber des ions métalliques (Cu ou Pb). Le type de tanin semble peut influencer la capacité d'absorption mais la structure cellulaire semble en revanche très significative (Tondi et al., 2009a). Ces mousses ont une grande capacité d'absorption des polluants anioniques et cationiques, comme le bleu de méthylène ou les produits pharmaceutiques. Ceci tout en ayant des propriétés comparables aux absorbants commerciaux (Sánchez-Martín et al., 2009, 2011b, 2011a, 2013).

Aussi, les mousses de tanins et phénoliques en général, possèdent une très bonne affinité avec l'eau et les solvants polaires (Tondi et al., 2009b). Ainsi, une application s'est révélée pour les mousses à base de tanins, remplacer les mousses florales synthétiques, généralement phénoliques. Avec cet objectif, il est possible de réaliser des mousses sans solvant, sans formaldéhyde, à porosité complètement ouverte (afin d'augmenter leur absorption de liquide) et en utilisant des catalyseurs alcalins (Basso et al., 2013a).

5 La lignine

Après la cellulose, la lignine est la substance organique polymère la plus abondance dans le monde (Fengel and Wegener, 1989). La lignine est un groupe de polymères phénoliques qui confèrent force et rigidité à la paroi cellulaire des plantes. La proportion de lignine varie entre 20-40% selon les espèces de plantes (Fengel and Wegener, 1989). La lignine peut être classée dans trois groupes principaux selon leur origine : les lignines de feuillus, les lignines de résineux et les lignines en provenance d'herbes (récoltes non-arborées ou herbacées) (Buranov and Mazza, 2008).

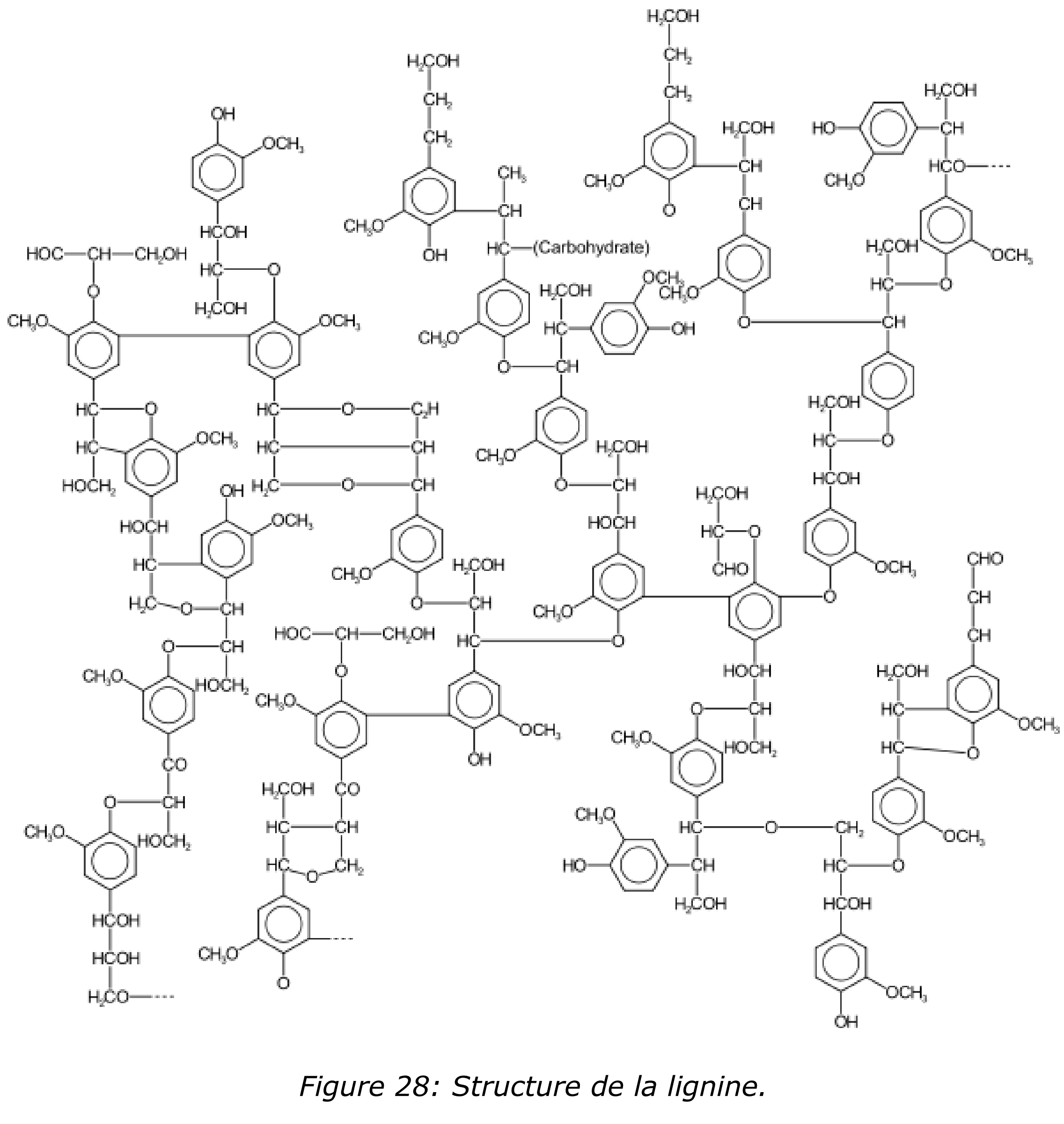

Figure 28: Structure de la lignine.

La composition de la lignine dépend de surcroît de facteurs, tels son âge et sa localisation dans la paroi cellulaire (Alonso, 2004). La formation de la lignine, sa structure et ses liaisons avec le reste de la paroi cellulaire demeurent difficilement explicables du fait de la grande hétérogénéité de polymères au niveau subcellulaire et le manque de méthode pour l'isolement non destructif de ce polymère (Radotic and Jeremic, 1998).

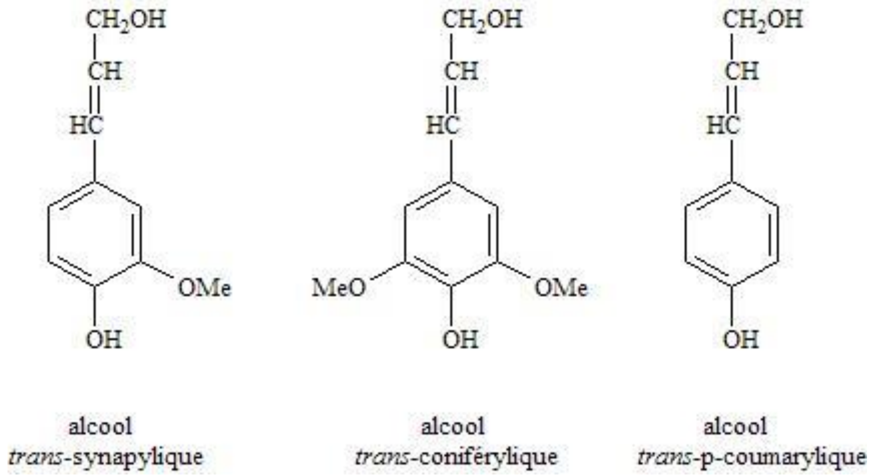

Figure 29: Les unités de base de la lignine.

La lignine est un polymère de type phénolique avec la présence de phénylpropane et des associations moléculaires bien définies (Jolivet et al., 2001) come l'alcool coniférylique, l'alcool sinapylique et l'alcool p-coumarylique (Figure 29). Ces associations font de la lignine un polymère naturel tridimensionnel comportant de nombreuses ramifications avec une quantité très importante de groupes fonctionnels qui renferment des centres actifs chimiques et biologiques (El Mansouri, 2006).

5.1 Formation de la lignine

La lignification est un processus qui débute au niveau de la lamelle moyenne au moment où la paroi secondaire s'épaissit, puis s'étend progressivement à l'ensemble des parois primaire et secondaires. La teneur en lignine est plus élevée dans la zone de la lamelle moyenne-paroi primaire dont l'épaisseur ne dépasse pas 1 μm (Brett and Waldron, 1990). Toutefois, la paroi secondaire, généralement très épaisse (1-5 μm), constitue l'essentiel de la masse des parois lignocellulosiques et contient la plupart des lignines de la plante. La lignification de la paroi cellulaire provoque la diffusion d'unités de phénylpropane, précurseurs de la lignine. Leur polymérisation commence par une déshydrogénation enzymatique (Figure 30) conduisant à la formation de radicaux phénoxy. A cause de la nature aléatoire de la réaction de polymérisation, il n'existe pas une structure définie pour la lignine.

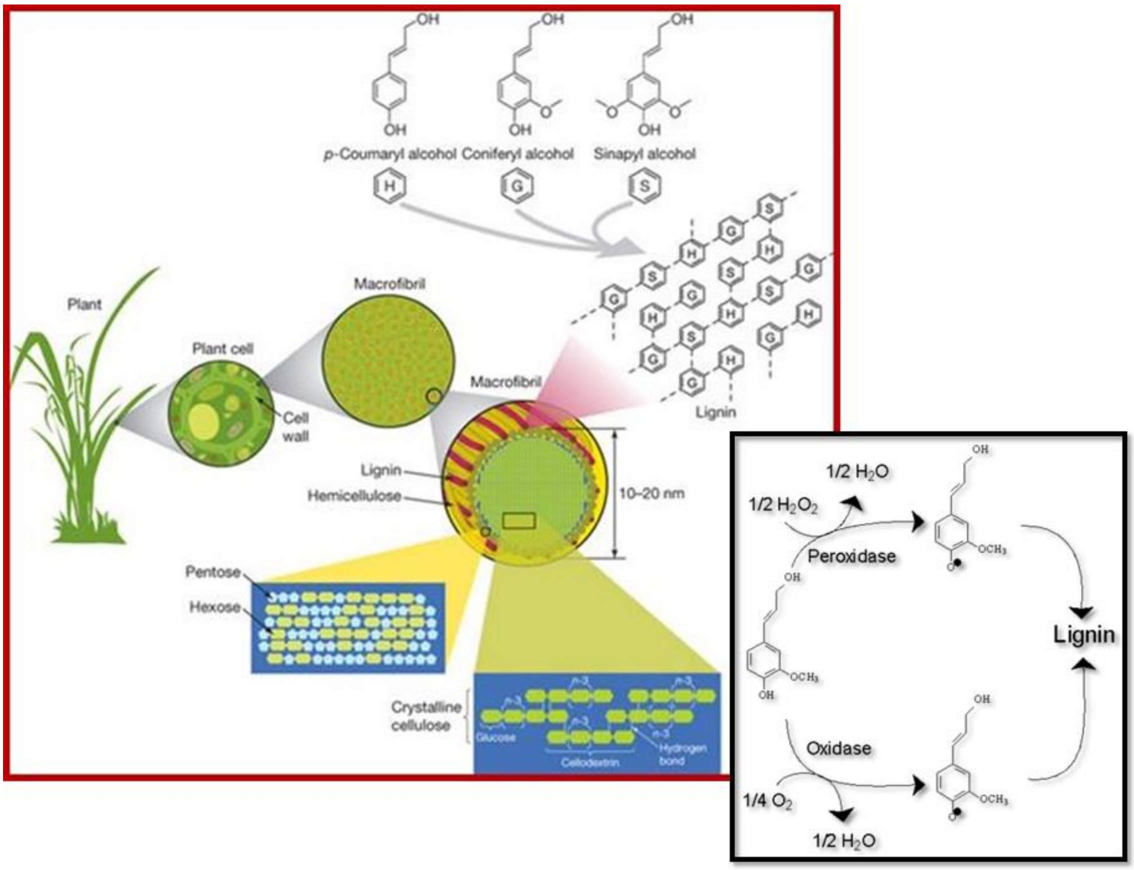

Figure 30: Déshydrogénation des monolignols par des peroxydases et des oxydases laccases à l'origine de la polymérisation de la lignine.

La polymérisation de la lignine s'effectue par radicalisation oxydative des phénols, suivie d'un couplage radicalaire combinatoire (Lapierre et al., 1995). La déshydrogénation des monolignols fait intervenir des peroxydases et/ou des laccases pour fournir la capacité oxydante dans la paroi cellulaire. Tous les composés phénoliques qui entrent dans la paroi cellulaire peuvent devenir des radicaux et ainsi s'incorporer dans le polymère de lignine en fonction de leur oxydation chimique et de leur propension au couplage (Wertz, 2010).

La lignine n'a pas de point de fusion, elle se ramollit entre 100 et 200ºC. Elle se décompose à partir de 270ºC. C'est un polymère thermoplastique qui peut être mis en œuvre avec la plupart des thermoplastiques pour faire des composites (Liu and Wang, 2010). Les propriétés physiques et chimiques de la lignine sont étroitement liées aux méthodes d'obtention, car elle est facilement modifiée par des composés chimiques d'où une variation très rapide de ses propriétés (El Hadji, 2008).

Dans les lignines se trouvent les groupes fonctionnels suivants :

- Hydroxyles phénoliques
- Hydroxyles aliphatiques
- Metoxiles
- Carbonyles
- Carboxyliques
- Sulfonates

5.2 Types de lignine

Selon le procédé d'obtention, les lignines peuvent être divisées en deux catégories (Gosselink et al., 2004) :

- Les lignosulfonates et les lignines Kraft, où le soufre a été utilisé pour leur obtention. Les lignines conventionnelles qui sont employées en industrie sont principalement obtenues à partir de bois de résineux.
- La deuxième catégorie correspond aux lignines sans soufre, comme traitement à la soude, procédé organosolv, par explosion à la vapeur ou de procédés de délignification par l'oxygène.

5.2.1 Lignine Kraft

La délignification se produit à travers l'action de NaOH et de Na_2S sur les liaisons éther de la molécule de lignine. La rupture de ces liaisons libère des groupes hydroxyles phénoliques en favorisant la dissolution de la lignine en milieu alcalin. Généralement, le processus de cuisson a lieu à une pression et temps entre 7-10 bar et 0.5-2h, respectivement, et à une température autour de 180ºC. La liqueur noire obtenue est concentrée dans des évaporateurs et le résidu est brulé pour produire énergie. Puis pour isoler la lignine Kraft, une méthode de précipitation acide en deux étapes est utilisée (Northey, 1992). La lignine Kraft est soluble en milieu aqueux basique ($pH>10.5$) et dans certains solvants organiques (Lin and Lin, 2000).

Figure 31: Lignine Kraft.

5.2.2 Lignosulfonate

Les lignosulfates sont produit par le procédé de sulfite pour la production de pâte à papier et il était historiquement le type le plus abondant de l'industrie de la lignine dans le marché. Dans la production de pâte au sulfite, de bois est chauffé à 140-170ºC avec une solution aqueuse de sulfite de sodium ou de le bisulfite, l'ammonium, le magnésium et le calcium. Le pH de la solution dépend du type, solubilité et caractéristiques de solubilité de dissociation du sel utilisé. Lors de processus de digestion en se produisant divers procédés chimiques, y compris la rupture des liaisons entre la lignine et les carbohydrates, la rupture de liaisons C-O d'interconnexion des unités lignine et la sulfonation des chaînes aliphatiques de lignine. Au cours de ce processus entre 4-8% de soufre est incorporée dans les molécules de lignine, la plupart sous forme de groupes sulfonate. Ce processus n'est pas sélectif pour l'élimination de la lignine, pour rendre plus pureté à la lignine doivent subir des processus de séparation ultérieurs (Chávez-Sifontes and Domine, 2013).

5.2.3 Lignine organosolv

Ces lignines sont obtenues à partir de la liqueur dans le processus de fabrication de la pâte de bois en utilisant des solvants organiques comme milieu de réaction. Dans ce cas, la lignine est précipitée dans un milieu aqueux après évaporation des solvants organiques (habituellement des alcools de bas poids moléculaire : méthanol ou éthanol). Le procédé de délignification avec des solvants organiques peut être catalysé en milieu acide ou basique, mais peut également être réalisée en l'absence de catalyseurs, mais elle nécessite des températures plus élevées. Le mécanisme de délignification en milieu basique se déroule par l'intermédiaire d'éther de rupture de liaison de type β–O-4, alors que le procédé en milieu acide provoque la rupture des liaisons de type α–O-4. Quelques procédés organosolvs développés sont organocell, acetosolv ou acetocell (Berg et al., 1995; Gottlieb et al., 1992), formacell (Nimz and Schone, 2000), milox et alcell.

5.3 Réactivité

Certaines caractéristiques de la lignine, telles que son hétérogénéité en lien avec sa distribution de poids moléculaire, la présence ou non de groupes fonctionnels et le type de liaison entre ses unités structurelles peuvent restreindre son utilisation (Gonçalves and Benar, 2001). La réactivité de la lignine est déterminée par sa structure particulière avec des groupes fonctionnels spécifiques et par ses modifications structurelles induites par les méthodes de séparation utilisées pour les différents matériaux. Cependant, il existe des traitements abondamment étudiés qui augmentent les sites actifs des lignines traditionnelles. Ces traitements sont : l'hydroxyméthylation (Benar et al., 1999), la phénolation (Ysbrandy et al., 1992), l'oxydation (Gonçalves and Benar, 2001), la diméthylation (Alonso et al., 2001, 2005; Chen, 1995), et la technique de fractionnement.

5.4 Applications

L'application principale de la lignine est son utilisation comme combustible pour la production d'énergie. Mais des colles à bois à base de lignine, sans formaldéhyde, ont satisfait aux conditions des normes internationales pour la fabrication de panneaux destinés à des utilisations intérieures et extérieures. Toutefois, pour l'utilisation commerciale de ces formulations, l'addition d'une colle synthétique comme une phénol-formaldéhyde ou un polymère isocyanate, comme PMDI, dans des quantités qui varient entre 20 et 40%, est nécessaire.

La lignine peut également être utilisée dans la production de biomatériaux, d'engrais, de charges pour peintures, vernis, colorants, émulsifiants, d'agents séquestrant, d'additifs dans l'asphalte ou sous forme de dispersants dans les ciments (Buranov and Mazza, 2008). Elle peut aussi être utilisée, comme liant dans les additifs alimentaires ou précurseur de la fabrication de la vanilline mais aussi dans les aliments pour animaux.

6 Les colles à bois/Les adhésif

L'industrie du bois emploie à l'heure actuelle quatre principales familles de colles thermodurcissables : les résines urée-formaldéhyde (UF), phénol-formaldéhyde (PF), mélanine-urée-formaldéhyde (MUF) et isocyanates. Chacune de ces résines correspond à un usage différent, principalement en fonction du besoin ou non de résister à l'humidité et/ou de répondre à plusieurs critères de résistance mécanique. Tous sont considérés comme des adhésifs synthétiques obtenus à partir du gaz naturel et du pétrole.

La plupart de ces colles synthétiques contiennent du formaldéhyde. Cependant, le formaldéhyde a été considérée jusqu'à maintenant comme cancérogène de catégorie 2 : « substance suspectées d'être cancérogènes pour l'être humain ». Il est désormais classé dans la catégorie 1B : « substance dont le potentiel cancérogène pour l'être humain est supposé par des données animales ». Ce changement a eu lieu le 1er avril 2015. Les acteurs de la recherche d'aujourd'hui se doivent de développer de nouveaux adhésifs plus respectueux de l'environnement et de la santé humaine.

L'utilisation industrielle des adhésifs organiques dérivés des produits de l'agriculture a débutée dès les années 1920. En plus d'une origine végétale, des adhésifs organiques peuvent également avoir une origine animale ou minérale. De nos jours, seuls les tanins et la lignine sont utilisés par l'industrie du bois et cela, en très faibles quantités. Pratiquement tous les tanins sont utilisés dans l'industrie du panneau. Et la lignine (organosolve et liqueur noire dérivée du procédé au sulfite en provenance des usines de papier) est employée comme co-réactif avec la colle PF commerciale pour ajouter une propriété spécifique à la résine.

6.1 Les panneaux de particules

Les panneaux de particules sont composés d'une ou plusieurs couches de particules de bois. Généralement, il y a trois couches : les couches extérieures sont composées de particules fines et la couche du milieu est composée quant à elle de particules plus grosses. Les taux d'encollage y sont également différents. Le taux d'encollage correspond à la quantité de résine utilisée par rapport à la quantité de particules. C'est donc le pourcentage de résine solide sur la masse particules anhydres. Les trois caractéristiques qui les définissent sont : une isotropie dans le plan, des caractéristiques mécaniques inférieures à celles du bois massif et un gonflement en épaisseur sous l'action de l'eau ou de l'humidité.

Les panneaux de particules sont définis par la norme NF EN 309. En France, deux labels de qualité existent : le panneau de particules CTB-S pour usage en milieu sec en construction répondant au moins au type P4 (selon la norme précédent), et le panneau de particules CTB-H répondant au moins au type P5. Leurs exigences sont données dans la norme NF EN 312.

Figure 32: Panneau de particules.

6.1.1 Les exigences de cohésion interne

La cohésion interne d'un panneau est sa résistance lorsqu'on applique une traction perpendiculaire à son plan. Cette valeur obtenue selon la norme (NF EN 319), généralement exprimée en N/mm^2, définit si le panneau satisfait aux exigences requises pour une application en tant que panneau travaillant en milieu sec ou humide.

La résistance à la traction perpendiculaire au plan de panneau de chaque éprouvette f_t est calculée selon la formule suivante :

$$f_t = \frac{F_{max}}{a \times b}$$

où :

F_{max} est la contrainte de rupture, en newton.

a, b sont la longueur et la largeur de l'éprouvette, en millimètre.

Pour un panneau travaillant en milieu sec (type P4), la valeur de cohésion interne doit être comprise entre 0.20 et 0.45 N/mm^2 et entre 0.25 et 0.5 N/mm^2 en milieu humide (type P5).

7 Références

Abdullah, U.H.B., Pizzi, A., 2013. Tannin-furfuryl alcohol wood panel adhesives without formaldehyde. Eur. J. Wood Wood Prod. 71, 131–132. doi:10.1007/s00107-012-0629-4

Abe, I., Funaoka, M., Kodama, M., 1987. Phenolic Nuclei of Condensed Tannins - Approaches by the phenyl mucleus-exchange method. Mokuzai Gakkaishi 33, 582–588.

Aguilar, R., Ramírez, J.A., Garrote, G., Vázquez, M., 2002. Kinetic study of the acid hydrolysis of sugar cane bagasse. J. Food Eng. 55, 309–318. doi:10.1016/S0260-8774(02)00106-1

Alonso, M.V., Oliet, M., Rodríguez, F., García, J., Gilarranz, M.A., Rodríguez, J.J., 2005. Modification of ammonium lignosulfonate by phenolation for use in phenolic resins. Bioresour. Technol. 96, 1013–1018. doi:10.1016/j.biortech.2004.09.009

Alonso, M.V., Rodríguez, J.J., Oliet, M., Rodríguez, F., García, J., Gilarranz, M.A., 2001. Characterization and structural modification of ammonic lignosulfonate by methylolation: Modification of Ammonic Lignosulfonate by Methylolation. J. Appl. Polym. Sci. 82, 2661–2668. doi:10.1002/app.2119

Alonso Rubio, M.V., 2004. Formulación y curado de resinas fenol-formaldehído tipo “resol” con parcial del fenol lignosulfonatos modificados. Universidad Complutense de Madrid, Madrid, España.

Aouf, C., Benyahya, S., Esnouf, A., Caillol, S., Boutevin, B., Fulcrand, H., 2014. Tara tannins as phenolic precursors of thermosetting epoxy resins. Eur. Polym. J. 55, 186–198. doi:10.1016/j.eurpolymj.2014.03.034

Auad, M.L., Zhao, L., Shen, H., Nutt, S.R., Sorathia, U., 2007. Flammability properties and mechanical performance of epoxy modified phenolic foams. J. Appl. Polym. Sci. 104, 1399–1407. doi:10.1002/app.24405

Ballerini, A., Despres, A., Pizzi, A., 2005. Non-toxic, zero emission tannin-glyoxal adhesives for wood panels. Holz Als Roh- Werkst. 63, 477–478. doi:10.1007/s00107-005-0048-x

Banhart, J., 2001. Manufacture, characterisation and application of cellular metals and metal foams. Prog. Mater. Sci. 46, 559–632. doi:10.1016/S0079-6425(00)00002-5

Basso, M.C., Giovando, S., Pizzi, A., Celzard, A., Fierro, V., 2013a. Tannin/furanic foams without blowing agents and formaldehyde. Ind. Crops Prod. 49, 17–22. doi:10.1016/j.indcrop.2013.04.043

Basso, M.C., Giovando, S., Pizzi, A., Lagel, M.C., Celzard, A., 2014a. Alkaline Tannin Rigid Foams. J. Renew. Mater. 2, 182–185. doi:10.7569/JRM.2013.634137

Basso, M.C., Lagel, M.C., Pizzi, A., Celzard, A., Abdalla, S., 2015. First Tools for Tannin-Furanic Foams Design. BioResources 10, 5233–5241. doi:10.1537/biores.10.3.5233-5241

Basso, M.C., Li, X., Fierro, V., Pizzi, A., Giovando, S., Celzard, A., 2011. Green, formaldehyde-free, foams for thermal insulation. Adv. Mater. Lett. 2, 378–382. doi:10.5185/amlett.2011.4254

Basso, M.C., Pizzi, A., Al-Marzouki, F., Abdalla, S., 2016. Horticultural/hydroponics and floral natural foams from tannins. Ind. Crops Prod. 87, 177–181. doi:10.1016/j.indcrop.2016.04.033

Basso, M.C., Pizzi, A., Celzard, A., 2013b. Dynamic Monitoring of Tannin-based Foam Preparation: Effects of Surfactant. BioResources 8. doi:10.15376/biores.8.4.5807-5816

Basso, M.C., Pizzi, A., Lacoste, C., Delmotte, L., Al-Marzouki, F., Abdalla, S., Celzard, A., 2014b. MALDI-TOF and 13C NMR Analysis of Tannin–Furanic–Polyurethane Foams Adapted for Industrial Continuous Lines Application. Polymers 6, 2985–3004. doi:10.3390/polym6122985

Benar, P., Gonçalves, A.R., Mandelli, D., Schuchardt, U., 1999. Eucalyptus organosolv lignins: study of the hydroxymethylation and use in resols. Bioresour. Technol. 68, 11–16. doi:10.1016/S0960-8524(98)00076-5

Berg, A., Janssen, W., Balle, S., Kunz, R.G., Klein, W., 1995. Delignification of cellulosic raw materials using acetic acid, nitric acid and ozone. US5385641A.
Bikard, J., 2009. Fabrication des mousses en polyuréthane. Tech. Ing.
Breitmaier, E., Voelter, W., 1990. Carbon-13 NMR spectroscopy: high-resolution methods and applications in organic chemistry and biochemistry, 3., completely rev. ed., reprint, corr. ed. VCH, Weinheim.
Brett, C., Waldron, K., 1990. Physiology and Biochemistry of Plant Cell Walls. Springer Netherlands : Imprint : Springer, Dordrecht.
Buranov, A.U., Mazza, G., 2008. Lignin in straw of herbaceous crops. Ind. Crops Prod. 28, 237–259. doi:10.1016/j.indcrop.2008.03.008
Cadahía, E., Conde, E., García-Vallejo, M.C., de Simón, B.F., 1996. Gel permeation chromatographic study of the molecular weight distribution of tannins in the wood, bark and leaves ofEucalyptus spp. Chromatographia 42, 95–100. doi:10.1007/BF02271062
Carneiro, A.C.O., Vital, B.R., Carvalho, A.M.M.L., Pereira, B.L.C., Andrade, B.G., 2010. Determinação da massa molar de taninos vegetais através da técnica da cromatografia de permeação em gel. Sci. For. 38, 419–429.
Carretero, M.E., 2000. Compuestos fenólicos: Taninos. Panor. Actual Medicam. 24, 633–636.
Celzard, A., Fierro, V., Amaral-Labat, G., Pizzi, A., Torero, J., 2011. Flammability assessment of tannin-based cellular materials. Polym. Degrad. Stab. 96, 477–482. doi:10.1016/j.polymdegradstab.2011.01.014
Celzard, A., Zhao, W., Pizzi, A., Fierro, V., 2010. Mechanical properties of tannin-based rigid foams undergoing compression. Mater. Sci. Eng. A 527, 4438–4446. doi:10.1016/j.msea.2010.03.091
Chávez-Sifontes, M., Domine, M.E., 2013. Lignina, estructura y aplicaciones: métodos de despolimerización para la obtención de derivados aromáticos de interés industrial. Avences En Cienc. E Ing. 4, 15–46.
Chen, C.M., 1995. Gluability of Kraft Lignin Copolymer Resins on Bonding Southern Pine Plywood. Holzforschung 49, 153–157. doi:10.1515/hfsg.1995.49.2.153
Chen, X., Li, H., Luo, H., Qiao, M., 2002. Liquid phase hydrogenation of furfural to furfuryl alcohol over Mo-doped Co-B amorphous alloy catalysts. Appl. Catal. Gen. 233, 13–20. doi:10.1016/S0926-860X(02)00127-8
Cheynier, V., Souquet, J.-M., Le Roux, E., Guyot, S., Rigaud, J., 1999. Size separation of condensed tannins by normal-phase high-performance liquid chromatography, in: Methods in Enzymology. Elsevier, pp. 178–184. doi:10.1016/S0076-6879(99)99018-3
Čop, M., Gospodarič, B., Kemppainen, K., Giovando, S., Laborie, M.-P., Pizzi, A., Sernek, M., 2015. Characterization of the curing process of mixed pine and spruce tannin-based foams by different methods. Eur. Polym. J. 69, 29–37. doi:10.1016/j.eurpolymj.2015.05.020
Delgado-Sánchez, C., Fierro, V., Li, S., Pasc, A., Pizzi, A., Celzard, A., 2017. Stability analysis of tannin-based foams using multiple light-scattering measurements. Eur. Polym. J. 87, 318–330. doi:10.1016/j.eurpolymj.2016.12.036
Donkin, M.J., Pearce, J., 1995. Tannin analysis by near infrared spectroscopy. J.-Soc. Leather Technol. Chem. 79, 8–11.
Drewes, S.E., Roux, D.G., 1963. Condensed tannins. 15. Interrelationships of flavonoid components in wattle-bark extract. Biochem. J. 87, 167–172.
El Hadji, B., 2008. Nouveaux matériaux composites thermoformables à base de fibres de cellulose. Université de Grenoble, France.
El Mansouri, N.E., 2006. Despolimerización de lignina para su aprovechamiento en adhesivos para producir tableros de partículas. Universitat Rovira i Virgili, Tarragona, España.

Fechtal, M., Riedl, B., 1993. Use of Eucalyptus and *Acacia mollissima* Bark Extract-Formaldehyde Adhesives in Particleboard Manufacture. Holzforschung 47, 349–357. doi:10.1515/hfsg.1993.47.4.349

Fengel, D., 1991. Chemical Studies on the Wood of Quebracho colorado. *(Schinopsis balansae* Engl.). Part 2. Investigations of the Lignin. Holzforschung 45, 395–401. doi:10.1515/hfsg.1991.45.6.395

Fengel, D., Wegener, G., 1989. Wood: chemistry, ultrastructure, reactions. de Gruyter, Berlin.

Foo, L.Y., 1983. Condensed Tannins: Preferential Substitution at the Interflavanoid Bond by Sulphite Ion.

Foo, L.Y., Hemingway, R.W., 1985. Condensed Tannins: Reactions of Model Compounds with Furfuryl Alcohol and Furfuraldehyde. J. Wood Chem. Technol. 5, 135–158. doi:10.1080/02773818508085184

Gandini, A., 1997. Furans in polymer chemistry. Prog. Polym. Sci. 22, 1203–1379. doi:10.1016/S0079-6700(97)00004-X

Garcia, R., Pizzi, A., 1998a. Polycondensation and autocondensation networks in polyflavonoid tannins. I. Final networks. J. Appl. Polym. Sci. 70, 1083–1091. doi:10.1002/(SICI)1097-4628(19981107)70:6<1083::AID-APP5>3.0.CO;2-K

Garcia, R., Pizzi, A., 1998b. Polycondensation and autocondensation networks in polyflavonoid tannins. II. Polycondensation versus autocondensation. J. Appl. Polym. Sci. 70, 1093–1109. doi:10.1002/(SICI)1097-4628(19981107)70:6<1093::AID-APP6>3.0.CO;2-J

Garcia, R., Pizzi, A., Merlin, A., 1997. Ionic polycondensation effects on the radical autocondensation of polyflavonoid tannins: An ESR study. J. Appl. Polym. Sci. 65, 2623–2633. doi:10.1002/(SICI)1097-4628(19970926)65:13<2623::AID-APP4>3.0.CO;2-D

Gardziella, A., Pilato, L.A., Knop, A., 2000. Phenolic Resins. Springer Berlin Heidelberg, Berlin, Heidelberg.

Gibson, L.J., Ashby, M.F., 1997. Cellular solids: structure and properties, 2. ed., 1. paperback ed. (with corr.), transferred to digital printing. ed, Cambridge solid state science series. Cambridge Univ. Press, Cambridge.

Gonçalves, A.R., Benar, P., 2001. Hydroxymethylation and oxidation of Organosolv lignins and utilization of the products. Bioresour. Technol. 79, 103–111.

Gosselink, R.J.A., de Jong, E., Guran, B., Abächerli, A., 2004. Co-ordination network for lignin—standardisation, production and applications adapted to market requirements (EUROLIGNIN). Ind. Crops Prod. 20, 121–129. doi:10.1016/j.indcrop.2004.04.015

Gottlieb, K., Preuss, A.W., Meckel, J., Berg, A., 1992. Acetocell pulping of spruce and chlorine-free bleaching. Presented at the Solvent Pulping Symposium Proceedings, Boston, pp. 35–39.

Grillet, A.M., Wyatt, N.B., Gloe, L.M., 2012. Polymer Gel Rheology and Adhesion, in: De Vicente, J. (Ed.), Rheology. InTech.

Haslam, E., 1989. Plant polyphenols: vegetable tannins revisited, Chemistry and pharmacology of natural products. Cambridge Univ. Pr, Cambridge.

Hellsten, E., 1986. The industrial applications of nonionic surfactants. Tenside Surfactants Deterg. 23, 337–341.

Hernes, P.J., Hedges, J.I., 2000. Determination of Condensed Tannin Monomers in Environmental Samples by Capillary Gas Chromatography of Acid Depolymerization Extracts. Anal. Chem. 72, 5115–5124. doi:10.1021/ac991301y

Hillis, W.E., Urbach, G., 1959. Reaction of polyphenols with formaldehyde. J. Appl. Chem. 9, 665–673. doi:10.1002/jctb.5010091207

Hoong, Y.B., Paridah, M.T., Luqman, C.A., Koh, M.P., Loh, Y.F., 2009. Fortification of sulfited tannin from the bark of Acacia mangium with phenol–formaldehyde for use as plywood adhesive. Ind. Crops Prod. 30, 416–421. doi:10.1016/j.indcrop.2009.07.012

Host, S., Rocher, M., 2001. Tensioactifs et oléagineux. ADEME 1, 81.

Hwang, J.W., Noh, S.M., Kim, B., Jung, H.W., 2015. Gelation and crosslinking characteristics of photopolymerized poly(ethylene glycol) hydrogels. J. Appl. Polym. Sci. 132, n/a-n/a. doi:10.1002/app.41939

Ikeda-Fukazawa, T., Ikeda, N., Tabata, M., Hattori, M., Aizawa, M., Yunoki, S., Sekine, Y., 2013. Effects of crosslinker density on the polymer network structure in poly- *N* , *N* -dimethylacrylamide hydrogels. J. Polym. Sci. Part B Polym. Phys. 51, 1017–1027. doi:10.1002/polb.23305

Jakobs, B., Breitzke, B., Stolz, M., Verzellino, R., 2005. Low foaming surfactant systems for industrial applications. SOFW J. 131, 63–68.

Jolivet, C., Guillet, B., Karroum, M., Andreux, F., Bernoux, M., Arrouays, D., 2001. Les phénols de la lignine et le 13C, traceurs de l’origine des matières organiques du sol. Comptes Rendus Académie Sci. - Ser. IIA - Earth Planet. Sci. 333, 651–657. doi:10.1016/S1251-8050(01)01673-1

Jurd, L., 1962. The hydrolyzable tannins, in: Wood Extractives and Their Significance to the Pulp and Paper Industries. Academic Press, New York and London, pp. 229–260.

Koumbi Mounanga, T., 2008. Tensioactifs antioxydants originaux pour la formulation de produits de préservation du bois. Université de Lorraine, Nancy.

Lacoste, C., Basso, M.-C., Pizzi, A., Celzard, A., Ella Ebang, E., Gallon, N., Charrier, B., 2015a. Pine (P. pinaster) and quebracho (S. lorentzii) tannin-based foams as green acoustic absorbers. Ind. Crops Prod. 67, 70–73. doi:10.1016/j.indcrop.2014.12.018

Lacoste, C., Basso, M.C., Pizzi, A., Laborie, M.-P., Celzard, A., Fierro, V., 2013a. Pine tannin-based rigid foams: Mechanical and thermal properties. Ind. Crops Prod. 43, 245–250. doi:10.1016/j.indcrop.2012.07.039

Lacoste, C., Basso, M.C., Pizzi, A., Laborie, M.-P., Garcia, D., Celzard, A., 2013b. Bioresourced pine tannin/furanic foams with glyoxal and glutaraldehyde. Ind. Crops Prod. 45, 401–405. doi:10.1016/j.indcrop.2012.12.032

Lacoste, C., Čop, M., Kemppainen, K., Giovando, S., Pizzi, A., Laborie, M.P., Sernek, M., Celzard, A., 2015b. Biobased foams from condensed tannin extracts from Norway spruce (Picea abies) bark. Ind. Crops Prod. 73, 144–153. doi:10.1016/j.indcrop.2015.03.089

Lacoste, C., Pizzi, A., Basso, M.-C., Laborie, M.-P., Celzard, A., 2014a. Pinus pinaster tannin/furanic foams: PART I. Formulation. Ind. Crops Prod. 52, 450–456. doi:10.1016/j.indcrop.2013.10.044

Lacoste, C., Pizzi, A., Laborie, M.-P., Celzard, A., 2014b. Pinus pinaster tannin/furanic foams: Part II. Physical properties. Ind. Crops Prod. 61, 531–536. doi:10.1016/j.indcrop.2014.04.034

Laib, A., Barou, O., Vico, L., Lafage-Proust, M.H., Alexandre, C., Rügsegger, P., 2000. 3D micro-computed tomography of trabecular and cortical bone architecture with application to a rat model of immobilisation osteoporosis. Med. Biol. Eng. Comput. 38, 326–332. doi:10.1007/BF02347054

Landrock, A.H., 1995. Handbook of plastic foams: types, properties, manufacture, and applications. Noyes Publications, Park Ridge, N.J., U.S.A.

Lapierre, C., Pollet, B., Rolando, C., 1995. New insights into the molecular architecture of hardwood lignins by chemical degradative methods. Res. Chem. Intermed. 21, 397–412. doi:10.1007/BF03052266

Larpent, C., 1995. Tensioatifs. Tech. Ing.

Le Perchec, P., 1994. Les molécules de la beauté, de l’hygiène et de la protection: une introduction à la science cosmétologique. Nathan, Paris.

Li, X., Basso, M.C., Braghiroli, F.L., Fierro, V., Pizzi, A., Celzard, A., 2012a. Tailoring the structure of cellular vitreous carbon foams. Carbon 50, 2026–2036. doi:10.1016/j.carbon.2012.01.004

Li, X., Basso, M.C., Fierro, V., Pizzi, A., Celzard, A., 2012b. Chemical Modification of Tannin/Furanic Rigid Foams by Isocyanates and Polyurethanes. Maderas Cienc. Tecnol. 0–0. doi:10.4067/S0718-221X2012005000001

Li, X., Basso, M.C., Fierro, V., Pizzi, A., Celzard, A., 2012c. Chemical Modification of Tannin/Furanic Rigid Foams by Isocyanates and Polyurethanes. Maderas-Cienc. Tecnol. 14, 257–265. doi:10.4067/S0718-221X2012005000001

Li, X., Essawy, H.A., Pizzi, A., Delmotte, L., Rode, K., Le Nouen, D., Fierro, V., Celzard, A., 2012d. Modification of tannin based rigid foams using oligomers of a hyperbranched poly(amine-ester). J. Polym. Res. 19. doi:10.1007/s10965-012-0021-4

Li, X., Pizzi, A., Lacoste, C., Fierro, V., Celzard, A., 2013. Physical Properties of Tannin/Furanic Resin Foamed With Different Blowing Agents. Bioresources 8, 743–752.

Lin, S.Y., Lin, I.S., 2000. Lignin, in: Wiley-VCH Verlag GmbH & Co. KGaA (Ed.), Ullmann's Encyclopedia of Industrial Chemistry. Wiley-VCH Verlag GmbH & Co. KGaA, Weinheim, Germany. doi:10.1002/14356007.a15_305

Liu, T., Wang, Q.W., 2010. Bio-Ethanol Lignin Waste/HDPE Composites: Preparation and Mechanical Properties. Adv. Mater. Res. 113–116, 606–609. doi:10.4028/www.scientific.net/AMR.113-116.606

Lorinc, A., 1974. Wetting and emulsifying power of solutions. Kolor. Ertesito 16, 11–12, 324–337.

Lunkenheimer, K., Malysa, K., Wienskol, G., Baranska, M., 2004. Method and procedure for swift characterization of foamability and foam stability. EP1416261 A2.

MacKintosh, F.C., Käs, J., Janmey, P.A., 1995. Elasticity of Semiflexible Biopolymer Networks. Phys. Rev. Lett. 75, 4425–4428. doi:10.1103/PhysRevLett.75.4425

Mansouri, H.R., Pizzi, A., 2006. Urea–formaldehyde–propionaldehyde physical gelation resins for improved swelling in water. J. Appl. Polym. Sci. 102, 5131–5136. doi:10.1002/app.24477

Mansouri, H.R., Thomas, R.R., Garnier, S., Pizzi, A., 2007. Fluorinated polyether additives to improve the performance of urea–formaldehyde adhesives for wood panels. J. Appl. Polym. Sci. 106, 1683–1688. doi:10.1002/app.26749

Martinez de Yuso, A., Lagel, M.C., Pizzi, A., Fierro, V., Celzard, A., 2014. Structure and properties of rigid foams derived from quebracho tannin. Mater. Des. 63, 208–212. doi:10.1016/j.matdes.2014.05.072

Masson, E., Merlin, A., Pizzi, A., 1996a. Comparative kinetics of induced radical autocondensation of polyflavonoid tannins. I. Modified and nonmodified tannins. J. Appl. Polym. Sci. 60, 263–269. doi:10.1002/(SICI)1097-4628(19960411)60:2<263::AID-APP14>3.0.CO;2-6

Masson, E., Pizzi, A., Merlin, A., 1996b. Comparative kinetics of the induced radical autocondensation of polyflavonoid tannins. III. Micellar reactions vs. cellulose surface catalysis. J. Appl. Polym. Sci. 60, 1655–1664. doi:10.1002/(SICI)1097-4628(19960606)60:10<1655::AID-APP18>3.0.CO;2-3

Masson, E., Pizzi, A., Merlin, M., 1997. Comparative kinetics of the induced radical autocondensation of polyflavonoid tannins. II. Flavonoid units effects. J. Appl. Polym. Sci. 64, 243–265. doi:10.1002/(SICI)1097-4628(19970411)64:2<243::AID-APP5>3.0.CO;2-R

Meikleham, N., Pizzi, A., Stephanou, A., 1994. Induced accelerated autocondensation of polyflavonoid tannins for phenolic polycondensates. I. 13C-NMR, 29Si-NMR, X-ray, and polarimetry studies and mechanism. J. Appl. Polym. Sci. 54, 1827–1845. doi:10.1002/app.1994.070541206

Meikleham, N.E., Pizzi, A., 1994. Acid- and alkali-catalyzed tannin-based rigid foams. J. Appl. Polym. Sci. 53, 1547–1556. doi:10.1002/app.1994.070531117

Merlin, A., Pizzi, A., 1996. An ESR study of the silica-induced autocondensation of polyflavonoid tannins. J. Appl. Polym. Sci. 59, 945–952. doi:10.1002/(SICI)1097-4628(19960207)59:6<945::AID-APP6>3.0.CO;2-P
Mori, F.A., 2000. Caracterização parcial dos taninos da casca e dos adesivos de três espécies de eucaliptos. Universidade Federal De Viçosa, Viçosa.
Muralidharan, D., 1997. Spectrophotometric analysis of catechins and condensed tannins using Ehrlich's reagent. J.-Soc. Leather Technol. Chem. 81, 231–233.
Nagaraja, B.M., Siva Kumar, V., Shasikala, V., Padmasri, A.H., Sreedhar, B., David Raju, B., Rama Rao, K.S., 2003. A highly efficient Cu/MgO catalyst for vapour phase hydrogenation of furfural to furfuryl alcohol. Catal. Commun. 4, 287–293. doi:10.1016/S1566-7367(03)00060-8
Nakagawa, K., Sugita, M., 1999. Spectroscopic characterisation and molecular weight of vegetable tannin. J.-Soc. Leather Technol. Chem. 83, 261–264.
Navarrete, P., 2011. Adhésifs naturels à base de tanin, tanin/lignine, et tanin/gluten pour la fabrication de panneaux de bois. Université Henri Poincaré Nancy 1, Épinal, France.
Navarrete, P., Mansouri, H.R., Pizzi, A., Tapin-Lingua, S., Benjelloun-Mlayah, B., Pasch, H., Rigolet, S., 2010. Wood Panel Adhesives from Low Molecular Mass Lignin and Tannin without Synthetic Resins. J. Adhes. Sci. Technol. 24, 1597–1610. doi:10.1163/016942410X500972
Nimz, H.H.H., Schone, M., 2000. Wood pulping with acetic acid with the addition of formic acid. US6139683A.
Northey, R.A., 1992. Low-Cost Uses of Lignin, in: Rowell, R.M., Schultz, T.P., Narayan, R. (Eds.), Emerging Technologies for Materials and Chemicals from Biomass. American Chemical Society, Washington, DC, pp. 146–175. doi:10.1021/bk-1992-0476.ch011
Osman, Z., Pizzi, A., 2002. Comparison of gelling reaction effectiveness of procyanidin tannins for wood adhesives. Holz Als Roh- Werkst. 60, 328–328. doi:10.1007/s00107-002-0289-x
Pasch, H., Pizzi, A., Rode, K., 2001. MALDI–TOF mass spectrometry of polyflavonoid tannins. Polymer 42, 7531–7539. doi:10.1016/S0032-3861(01)00216-6
Pine, D.J., Weitz, D.A., Zhu, J.X., Durian, D.J., Yodh, A., Kao, M., 1994. Diffusing-wave spectroscopy and interferometry. Macromol. Symp. 79, 31–44. doi:10.1002/masy.19940790105
Pizzi, A., 2016. Wood products and green chemistry. Ann. For. Sci. 73, 185–203. doi:10.1007/s13595-014-0448-3
Pizzi, A., 1994. Advanced wood adhesives technology. M. Dekker, New York.
Pizzi, A. (Ed.), 1983. Wood adhesives: chemistry and technology. M. Dekker, New York.
Pizzi, A., 1982. Condensed tannins for adhesives. Ind. Eng. Chem. Prod. Res. Dev. 21, 359–369. doi:10.1021/i300007a005
Pizzi, A., 1980. Tannin-Based Adhesives. J. Macromol. Sci. Part C 18, 247–315. doi:10.1080/00222358008081043
Pizzi, A., 1979. Sulphited tannins for exterior wood adhesives. Colloid Polym. Sci. 257, 37–40. doi:10.1007/BF01539014
Pizzi, A., 1978. Tannin-formaldehyde exterior wood adhesives through flavonoid B-ring cross linking. J. Appl. Polym. Sci. 22, 2397–2399. doi:10.1002/app.1978.070220831
Pizzi, A., 1977. Chemestry and technology of cold and thermosetting wattle tannin based wood adhesive. University of the Orange Free State, Orange, South Africa.
Pizzi, A., Meikleham, N., 1995. Induced accelerated autocondensation of polyflavonoid tannins for phenolic polycondensates. III. CP-MAS 13C-NMR of different tannins and models. J. Appl. Polym. Sci. 55, 1265–1269. doi:10.1002/app.1995.070550812
Pizzi, A., Meikleham, N., Dombo, B., Roll, W., 1995a. Autocondensation-based, zero-emission, tannin adhesives for particleboard. Holz Als Roh- Werkst. 53, 201–204. doi:10.1007/BF02716424

Pizzi, A., Meikleham, N., Stephanou, A., 1995b. Induced accelerated autocondensation of polyflavonoid tannins for phenolic polycondensates. II. Cellulose effect and application. J. Appl. Polym. Sci. 55, 929–933. doi:10.1002/app.1995.070550611
Pizzi, A., Mittal, K.L., 2003. Handbook of Adhesive Technology, Revised and Expanded. CRC Press.
Pizzi, A., Roux, D.G., 1978. Resorcinol/wattle flavonoids condensates for cold-setting adhesives. J. Appl. Polym. Sci. 22, 2717–2718. doi:10.1002/app.1978.070220929
Pizzi, A., Scharfetter, H.O., 1978. The chemistry and development of tannin-based adhesives for exterior plywood. J. Appl. Polym. Sci. 22, 1745–1761. doi:10.1002/app.1978.070220623
Pizzi, A., Stephanou, A., 1994a. A 13C NMR study of polyflavonoid tannin adhesive intermediates. I. Noncolloidal performance determining rearrangements. J. Appl. Polym. Sci. 51, 2109–2124. doi:10.1002/app.1994.070511302
Pizzi, A., Stephanou, A., 1994b. A 13C NMR study of polyflavonoid tannin adhesive intermediates. II. Colloidal state reactions. J. Appl. Polym. Sci. 51, 2125–2130. doi:10.1002/app.1994.070511303
Pizzi, A., Stephanou, A., 1993. On the chemistry, behavior, and cure acceleration of phenol–formaldehyde resins under very alkaline conditions. J. Appl. Polym. Sci. 49, 2157–2170. doi:10.1002/app.1993.070491212
Pizzi, A., Tekely, P., 1995. 13C-NMR of Zn2 acetate-induced autocondensation of polyflavonoid tannins for phenolic polycondensates. J. Appl. Polym. Sci. 56, 633–636. doi:10.1002/app.1995.070560512
Pizzi, A., Valenzuela, J., Westermeyer, C., 1993. Non-Emulsifiable, Water-Based, Mixed Diisocyanate Adhesive Systems for Exterior Plywood. Part II. Theory Application and Industrial Results. Holzforschung 47, 68–71. doi:10.1515/hfsg.1993.47.1.68
Plomley, K.F., 1966. Tannin-formaldehyde adhesives, Division of Forest Products Technological Paper. Commonwealth Scientific and Industrial Research Organization, Melbourne, Australia.
Porter, L.J., 1988. Flavans and proanthocyanidins, in: Harborne, J.B. (Ed.), The Flavonoids: Advances in Research since 1980. Springer US, Boston, MA, pp. 21–62. doi:10.1007/978-1-4899-2913-6_2
Radotic, K., Jeremic, M., 1998. Two pathways of lignin synthesis: a comparative study. Biblid 0021-3225 34, 491–501.
Rafati, R., Haddad, A.S., Hamidi, H., 2016. Experimental study on stability and rheological properties of aqueous foam in the presence of reservoir natural solid particles. Colloids Surf. Physicochem. Eng. Asp. 509, 19–31. doi:10.1016/j.colsurfa.2016.08.087
Robbins, C.T., Hanley, T.A., Hagerman, A.E., Hjeljord, O., Baker, D.L., Schwartz, C.C., Mautz, W.W., 1987. Role of Tannins in Defending Plants Against Ruminants: Reduction in Protein Availability. Ecology 68, 98–107. doi:10.2307/1938809
Rossouw, D. du T., 1979. Reaction kinetics of phenols and tannin with aldehydes. University of South Africa, Pretoria.
Rossouw, D. du T., Pizzi, A., McGillivray, G., 1980. The kinetics of condensation of phenolic polyflavonoid tannins with aldehydes. J. Polym. Sci. Polym. Chem. Ed. 18, 3323–3343. doi:10.1002/pol.1980.170181201
Roux, D.G., 1972. Recent advances in the chemistry and chemical utilization of the natural condensed tannins. Phytochemistry 11, 1219–1230. doi:10.1016/S0031-9422(00)90068-2
Roux, D.G., Ferreira, D., Botha, J.J., Garbutt, D.C.F., 1976. Heartwood extracts of the black wattle (Acacia mearnsii) as a possible source of resorcinol. Appl Polym 28, 1365–1376.
Roux, D.G., Ferreira, D., Hundt, H.K.L., Malan, E., 1975. Structure stereochemistry and reactivity of natural condensed tannins as basis for their extended industrial application. Appl Polym 28.

Roux, D.G., Paulus, E., 1961. Condensed tannins. 8. The isolation and distribution of interrelated heartwood components of Schinopsis Spp. Biochem. J. 78, 785–789.
Sánchez-Martín, J., Beltrán-Heredia, J., Carmona-Murillo, C., 2011a. Adsorbents from Schinopsis balansae: Optimisation of significant variables. Ind. Crops Prod. 33, 409–417. doi:10.1016/j.indcrop.2010.10.038
Sánchez-Martín, J., Beltrán-Heredia, J., Delgado-Regaña, A., Rodríguez-González, M.A., Rubio-Alonso, F., 2013. Adsorbent tannin foams: New and complementary applications in wastewater treatment. Chem. Eng. J. 228, 575–582. doi:10.1016/j.cej.2013.05.009
Sánchez-Martín, J., Beltrán-Heredia, J., Gibello-Pérez, P., 2011b. Adsorbent biopolymers from tannin extracts for water treatment. Chem. Eng. J. 168, 1241–1247. doi:10.1016/j.cej.2011.02.022
Sánchez-Martín, J., González-Velasco, M., Beltrán-Heredia, J., 2009. *Acacia mearnsii de Wild* Tannin-Based Flocculant in Surface Water Treatment. J. Wood Chem. Technol. 29, 119–135. doi:10.1080/02773810902796146
Sauget, A., Zhou, X., Pizzi, A., 2014. MALDI-ToF Analysis of Tannin-Resorcinol Resins by Alternative Aldehydes. J. Renew. Mater. 2, 186–200. doi:10.7569/JRM.2013.634138
Schofield, P., Mbugua, D.M., Pell, A.N., 2001. Analysis of condensed tannins: a review. Anim. Feed Sci. Technol., Tannins:Analysis and Biological Effects in Ruminant Feeds 91, 21–40. doi:10.1016/S0377-8401(01)00228-0
Sobisch, T., 1994. Solubilization inaqueous solutions of surfactant mixtures. Tenside Surfactants Deterg. 31, 36–38.
Soo Bae, Y., Malan, J.C.S., Karchesy, J.J., 1994. Sulfonation of Procyanidin Polymers: Evidence of Intramolecular Rearrangement and Aromatic Ring Substitution. Holzforschung 48, 119–123. doi:10.1515/hfsg.1994.48.2.119
Spina, S., Zhou, X., Segovia, C., Pizzi, A., Romagnoli, M., Giovando, S., Pasch, H., Rode, K., Delmotte, L., 2013a. Phenolic resin wood panel adhesives based on chestnut (*Castanea sativa*) hydrolysable tannins. Int. Wood Prod. J. 4, 95–100. doi:10.1179/2042645312Y.0000000020
Spina, S., Zhou, X., Segovia, C., Pizzi, A., Romagnoli, M., Giovando, S., Pasch, H., Rode, K., Delmotte, L., 2013b. Phenolic resin adhesives based on chestnut (*Castanea sativa*) hydrolysable tannins. J. Adhes. Sci. Technol. 27, 2103–2111. doi:10.1080/01694243.2012.697673
Szczurek, A., Fierro, V., Pizzi, A., Stauber, M., Celzard, A., 2014. A new method for preparing tannin-based foams. Ind. Crops Prod. 54, 40–53. doi:10.1016/j.indcrop.2014.01.012
Thébault, M., Pizzi, A., Dumarçay, S., Gerardin, P., Fredon, E., Delmotte, L., 2014. Polyurethanes from hydrolysable tannins obtained without using isocyanates. Ind. Crops Prod. 59, 329–336. doi:10.1016/j.indcrop.2014.05.036
Thompson, D., Pizzi, A., 1995. Simple 13C-NMR methods for quantitative determinations of polyflavonoid tannin characteristics. J. Appl. Polym. Sci. 55, 107–112. doi:10.1002/app.1995.070550111
Tondi, G., Oo, C.W., Pizzi, A., Trosa, A., Thevenon, M.F., 2009a. Metal adsorption of tannin based rigid foams. Ind. Crops Prod. 29, 336–340. doi:10.1016/j.indcrop.2008.06.006
Tondi, G., Pizzi, A., 2009. Tannin-based rigid foams: Characterization and modification. Ind. Crops Prod. 29, 356–363. doi:10.1016/j.indcrop.2008.07.003
Tondi, G., Pizzi, A., Olives, R., 2008. Natural tannin-based rigid foams as insulation for doors and wall panles. Maderas Cienc. Tecnol. 10, 219–227. doi:10.4067/S0718-221X2008000300005
Tondi, G., Zhao, W., Pizzi, A., Du, G., Fierro, V., Celzard, A., 2009b. Tannin-based rigid foams: A survey of chemical and physical properties. Bioresour. Technol. 100, 5162–5169. doi:10.1016/j.biortech.2009.05.055
Venter, P.B., Sisa, M., van der Merwe, M.J., Bonnet, S.L., van der Westhuizen, J.H., 2012. Analysis of commercial proanthocyanidins. Part 1: The chemical composition of

quebracho (Schinopsis lorentzii and Schinopsis balansae) heartwood extract. Phytochemistry 73, 95–105. doi:10.1016/j.phytochem.2011.10.006

Vieira, M.C., Lelis, R.C.C., Silva, B.C. da, Oliveira, G. de L., 2011. Tannin Extraction from the Bark of Pinus oocarpa var. oocarpa with Sodium Carbonate and Sodium Bisulfite. Floresta E Ambiente 18, 1–8. doi:10.4322/floram.2011.017

Wang, H., Han, X., Yu, C., Wang, Y., Ma, L., 2006. Antifoaming study on copolymer starch-PVA coated material. Zhongguo Turans Yu Feiliao 3, 31–34.

Watanabe, Y., Kabir, M.H., Gong, J., Furukawa, H., 2013. Nanoscale imaging of mesh size distribution in gel engineering materials with visual scanning microscopic light scattering, in: Varadan, V.K. (Ed.), . p. 86911C. doi:10.1117/12.2009094

Weaire, D., Phelan, R., 1996. The physics of foam. J. Phys. Condens. Matter 8, 9519–9524. doi:10.1088/0953-8984/8/47/055

Weitz, D.A., Zhu, J.X., Durian, D.J., Gang, H., Pine, D.J., 1993. Diffusing-wave spectroscopy: The technique and some applications. Phys. Scr. T49B, 610–621. doi:10.1088/0031-8949/1993/T49B/040

Wertz, J.L., 2010. La lignine. Note de synthèse (Document ValBiom-Gembloux AgroBio Tech).

Winter, H.H., 2002. The Critical Gel, in: Borsali, R., Pecora, R. (Eds.), Structure and Dynamics of Polymer and Colloidal Systems. Springer Netherlands, Dordrecht, pp. 439–470.

Wu, X.Q., Schork, F.J., 2001. Kinetics of miniemulsion polymerization of vinyl acetate with nonionic and anionic surfactants. J. Appl. Polym. Sci. 81, 1691–1699. doi:10.1002/app.1601

Ysbrandy, R.E., Sanderson, R.D., Gerischer, G.F.R., 1992. Adhesives from Autohydrolysis Bagasse Lignin, a Renewable Resource. Part I. The Physical Properties of Laminates made with Phenolated Lignin Novolacs. Holzforschung 46, 249–252. doi:10.1515/hfsg.1992.46.3.249

Zhang, X.., Macosko, C.., Davis, H.., Nikolov, A.., Wasan, D.., 1999. Role of Silicone Surfactant in Flexible Polyurethane Foam. J. Colloid Interface Sci. 215, 270–279. doi:10.1006/jcis.1999.6233

Zhao, W., Pizzi, A., Fierro, V., Du, G., Celzard, A., 2010. Effect of composition and processing parameters on the characteristics of tannin-based rigid foams. Part I: Cell structure. Mater. Chem. Phys. 122, 175–182. doi:10.1016/j.matchemphys.2010.02.062

Zhou, X., Pizzi, A., Sauget, A., Nicollin, A., Li, X., Celzard, A., Rode, K., Pasch, H., 2013. Lightweight tannin foam/composites sandwich panels and the coldset tannin adhesive to assemble them. Ind. Crops Prod. 43, 255–260. doi:10.1016/j.indcrop.2012.07.020

Deuxième partie : Résultats

Résultats

Les résultats des travaux effectués au cours de cette thèse sont présentés ci-après sous la forme de publications scientifique. Chacune comprend une introduction avec le contexte de la recherche effectuée, une description des techniques et méthodes utilisées pour mener l'enquête et des résultats proprement obtenus et leurs propres conclusions.

Cette partie organise les travaux de recherche réalisés en quatre sections:

- Différentiation des tanins en fonction des traitements subis lors de l'extraction.
  - Understanding and distinguishing condensed tannins with the same origin but influenced by sulfitation.
- Les réactions avec des tanins et la lignine.
  - Polycondensation resins by flavonoid tannins reaction with amines.
  - Polycondensation resins by lignin reaction with (poly)amines.
  - Isocyanate-free polyurethanes by coreaction of condensed tannins with aminated tannins.
  - Polyurethanes from kraft lignin without using isocyanates.
- Adhésifs de tanins pour panneaux de particules.
  - Lignin-derived non-toxic aldehydes for ecofriendly tannin adhesives for wood panels.
- Mousses projetables de tanin.
  - Mechanically blown wall-projected tannin-based foams.

1 « Understanding and distinguishing condensed tannins with the same origin but influenced by sulfitation ».

Auteurs: F.J. Santiago-Medina[1], C. Delgado-Sánchez[2], A. Pizzi[1,3], A. Celzard[2], V. Fierro[2], L. Delmotte[4], C. Vaulot[4].

[1] LERMAB, ENSTIB, University of Lorraine, Épinal, France.

[2] IJL, ENSTIB, University of Lorraine, Épinal, France.

[3] Department of Physics, King Abdulaziz Iniversity, Jeddah, Saudi Arabia.

[4] Material Science Institute of Mulhouse, UMR CNRS 7361, University of Haute Alsace, Mulhouse, France.

Résumé:

La sulfitation est l'un des traitements les plus anciens utilisés pour l'extraction des tanins Quebracho pour augmenter leur solubilité dans l'eau froide. Le sulfite de sodium est bien connu pour réagir avec le tanin sur les sites C2 et C4 des oligomères de tanin, conduisant à l'ouverture du cycle C du pyranhe hétérocycle ou à la fission des liaisons interflavanyl. On s'attend à ce que deux tanins sulfatés extraits selon le même procédé à partir de la même source aient la même structure et qu'ils présentent le même comportement. Cependant, on a observé que ces deux tanins de Quebracho extraits à part entière peuvent présenter des comportements différents, comme leurs réactivités, qui influent sur leur aptitude à certaines applications. Des techniques telles que le temps de gel, la microréologie et la réactivité moussante peuvent quantifier la différence de comportement, mais sans déterminer ses causes. Une autre technique, comme la chromatographie de perméation gel, détermine que la diminution de la distribution de masse moléculaire joue un rôle important dans les propriétés du tanin.

Submitted to *Proligno*

Understanding and distinguishing condensed tannins with the same origin but influenced by sulfitation

***Francisco José* SANTIAGO-MEDINA**[1]
PhD student – LERMAB, ENSTIB, University of Lorraine
Address: 27 rue Philippe Séguin, BP21042, 88051 Epinal, France
E-mail: francisco-jose.santiago-medina@univ-lorraine.fr

***Clara* DELGADO-SÁNCHEZ**
PhD student – IJL, ENSTIB, University of Lorraine
Address: 27 rue Philippe Séguin, BP21042, 88051 Epinal, France
E-mail: clara.delgado-sanchez@univ-lorraine.fr

***Antonio* PIZZI**
Prof. Dr. – LERMAB, ENSTIB, University of Lorraine, France
Department of Physics, King Abdulaziz Iniversity, Jeddah, Saudi Arabia
Address: 27 rue Philippe Séguin, BP21042, 88051 Epinal, France
E-mail: antonio.pizzi@univ-lorraine.fr

***Alain* CELZARD**
Prof. Dr. – IJL, ENSTIB, University of Lorraine
Address: 27 rue Philippe Séguin, BP21042, 88051 Epinal, France
E-mail: alain.celzard@univ-lorraine.fr

***Vanessa* FIERRO**
Dr. – IJL, ENSTIB, University of Lorraine
Address: 27 rue Philippe Séguin, BP21042, 88051 Epinal, France
E-mail: vanessa.fierro@univ-lorraine.fr

***Luc* DELMOTTE**
Dr. – Material Science Institute of Mulhouse, UMR CNRS 7361, University of Haute Alsace
Address: 15 rue Jean Starcky, BP2488, 68057 Mulhouse, France
E-mail: luc.delmotte@uha.fr

***Cyril* VAULOT**
Dr. – Material Science Institute of Mulhouse, UMR CNRS 7361, University of Haute Alsace
Address: 15 rue Jean Starcky, BP2488, 68057 Mulhouse, France
E-mail: cyril.vaulot@uha.fr

[1] Corresponding author at: LERMAB, University of Lorraine, 27 rue Philippe Seguin, BP21042, 88051 Épinal, France. Fax: +33 3 29 29 61 38. E-mail address: francisco-jose.santiago-medina@univ-lorraine.fr (F.J. Santiago-Medina), antonio.pizzi@univ-lorraine.fr (A. Pizzi).

ABSTRACT

Sulfitation is one of the oldest treatments used for the extraction of quebracho tannins to increase their solubility in cold water. Sodium sulfite is well-known to react with the tannin at the C2 and C4 sites of tannin oligomers, leading to the opening of the heterocycle pyran C-ring or to interflavanyl bond fission. Two sulphited tannins extracted according to the same process from the same source should be expected to have the same structure and thus, to present the same behavior. However, it has been observed that these two quebracho tannins extracted equally can exhibit different behaviors, as their reactivities, impinging on their suitability for certain applications. Techniques such as gel time, microrheology and foaming reactivity can quantified the difference in behavior, but without determining its causes. Other technique, such as Gel Permeation Chromathography determines that the decrease in molecular mass distribution plays an important role in the tannin properties.

KEYWORDS

GPC; Microrheology; Quebracho tannin; Reactivity; Sulfitation;

INTRODUCTION

Condensed tannins are natural polyphenolic compounds, which are attracting increasing interest for diverse industrial applications (Pizzi, 1994), such as wood adhesive (Abdullah and Pizzi, 2013; Navarrete et al., 2010; Pizzi, 1983, 1994). They are polyflavonoid oligomers mostly composed of flavan-3-ols repeating units linked by carbon-carbon bonds, and smaller amounts of polysaccharides and simple sugars (Schofield et al., 2001). They are extracted mainly from tree barks or wood.

Quebracho is commercial tannin extracted from the heartwood of either *Schinopsis lorentzii* (red “santiagueño” quebracho) from the western Chaco region of Argentina, Bolivia and Paraguay and *Schinopsis balansae* (red “chaqueno” quebracho) from the eastern Chaco region of Argentina. Usually, hot-water soluble quebracho is extracted under pressure with boiling water (around 130ºC) (Fengel, 1991; Venter et al., 2012). However, due to the relative solubility in water of the tannins extracted by this process and their high viscosity, the use of this tannin in certain applications can be difficult. Thus, to enhance its solubility and reduce its viscosity (Pizzi, 1982), a cold-water soluble quebracho is prepared by treating the hot-water soluble extract with bisulfite or by direct extraction of wood with a hot aqueous bisulfite solution. The treatment with bisulfite further increases the extraction yields when it is compared with just a hot water extraction.(Hoong et al., 2009; Vieira et al., 2011).

Sulfitation changes the physical properties of condensed tannins (Carneiro et al., 2010; Fechtal and Riedl, 1993; Hoong et al., 2009; Pizzi, 1979). It is for this reason that is of interest to study the molecular weight of quebracho tannin because several of its properties, which are important to the processability and application, are directly related to its molar mass. Gel permeation chromatography (GPC) is a method that provides information on molecular weight and molecular weight distribution of polymers, including tannins.

There activity of tannins is likely affected by sulfitation. Thus, this is a determinant parameter in tannins characterization due to its influence in their applicability. A direct indication of tannin reactivity is obtained by the gel time test. The gel time is defined as the point at which the polycondensates formed by the reaction of an aqueous tannins solution with formaldehyde become an elastic, rubbery solid. It is a rather simple test, easy and rapid to carry out. The gel time is strongly dependent on the pH of the solution (Pizzi, 1994). Conversely, passive microrheology is a technique that is increasingly used to investigate non-invasively the viscoelastic microstructure properties and the gel point transition for polymers and hydrogels. Passive microrheology consists of using micron size particles to measure the local deformation of a sample resulting from its thermal energy, that is to say the Brownian motion. There are several advantages in using this technique: it is rapid, highly sensitive, requires small sample volumes and minimizes the risk of altering the material microstructure since external forces are not applied.

The present work is aimed at attempting to discern between two commercial condensed tannins from the same source but presenting different reactivities and properties. Gel time test, microrheology test and gel permeation chromatography were used to identify what causes the difference in behavior of the two tannins, which their source and structure appeared to be identical.

MATERIALS AND METHODS

Materials

Two sulphited quebracho tannin powders with a polyphenolic content between 82% and 84%, hereinafter QL and QC respectively, were kindly supplied by the company SilvaChimica (St Michele Mondovi, Italy). They were used for their characterization using a number of different techniques. Sodium hydroxide pearls were supplied by Carlo Erba Reagents S.A.S. (France) and paraformaldehyde at 95% by EMD Millipore Corporation (USA). Phenol sulfonic acid was supplied by Capital Resin Corporation (USA). Furfuryl alcohol at 98%, ethylene glycol and Kolliphor ELP, namely ethoxylatedcastor oil were provided by Sigma-Aldrich.

Elemental analysis

The samples of elemental analyses were done with a CHONS elemental instrument (Vario El cube, Elementar, Germany) to determine their carbon (C), hydrogen (H), nitrogen (N), sulfur (S) and oxygen (O) contents. Based on the data obtained, the sulfonic acid content was also quantified according to Eq. (1).

$$F{:}S = \frac{\left[\frac{C\%}{12\times 15}\right]}{\left[\frac{S\%}{32}\right]} \text{ [mol/mol]} \qquad (1)$$

where: *F:S* is the molar ratio of flavon-3-ol unit and sulfonic acid group, in mol/mol;
C% is the weight percentage of carbon;
S% is the weight percentage of sulfur;
12 is the molar mass of carbon;
32 is the molar mass of sulfur;
15 is the number of carbon atoms in a flavon-3-ol unit.

Viscosity

A solution of 40% (w/w) tannin/water was prepared and its pH adjusted to 7 with a NaOH 33% water solution. The viscosity was measured at 25°C using a Brookfield viscometer RV with a spindle Nr. 21. The measure of viscosity was repeated 3 times for each tannin and the results averaged.

Gel permeation chromatography (GPC)

Relative molecular weights were determined by GPC in dimethylformamide (DMF) containing LiBr at a concentration of 0,01 mol/L at 50°C. Solutions of samples with concentrations of 5.00 mg/mL were prepared and filtered (PTFE membrane; 0.20 µm) before injection. The flow rate was 1.0 mL/min. The following Agilent 1100 Infinity series setup was used: a G1310A isocratic pump; a G1322A degasser; a G1329A auto-sampler; a G1316A thermostated column compartment equipped with set of Polymer Laboratories PL gel MIXED D columns (nominal particle size: 5 µm) composed of a guard column (50×7.5 mm) and two columns (300×7.5 mm); a G1314A variable wavelength detector; a G7800A multidetector suite equipped with a MDS refractive index detector. Conventional calibration was performed using a set of EasiVial poly(methyl methacrylate) standards. Agilent GPC/SEC software and multi-detector upgrade were used to determine molar masses values and distributions.

Gel time

10 g of a 45% (w/w) tannin water solution to which was added 5% of paraformaldehyde fine powder on tannin solid content were mixed in a test tube and placed in a water bath, which was maintained at boiling temperature (just below 100ºC) at normal atmospheric pressure. A wire spring was inserted in the test tube and rapidly moved up and down and the time to gelling is measured by stopwatch. The test was duplicated and the average value was reported. The pH of the tannin solutions was adjusted to 7 using a sodium hydroxide 33% water solution (NaOH). This is a standard FESYP (European Federation of Panels Manufacturers) test and is used extensively in Europe for wood adhesives (Pizzi and Tekely, 1995).

Foamat Test

The reactivity of both samples of quebracho tannin was tested by using them to prepare tannin rigid foams. The same formulation was used in both cases. This is: a solution containing 30 g of tannin, 24 g of furfuryl alcohol, 6 g of water, 2.2 g of ethylene glycol and 2 g of Kolliphor ELP were strongly stirred for some minutes until homogeneity. 7 g of phenol sulfonic acid was then added and mixed with the resin for 15 s. Finally, the catalyzed resin was poured into the chamber of a FOAMAT 281 foaming measuring equipment (FormatMesstechnik GmbH, Karlsruhe, Germany). This equipment measures and records simultaneously the expansion, hardening, and temperature and pressure variation during the foaming process. The chamber is composed by a carton cylinder set on the manometer sensor. The pressure generated by the expansion is measured by the force applied onto this metal plate sensor. A K-type thermocouple is immersed into the mixture and measures the temperature variation. The CMD-sensor measures the foam electrochemical properties during the transition from liquid to solid state. It is a dielectric polarization sensor composed of two comb-shaped electrodes disposed on a printed circuit in such a manner as to form a type of flat condenser at the bottom of the foaming chamber. Then, the contact is ensured by both (i) the blowing pressure right from the beginning and (ii) the direct correlation between the dielectric polarization negative slope and the rate of the molecular movements decrease in the resin due to the progress of cross-linking. The foam height is constantly monitored by an ultrasound sensor according to the pulse-echo method. The software “Mousse”, version 3.80, was used to collect and process the datas.

Microrheology studies.

The polycondensation of the two quebracho tannins was investigated by a non-contact (laser) microrheometer (Rheolaser™ model Rheolab 6, Formulaction), which follows the fluctuations of scattered light intensity on a limited volume of sample as a function of time. It provides information on the dynamics of the light-scattering particles, directly related to the viscoelastic properties (elastic modulus G’ and viscous G” shear modulus) of the material. The passive microrheology analysis is based on the Multi-Speckle Diffusing Wave Spectroscopy (MSDWS) (Pine et al., 1994; Weitz et al., 1993). This technique relates the Brownian motion, which is reported as the Mean Square Displacement (MSD) like a function of decorrelation time, thus like a function of frequency. A single measurement with Rheolaser™ Master is sufficient to scan all frequencies.

Microrheology. Sample preparation

A tannin 45% water solution was prepared, and its pH adjusted to 7 using very low proportions of solid sodium hydroxide (NaOH). 2 mL of 0.02 g TiO_2 nanoparticles (typical diameter 50 nm) suspended in water were added to each sample solution in order to record scattering in the tannin solution. The solution was then mixed with paraformaldehyde powder (5% by weight on solid tannin content). The final mixture was poured into a cylindrical glass tube (diameter 25 mm) and immediately placed in the sample holder of the Rheolaser™ preheated at 80°C. The samples were maintained at this temperature during 3 days whereas the MSD data were continuously recorded. The test was duplicated for each tannin solution and their average values reported.

RESULTS AND DISCUSSION

Gel time

The extractions of tannin can be done following different methods, as employing sulfite during the extraction to obtain cold water soluble quebracho tannin. When the extractions of tannin from the same type of source have been done using the same process, it is expected that the extracted tannins would show a very similar or practically identical behavior. However, it was found that between the two quebracho tannins studied, there was a considerable difference in reactivity. The gel time test is a very simple but useful test to evaluate the reactivity of tannin with an aldehyde under the same conditions. This test has been widely used as a standard test to evaluate wood adhesives reactivity because of its simplicity. The gel time results are gathered in the Table 1. These results showed that the solution of tannin with QC quebracho forms a gel around one minute faster than the solution with QL quebracho tannin. Indicating the low-reactivity of QL.

Table 1 – Results of gel time test for QC and QL

Sample	Gel time (pH=7) [s]	Gel time (by Foamat) [s]
QL	202 ±3	146 ±5
QC	144 ±4	56 ±3

Foaming process

The reactivity of both samples of tannin was also evaluated by using them in the formulation of standard foams. Fig. 1 shows the variation of the temperature and the height of the foam during foaming. The curves of temperatures and height present similar shapes with a temperature increase up to 104ºC. However, the induction, time from addition of the acid to start of foaming, happened latter when QL tannin was used. Almost 100s of difference were measured between the induction times of both quebracho tannins. Thus, the difference in reactivity between both tannins delays the onset of the foaming for QL tannin. This result along with the values obtained by gel time raises the question of why should this difference of reactivity between the two tannins exists.

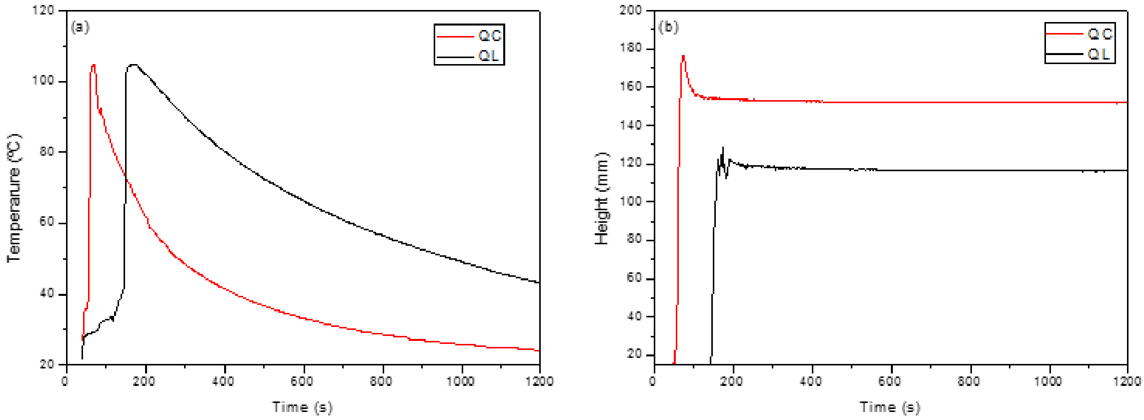

Fig. 1. a – Temperature and; b – height of tannin based foams from QL and QC as a function of time.

To explain the difference in reactivity, the two tannin extracts have been characterized by elemental analysis, GPC, FTIR, solid ^{13}C NMR, and MALDI-TOF. The result of the last three techniques are not shown in this work because they showed no difference between both tannins. Furthermore, a microrheology study allowed to confirm the difference in reactivity and to reveal some viscoelastic properties of the gel obtained.

Confirmation by microrheology. Gel time and properties of the gel formed.

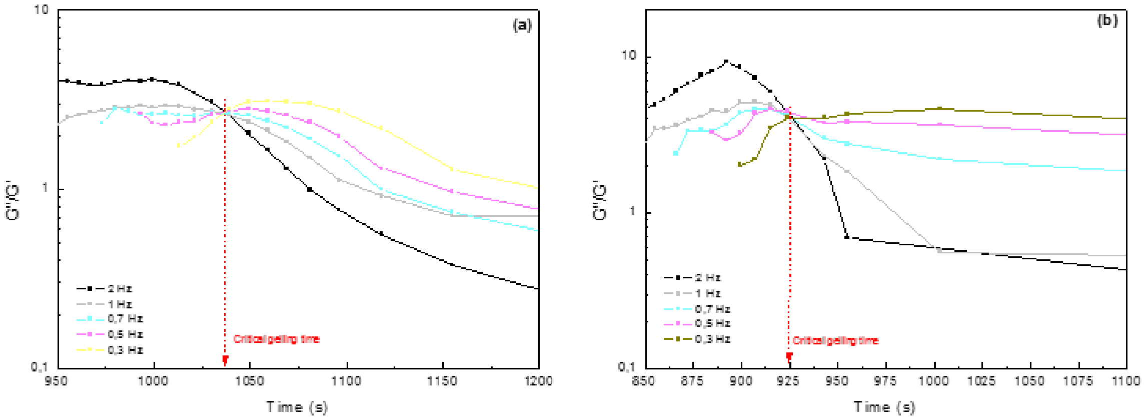

Fig. 2. Determination of critical gel point of a – QL and; b – Qc tannin.

The difference of reactivity can be confirmed by calculating the gel time using rheological parameters. For non-ideal gels wherein network defects or physical entanglements are present, the cross-over point depends on the applied frequency (Grillet et al., 2012). This is the case of the gels from the QL and QC tannins. Fig. 2 and Table 2 show both tannins gel points, as well as the viscoelastic parameters of the gels formed. At the critical gel point, the ratio of the shear moduli, G”/G’= tan(δ), is independent of the frequency. The critical gel point is the time when the curves of tan(δ) at various frequencies coincide (Winter, 2002) (Fig. 2). This clearly confirms the higher reactivity of QC, as previously found by the gel time test and foaming assays, showing around a 2 minutes shorter gel time than QL in its reaction with formaldehyde.

Table 2 – Critical gel point, viscosity and viscoelastic parameters of the gel formed (at 1 Hz) at pH=7.

Sample	Critical Gelling Time (s)	Viscosity (cP)		G’ (Pa)	G’’ (Pa)	G’’/G’	δ
		10 rpm	20 rpm				
QL	1038	1360±11	1230±8	70.7	12.6	0.178	10.11
QC	925	300±10	276±9	114	11.8	0.104	5.94

It is also interesting to study some of the viscoelastic properties of the gels. To obtain the viscoelastic parameters of the gels (Table 2), both gels have been compared at low frequencies (1Hz). As both gel and sol polymers are rearranging due to Brownian motion so the measured properties are dominated by the elastic deformation equilibrium of the gelled network. The viscoelastic parameters, and thus, the phase angle δ show the relative contribution of the liquid viscous part and the solid elastic part in the material in question. The viscoelastic results in Table 2 show that the QC gel is stiffer than the QL one because it has a higher elastic modulus and a smaller phase angle.

$$G' = \frac{k_B T}{\xi^3} \qquad (2)$$

A low frequency, the storage modulus G’ (ω) is related to the mesh size ξ that describes the average spacing between chains or the size of voids between filaments. The mesh size ξ decreases with the increasing concentration of chains. For a densely crosslinked gel, ξ is also the typical distance between crosslinks, and therefore entanglement points. The relation between these parameters is given by Eq. (2). Where k_B is the Boltzmann constant and T is the temperature of the sample (MacKintosh et al., 1995).

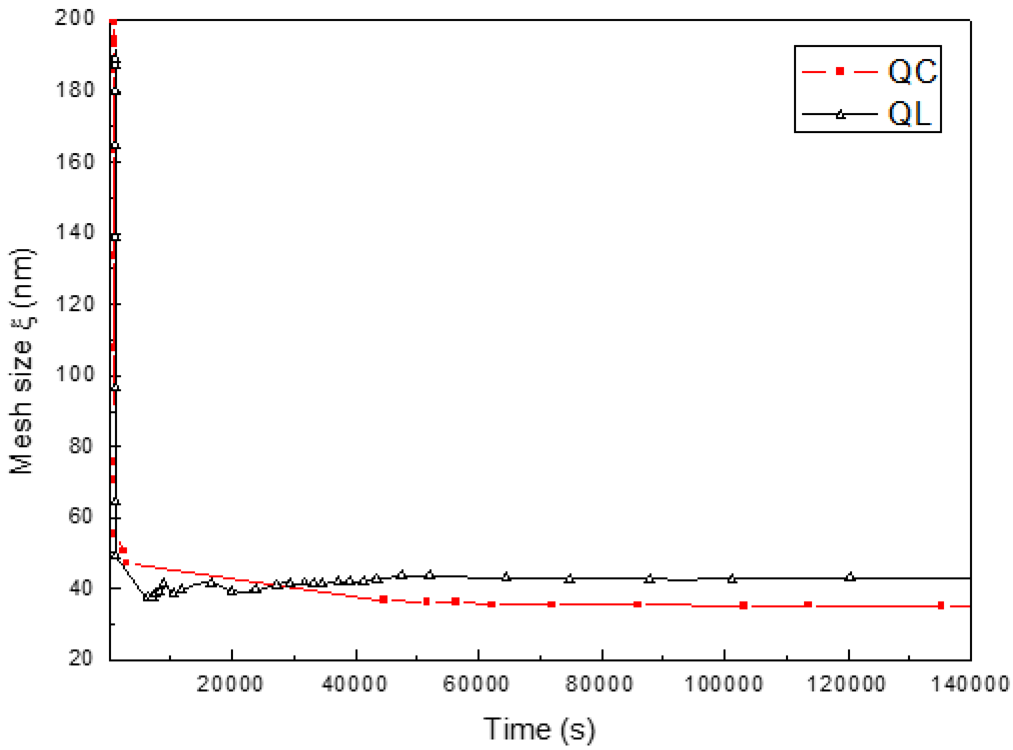

Fig. 3. Mesh size in function of the gelation time at 1 Hz.

This relation allows calculating the mesh size as a function of time (Fig. 3) and, especially, to get the value of the mesh size at the end of the process when the gel is stable. Fig. 3 shows that QC gel has a smaller mesh size than QL one. Thus, QC gel is more crosslinked than QL and therefore, the mechanical properties of the gel should be better (measures not taken) (Hwang et al., 2015; Ikeda-Fukazawa et al., 2013; Watanabe et al., 2013). This confirms what previously found about the viscoelastic parameters and that the QC gel is the toughest one.

GPC analysis

The determination of the relative distribution of the molecular weights of the flavonoid oligomer species was performed by GPC with a refractive index detector and a variable wavelength detector (results not shown). The GPC chromatograms (Fig. 4) show the refractive index detector response as a function of elution times of both tannins, and the different molecular mass averages are shown in Table 3. The GPC results show a narrow molecular weight distribution in the QC tannin, as it can be observed from its lower polydispersity, while the GPC chromatogram of the QL tannin displays a proportion of material at lower elution time. This means that in the QL quebracho tannin there is a range of oligomers of higher molecular weight than in the QC one, doing its average molecular weight higher (M_w=4158 g mol^{-1}) than for QC (M_w=3119 g mol^{-1}). In addition, the QC tannin shows two well-defined peaks in its chromatogram, the first one at 18.98 min, which coincide with the maximum of QL. Whereas the second one, at 20.01 min, should be attributed to monomers and structures of lower molecular weight generated by sulphitation, leading to a decrease in the average molecular weight of QC (Foo, 1983; Soo Bae et al., 1994). The absence of these heavier oligomers and the presence of a higher amount of lower molecules in QC decreases the degree of chain entanglement in this tannin. This allows an easier rearrangement of the molecules in solution, thus showing a lower viscosity (Table 2). But the decrease in the molecular weight due to sulfitation is not the only cause of the decrease in viscosity in QC tannin. As there are two further reasons which explain the decrease of viscosity. The sulfitation introduces a sulphonic acid group at the C2 or C4 position (Fig. 5) of the flavonoid causing increase solubility of the tannin in cold water due to the presence of a linked sulphonic acid group, which produces an increment in the polarity of the molecules. In addition, the inclusion of a sulphonic acid group at the C2 position opens the heterocyclic ring rendering the flavonoid unit much more flexible hence much more mobile and more accessible the most reactive parts of the tannin molecule, consequently increasing its reactivity (Foo, 1983; Pizzi, 1979).The sulfonic group is preferentially linked at the tannin C2 site because the terminal units in quebracho tannin, which present at least 82% of resorcinol unit as A-ring (Abe et al., 1987), are catechin or robitenidin units (Pasch et al., 2001; Pizzi, 1994).

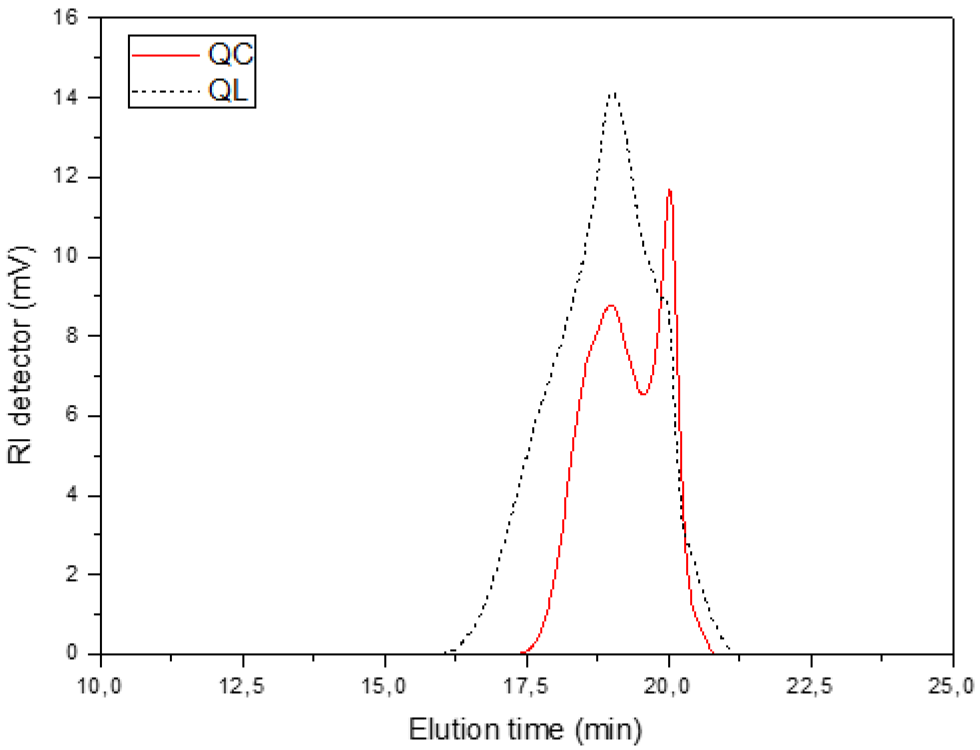

Fig. 4. GPC chromatograms of both quebracho tannins.

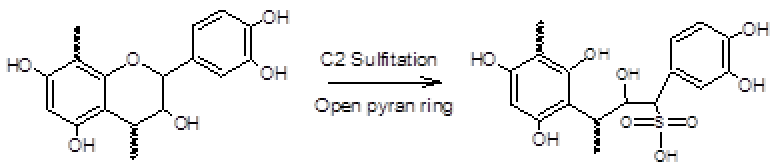

Fig. 5. Structure obtained by opening of the pyran ring.

Table 3 – Gel permeation chromatography results.

Sample	Mn	Mw	Mp	Mz	Mz+1	Mv	Mw/Mn=PD
QL	3039	4158	3462	5610	7228	5381	1,36
QC	2639	3119	1915	3646	4153	3569	1,18

Elemental analysis

The proportions of C, H, N and S as well as the F:S ratio obtained by elemental analysis are shown in Table 4. The F:S value is 7,16 for QC, while for QL the value is 40,37, indicating the higher sulfonic acid group content in polyflavonoids of QC. It means that QC tannins has five time more amount of sulfur than QL. The results obtained by elemental analysis indicate that the two quebracho tannins had different concentrations of sulfite during their extraction process. Moreover, this confirms previous research work where it was shown that the greater the degree of sulfitation, the lower the molecular weight of the tannin, and thus its polydispersity (Carneiro et al., 2010; Fechtal and Riedl, 1993; Mori, 2000).

Table 4 – Elemental component of condensed tannins in QC and QL.

Sample	N (wt%)	C (wt%)	H (wt%)	S (wt%)	O (wt%)	F:S (mol:mol)
QC	0.17	56.80	4.86	1.41	36.76	7.16
QL	0.20	56.77	5.04	0.25	37.74	40.37

CONCLUSIONS

Sulfitation is one of the most well-known processes used during the extraction of quebracho tannin. The variation of its concentration during this stage has demonstrated that produce changes in the chemical properties of condensed tannin through the modification of theirs physical properties. The introduction of a sulfonic acid group at the C2 site of tannin units causes the modification of the polarity and the structure of the tannin molecules, rendering molecules more soluble in polar solvents, increasing the flexibility of their structure and reducing the molecular weight of the tannin. Finally, these changes contribute to increase the reactivity of the tannin when it undergoes a greater degree of sulfitation during its extraction. This reactivity is easily measurable using a simple gel time test while the GPC analysis is confirmed as an excellent technique to determine differences between the molecular weights of condensed tannins. These two tannins can be used to prepare wood adhesives for particle boards and/or in the formulation of tannin rigid foams, where theirs different reactivity will affect directly to some parameters of the foam, as the induction time.

ACKNOWLEDGES

Thanks are due to Dr. Julien Poly for recording the GPC spectrum. The authors gratefully acknowledge the financing of the present research by a contract with the Pole of excellence Axelera and by LERMAB laboratory of the University of Lorraine.

REFERENCES

Abdullah, U.H.B. and Pizzi, A., (2013) Tannin-furfuryl alcohol wood panel adhesives without formaldehyde. Eur. J. Wood Wood Prod. **71**, 131–132.

Abe, I., Funaoka, M. and Kodama, M., (1987) Phenolic Nuclei of Condensed Tannins - Approaches by the phenyl mucleus-exchange method. Mokuzai Gakkaishi **33**, 582–588.

Carneiro, A.C.O., Vital, B.R., Carvalho, A.M.M.L., Pereira, B.L.C. and Andrade, B.G., (2010) Determinação da massa molar de taninos vegetais através da técnica da cromatografia de permeação em gel. Sci. For. **38**, 419–429.

Fechtal, M. and Riedl, B., (1993) Use of Eucalyptus and *Acacia mollissima* Bark Extract-Formaldehyde Adhesives in Particleboard Manufacture. Holzforschung **47**, 349–357.

Fengel, D., (1991) Chemical Studies on the Wood of Quebracho colorado. *(Schinopsis balansae* Engl.). Part 2. Investigations of the Lignin. Holzforschung **45**, 395–401.

Foo, L.Y., (1983) Condensed Tannins: Preferential Substitution at the Interflavanoid Bond by Sulphite Ion.

Grillet, A.M., Wyatt, N.B. and Gloe, L.M., (2012) Polymer Gel Rheology and Adhesion, in: De Vicente, J. (Ed.), Rheology. InTech.

Hoong, Y.B., Paridah, M.T., Luqman, C.A., Koh, M.P. and Loh, Y.F., (2009) Fortification of sulfited tannin from the bark of Acacia mangium with phenol–formaldehyde for use as plywood adhesive. Ind. Crops Prod. **30**, 416–421.

Hwang, J.W., Noh, S.M., Kim, B. and Jung, H.W., (2015) Gelation and crosslinking characteristics of photopolymerized poly(ethylene glycol) hydrogels. J. Appl. Polym. Sci. **132**, n/a-n/a.

Ikeda-Fukazawa, T., Ikeda, N., Tabata, M., Hattori, M., Aizawa, M., Yunoki, S. and Sekine, Y., (2013) Effects of crosslinker density on the polymer network structure in poly- *N* , *N* - dimethylacrylamide hydrogels. J. Polym. Sci. Part B Polym. Phys. **51**, 1017–1027.

MacKintosh, F.C., Käs, J. and Janmey, P.A., (1995) Elasticity of Semiflexible Biopolymer Networks. Phys. Rev. Lett. **75**, 4425–4428.

Mori, F.A., (2000) Caracterização parcial dos taninos da casca e dos adesivos de três espécies de eucaliptos.

Navarrete, P., Mansouri, H.R., Pizzi, A., Tapin-Lingua, S., Benjelloun-Mlayah, B., Pasch, H. and Rigolet, S., (2010) Wood Panel Adhesives from Low Molecular Mass Lignin and Tannin without Synthetic Resins. J. Adhes. Sci. Technol. **24**, 1597–1610.

Pasch, H., Pizzi, A. and Rode, K., (2001) MALDI–TOF mass spectrometry of polyflavonoid tannins. Polymer **42**, 7531–7539.

Pine, D.J., Weitz, D.A., Zhu, J.X., Durian, D.J., Yodh, A. and Kao, M., (1994) Diffusing-wave spectroscopy and interferometry. Macromol. Symp. **79**, 31–44.

Pizzi, A., (1979) Sulphited tannins for exterior wood adhesives. Colloid Polym. Sci. **257**, 37–40.

Pizzi, A., (1982) Condensed tannins for adhesives. Ind. Eng. Chem. Prod. Res. Dev. **21**, 359–369.

Pizzi, A. (Ed.), (1983) Wood adhesives: chemistry and technology. M. Dekker, New York.

Pizzi, A., (1994) Advanced wood adhesives technology. M. Dekker, New York.

Pizzi, A. and Tekely, P., (1995) 13C-NMR of Zn2 acetate-induced autocondensation of polyflavonoid tannins for phenolic polycondensates. J. Appl. Polym. Sci. **56**, 633–636.

Schofield, P., Mbugua, D.M. and Pell, A.N., (2001) Analysis of condensed tannins: a review. Anim. Feed Sci. Technol., Tannins:Analysis and Biological Effects in Ruminant Feeds **91**, 21–40.

Soo Bae, Y., Malan, J.C.S. and Karchesy, J.J., (1994) Sulfonation of Procyanidin Polymers: Evidence of Intramolecular Rearrangement and Aromatic Ring Substitution. Holzforschung **48**, 119–123.

Venter, P.B., Sisa, M., van der Merwe, M.J., Bonnet, S.L. and van der Westhuizen, J.H., (2012) Analysis of commercial proanthocyanidins. Part 1: The chemical composition of quebracho (Schinopsis lorentzii and Schinopsis balansae) heartwood extract. Phytochemistry **73**, 95–105.

Vieira, M.C., Lelis, R.C.C., Silva, B.C. da and Oliveira, G. de L., (2011) Tannin Extraction from the Bark of Pinus oocarpa var. oocarpa with Sodium Carbonate and Sodium Bisulfite. Floresta E Ambiente **18**, 1–8.

Watanabe, Y., Kabir, M.H., Gong, J. and Furukawa, H., (2013) Nanoscale imaging of mesh size distribution in gel engineering materials with visual scanning microscopic light scattering, in: Varadan, V.K. (Ed.), . p. 86911C.

Weitz, D.A., Zhu, J.X., Durian, D.J., Gang, H. and Pine, D.J., (1993) Diffusing-wave spectroscopy: The technique and some applications. Phys. Scr. **T49B**, 610–621.

Winter, H.H., (2002) The Critical Gel, in: Borsali, R., Pecora, R. (Eds.), Structure and Dynamics of Polymer and Colloidal Systems. Springer Netherlands, Dordrecht, pp. 439–470.

2 « Polycondensation resins by flavonoid tannins reaction with amines »

Auteurs: F.J. Santiago-Medina[1], A. Pizzi[1,2], M.C. Basso[1], L. Delmotte[3] et A. Celzard[4].

[1] LERMAB, University of Lorraine, 27 rue Philippe Seguin, 88000 Épinal, France.

[2] Department of Physics, King Abdulaziz University, 21589 Jeddah, Saudi Arabia.

[3] Material Science Institute of Mulhouse, CNRS LRC 7228, 15 rue Jean Starcky, BP 2488, 68057 Mulhouse Cedex, France.

[4] IJL, University of Lorraine, 27 rue Philippe Seguin, 88000 Épinal, France.

Résumé :

La réaction d'un tanin flavonoïde condensé, à savoir l'extrait de tanin de mimosa avec une hexaméthylène diamine, a été étudiée. À cette fin, la catéchine a également été utilisée comme composé modèle flavonoïde et traitée dans les mêmes conditions. Les études de résonance magnétique nucléaire (^{13}C NMR) et les études de spectroscopie de masse de l'ionisation de désorption par laser assistée par matrice (MALDI-ToF) ont révélé que des composés de polycondensation conduisant à des résines ont été obtenus par réaction des amines avec les goupes hydroxy phénoliques du tanin. Simultanément, une deuxième réaction conduisant à la formation de liaisons ioniques entre les deux groupes s'est produite. Ces nouvelles réactions ont montré qu'ils conduisent clairement à la réaction de plusieurs groupes hydroxyle phénoliques et à l'oligomérisation des unités de flavonoïdes, pour former des résines durcies.

Published by *Polymers*

polymers

MDPI

Article

Polycondensation Resins by Flavonoid Tannins Reaction with Amines

Francisco-Jose Santiago-Medina [1], Antonio Pizzi [1,2,*], Maria Cecilia Basso [1], Luc Delmotte [3] and Alain Celzard [4]

1 LERMAB, University of Lorraine, 27 rue Philippe Seguin, 88000 Epinal, France; francisco-jose-santiago-medina@univ-lorraine.fr (F.-J.S.-M.); cecilia-c-c@hotmail.com (M.C.B.)
2 Department of Physics, King Abdulaziz University, 21589 Jeddah, Saudi Arabia
3 Institut de Science des Matériaux de Mulhouse, CNRS LRC 7228, 15, rue Jean Starcky, BP 2488, 68057 Mulhouse Cedex, France; luc.delmotte@uha.fr
4 Institute Jean Lamour, University of Lorraine, 27 rue Philippe Seguin, 88000 Epinal, France; alain.celzard@univ-lorraine.fr
* Correspondence: antonio.pizzi@univ-lorraine.fr; Tel.: +33-62-312-6940

Academic Editor: Naozumi Teramoto
Received: 6 December 2016; Accepted: 20 January 2017; Published: 25 January 2017

Abstract: Reaction of a condensed flavonoid tannin, namely mimosa tannin extract with a hexamethylene diamine, has been investigated. For that purpose, catechin was also used as a flavonoid model compound and treated in similar conditions. Solid-state cross-polarisation/magic-angle spinning (CP-MAS) carbon 13 nuclear magnetic resonance (^{13}C NMR) and matrix assisted laser desorption ionisation time of flight (MALDI-ToF) mass spectroscopy studies revealed that polycondensation compounds leading to resins were obtained by the reaction of the amines with the phenolic hydroxy groups of the tannin. Simultaneously, a second reaction leading to the formation of ionic bonds between the two groups occurred. These new reactions have been shown to clearly lead to the reaction of several phenolic hydroxyl groups, and flavonoid unit oligomerisation, to form hardened resins.

Keywords: flavonoid tannin amines reactions; oligomers distribution; resins; MALDI-ToF; CP-MAS ^{13}C NMR

1. Introduction

Condensed polyflavonoid tannin extracts are mostly composed of flavan-3-ols repeating units and smaller fractions of polysaccharides and simple sugars [1]. The repeating units are linked to each other by C4–C6 or C4–C8, the former predominating in tannins in which fisetinidin (resorcinol A-ring; catechol B-ring) and robinetinidin (resorcinol A-ring; pyrogallol B-ring) are the predominant repeating units. While the reactions of these natural oligomeric materials have been used extensively to give polycondensates with aldehydes [2], even reactions of self-condensation have been studied and shown to lead to useful physically and chemically crosslinked networks [3–7].

Reactions of amination of phenols are well known, with the original approach to this reaction being by metal catalysis [8,9]. More recently, direct amination of phenols without the use of a metal catalyst has come to the fore and gained interest and importance [10,11].

Reactions of amination of flavonoid tannins to convert part of the phenolic hydroxyl groups of the B-ring to –NH_2 have been studied before [12–14]; they have been exclusively with ammonia, although the literature on this is limited to just three articles [12–14]. There appear to be no references on the reaction of amines, diamines, or polyamines with condensed tannins in the relevant literature. The oldest of the articles on the ammonia reaction with flavonoid tannins was aimed to even more efficiently bind formaldehyde gas emitted from tannin adhesive resins for wood panels [12]. In this study, amination of pyrogallol B-rings of condensed tannins to form 4′-amino-3′,5′-dyhydroxybenzene type B-rings by NH_3 treatment was described. The amination of the pyrogallol B-ring by NH_3/water is a regioselective amino-substitution of phenolic hydroxyl groups and proceeds under relatively mild conditions without a catalyst [12–14]. While early reports indicated that only one hydroxy group of the flavonoid B-ring is aminated [12], later work showed that multiamination also proceeds with relative ease [14], mainly to prepare carbonized materials richer in nitrogen. These amination reactions, however, did not appear to lead to long oligomers and finally to crosslinked resins. To obtain then polycondensation resins without the use of any aldehyde, the reaction of condensed tannins with a diamine were investigated in the work presented here. The aim of this work was to obtain thermoset resins having a very rapid initial gelling either (i) by using only amines and polyamines as the only hardener; or (ii) to use two hardeners, of which the amine was the one giving just the initial immobilization of the resin—for example, for spray-projected coatings to avoid initial running down on vertical walls.

The reactions of diamines with condensed tannin to form resins were investigated here, using first catechin as a flavonoid model compound, followed by the same reactions on a condensed tannin analysed by extensive MALDI-ToF spectroscopy and solid-state cross-polarisation/magic-angle spinning (CP-MAS) ^{13}C NMR studies. The findings are presented in this article.

2. Materials and Methods

2.1. Materials and Reactions

Catechin crystals (purity > 98%, high pressure liquid chromatography (HPLC) quality) was supplied by Sigma Aldrich (St. Louis, MO, USA) as (+)-catechin hydrate. Tannin extract was a commercial product, namely mimosa tannin extracted from barks of *Acacia mearnsii* (De Wild), supplied by SilvaChimica (St Michele Mondovi, Italy). It contained 80%–82% of actual phenolic flavonoid materials, 4%–6% of water, 1% of amino and imino acids, with the remainder being monomeric and oligomeric carbohydrates, generally broken pieces of hemicelluloses (see Figure 1).

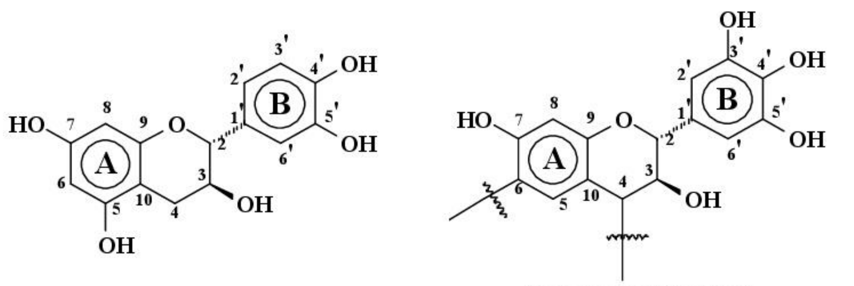

Figure 1. Structure of catechin and structure of the predominant flavonoid unit of mimosa tannin, robinetinidin, with its predominant C4 and C6 sites linked C4–C6 to other flavonoid units.

From these two compounds, the following experiments have been carried out.

The samples were prepared as follow:

(1) Catechin (0.5 g) was mixed with 0.5 g of hexamethylenediamine (HMDA) (70% solution in water). Three samples were prepared with the proportions above. Then, each sample was reacted in an oven at 65, 100, and 185 °C overnight, respectively.
(2) Catechin (0.5 g) was mixed with 0.5 g of HMDA (70% solution in water) and 0.15 g of a 65 wt % aqueous solution of *p*-toluenesulfonic acid (pTSA). Again, three samples were prepared with the proportions above, and they were reacted in an oven at 65, 100, and 185 °C overnight, respectively.

(3) Catechin (0.5 g) was mixed with 0.5 g of HMDA (70% solution in water) and 0.15 g of a 33 wt % aqueous solution of NaOH. Three samples were prepared with the proportions above. After that, they were reacted in an oven at 65, 100, and 185 °C overnight, respectively.
(4) Mimosa tannin (2 g) was mixed with 2 g of hexamethylenediamine (HMDA) (70% solution in water). Three samples were prepared with the proportions above, and they were reacted in an oven at 65, 100, and 185 °C overnight, respectively.
(5) Mimosa tannin (2 g) was mixed with 2 g of HMDA (70% solution in water) and 0.6 g of a 65 wt % aqueous solution *p*-toluenesulfonic acid (pTSA). Three samples were prepared with the proportions above. Then, they were reacted in an oven at 65, 100, and 185 °C overnight, respectively.
(6) Mimosa tannin (2 g) was mixed with 2 g of HMDA (70% solution in water) and 0.6 g of a 33 wt % aqueous solution NaOH. Again, three samples were prepared with the proportions above, and they were reacted in an oven at 65, 100, and 185 °C overnight, respectively.

The samples were mixed with a spatula because they become a paste after the addition of catechin or mimosa tannin. After the reaction in the oven, the samples prepared at 100 and 185 °C become a dry solid, while the samples prepared at 65 °C remained like a paste.

In the case of the mimosa tannin samples at 185 °C, they have not been analysed by MALDI because the spectra were not good enough due to the difficulty of their solubility in the acetone–water solution for their MALDI-ToF analysis.

2.2. Matrix-Assisted Laser Desorption Ionisation Time-of-Flight (MALDI-ToF) Mass Spectrometry Analysis

The spectra were recorded on a KRATOS Kompact MALDI AXIMA TOF 2 instrument (KRATOS Ana lytical, Shimadzu Europe Ltd., Manchester, UK). The irradiation source was a pulsed nitrogen laser with a wavelength of 337 nm. The time period of a laser pulse was 3 ns. The measurements were carried out using the following conditions: polarity = positive, flight path = linear, mass = high (20 kV acceleration voltage), 100–150 pulses per spectrum. The delayed extraction technique was used by applying delay times of 200–800 ns.

2.3. CP-MAS ^{13}C NMR

Solid-state CP-MAS (cross-polarisation/magic-angle spinning) ^{13}C NMR spectra of the aforementioned oven-dried solids were recorded on a Brüker MSL 300 spectrometer (Brüker France, Wissembourg, France) at a frequency of 75.47 MHz. Chemical shifts were calculated relative to tetramethyl silane (TMS). The rotor was spun at 4 kHz on a double-bearing 7 mm Bruker probe. The spectra were acquired with 5 s recycle delays, a 90° pulse of 5 s and a contact time of 1 ms. The number of transients was 3000.

The ^{13}C NMR spectra were simulated with ACD/I-Lab version 12.0 (Advanced Chemistry Development Inc., Strasbourg, France) and with a free program online nmrdb.org [15] (https://www.nmrdb.org/).

3. Results and Discussion

3.1. Reactions of Catechin with Hexamethylene Diamine

3.1.1. MALDI-ToF

While some of the peaks obtained by MALDI-ToF in the products obtained by reactions at 185 °C are the same as those in the cases at 100 °C, a greater number of different types of compounds are observed in the reactions at 100 °C. For the MALDI-ToF analysis of the reactions of catechin as a model compound, the spectra of the NaOH-catalysed reaction will be discussed, as the peaks are practically the same for the acid-catalysed and uncatalysed cases, the main differences being their relevant proportions. Two types of reactions appear to occur from the calculation of the MALDI masses found, namely (i) the formation of secondary amines by reaction of the hexamethylene diamine on the –OH groups of the flavonoid units; and (ii) the formation of $–O^{-}\ {}^{+}NH_3$-salts between the amino group and some of the phenolic –OH groups of the tannin flavonoids.

Thus, in the spectra obtained, the main peaks observed are reported in Table 1, and Figures 2 and 3. There appears to be a clear period of 40 Da. This is a diamine with $2Na^+$ (not an unusual occurrence), thus $116 + 23 + 23 - 2 = 160$ Da, giving the $160/4 = 40$ Da period. The series of peaks that appears is then 798-758-718-678-634-594-553(small)-513 Da. From this series, for example, the repetition of peaks follows a 160 Da period such as $513 + 160 = 673$ Da (678 Da), $594 + 160 = 754$ Da (758 Da) (this is salt $4 \times 117 = 755$ Da), and $638 + 160 = 798$ Da $= 755 + 2Na^+ = 801 - 2H^+ = 799$ Da.

Table 1. MALDI-ToF peaks interpretation. NaOH-catalysed reaction of catechin and hexamethylenediamine at 100 °C *.

289.9 Da = Catechin alone
509–512 Da = catechin-(hexamethylenediamine)$_2$ (509 Da calculated)
524.6 Da = catechin-(hexamethylenediamine)$_2$ ionic salt
526 Da = 524 diprotonated
552.8 Da = catechin-(hexamethylenediamine)$_2$ + 3 × Na^+ (calculated 553 Da)
579.7 Da = catechin-(hexamethylenediamine)$_2$ + 4 × Na^+ (calculated 582 Da)
602.7 Da = catechin dimer + Na^+ (calculated 601 Da)
605 Da = catechin-(hexamethylenediamine)$_3$ + Na^+
631.6–633.7 Da = catechin-(hexamethylenediamine)$_3$ + 2 × Na^+ (calculated 630 Da)
664 Da = catechin-hexamethylenediamine-catechin (660 Da calculated)
However, also:
638 + 1 × Na^+ = catechin-(hexamethylenediamine)$_3$ ionic salt (calculated 661 Da)
678 Da = catechin-(hexamethylenediamine)$_3$ + 4 × Na^+ (calculated 675 Da)
758 Da = catechin-hexamethylenediamine-catechin-hexamethylenediamine
798 Da = catechin-(hexamethylenediamine)$_4$ + 2 × Na^+, ionic salt.
1169 Da = hexamethylenediamine-catechindimer-hexamethylenediamine-catechin-hexamethylenediamine + 1 × Na^+
1459 Da = hexamethylenediamine-catechindimer-hexamethylenediamine-catechindimer-hexamethylenediamine, diprotonated

* In the spectra, there is a clear period of 40 Da. This is a diamine with $2Na^+$, thus $116 + 23 + 23 - 2 = 160$ Da, thus with $2 \times Na^+$, not an unusual occurrence. Also, $160/4 = 40$ Da period, thus a series 798-758-718-678-634-594-553(small)-513 Da Thus, $513 + 160 = 673$ Da (678 Da); thus $594 + 160 = 754$ Da (758 Da). This is a salt $4 \times 117 = 755$ Da; thus $638 + 160 = 798$ Da $= 755$ Da $+ 2Na^+ = 801$ Da $- 2H^+ = 799$ Da.

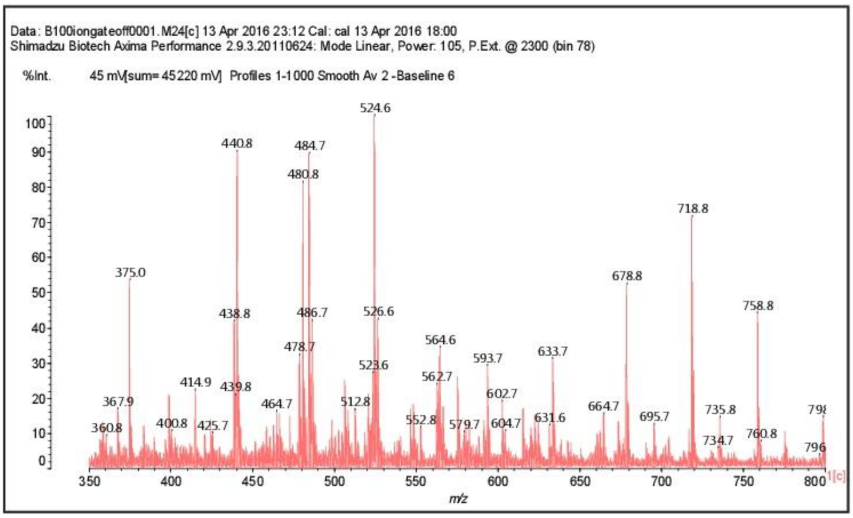

Figure 2. MALDI-ToF spectrum of the reaction of catechin with hexamethylene diamine at 185 °C, NaOH-catalysed. Range 350–800 Da.

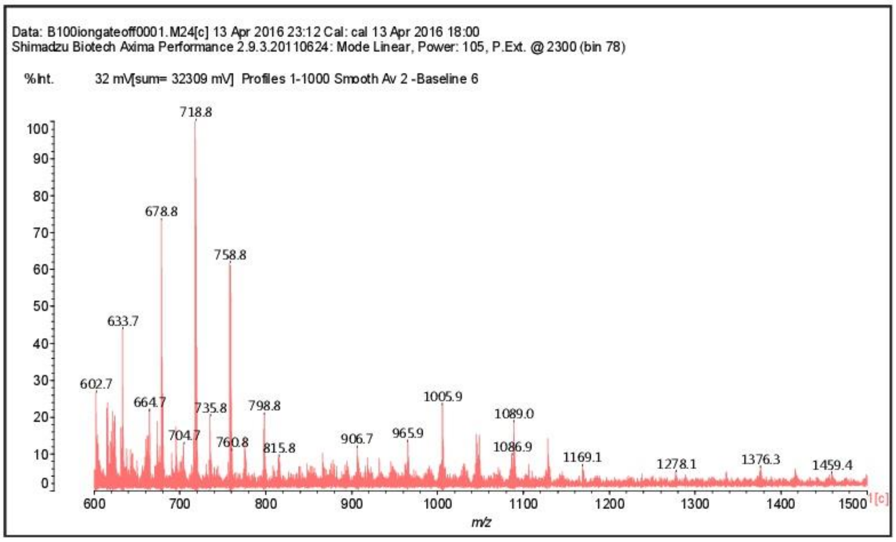

Figure 3. MALDI-ToF spectrum of the reaction of catechin with hexamethylene diamine at 185 °C, NaOH-catalysed. Range 600–1500 Da.

The structures of the type of compounds more characteristic that formed (see Table 1) are thus as follows. At 509–512 Da (Figure 4), where the bonds formed are covalent.

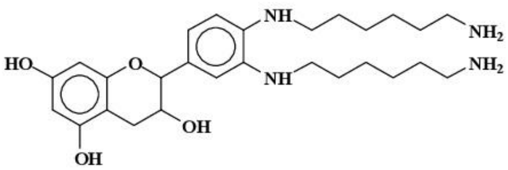

Figure 4. Example of covalent bonds structure at 509–512 Da.

At 524.6 Da (Figure 5), where the bonds formed are strongly ionic, thus forming a salt.

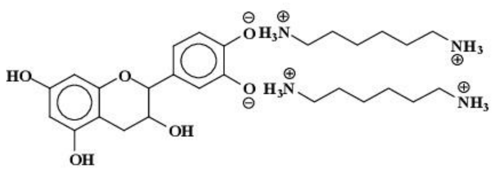

Figure 5. Example of ionic bonds salt structure at 524.6 Da.

Additionally, mixed-bond species, such as the oligomer at 548 Da (Figure 6):

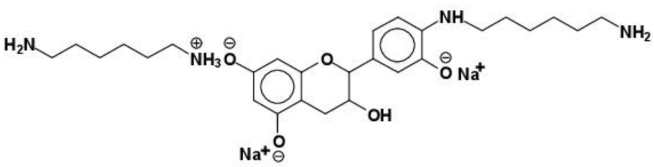

Figure 6. Example of mixed ionic and covalent bonds structure at 548 Da.

It must be pointed out that the structure shown above is the most likely, rather than the Na^+ being attached to the N of the amine. This is so because, in general, a strong base is needed to abstract a proton from an amine. The NaOH used in the catalysis of the reaction is not strong enough for this. Furthermore, such sodium amides are strong bases themselves, which are not likely to coexist in the presence of protic compounds such as phenols. It is then most likely that the 548 Da peak belongs to a molecule that is the sodium salt of the phenolate ion. This is equally valid for structures such as the 564 Da peak observed for the mimosa tannin and other structures where Na^+ is present. (Table 2).

Dimers of two catechin monomers linked covalently through an hexamethylenediamine occurs, such as the peak occurring at 664 Da (Figure 7):

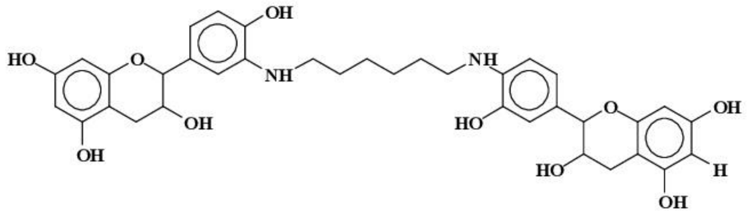

Figure 7. Example of covalent bonds dimer structure at 664 Da.

This can, however, also be interpreted as $638 + 1 \times Na^+ = 661$ Da, thus an ionic salt such as (Figure 8):

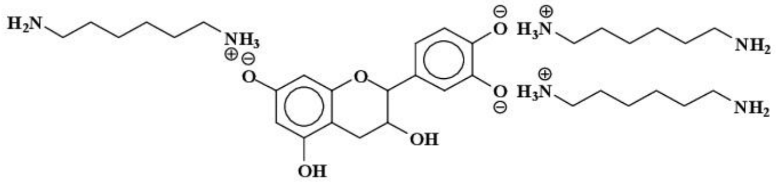

Figure 8. Example of ionic bonds salt structure at 661 Da.

Equally, at 758 Da (Figure 9):

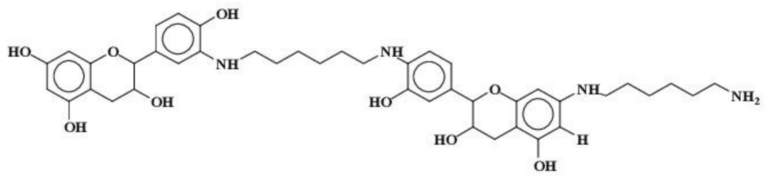

Figure 9. Example of covalent bonds dimer at 758 Da.

At 798 Da (Figure 10):

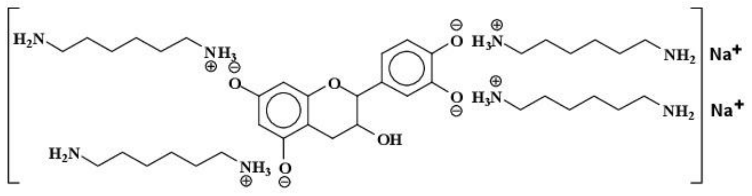

Figure 10. Example of ionic bonds salt structure at 798 Da.

At 880 Da (Figure 11):

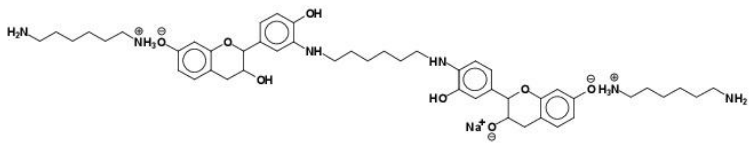

Figure 11. Example of covalent bonds dimer mixed with ionic salt bonds at 880 Da.

At 1070 Da (Figure 12):

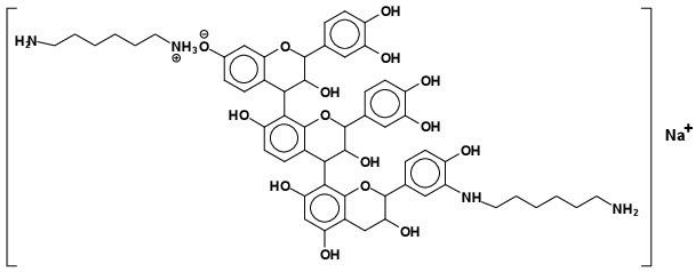

Figure 12. Example of a flavonoid trimer structure with amine reacted with mixed covalent bonds and ionic salt bonds at 1070 Da.

Higher oligomers in which catechin has dimerised also occurs, this being a fairly common reaction [16,17]. In these, the catechin dimer is linked covalently to either a catechin monomer or another catechin dimer, such as those shown by the peaks for the oligomers at 1169 Da = 1145 + 1 × Na^+ (Figure 2) and at 1404 and 1459 Da, deprotonated.

At 1169 Da (Figure 13):

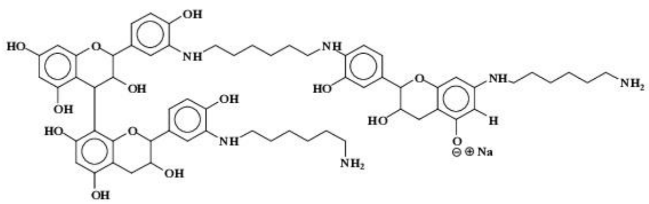

Figure 13. Example of flavonoid dimer and monomer covalently bridged by a diamine with other covalently linked diamines at 1169 Da.

At 1404 Da (Figure 14):

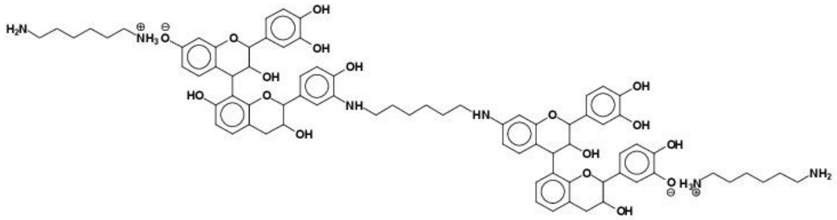

Figure 14. Example of two flavonoid dimers covalently bridged by a diamine with other ionic salt bonds linked diamines at 1404 Da.

At 1459 Da, deprotonated (Figure 15):

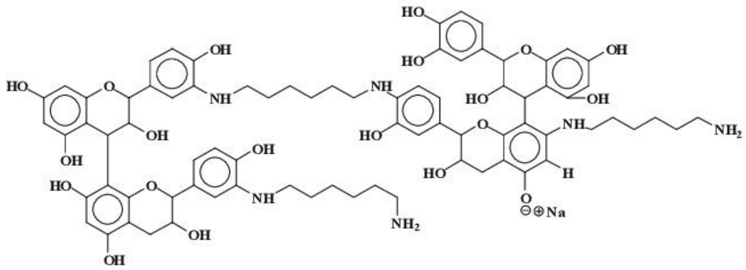

Figure 15. Example of two flavonoid dimers covalently bridged by a diamine with other covalently linked diamines at 1459 Da.

It must be made clear that the structures above are not the only possible isomers deduced from the peaks of the MALDI-ToF spectra, but that other isomer possibilities do exist for them. The existence of different isomers becomes clearer and is also confirmed later by the CP-MAS ^{13}C NMR analysis.

3.1.2. CP-MAS ^{13}C NMR

In regard to the NMR spectra: the reactions occurring appear to be more advanced when the temperature is higher, while the reaction appears almost not to occur at the lower temperature of 65 °C. For this reason, the case of the reaction of catechin as a model compound with hexamethylene diamine catalysed by pTSA at 185 °C will be discussed first. The corresponding CP-MAS ^{13}C NMR spectrum is shown in Figure 4.

In Figure 16, first of all, the aliphatic carbon in position alpha to an –NH of the diamine reacted covalently with the tannin must have a shift of 43–44 ppm, while the same for an aliphatic amine not reacted should have a calculated shift of 41–42 ppm. Looking at the spectra of the 185 °C reactions, either pTSA- and NaOH-catalysed or uncatalysed (one reported in Figure 4, the others reported in the Supplementary Material), it can be noticed that the shift is at 42.9 ppm (uncatalysed), 43.2 ppm (NaOH-catalysed), and 43.5 ppm (pTSA-catalysed) indicating that at 185 °C, the amine has reacted covalently. This is confirmed by other indications. The shift for the C in β of the covalently reacted diamine should be at 30 ppm, while the unreacted one should be at 33–34 ppm. This peak is not visible at all in uncatalysed and pTSA-catalysed, as it is covered totally by the huge peak at 27–28 ppm, but appears as a slight shoulder at 33 ppm for the NaOH-catalysed case. It must be clearly pointed out that the shift of the top of the 43–44 ppm wide peak clearly changes when comparing the CP-MAS ^{13}C NMR spectra of the three cases when the reaction is carried out at 100 °C (all spectra reported in the Supplementary Material). Thus, they are respectively at 41.9 ppm (pTSA-catalysed), 42.6 ppm (NaOH-catalysed), and 42.3 ppm. This indicates that, just based on NMR evidence, the type of bonds obtained in the reaction at 100 °C appears to be more uncertain, or at least that ionic bonds and covalent bonds are in different proportions according to the presence of different catalysts, or their absence. This implies that at the higher temperature of 185 °C, the reaction shift more towards the formation of covalently bound amines, the most found in pTSA catalysis, followed by NaOH catalysis, and least in the uncatalysed case.

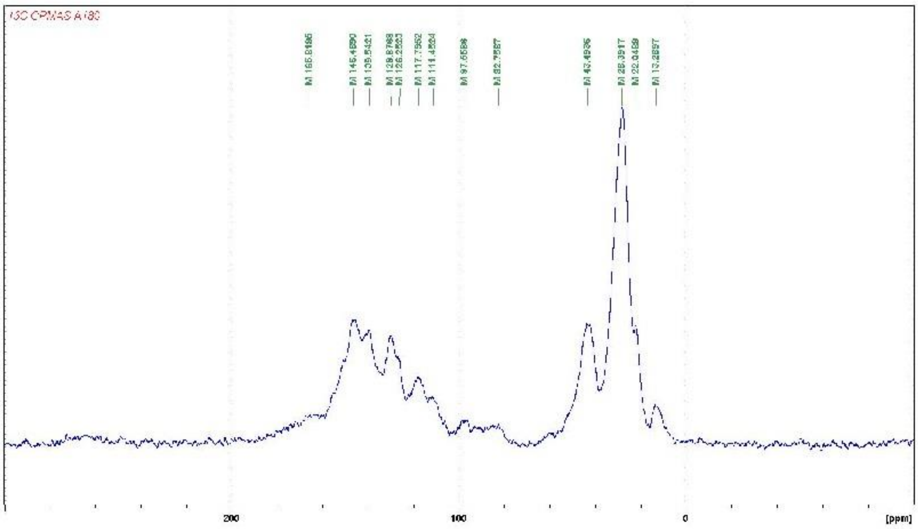

Figure 16. Cross-polarisation/magic-angle spinning (CP-MAS) ^{13}C NMR spectrum of the reaction of catechin with hexamethylene diamine at 185 °C, *p*-toluenesulfonic acid (pTSA)-catalysed.

The other clear indication of the existence of the formation of covalent bonds between the amine and the catechin –OH groups is the considerable decrease of the peak at 155–157 ppm, indicating that the carbons C5 and C7 carrying the –OH groups on the A-ring have markedly decreased as they have reacted. This species formed by this reaction is defined by the appearance of a new peak at 139.5 ppm. This peak belongs to a flavonoid C5 and a C7 that have reacted covalently with an amine, indicating that the interpretation given to the MALDI spectra has been incomplete because there has been considerable reaction on the A-ring to form the following types of linkages (Figure 17).

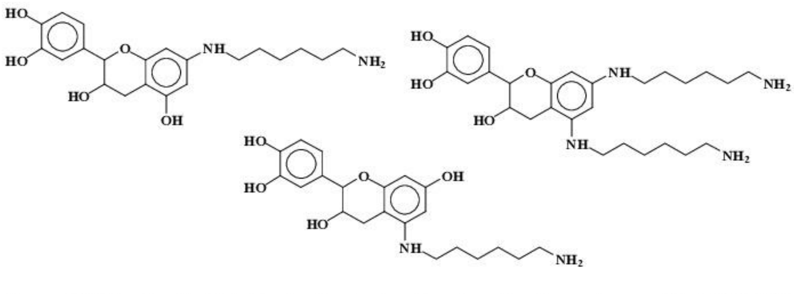

Figure 17. Covalently linked catechin A-ring-diamine structures observed by ^{13}C NMR.

This is not all. The total disappearance in the 180 °C spectra of the catechin C3 peak at 68–72 ppm indicates that even the alcoholic –OH on the C3 site has reacted covalently with the amine to form linkages of the type (Figure 18):

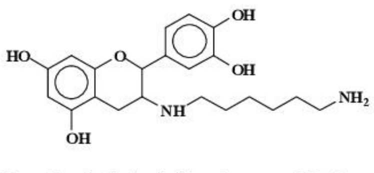

Figure 18. Covalently linked diamine onto C3 site of catechin.

This being a rather unexpected occurrence.

The first question to be asked is then: are covalent bonds with the amine formed also with the carbons of the B-ring, as interpreted from the oligomers representation shown in the interpretation of the MALDI spectra?

The answer to this question is clearly yes, as the covalent bonds are also formed at 185 °C on the B-ring as the 145–146 ppm peak belonging to the aromatic B-ring carbons carrying the phenolic –OH groups is also markedly smaller in all the catalysed and uncatalysed spectra at 185 °C. Moreover, the covalent bond formed transmit at 134–135 ppm, indicating that the 138–139 ppm peak belongs to both the covalently reacted A- and B-rings of catechin. Thus, linkages such as Figure 19 also occur.

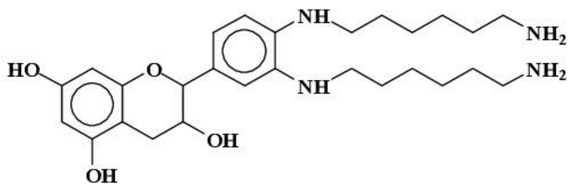

Figure 19. Covalently linked diamine onto catechin B-ring sites.

The simulation of the spectra with ACD/I-Lab yields a value of 41.8 ppm for the reacted amine, and 38.7 ppm for the unreacted amine. The online software at nmrdb.org [15] yields 44.0 ppm for the covalently reacted amine formed and 41.9 ppm for the nonreacted amine. The superposition of the pTSA-catalysed spectra at 185 and 100 °C shown in Figure 20 indicates that the formation of the amine is indeed occurring.

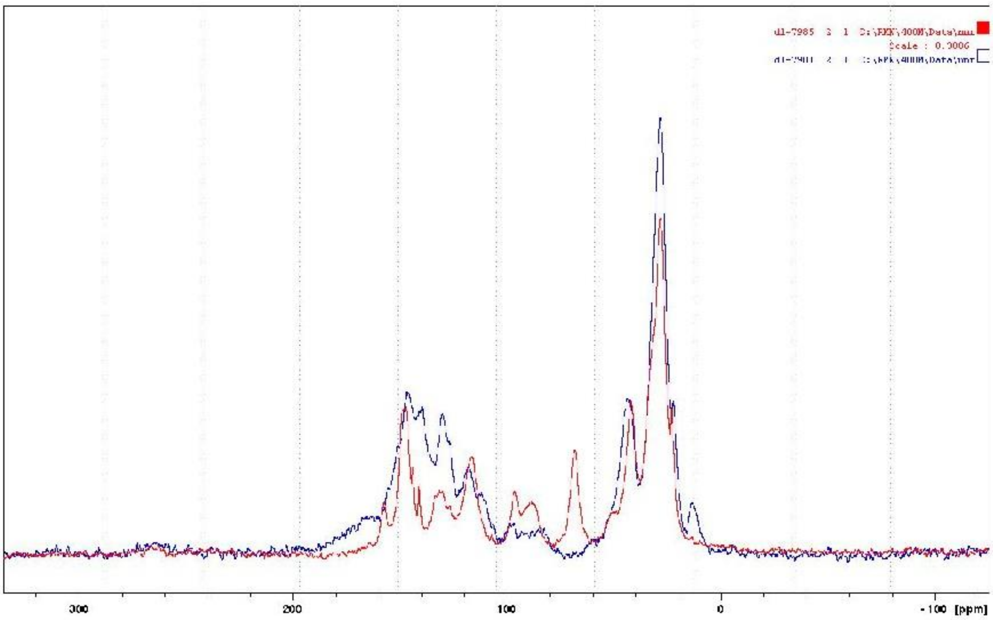

Figure 20. Superposition for comparison of the CP-MAS ^{13}C NMR spectra of the reactions of catechin with hexamethylene diamine at 185 °C (blue curve) and at 100 °C (red curve), both pTSA-catalysed.

Furthermore, on the pTSA-catalysed 185 °C spectrum, a rotation band at 13 ppm occurs. If the rate of rotation that has caused it is subtracted, a well-defined peak at 133.8 ppm is obtained. This peak is hidden by other species. This chemical shift can also be simulated with an amination of the –OH group on the C3 of catechin and corresponds to the to the shift of the carbon in C1′. Moreover, the disappearing of the peak at 68 ppm observed on the pTSA-catalysed 100 °C spectrum and absent on the pTSA-catalysed 185 °C spectrum shows that the C3 carbon of the catechin has lost its –OH group, substituted with an –NH group (calculated at 67.6 ppm for catechin and 68 ppm for the 100 °C case, and at 55.8 ppm for the amination on C3 corresponding to the large peak at 55–59 ppm for the 180 °C case).

The second question is: do the ionic-type salt bonds, apparent in the MALDI spectra, really occur?

The response is also clearly positive. The huge peak at 27–29 ppm belongs to either diamine not reacted or to diamine linked as a totally ionised salt to structures of the type which follows. Thus, in both strongly acid- and strongly alkaline-catalysed reactions at 185 °C, it is certain that the rest of the amine is coordinated to catechin with linkages such as Figure 21, where the salts are formed with the –OHs of both the B- and A-rings of the catechin. It must be considered that unreacted diamine might be mixed with this, although the MALDI clearly indicates that the ionic bonds do exist. The presence of the 33 ppm shoulder in the spectrum of the alkali-catalysed 185 °C reaction product indicates that, for the amine, β carbons confirm that ionic bonds in quantity do occur.

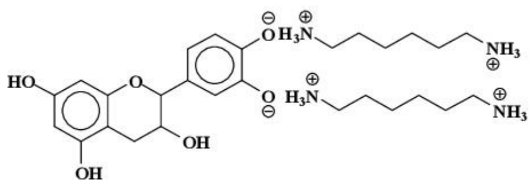

Figure 21. Example of structure of diamines linked to catechin B-ring sites by ionic salt bonds.

In the case of the uncatalysed reaction, the amine should also be present in the same manner, thus partly ionically linked to the catechin or unreacted.

The last question to be answered by the NMR analysis is: what happens at lower temperature, namely at 100 °C?

The spectra are not reported here (they are available in the Supplementary Material), but the reaction is clearly less advanced, as should be expected. First of all, the C3 of the catechin has not reacted at all as the alcoholic C3–OH site shift exists and is big. Second, there is a clear covalent reaction of the amine on the catechin A-ring and some (lesser) reaction on the B-ring in the case of the pTSA-catalysed 100 °C spectrum. The reaction on the A-ring is also clear for the NaOH-catalysed 100 °C spectrum and also, but to a lesser extent, for the uncatalysed 100 °C spectrum. For these latter two, it does not appear that reaction on the B-ring does occur, or at least its proportion is minimal. Furthermore, no reactions on C3 appear to have occurred.

3.2. Reaction of Mimosa Tannin Extract with Hexamethylene Diamine

The same reactions were repeated by using mimosa tannin extract instead of the catechin model compound. The MALDI-ToF spectra of the reaction alkaline catalysis are shown in Figures 6 and 7. The oligomer species obtained under alkaline catalysis are listed in Table 2. The MALDI spectra for the acid-catalysed and uncatalysed reactions at 100 °C and 65 °C are reported in the Supplementary Material.

From Figures 22 and 23, the same period of 40 Da is observed as in the case of catechin due to a diamine with 2 × Na^+, thus 116 + 23 + 23 − 2 = 160 Da, thus 160/4 = 40 Da period: 801-761-719-677-638-596-554-514-474-430-390-350, is observed. The same type of reactions observed for the case of the catechin model compound appears to occur. Thus, both (1) substitution of the flavonoid units' hydroxyl groups with the amino group of the amine and (2) the formation of $–O^-$ Na^+ salts appear to occur. Compounds in which one, two, and even three diamines are linked covalently to a flavonoid monomer unit are observed as, for example, the peaks at 374, 524, and 621 Da (Table 2). Equally, species in which one or more HMDA molecules are linked covalently to a flavonoid dimer occur as, for example, the ones represented by the peaks at 743 and 758 Da (Table 2), as well as species in which HMDA constitutes a bridge between two species such as two flavonoid dimers as, for example, the compounds at peaks 1260 and 1330 Da (Table 2). Conversely, species in which the amine is not covalently linked to a flavonoid unit, but rather a salt has been formed, are also present, such as, for example, the species at 390, 428–430, 661 Da, and many others as indicated in Table 2. Moreover, mixed species in which some HMDA molecules are linked covalently and some are linked by a salt bond to the same flavonoid are also present, as, for example, the species at peaks 638, 677, 761, and 1404 Da. Unreacted flavonoid oligomers—such as those represented by the peaks at 612, 881, 1178 Da, and others—are also present (Table 2).

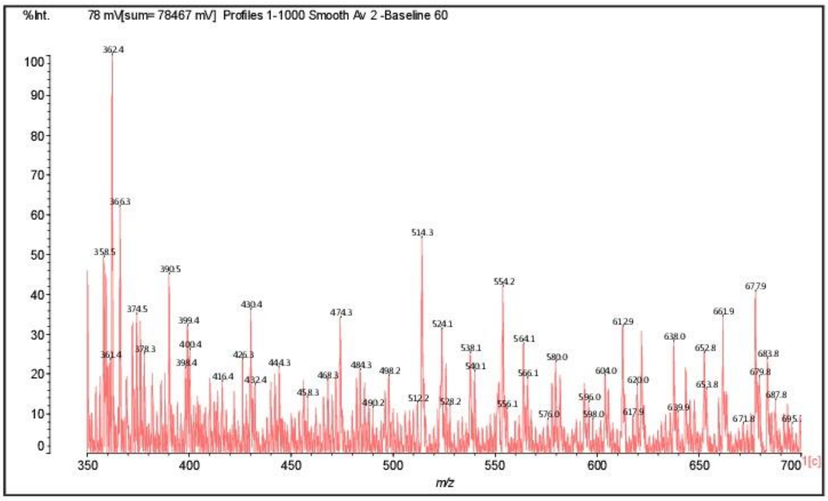

Figure 22. MALDI-ToF spectrum of the reaction of mimosa tannin extract with hexamethylene diamine at 100 °C, pTSA-catalysed. Range 350–700 Da.

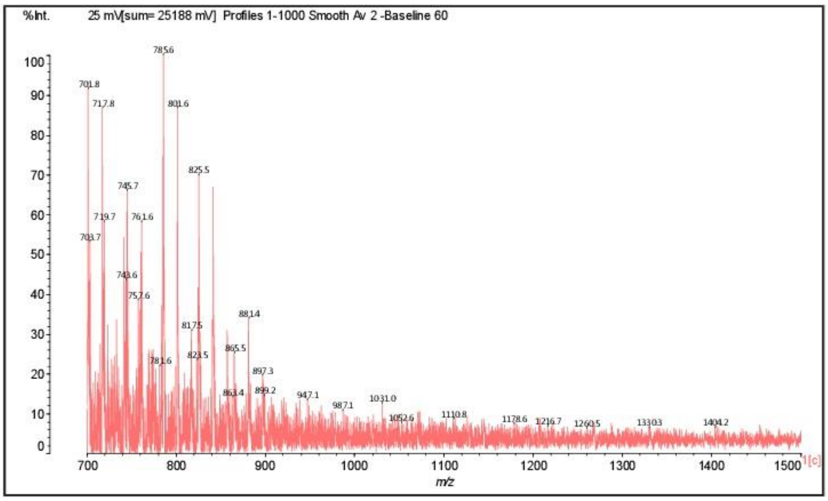

Figure 23. MALDI-ToF spectrum of the reaction of mimosa tannin extract with hexamethylene diamine at 100 °C, pTSA-catalysed. Range 700–1500 Da.

Table 2. Oligomer species formed during the reaction at 100 °C between mimosa tannin extract and hexamethylene diamine in the NaOH-catalysed reaction.

Experimental	Calculated (Da)	Description of Calculation (Da)	Description	Number Ionic Bonds	Number Covalent Bonds
372–374	372	274 + 116 − 18	F-HMDA	-	1
390	390	274 + 116	F(−)(+)HMDA	1	-
410	410	290 − 17 + 114 + 23	F-HMDA(−)(+)Na	-	1
426	426	306 + 114 − 17 + 23	G-HMDA(−)(+)Na	-	1
428–430	428	290 + 115 + 23	C(−)(+)HMDA(−)(+)Na	1	-
444	444	306 + 115 + 23	G(−)(+)HMDA(−)(+)Na	1	-
488	488	274 − 17 + 115 + 116	HMDA(+)(−)F-HMDA	1	1
468	468	274 + 114 × 2 − 17 × 2	(HMDA-F-HMDA) less 2H$^+$	-	2
484	484	290 + 114 × 2 − 17 × 2	(HMDA-C-HMDA) less 2H$^+$	-	2
500	500	304 + 2 + 114 × 2 − 17 − 17	(HMDA-G-HMDA) less 2H+	-	2
524	524	306 + 114 + 115 – 17 − 17 + 23	(G[HMDA]$_2$)(−)(+)Na	-	2
525	525	290 + 114 + 115 − 17 + 23	HMDA-C(−)(+)HMDA(−)(+)Na	1	1
528	528	274 + 116 + 114 + 23	HMDA(+)(−)F(−)(+)HMDA(−)(+)Na	2	-
540	542	306 + 115 × 2 − 17 + 23	[HMDA(+)(−)G-HMDA](−)(+)Na	1	1
562	562	272 + 288 + 2	Dimer	-	-
564	564	306 + 114 + 115 − 17 + 23 × 2	Na(+)(−)HMDA(+)(−)G-HMDA(−)(+)Na	1	1
578	578	288 + 288 + 2	Dimer	-	-
612	610	304 + 304 + 2	Dimer	-	-
617	618	306 + 115 × 2 − 17 × 2 + 116	HMDA(+)(−)G(HMDA)$_2$	1	2
621	622	306 + 115 × 2+ 114 − 17 × 3 + 23	[G(HMDA)$_3$](−)(+)Na	-	3
638	640	306 + 115 × 3 − 17 − 17 + 23	[HMDA(+)(−)G(HMDA)$_2$](−)(+)Na	1	2
643	644	272 + 272 + 2 + 114 − 17	F-F-HMDA	-	1
642	642	272 + 288 + 2 + 114 − 17 × 2	F-HMDA-C	-	2
653	654	306 + 116 × 3	G[(−)(+)HMDA]$_3$	3	-
661	660	272 + 288 + 2 + 115 − 17	F-C-HMDA	-	1
661	662	272 + 272 + 2 + 116	F-F(−)(+)HMDA	1	-
677	676	306 + 116 × 2+ 115 + 23	[HMDA(+)(−)]$_2$ G (−)(+)HMDA(−)(+)Na	3	-
677	678	272 + 288 + 2 + 116	F-C(−)(+)HMDA	1	-
682	682	272 + 288 + 2 + 114 − 17 + 23	[F-C-HMDA]	-	1
687	688	272 + 2 + 115 × 3 + 114 − 17 × 4 + 23	[F(HMDA)$_4$](−)(+)Na	-	4
695	694	288 + 288 + 2 + 116	C-C(−)(+)HMDA	1	-
701	701	272 + 288 + 2 + 116 + 23	[F-C(−)(+)HMDA](−)(+)Na	1	-
716	717	288 + 288 + 2 + 116 + 23	[C-C(−)(+)HMDA](−)(+)Na	1	-
723	723	272 + 272 + 2 + 114 + 115 − 17 × 3	F-HMDA-F-HMDA	-	3
745	744	274 + 274 + 114 + 116 − 17 × 2	F-HMDA-F(−)(+)HMDA	-	-
740–743	742	274 + 274 + 2 + 115 × 2 − 17 × 2	HMDA-F-F-HMDA	-	2
757	758	272 + 288 + 2 + 115 × 2 − 17 × 2	HMDA-F-C-HMDA	-	2
761	760	274 + 290 + 114 − 17 × 2 + 116	F-HMDA-C(−)(+)HMDA	1	2
857	857	272 + 272 + 288 + 2 + 23	Trimer	-	-
865	866	272 + 288 + 304 + 2	Trimer	-	-
881	880	272 × 2 + 2 + 115 × 3 − 17 × 2 + 23	[(HMDA(+)(−))$_2$ (F-HMDA-F)](−)(+)Na	2	2
881	882	288 × 2 + 304 + 2	Trimer	-	-
898	898	272 × 2 + 2+ 114 × 3 − 17 + 23	[(HMDA(+)(−))$_2$ F-F-HMDA](−)(+)Na	2	1
898	898	288 + 304 × 2 + 2	Trimer	-	-
906	905	288 × 2 + 304 + 2 + 23	Trimer	-	-
921	921	288 + 304 × 2 + 2 + 23	Trimer	-	-
1052	1052	857 + 114 + 115 − 17 × 2	[(F-C-F)(HMDA)$_2$](−)(+)Na	-	2
1069	1070	857 + 115 × 2 − 17	[HMDA-(F-C-F)(−)(+)HMDA](−)(+)Na	1	1
1178	1178	288 × 4 + 2 + 23	Tetramer	-	-
1260	1258	288 × 2 + 2 + 116 − 18 × 2 + 288 × 2 + 2 + 23 − 1	[C-C-HMDA-C-C](−)(+)Na	-	2
1330	1334	288 × 2 + 2 + 116 × 2 − 18 × 3 + 288 × 2 + 2	C-C-HMDA-C-C-HMDA	-	3
1404	1404	272 × 2 + 2 + 116 × 3 − 18 × 2 + 272 × 2 + 2	HMDA(+)(−)F-F-HMDA-F-F(−)(+)HMDA	2	2

F = fisetinidin; C = catechin or robinetinidin; G = gallocatechin; HMDA = hexamethylenediamine; "-" = covalent bond; "(+)(−)" = ionic bond; "(+)(−)Na = Na$^+$ linked to flavonoid units phenolic –OHs as –O$^-$ Na$^+$.

The MALDI analysis of the catechin–HMDA reaction was done at 185 °C (and 100 and 65 °C in the Supplementary Material attached to this article), but was done at 100 °C for the mimosa tannin HMDA reaction for reasons of solubility. The catechin–HMDA sample at 185 °C, while solid, shows still more than sufficient solubility in acetone for analysis by MALDI. This is, however, not the case for the mimosa tannin–HMDA reaction that, at 185 °C, has hardened and is practically insoluble. This is why the MALDI was done on the 100 °C tannin/HMDA reaction: it was much less polymerised and the majority of it was still soluble in acetone. Equally, it was the reason why the NMR of the solids of the catechin-hardened material was done. It must be pointed out that the number average degree of polymerisation (DPn) of mimosa tannin is around 4.5, thus 4–5 flavonoid units linked together. This is why a hardened tridimensional network is reached more rapidly in the reaction of HMDA with the tannin than with a catechin monomer.

4. Conclusions

A novel reaction of amines with flavonoid tannin is described. The reaction of hexamethylenediamine with catechin, a flavonoid monomer used as a model compound of condensed tannins, and with mimosa tannin were studied. The reactions were carried out at three different temperatures: 65, 100, and 185 °C. The reaction products obtained were analysed by MALDI-TOF and CP-MAS ^{13}C NMR, and the structures of the chemical species formed were indicated. Two reactions occurred under both alkaline and acid conditions, namely (i) the reaction of the amine with the phenolic hydroxy groups of the tannin, leading to polycondensation resins; and (ii) a reaction leading to the formation of ionic bonds between the protonated amino groups of the amine and the hydroxyl groups of the flavonoid structure for both the catechin and the tannin. Hardened, insoluble resins were formed for the tannin at the higher temperature, and resins insoluble in water but soluble in acetone were formed at 100 °C.

- At 185 °C, there are covalent bonds between the amine and the A- and B-rings of the catechin and also with the aliphatic C3 site of the catechin. The A-ring appears to react first, before the B-rings.
- At 185 °C, there is a high proportion of ionic bonds between the amine and the A- and B-rings of the catechin, while presence of some unreacted amine cannot be excluded.
- At 100 °C, the proportion of ionic bonds appears to predominate.
- At 100 °C, there are covalent bonds between the amine and the A- and B-rings of the catechin for the pTSA-catalysed reaction (reaction A), with the A-rings having reacted more.
- At 100 °C, there are covalent bonds between the amine and the A-rings of the catechin for the NaOH-catalysed reaction, but less or even no reaction on the B-ring. There are even fewer covalent bonds in the uncatalysed reaction.
- At 180 °C, and to a lesser extent also at 100 °C, mimosa tannin reacting with hexamethylene diamine forms hard, condensed solids, be it uncatalysed or alkali- or acid-catalysed.
- At 180 °C, the condensation solid formed is hardly soluble in acetone water.
- The reaction of mimosa tannin or similar condensed tannins with a diamine is fast.
- In regard to the influence of different catalysts, their influence is minimal other than to accelerate the reaction. To this purpose, reactions at three different temperatures (but without any catalysts) were done with similar results, and the analysis results are shown in the Supplementary Material.

Supplementary Materials: The following are available online at www.mdpi.com/2073-4360/9/2/37/s1, Table S1: Structures determined by MALDI ToF of the reaction of mimosa + hexamethylenediamine + NaOH at 100 °C, Table S2: Structures determined by MALDI ToF of the reaction of mimosa +hexamethylenediamine + pTSA at 100 °C, Table S3: Structures determined by MALDI ToF of the uncatalysed reaction of mimosa + hexamethylenediamine at 100 °C, Table S4: Structures determined by MALDI ToF of the reaction of mimosa + hexamethylenediamine + NaOH at 65 °C, Table S5: Structures determined by MALDI ToF of the reaction of mimosa + hexamethylenediamine + pTSA at 65 °C, Table S6: Structures determined by MALDI ToF of the uncatalysed reaction of mimosa + hexamethylenediamine at 65 °C, Table S7: Structures determined by MALDI ToF of the uncatalysed reaction of catechin monomer + hexamethylenediamine at 185 °C, Table S8: Structures determined by MALDI ToF of the uncatalysed reaction of catechin monomer + hexamethylenediamine at 100 °C, Table S9: Structures determined by MALDI ToF of the uncatalysed reaction of catechin monomer + hexamethylenediamine at 65 °C, Figure S1: MALDI ToF spectrum of the reaction of mimosa + hexamethylenediamine + NaOH at 100 °C. 350–700 Da range, Figure S2: MALDI ToF spectrum of the reaction of mimosa + hexamethylenediamine + NaOH at 100 °C. 700–1500 Da range, Figure S3: MALDI ToF spectrum of the reaction of mimosa + hexamethylenediamine + pTSA at 100 °C. 700–2200 Da range, Figure S4: MALDI ToF spectrum of the uncatalysed reaction of mimosa + hexamethylenediamine at 100 °C. 350–700 Da range, Figure S5: MALDI ToF spectrum of the uncatalysed reaction of mimosa + hexamethylenediamine at 100 °C. 700–1500 Da range. Figure S6: MALDI ToF spectrum of the reaction of mimosa + hexamethylenediamine + NaOH at 65 °C. 350–700 Da range, Figure S7: MALDI ToF spectrum of the reaction of mimosa + hexamethylenediamine + NaOH at 65 °C. 700–1500 Da range, Figure S8: MALDI ToF spectrum of the reaction of mimosa + hexamethylenediamine + pTSA at 65 °C 350–700 Da range, Figure S9: MALDI ToF spectrum of the reaction of mimosa + hexamethylenediamine + pTSA at 65 °C 700–1500 Da range, Figure S10: MALDI ToF spectrum of the uncatalysed reaction of mimosa + hexamethylenediamine at 65 °C. 350–700 Da range, Figure S11: MALDI ToF spectrum of the uncatalysed reaction of mimosa + hexamethylenediamine at 65 °C. 700–1500 Da range, Figure S12: MALDI ToF of the uncatalysed reaction of catechin monomer + hexamethylenediamine at 185 °C. 330–600 Da range, Figure S13: MALDI ToF of the uncatalysed reaction of catechin monomer + hexamethylenediamine at 185 °C. 350–2000 Da range, Figure S14: MALDI ToF spectrum of the uncatalysed reaction of catechin monomer + hexamethylenediamine at 100 °C. 350–800 Da range, Figure S15: MALDI ToF spectrum of the uncatalysed reaction of catechin monomer + hexamethylenediamine at 100 °C. 600–2000 Da range, Figure S16: MALDI ToF spectrum of the uncatalysed reaction of catechin monomer + hexamethylenediamine at 65 °C. 330–600 Da range, Figure S17: MALDI ToF spectrum of the uncatalysed reaction of catechin monomer + hexamethylenediamine at 65 °C. 600–1500 Da range, Figure S18: MALDI ToF spectrum of the reaction of catechin monomer + hexamethylenediamine + NaOH at 185 °C. 350–800 Da range, Figure S19: MALDI ToF spectrum of the reaction of catechin monomer + hexamethylenediamine + NaOH at 185 °C. 600–1500 Da range, Figure S20: MALDI ToF spectrum of the reaction of catechin monomer + hexamethylenediamine + NaOH at 100 °C. 350–800 Da range, Figure S21: MALDI ToF spectrum of the reaction of catechin monomer + hexamethylenediamine + NaOH at 100 °C. 600–1500 Da range, Figure S22: MALDI ToF spectrum of the reaction of catechin monomer + hexamethylenediamine + NaOH at 65 °C. 350–800 Da range, Figure S23: MALDI ToF spectrum of the reaction of catechin monomer + hexamethylenediamine + NaOH at 65 °C. 600–1500 Da range, Figure S24: MALDI ToF spectrum of the reaction of catechin monomer + hexamethylenediamine + pTSA at 185 °C. 350–800 Da range, Figure S25: MALDI ToF spectrum of the reaction of catechin monomer + hexamethylenediamine + pTSA at 100 °C. 350–800 Da range, Figure S26: MALDI ToF spectrum of the reaction of catechin monomer + hexamethylenediamine + pTSA at 100 °C. 600–1500 Da range, Figure S27: MALDI ToF spectrum of the reaction of catechin monomer + hexamethylenediamine + pTSA at 65 °C. 350–800 Da range, Figure S28: MALDI ToF spectrum of the reaction of catechin monomer + hexamethylenediamine + pTSA at 65 °C. 400–900 Da range, Figure S29: CP MAS ^{13}C NMR spectrum of the reaction of catechin monomer + hexamethylenediamine + pTSA at 185 °C, Figure S30: CP MAS ^{13}C NMR spectrum of the reaction of catechin monomer + hexamethylenediamine + pTSA at 100 °C, Figure S31: CP MAS ^{13}C NMR spectrum of the reaction of catechin monomer + hexamethylenediamine + NaOH at 185 °C, Figure S32: CP MAS ^{13}C NMR spectrum of the reaction of catechin monomer + hexamethylenediamine + NaOH at 100 °C, Figure S33: CP MAS ^{13}C NMR spectrum of the uncatalysed reaction of catechin monomer + hexamethylenediamin at 185 °C, Figure S34: CP MAS ^{13}C NMR spectrum of the uncatalysed reaction of catechin monomer + hexamethylenediamin at 100 °C. Thus, (1) MALDI-ToF spectra and tables of reaction products of the uncatalysed, NaOH-catalysed, and pTSA-catalysed reactions of mimosa tannin extract with hexamethylene diamine at 100 and 65 °C. (2) MALDI-ToF spectra and tables of reaction products of the uncatalysed reactions of catechin with hexamethylene diamine at 185, 100, and 65 °C.

Acknowledgments: The authors acknowledge the funding from the BRIIO project financed by the conventions of the French state (FUI) Nr. 1410042V and Nr. 1410043V through Bpifrance financement.

Author Contributions: Antonio Pizzi, Francisco Santiago-Medina, and Maria Cecilia Basso conceived of and designed the experiments; Francisco Santiago-Medina performed the MALDI-ToF analysis; F. Santiago-Medina and Antonio Pizzi analysed and interpreted the MALDI-ToF spectra; Luc Delmotte performed the CP-MAS ^{13}C NMR analysis and the simulation with the ACP/I-lab and mndb programmes and Antonio Pizzi analysed and interpreted the CP-MAS ^{13}C NMR data; Alain Celzard contributed parallel analysis tools; Antonio Pizzi wrote the paper.

Conflicts of Interest: The authors declare no conflict of interest.

References

1. Pizzi, A. Tannin-based wood adhesives. In *Wood Adhesives Chemistry and Technology*; Pizzi, A., Ed.; Marcel Dekker: New York, NY, USA, 1983; pp. 177–246. Available online: https://www.amazon.fr/Wood-Adhesives-Pizzi/dp/0824715799/ref=sr_1_5?s=english-books&ie=UTF8&qid=1482513734&sr=1-5&keywords=Wood+Adhesives+Chemistry+and+Technology (accessed on November 1983).
2. Pizzi, A. *Advanced Wood Adhesives Technology*; Marcel Dekker: New York, NY, USA, 1994; pp. 1–304. Available online: https://books.google.fr/books?hl=fr&lr=&id=xpZVVkiaQDsC&oi=fnd&pg=PA19&dq=2.%09Pizzi,+A.+Advanced+wood+adhesives+technology,+Marcel+Dekker,+New+York,+1994&ots=9ktO_3O1NO&sig=3mcurFkvpjL9SrStZElkRavCI1Y#v=onepage&q=2.%09Pizzi%2C%20A.%20Advanced%20wood%20adhesives%20technology%2C%20Marcel%20Dekker%2C%20New%20York%2C%201994&f=false (accessed on August 1994).
3. Garcia, R.; Pizzi, A. Polycondensation and autocondensation networks in polyflavonoid tannins. I. Final networks. *J. Appl. Polym. Sci.* **1998**, *70*, 1083–1091. [CrossRef]
4. Garcia, R.; Pizzi, A. Polycondensation and autocondensation networks in polyflavonoid tannins. II. Polycondensation vs. Autocondensation. *J. Appl. Polym. Sci.* **1998**, *70*, 1093–1110. [CrossRef]
5. Masson, E.; Merlin, A.; Pizzi, A. Comparative kinetics of the induced radical autocondensation of polyflavonoid tannins. I. Modified and non-modified tannins. *J. Appl. Polym. Sci.* **1996**, *60*, 263–269. [CrossRef]

6. Masson, E.; Pizzi, A.; Merlin, A. Comparative kinetics of the induced radical autocondensation of polyflavonoid tannins. III. Micellar reactions vs. cellulose surface catalysis. *J. Appl. Polym. Sci.* **1996**, *60*, 1655–1664. [CrossRef]
7. Masson, E.; Pizzi, A.; Merlin, A. Comparative kinetics of: The induced radical autocondensation of polyflavonoid tannins. II. Flavonoid units effects. *J. Appl. Polym. Sci.* **1997**, *64*, 243–265. [CrossRef]
8. Itoh, M.; Hattori, H.; Tanabe, K. The acidic properties of TiO_2-SiO_2 and its catalytic activities for the amination of phenol, the hydration of ethylene and the isomerization of butane. *J. Catal.* **1974**, *35*, 225–231. [CrossRef]
9. Iranpoor, N.; Panahi, F. Direct Nickel-catalyzed amination of phenols via C-O Bond activation using 2,4,6-Trichloro-1,3,5-triazine (TCT) as reagent. *Adv. Synth. Catal.* **2014**, *356*, 3067–3073. [CrossRef]
10. Yu, J.; Wang, Y.; Zhang, P.; Wu, J. Direct amination of phenols under metal-free conditions. *Synlett* **2013**, *24*, 1448–1454.
11. Kim, H.J.; Kim, J.; Cho, S.H.; Chang, S. Intermolecular oxidative C-N bond formation under metal-free conditions: Control of chemoselectivity between aryl sp2 and benzylic sp3 C-H Bond imidation. *J. Am. Chem. Soc.* **2011**, *133*, 16382–16385. [CrossRef] [PubMed]
12. Hashida, K.; Makino, R.; Ohara, S. Amination of pyrogallol nucleus of condensed tannins and related polyphenols by ammonia water treatment. *Holzforschung* **2009**, *63*, 319–326. [CrossRef]
13. Kida, K.; Suzuki, M.; Takagaki, A.; Nanjo, F. Deodorizing effects of tea catechins on amines and ammonia. *Biosci. Biotechnol. Biochem.* **2002**, *66*, 373–377. [CrossRef] [PubMed]
14. Braghiroli, F.; Fierro, V.; Pizzi, A.; Rode, K.; Radke, W.; Delmotte, L.; Parmentier, J.; Celzard, A. Condensation reactions of flavonoid tannins with ammonia. *Ind. Crop. Prod.* **2013**, *44*, 330–335. [CrossRef]
15. Binev, Y.; Marques, M.M.; Aires-de-Sousa, J. Prediction of 1H NMR coupling constants with associative neural networks trained for chemical shifts. *J. Chem. Inf. Model.* **2007**, *47*, 2089–2097. [CrossRef] [PubMed]
16. Ohara, S.; Hemingway, R.W. Condensed tannins: The formation of a diarylpropanol-catechinic acid dimer from base-catalyzed reactions of (+)-catechin. *J. Wood Chem. Technol.* **1991**, *11*, 195–208. [CrossRef]
17. Hashida, K.; Ohara, S.; Makino, R. Base-catalyzed reactions of (−)-epicatechin: Formation of enantiomers of base-catalyzed reaction products from (+)-catechin. *J. Wood Chem. Technol.* **2003**, *23*, 227–232. [CrossRef]

2.1 Matériel supplémentaire de « Polycondensation resins by flavonoid tannins reaction with amines »

Polymers **2017**, *9*, 37; doi:10.3390/polym9020037 S1 of S25

Supplementary Materials: Polycondensation Resins by Flavonoid Tannins Reaction with Amines

Francisco-Jose Santiago-Medina, Antonio Pizzi, Maria Cecilia Basso, Luc Delmotte and Alain Celzard

1. Mimosa Tannin Reactions

For each sample the number refers to the temperature (65, 100 and 185 °C) and the letter sAB = mimosa + hexamethylenediamine A = mimosa + hexamethylenediamine + pTSA and B = mimosa + hexamethylenediamine + NaOH.

In the case of the samples at 180 °C, they have not been analysed because the spectra are not very good due to these samples unable to be well-dissolved in the acetone–water solution before theirs measurements in the MALDI.

AB is mimosa + hexamethylenediamine without no acid or base catalyst

Legend

F = fisitinidin

C = catechin

G = gallocatechin

HMDA= Hexamethylenediamine

"-" = covalent bond

"(+)(−)" = ionic bond

"(+)(−)Na = Na^+ linked to flavonoid units phenolic –OHs as $–O^-Na^+$

B100

Table S1. Structures determined by MALDI ToF of the reaction of mimosa + hexamethylenediamine + NaOH at 100 °C.

Experimental	Calculated (Da)	Descrip. Cal (Da)	Description	Number Ionic Bonds	Number Covalent Bonds
372	372	274 + 116 − 18	F-HMDA	-	1
390	390	274 + 116	F(−)(+)HMDA	1	-
410	410	290 – 17 + 114 + 23	F-HMDA(−)(+)Na	-	1
426	426	306 + 114 – 17 + 23	G-HMDA(−)(+)Na	-	1
428	428	290 + 115 + 23	C(−)(+)HMDA(−)(+)Na	1	-
444	444	306 + 115 + 23	G(−)(+)HMDA(−)(+)Na	1	-
488	488	274 – 17 + 115 + 116	HMDA(+)(−)F-HMDA	1	1
468	468	274 + 114 × 2 – 17 × 2	(HMDA-F-HMDA) less 2H+	-	2
484	484	290 + 114 × 2 – 17 × 2	(HMDA-C-HMDA) less 2H+	-	2
500	500	304 + 2 + 114 × 2 – 17 − 17	(HMDA-G-HMDA) less 2H+	-	2
524	524	306 + 114 + 115 – 17 − 17+ 23	(G[HMDA]$_2$)(−)(+)Na	-	2
525	525	290 + 114 + 115 – 17 + 23	HMDA-C(−)(+)HMDA(−)(+)Na	1	1
528	528	274 + 116 + 114 + 23	HMDA(+)(−)F(−)(+)HMDA(−)(+)Na	2	-
540	542	306 + 115 × 2 − 17 + 23	[HMDA(+)(−)G-HMDA](−)(+)Na	1	1
562	562	272 + 288 + 2	Dimer	-	-
564	564	306 + 114 + 115 – 17 + 23 × 2	Na(+)(−)HMDA(+)(−)G-HMDA(−)(+)Na	1	1
578	578	288 + 288 + 2	Dimer	-	-
612	610	304 + 304 + 2	Dimer	-	-
617	618	306 + 115 × 2 – 17 × 2 + 116	HMDA(+)(−)G(HMDA)$_2$	1	2
621	622	306 + 115 × 2 + 114 – 17 × 3 + 23	[G(HMDA)$_3$](−)(+)Na	-	3
638	640	306 + 115 × 3 – 17 – 17 + 23	[HMDA(+)(−)G(HMDA)$_2$](−)(+)Na	1	2
643	644	272 + 272 + 2 + 114 − 17	F-F-HMDA	-	1

642	642	272 + 288 + 2 + 114 – 17 × 2	F-HMDA-C	-	2
653	654	306 + 116 × 3	G[(−)(+)HMDA]$_3$	3	-
661	660	272 + 288 + 2 + 115 − 17	F-C-HMDA	-	1
661	662	272 + 272 + 2 + 116	F-F(−)(+)HMDA	1	-
677	676	306 + 116 × 2 + 115 + 23	[HMDA(+)(−)]$_2$ G (−)(+)HMDA(−)(+)Na	3	-
677	678	272 + 288 + 2 + 116	F-C(−)(+)HMDA	1	-
682	682	272 + 288 + 2 + 114 – 17 + 23	[F-C-HMDA]	-	1
687	688	272 + 2 + 115 × 3 + 114 ×17 × 4 + 23	[F(HMDA)$_4$](−)(+)Na	-	4
695	694	288 + 288 + 2 + 116	C-C(−)(+)HMDA	1	-
701	701	272 + 288 + 2 + 116 + 23	[F-C(−)(+)HMDA](−)(+)Na	1	-
716	717	288 + 288 + 2 + 116 + 23	[C-C(−)(+)HMDA](−)(+)Na	1	-
723	723	272 + 272 + 2 + 114 + 115 – 17 × 3	F-HMDA-F-HMDA	-	3
745	744	274 + 274 + 114 + 116 – 17 × 2	F-HMDA-F(−)(+)HMDA	-	-
740-743	742	274 + 274 + 2 + 115 × 2 – 17 × 2	HMDA-F-F-HMDA	-	2
757	758	272 + 288 + 2 + 115 × 2 – 17 × 2	HMDA-F-C-HMDA	-	2
761	760	274 + 290 + 114 – 17 × 2 + 116	F-HMDA-C(−)(+)HMDA	1	2
857	857	272 + 272 + 288 + 2 + 23	Trimer	-	-
865	866	272 + 288 + 304 + 2	Trimer	-	-
881	880	272 × 2 + 2 + 115 × 3 – 17 × 2 + 23	[(HMDA(+)(−))$_2$ (F-HMDA-F)](−)(+)Na	2	2
881	882	288 × 2 + 304 + 2	Trimer	-	-
898	898	272 × 2 + 2 + 114 × 3 – 17 + 23	[(HMDA(+)(−))$_2$ F-F-HMDA](−)(+)Na	2	1
898	898	288 + 304 × 2 + 2	Trimer	-	-
906	905	288 × 2 + 304 + 2 + 23	Trimer	-	-
921	921	288 + 304 × 2 + 2 + 23	Trimer	-	-
1052	1052	857 + 114 + 115 – 17 × 2	[(F-C-F)(HMDA)$_2$](−)(+)Na	-	2
1069	1070	857 + 115 × 2 – 17	[HMDA-(F-C-F)(−)(+)HMDA](−)(+)Na	1	1
1178	1178	288 × 4 + 2 + 23	Tetramer	-	-
1260	1258	288 × 2 + 2 + 116 – 18 × 2+288 × 2+2+23-1	[C-C-HMDA-C-C](−)(+)Na	-	2
1330	1334	288x2+2+116 × 2-18 × 3 + 288 × 2 + 2	C-C-HMDA-C-C-HMDA	-	3
1404	1404	272 × 2 + 2 + 116 × 3 – 18 × 2 + 272 × 2 + 2	HMDA(+)(−)F-F-HMDA-F-F(−)(+)HMDA	2	2

Period of 40 Da due to a diamine with 2Na$^+$, thus 116 + 23 + 23 − 2 = 160 Da, thus 160/4 = 40 Da period: 801-61-719-677-638-596-554-514-474-430-390-350.

B100

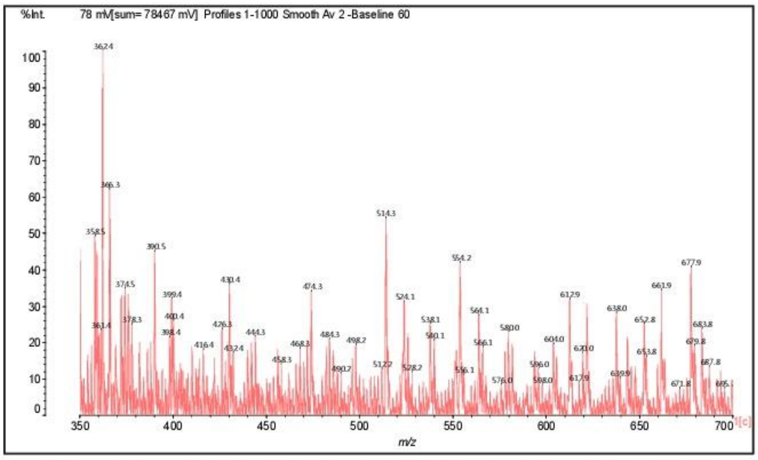

Figure S1. MALDI ToF spectrum of the reaction of mimosa + hexamethylenediamine + NaOH at 100 °C; 350–700 Da range.

B100

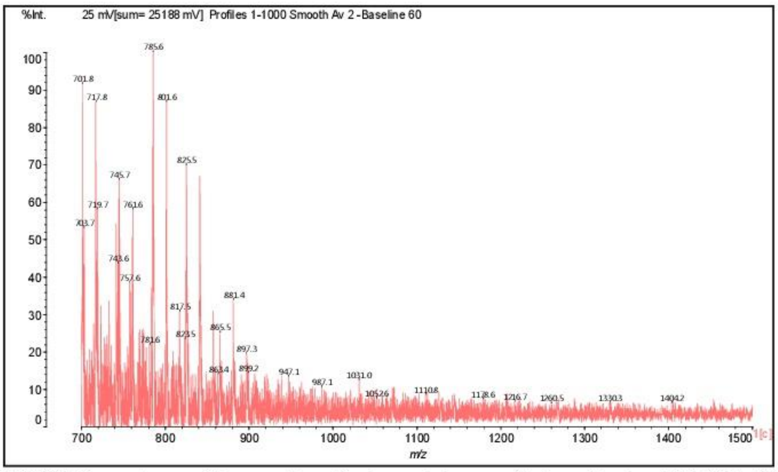

Figure S2. MALDI ToF spectrum of the reaction of mimosa + hexamethylenediamine + NaOH at 100°C; 700–1500 Da range.

A100

Table S2. Structures determined by MALDI ToF of the reaction of mimosa + hexamethylenediamine + pTSA at 100 °C.

Experimental	Calculated (Da)	Descrip. Cal (Da)	Description	Number Ionic Bonds	Number Covalent Bonds
371	372	274 + 116 − 18	F-HMDA	-	1
390	390	274 + 116	F(−)(+)HMDA	1	-
410	410	290 − 17 + 114 + 23	F-HMDA(−)(+)Na		1
412	412	274 + 115 + 23	F(−)(+)HMDA(−)(+)Na	1	
428	428	290 + 115 + 23	C(−)(+)HMDA(−)(+)Na	1	
444	444	306 + 115 + 23	G(−)(+)HMDA(−)(+)Na	1	
486 or 490	488	274 − 17 + 115 + 116	HMDA(+)(−)F-HMDA	1	1
486	484	290 + 114 × 2 − 17 × 2	(HMDA-C-HMDA) +2H+	-	2
524	524	306 + 114 + 115 − 17 − 17 + 23	(G[HMDA]$_2$)(−)(+)Na	-	2
526	525	290 + 114 + 115 − 17 + 23	HMDA-C(−)(+)HMDA(−)(+)Na	1	1
528	528	274 + 116 + 114 + 23	HMDA(+)(−)F(−)(+)HMDA(−)(+)Na	2	
540	542	306 + 115 × 2 − 17 + 23	[HMDA(+)(−)G-HMDA](−)(+)Na	1	1

564	564	306 + 114 + 115 – 17 + 23 × 2	Na(+)(−)HMDA(+)(−)G-HMDA(−)(+)Na	1	1
568	568	274 + 115 × 3 – 17 × 3	F[HMDA]$_3$	-	3
578	578	288 + 288 + 2	Dimer (small)	-	-
612	610	304 + 304 + 2	Dimer	-	-
621	622	306 + 115 × 2 + 114 – 17 × 3 + 23	[G(HMDA)$_3$](−)(+)Na	-	3
626	626	274 + 114 × 3 – 17 + 23	[HMDA-F((−)(+)HMDA)$_2$](−)(+)Na	2	1
640	640	306 + 115 × 3 – 17 – 17 + 23	[HMDA(+)(−)G(HMDA)$_2$](−)(+)Na	1	2
643	644	272 + 272 + 2 + 114 − 17	F-F-HMDA	-	1
643	642	272 + 288 + 2 + 114 – 17 × 2	F-HMDA-C	-	2
661	660	272 + 288 + 2 + 115 − 17	F-C-HMDA	-	1
661	662	272 + 272 + 2 + 116	F-F(−)(+)HMDA	1	-
677	676	306 + 116 × 2 + 115 + 23	[HMDA(+)(−)]$_2$ G (−)(+)HMDA(−)(+)Na	3	-
679	678	272 + 288 + 2 + 116	F-C(−)(+)HMDA	1	-
683	682	272 + 288 + 2 + 114 – 17 + 23	[F-C-HMDA]	-	1
695	694	288 + 288 + 2 + 116	C-C(−)(+)HMDA	1	-
700	701	272 + 288 + 2 + 116 + 23	[F-C(−)(+)HMDA](−)(+)Na	1	-
706	706	274 + 115 × 4 – 17 × 3 + 23	[(HMDA)$_3$F(−)(+)HMDA](−)(+)Na	1	3
717	717	288 + 288 + 2 + 116 + 23	[C-C(−)(+)HMDA](−)(+)Na	1	-
723	723	272 + 272 + 2 + 114 + 115 – 17 × 3	F-HMDA-F-HMDA	-	3
745	744	274 + 274 + 114 + 116 – 17 × 2	F-HMDA-F(−)(+)HMDA	-	-
758	758	272 + 288 + 2 + 115 × 2 – 17 × 2	HMDA-F-C-HMDA	-	2
761	760	274 + 290 + 114 – 17 × 2 + 116	F-HMDA-C(−)(+)HMDA	1	2
761	760	272 + 272 + 2 + 115 – 17 + 116	HMDA-F-F(−)(+)HMDA	1	1
777	776	272 + 288 + 2 + 114 × 2 − 17	HMDA-F-C(−)(+)HMDA	1	1
857	857	272 + 272 + 288 + 2 + 23	Trimer	-	-
880	880	272 – 2 + 2 + 115 × 3 – 17 × 2 + 23	[(HMDA(+)(−))$_2$ (F-HMDA-F)](−)(+)Na	2	2
882	882	288 × 2 + 304 + 2	Trimer	-	-
897	898	272 × 2 + 2 + 114 × 3 – 17 + 23	[(HMDA(+)(−))$_2$ F-F-HMDA](−)(+)Na	2	1
897	898	288 + 304 × 2 + 2	Trimer	-	-
906	905	288 × 2 + 304 + 2 + 23	Trimer	-	-
921	921	288 + 304 × 2 + 2 + 23	Trimer	-	-

Two period of around 44 and 43 Da, respectively, are clear. The first from 1260 Da until 1876 Da and the second one from 1849 Da until 2067 Da. Something similar is found in the spectrum of the samples prepared at 180 °C, which they could barely be dissolved. Thus, it can be quite likely to be a measurement error. A third period of 40 Da, due to a diamine with 2 Na^+ + 116 + 23 + 23 − 2 = 160/4, is observed from 801 Da until 350 Da.

A 100

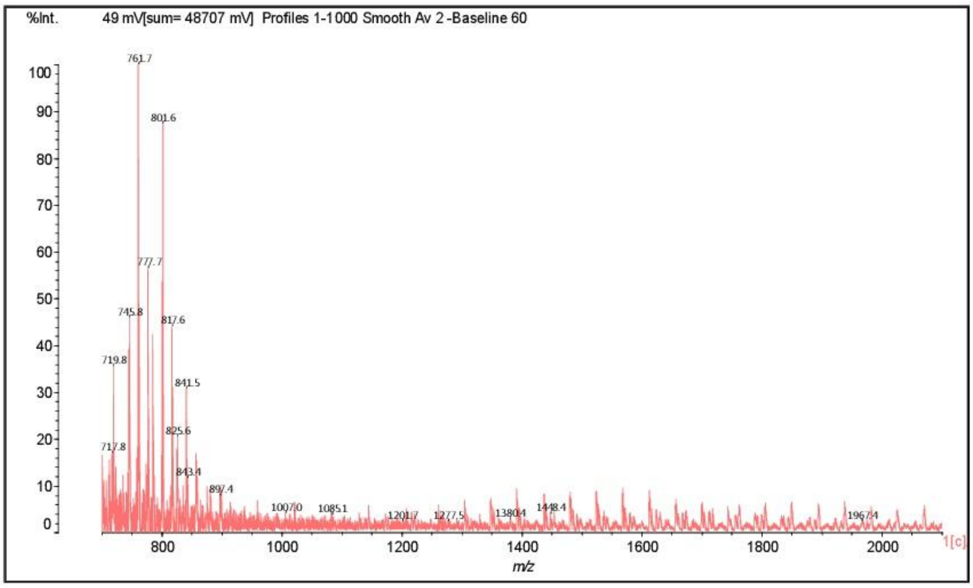

Figure S3. MALDI ToF spectrum of the reaction of mimosa + hexamethylenediamine + pTSA at 100°C; 700–2200 Da range.

Polymers **2017**, *9*, 37; doi:10.3390/polym9020037

sAB100

Table S3. Structures determined by MALDI ToF of the uncatalysed reaction of mimosa + hexamethylenediamine at 100°C.

Experimental	Calculated (Da)	Descrip. Cal (Da)	Description	Number Ionic Bonds	Number Covalent Bonds
371	372	274 + 116 − 18	F-HMDA	-	1
390	390	274 + 116	F(−)(+)HMDA	1	-
410	410	290-17 + 114 + 23	F-HMDA(−)(+)Na		1
444	444	306 + 115 + 23	G(−)(+)HMDA(−)(+)Na	1	
488	488	274 – 17 + 115 + 116	HMDA(+)(−)F-HMDA	1	1
468	468	274 + 114 × 2 – 17 × 2	(HMDA-F-HMDA) less 2H+	-	2
486	484	290 + 114 × 2 – 17 × 2	(HMDA-C-HMDA) +2H+	-	2
508	507	290 + 115 + 114 – 17 × 2 + 23	[C(HMDA)$_2$](+)(−)Na	-	2
524	524	306 + 114 + 115 – 17 – 17 + 23	(G[HMDA]$_2$)(−)(+)Na	-	2
526	525	290 + 114 + 115 – 17 + 23	HMDA-C(−)(+)HMDA(−)(+)Na	1	1
528	528	274 + 116 + 114 + 23	HMDA(+)(−)F(−)(+)HMDA(−)(+)Na	2	-
560	560	306 + 114 × 2 + 3 + 23	[G((−)(+)HMDA)$_2$](−)(+)Na	2	-
564	564	306 + 114 + 115 – 17 + 23 × 2	Na(+)(−)HMDA(+)(−)G-HMDA(−)(+)Na	1	1
567	568	274 + 115 × 3 – 17 × 3	F[HMDA]$_3$	-	3
579	578	288 + 288 + 2	Dimer	-	-
612	610	304 + 304 + 2	Dimer	-	-
619	618	306 + 115 × 2 – 17 × 2 + 116	HMDA(+)(−)G(HMDA)$_2$	1	2
622	622	306 + 115 × 2 + 114 – 17 × 3 + 23	[G(HMDA)$_3$](−)(+)Na	-	3
640	640	306 + 115 × 3 – 17 – 17 + 23	[HMDA(+)(−)G(HMDA)$_2$](−)(+)Na	1	2
643	644	272 + 272 + 2 + 114 – 17	F-F-HMDA	-	1
643	642	272 + 288 + 2 + 114 – 17 × 2	F-HMDA-C	-	2
661	660	272 + 288 + 2 + 115 – 17	F-C-HMDA	-	1
661	662	272 + 272 + 2 + 116	F-F(−)(+)HMDA	1	-
677	676	306 + 116 × 2 + 115 + 23	[HMDA(+)(−)]$_2$ G (−)(+)HMDA(−)(+)Na	3	-
679	678	272 + 288 + 2 + 116	F-C(−)(+)HMDA	1	-
683	682	272 + 288 + 2 + 114 – 17 + 23	[F-C-HMDA]	-	1
695	694	288 + 288 + 2 + 116	C-C(−)(+)HMDA	1	-
700	701	272 + 288 + 2 + 116 + 23	[F-C(−)(+)HMDA](−)(+)Na	1	-
719	717	288 + 288 + 2 + 116 + 23	[C-C(−)(+)HMDA](−)(+)Na	1	-
723	723	272 + 272 + 2 + 114 + 115 – 17 × 3	F-HMDA-F-HMDA	-	3
759	758	272 + 288 + 2 + 115 × 2 – 17 × 2	HMDA-F-C-HMDA	-	2
761	760	274 + 290 + 114 – 17 × 2 + 116	F-HMDA-C(−)(+)HMDA	1	2
761	760	272 + 272 + 2 + 115 – 17 + 116	HMDA-F-F(−)(+)HMDA	1	1
776	776	272 + 288 + 2 + 114 × 2 – 17	HMDA-F-C(−)(+)HMDA	1	1
857	857	272 + 272 + 288 + 2 + 23	Trimer	-	-
1069	1070	857 + 115 × 2 – 17	[HMDA-(F-C-F)(−)(+)HMDA](−)(+)Na	1	1

The same period of 40 Da from 801 until 350 is observed.

sAB100

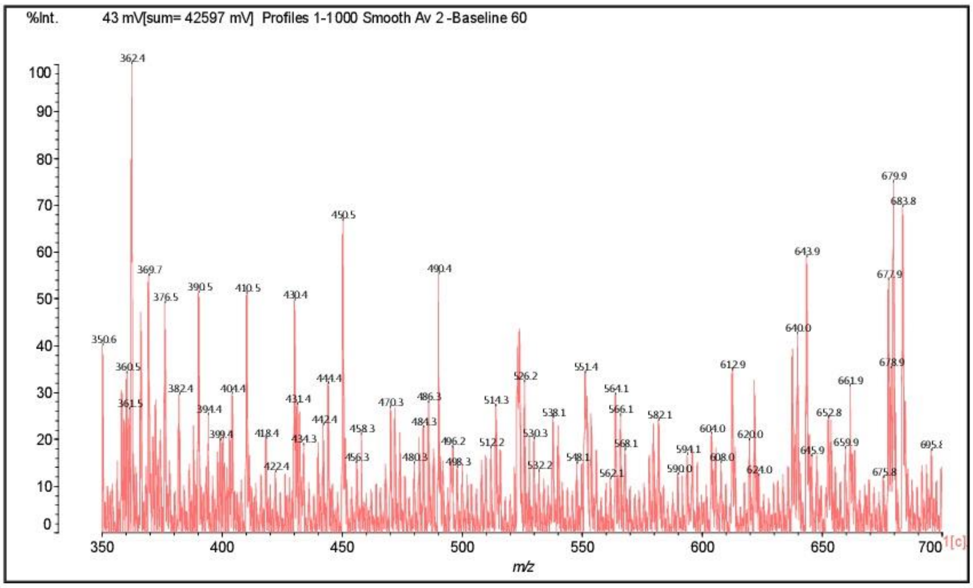

Figure S4. MALDI ToF spectrum of the uncatalysed reaction of mimosa + hexamethylenediamine at 100 °C; 350–700Da range.

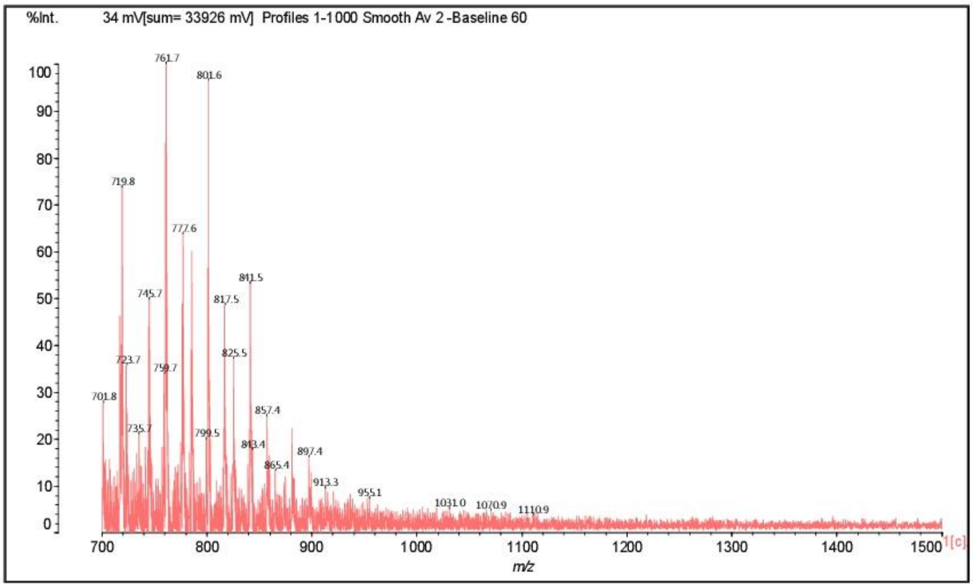

Figure S5. MALDI ToF spectrum of the uncatalysed reaction of mimosa + hexamethylenediamine at 100 °C; 700–1500 Da range.

In the three next samples, which were prepared at 65 °C, have also been found the same period of 40 Da, from 801 Da until 350 Da.

B65

Table S4. Structures determined by MALDI ToF of the reaction of mimosa + hexamethylenediamine + NaOH at 65 °C.

Experimental	Calculated (Da)	Descrip. Cal (Da)	Description	Number Ionic Bonds	Number Covalent Bonds
372	372	274 + 116 – 18	F-HMDA	-	1
390	390	274 + 116	F(−)(+)HMDA	1	-
445	444	306 + 115 + 23	G(−)(+)HMDA(−)(+)Na	1	
488	488	274 – 17 + 115 + 116	HMDA(+)(−)F-HMDA	1	1
466	468	274 + 114 × 2 – 17 × 2	(HMDA-F-HMDA) less 2H+	-	2
485	484	290 + 114 × 2 – 17 × 2	(HMDA-C-HMDA) +2H+	-	2
502	502	274 + 114 + 114	F[(−)(+)HMDA]$_2$ less 2H+	2	
507	507	290 + 115 + 114 – 17 × 2 + 23	[C(HMDA)$_2$](+)(−)Na	-	2
523	524	306 + 114 + 115 – 17 – 17 + 23	(G[HMDA]$_2$)(−)(+)Na	-	2
526	525	290 + 114 + 115 – 17 + 23	HMDA-C(−)(+)HMDA(−)(+)Na	1	1
542	542	306 + 115 × 2 – 17 + 23	[HMDA(+)(−)G-HMDA](−)(+)Na	1	1
563	562	272 + 288 + 2	Dimer	-	
563	564	306 + 114 + 115 – 17 + 23 × 2	Na(+)(−)HMDA(+)(−)G-HMDA(−)(+)Na	1	1
578	578	288 + 288 + 2	Dimer	-	-
612	610	304 + 304 + 2	Dimer	-	-
619	618	306 + 115 × 2 – 17 × 2 + 116	HMDA(+)(−)G(HMDA)$_2$	1	2
622	622	306 + 115 × 2 + 114 – 17 × 3 + 23	[G(HMDA)$_3$](−)(+)Na	-	3
643	644	272 + 114 × 3 + 2 + 23	-	3	-
643	644	272 + 272 + 2 + 114 – 17	F-F-HMDA	-	1
643	642	272 + 288 + 2 + 114 – 17 × 2	F-HMDA-C	-	2
652	654	306 + 116 × 3	G[(−)(+)HMDA]$_3$	3	-
661	660	272 + 288 + 2 + 115 – 17	F-C-HMDA	-	1
661	662	272 + 272 + 2 + 116	F-F(−)(+)HMDA	1	-
677	676	306 + 116 × 2 + 115 + 23	[HMDA(+)(−)]$_2$ G (−)(+)HMDA(−)(+)Na	3	-
678	678	272 + 288 + 2 + 116	F-C(−)(+)HMDA	1	-
683	682	272 + 288 + 2 + 114 – 17 + 23	[F-C-HMDA]	-	1
693	694	288 + 288 + 2 + 116	C-C(−)(+)HMDA	1	-
700	701	272 + 288 + 2 + 116 + 23	[F-C(−)(+)HMDA](−)(+)Na	1	-
719	717	288 + 288 + 2 + 116 + 23	[C-C(−)(+)HMDA](−)(+)Na	1	-
723	723	272 + 272 + 2 + 114 + 115 – 17 × 3	F-HMDA-F-HMDA	-	3
759	758	272 + 288 + 2 + 115 × 2 – 17 × 2	HMDA-F-C-HMDA	-	2
761	760	274 + 290 + 114 – 17 × 2 + 116	F-HMDA-C(−)(+)HMDA	1	2
761	760	272 + 272 + 2 + 115 – 17 + 116	HMDA-F-F(−)(+)HMDA	1	1
776	776	272 + 288 + 2 + 114 × 2 – 17	HMDA-F-C(−)(+)HMDA	1	1
857	857	272 + 272 + 288 + 2 + 23	Trimer	-	-
865	866	272 + 288 + 304 + 2	Trimer	-	-
908	905	288 × 2 + 304 + 2 + 23	Trimer	-	-

Polymers **2017**, *9*, 37; doi:10.3390/polym9020037

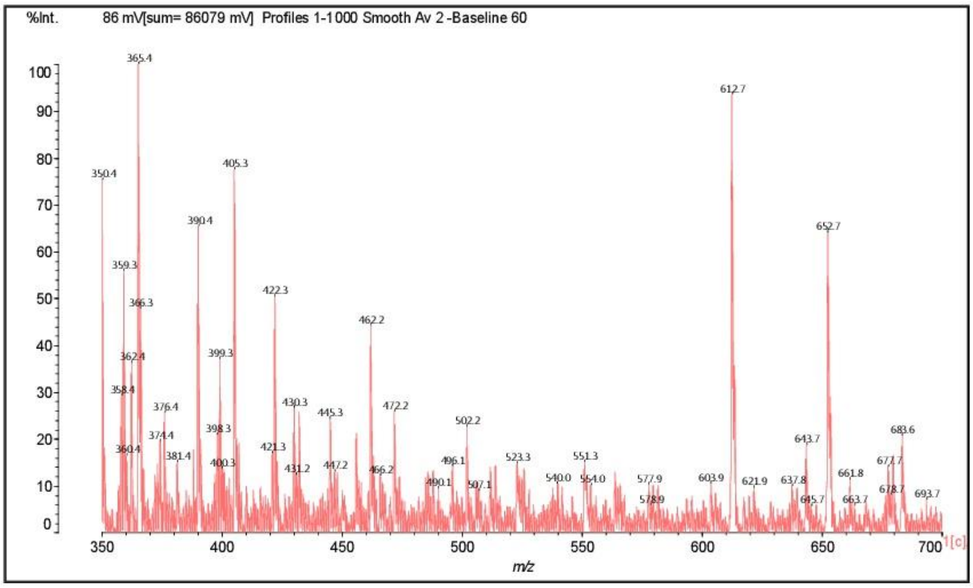

Figure S6. MALDI ToF spectrum of the reaction of mimosa + hexamethylenediamine + NaOH at 65 °C; 350–700 Da range.

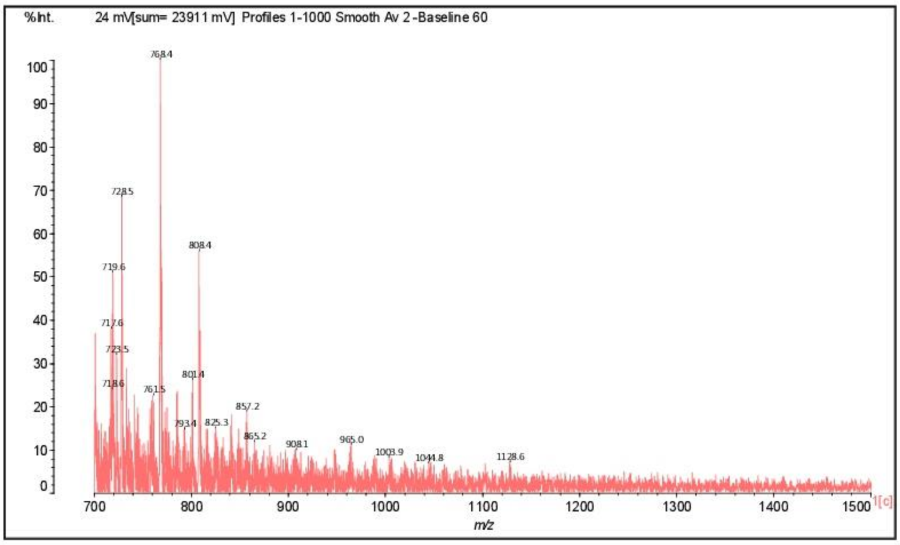

Figure S7. MALDI ToF spectrum of the reaction of mimosa + hexamethylenediamine + NaOH at 65 °C; 700–1500 Da range.

A65

Table S5. Structures determined by MALDI ToF of the reaction of mimosa + hexamethylenediamine + pTSA at 65 °C.

Experimental	Calculated (Da)	Descrip. Cal (Da)	Description	Number Ionic Bonds	Number Covalent Bonds
372	372	274 + 116 – 18	F-HMDA	-	1
390	390	274 + 116	F(−)(+)HMDA	1	-
410	410	290 – 17 + 114 + 23	F-HMDA(−)(+)Na		1
412	412	274 + 115 + 23	F(−)(+)HMDA(−)(+)Na	1	-
428	428	290 + 115 + 23	C(−)(+)HMDA(−)(+)Na	1	-

446	444	306 + 115 + 23	G(−)(+)HMDA(−)(+)Na	1	-
488	488	274 – 17 + 115 + 116	HMDA(+)(−)F-HMDA	1	1
486	486	290 + 115 × 2 – 17 × 2	(HMDA-C-HMDA)	-	2
501	500	304 + 2 + 114 × 2 – 17 – 17	(HMDA-G-HMDA) less 2H+	-	2
526	524	306 + 114 + 115 – 17 – 17 + 23	(G[HMDA]$_2$)(−)(+)Na	-	2
526	525	290 + 114 + 115 – 17 + 23	HMDA-C(−)(+)HMDA(−)(+)Na	1	1
540	542	306 + 115 × 2 – 17 + 23	[HMDA(+)(−)G-HMDA](−)(+)Na	1	1
568	568	274 + 115 × 3 – 17 – 17 – 17	F(HMDA)$_3$	-	3
612	610	304 + 304 + 2	Dimer	-	-
623	622	306 + 115 × 2 + 114 – 17 × 3 + 23	[G(HMDA)$_3$](−)(+)Na	-	3
639	640	306 + 115 × 3 – 17 – 17 + 23	[HMDA(+)(−)G(HMDA)$_2$](−)(+)Na	1	2
643	644	274 + 116 × 3 + 23 – 1	[F((−)(+)HMDA)$_3$](−)(+)Na	3	-
643	644	272 + 272 + 2 + 114 – 17	F-F-HMDA	-	1
642	642	272 + 288 + 2 + 114 – 17 × 2	F-HMDA-C	-	2
655	654	306 + 116 × 3	G[(−)(+)HMDA]$_3$	3	-
659	658	306 + 116 × 3 – 18 + 23 – 1	[HMDA-G((−)(+)HMDA)$_2$](−)(+)Na	2	1
659	660	272 + 288 + 2 + 115 – 17	F-C-HMDA	-	1
661	662	272 + 272 + 2 + 116	F-F(−)(+)HMDA	1	-
677	676	306 + 116 × 2 + 115 + 23	[HMDA(+)(−)]$_2$ G (−)(+)HMDA(−)(+)Na	3	-
679	678	272 + 288 + 2 + 116	F-C(−)(+)HMDA	1	-
682	682	272 + 288 + 2 + 114 – 17 + 23	[F-C-HMDA]	-	1
695	694	288 + 288 + 2 + 116	C-C(−)(+)HMDA	1	-
723	723	272 + 272 + 2 + 114 + 115 – 17 × 3	F-HMDA-F-HMDA	-	3
723	724	274 + 116 × 4 – 18 × 2 + 23 – 1	[(HMDA)$_2$F((−)(+)HMDA)$_2$](−)(+)Na	2	2
745	744	274 + 274 + 114 + 116 – 17 × 2	F-HMDA-F(−)(+)HMDA	-	-
740-743	742	274 + 274 + 2 + 115 × 2 – 17 × 2	HMDA-F-F-HMDA	-	2
759	758	272 + 288 + 2 + 115 × 2 – 17 × 2	HMDA-F-C-HMDA	-	2
761	760	274 + 290 + 114 – 17 × 2 + 116	F-HMDA-C(−)(+)HMDA	1	2
761	760	272 + 272 + 2 + 115 – 17 + 116	HMDA-F-F(−)(+)HMDA	1	1
777	776	272 + 288 + 2 + 115 – 17 + 116	HMDA-F-C(−)(+)HMDA	1	1
857	857	272 + 272 + 288 + 2 + 23	Trimer	-	-
865	866	272 + 288 + 304 + 2	Trimer	-	-
897	898	272 × 2 + 2 + 114 × 3 – 17 + 23	[(HMDA(+)(−))$_2$ F-F-HMDA](−)(+)Na	2	1
897	898	288 + 304 × 2 + 2	Trimer	-	-
906	905	288 × 2 + 304 + 2 + 23	Trimer	-	-
925	921	288 + 304 × 2 + 2 + 23	Trimer	-	-

Polymers **2017**, *9*, 37; doi:10.3390/polym9020037

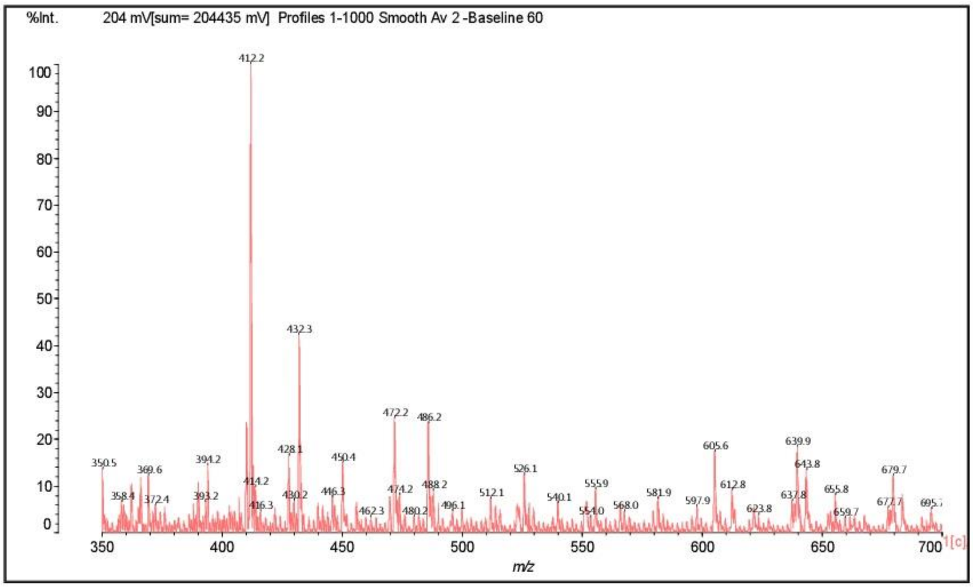

Figure S8. MALDI ToF spectrum of the reaction of mimosa + hexamethylenediamine + pTSA at 65 °C; 350–700 Da range.

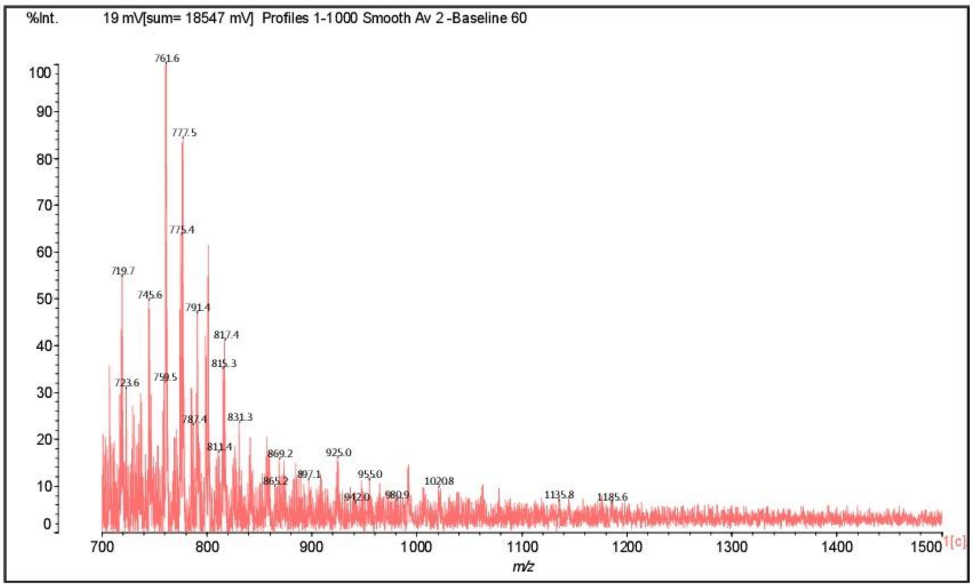

Figure S9. MALDI ToF spectrum of the reaction of mimosa + hexamethylenediamine + pTSA at 65 °C; 700–1500 Da range.

Polymers **2017**, *9*, 37; doi:10.3390/polym9020037

sAB65

Table S6. Structures determined by MALDI ToF of the uncatalysed reaction of mimosa + hexamethylenediamine at 65 °C.

Experimental	Calculated (Da)	Descrip. Cal (Da)	Description	Number Ionic Bonds	Number Covalent Bonds
390	390	274 + 116	F(−)(+)HMDA	1	-
410	410	290 − 17 + 114 + 23	F-HMDA(−)(+)Na	-	1
444	444	306 + 115 + 23	G(−)(+)HMDA(−)(+)Na	1	-
488	488	274 − 17 + 115 + 116	HMDA(+)(−)F-HMDA	1	1
468	468	274 + 114 × 2 − 17 × 2	(HMDA-F-HMDA) less 2H+	-	2
486	486	290 + 115 × 2 − 17 × 2	(HMDA-C-HMDA)	-	2
508	508	290 + 115 × 2 − 17 × 2 + 23 − 1	[C(HMDA)$_2$](−)(+)Na	-	2
524	524	306 + 114 + 115 − 17 − 17 + 23 − 1	(G[HMDA]$_2$)(−)(+)Na	-	2
526	525	290 + 114 + 115 − 17 + 23	HMDA-C(−)(+)HMDA(−)(+)Na	1	1
528	528	274 + 116 + 114 + 23	HMDA(+)(−)F(−)(+)HMDA(−)(+)Na	2	
560	560	306 + 116 × 2 + 23 − 1	[G((−)(+)HMDA)$_2$](−)(+)Na	2	-
566	568	274 + 115 × 3 − 17 − 17 − 17	F(HMDA)$_3$	-	3
580	578	288 + 288 + 2	Dimer	-	-
612	610	304 + 304 + 2	Dimer	-	-
619	618	306 + 115 × 2 − 17 × 2 + 116	HMDA(+)(−)G(HMDA)$_2$	1	2
621	622	306 + 115 × 2 + 114 − 17 × 3 + 23	[G(HMDA)$_3$](−)(+)Na	-	3
639	640	306 + 115 × 3 − 17 − 17 + 23	[HMDA(+)(−)G(HMDA)$_2$](−)(+)Na	1	2
643	644	274 + 116 × 3 + 23 − 1	[F((−)(+)HMDA)$_3$](−)(+)Na	3	-
643	644	272 + 272 + 2 + 114 − 17	F-F-HMDA	-	1
642	642	272 + 288 + 2 + 114 − 17 × 2	F-HMDA-C	-	2
653	654	306 + 116 × 3	G[(−)(+)HMDA]$_3$	3	-
661	660	272 + 288 + 2 + 115 − 17	F-C-HMDA	-	1
661	662	272 + 272 + 2 + 116	F-F(−)(+)HMDA	1	-
677	676	306 + 116 × 2 + 115 + 23	[HMDA(+)(−)]$_2$ G (−)(+)HMDA(−)(+)Na	3	-
679	678	272 + 288 + 2 + 116	F-C(−)(+)HMDA	1	-
683	682	272 + 288 + 2 + 114 − 17 + 23	[F-C-HMDA]	-	1
695	694	288 + 288 + 2 + 116	C-C(−)(+)HMDA	1	-
719	717	288 + 288 + 2 + 116 + 23	[C-C(−)(+)HMDA](−)(+)Na	1	-
723	723	272 + 272 + 2 + 114 + 115 − 17 × 3	F-HMDA-F-HMDA	-	3
723	724	274 + 116 × 4 − 18 × 2 + 23 − 1	[(HMDA)$_2$F((−)(+)HMDA)$_2$](−)(+)Na	2	2
759	758	272 + 288 + 2 + 115 × 2 − 17 × 2	HMDA-F-C-HMDA	-	2
761	760	274 + 290 + 114 − 17 × 2 + 116	F-HMDA-C(−)(+)HMDA	1	2
761	760	272 + 272 + 2 + 115 − 17 + 116	HMDA-F-F(−)(+)HMDA	1	1
777	776	272 + 288 + 2 + 115 − 17 + 116	HMDA-F-C(−)(+)HMDA	1	1
857	857	272 + 272 + 288 + 2 + 23	Trimer	-	-
1366	1368	288 × 2 + 2 + 116 × 2 − 18 × 3 + 304 × 2 + 2 (Or 288 × 4 + 2 + 116 × 2 − 18)	C-G-HMDA-C-G-HMDA or HMDA-C-C-C-C(−)(+)HMDA	-	3
1480	1482	288 × 2 + 304 × 2 + 2 + 116 × 3 − 18 × 3	(G-C-C-G)(HMDA)$_3$	-	3

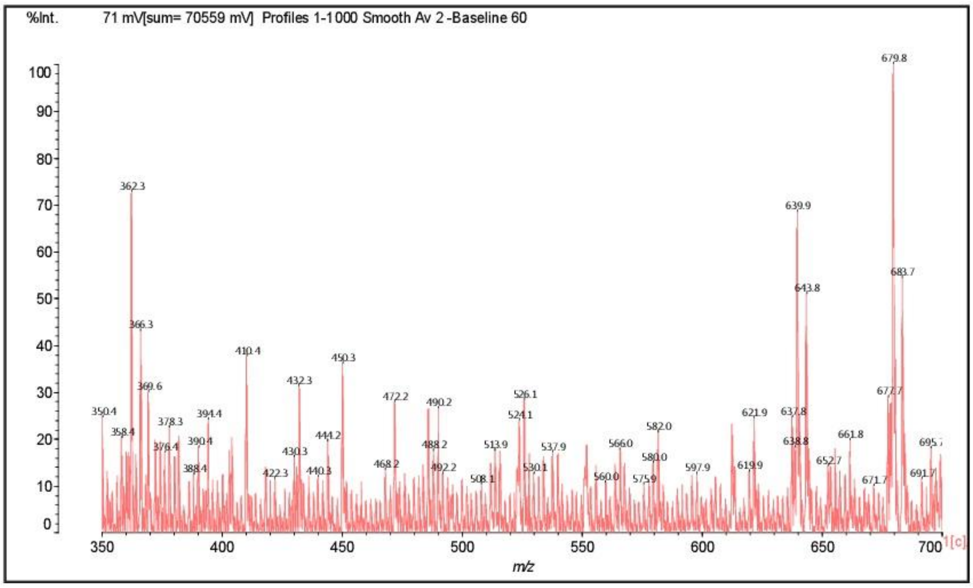

Figure S10. MALDI ToF spectrum of the uncatalysed reaction of mimosa + hexamethylenediamine at 65 °C; 350–700 Da range.

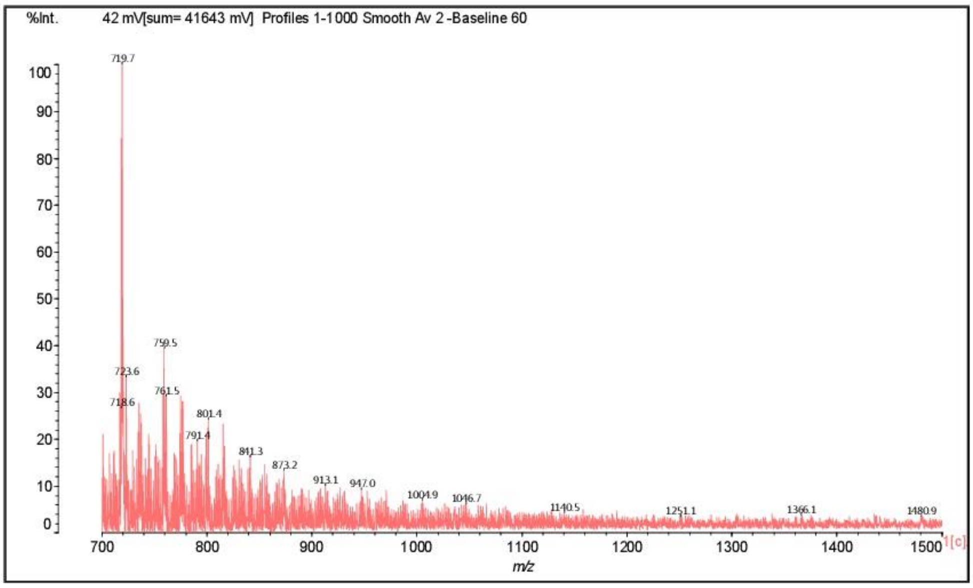

Figure S11. MALDI ToF spectrum of the uncatalysed reaction of mimosa + hexamethylenediamine at 65 °C; 700–1500 Da range.

Polymers **2017**, *9*, 37; doi:10.3390/polym9020037 S13 of S25

2. Catechin Model Compound Reactions

[M+Na$^+$] = Cat (288 Da) + HMDA (114 Da) + 2H (end group) + 23 Na$^+$
Cat = catechin
HMDA = hexamethylenediamine

sAB185

Table S7. Structures determined by MALDI ToF of the uncatalysed reaction of catechin monomer + hexamethylenediamine at 185 °C.

Experimental [Mn + Na$^+$] (on the Graph) (Da)	Calculated [Mn + Na$^+$] (Da)	Description
23.1	23	Na$^+$
39.1	35.5	Cl$^-$
117	116	HMDA
137	139	HMDA + Na$^+$
289.9	290	Cat
315.8	313	Cat + Na$^+$
370.7	367	3× HMDA + Na$^+$
401.8	404	Cat + HMDA
428.8	427	Cat + HMDA + Na$^+$
522.5	518	HMDA + Cat + HMDA
544.5	541	HMDA + Cat + HMDA + Na$^+$
698.6	692	Cat + HMDA + Cat
711.4	709	6× HMDA + Na$^+$
888.8	889	Cat + Cat + Cat + Na$^+$
1103.2	1096	Cat + HMDA + Cat + HMDA + Cat
1220.5	1208	Cat + HMDA + Cat + HMDA + Cat + HMDA
1279.4	1268	Cat + Cat + HMDA + Cat + Cat
1397.6	1405	Cat + HMDA + Cat + Cat + HMDA + Cat + Na$^+$
1454.7	1459	HMDA +Cat + HMDA + Cat + HMDA + Cat + HMDA + HMDA + Na$^+$
1513.9	1519	Cat + HMDA + Cat + HMDA + Cat +HMDA + Cat + Na$^+$

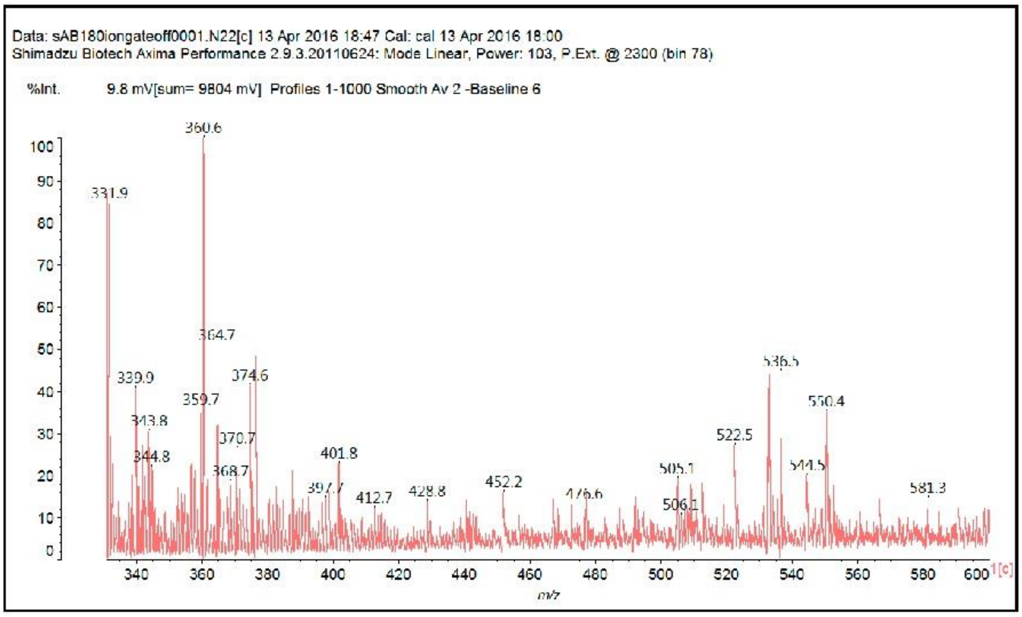

Figure S12. MALDI ToF of the uncatalysed reaction of catechin monomer + hexamethylenediamine at 185 °C; 330–600 Da range.

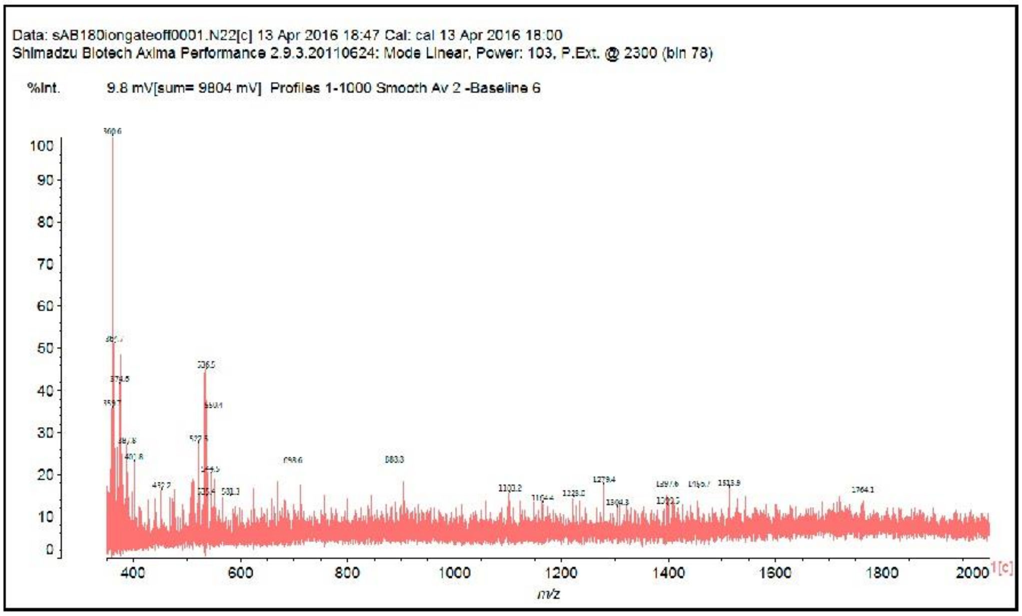

Figure S13. MALDI ToF of the uncatalysed reaction of catechin monomer + hexamethylenediamine at 185 °C; 350–2000 Da range.

sAB100

Table S8. Structures determined by MALDI ToF of the uncatalysed reaction of catechin monomer + hexamethylenediamine at 100 °C.

Experimental [Mn + Na⁺] (on the Graph) (Da)	Calculated [Mn + Na⁺] (Da)	Description
23.0	23	Na^+
38.9	35.5	Cl^-
117.2	116	HMDA
137.1	139	HMDA + Na^+
289.9	290	Cat
314.7	313	Cat + Na^+
368.6	367	3 × HMDA + Na^+
424.7	427	Cat + HMDA + Na^+
520.8	518	HMDA + Cat + HMDA
540.8–546.6	541	HMDA + Cat + HMDA + Na^+
719.6	715	Cat + HMDA + Cat + Na^+
893	889	Cat + Cat + Cat + Na^+
1087	1094	Cat + HMDA + Cat + HMDA + Cat
1221.7	1208	Cat + HMDA + Cat + HMDA + Cat + HMDA
1338.8	1345	HMDA + Cat + HMDA + Cat + HMDA + Cat + HMDA + Na^+
1397.3	1382	Cat + HMDA + Cat + Cat + HMDA + Cat
1455.2	1459	HMDA + Cat + HMDA + Cat + HMDA + Cat + HMDA + HMDA + Na^+
1746.7	1745	HMDA + Cat + HMDA + Cat + HMDA + Cat + HMDA + Cat + HMDA + Na^+

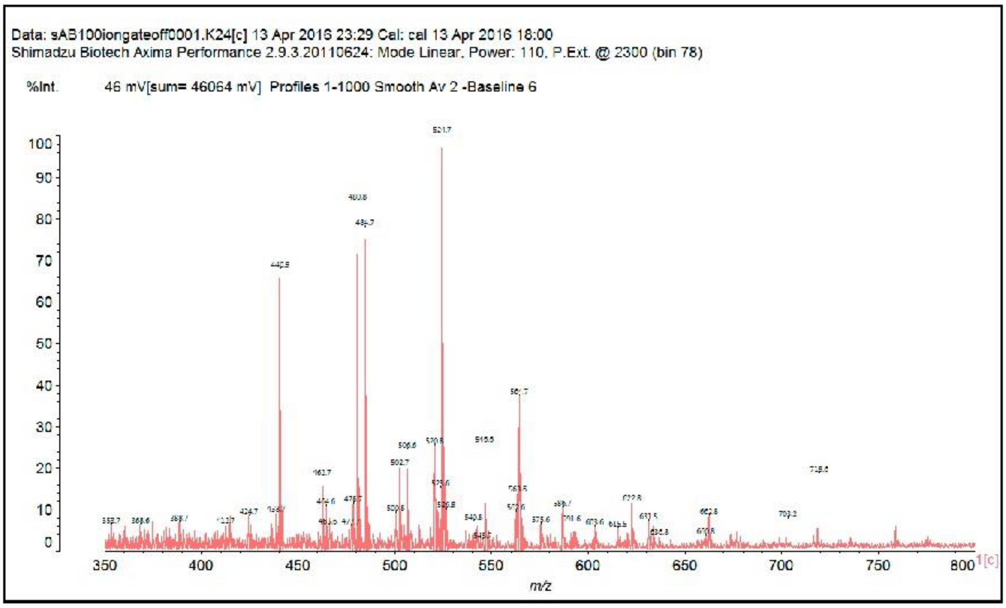

Figure S14. MALDI ToF spectrum of the uncatalysed reaction of catechin monomer + hexamethylenediamine at 100 °C; 350–800 Da range.

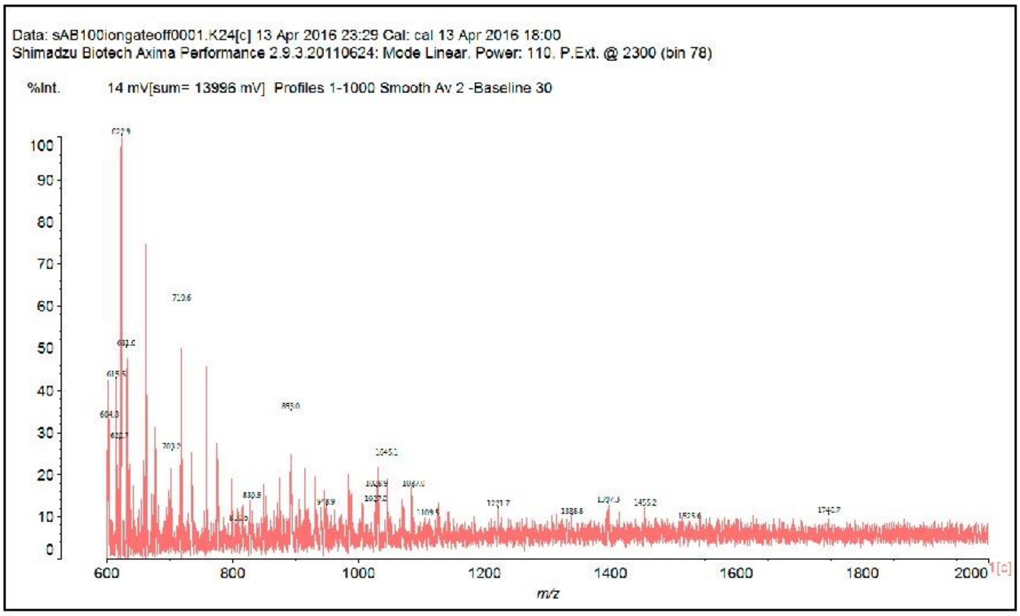

Figure S15. MALDI ToF spectrum of the uncatalysed reaction of catechin monomer + hexamethylenediamine at 100 °C; 600–2000 Da range.

sAB65

Table S9. Structures determined by MALDI ToF of the uncatalysed reaction of catechin monomer + hexamethylenediamine at 65 °C.

Experimental [Mn + Na⁺] (on the Graph) (Da)	Calculated [Mn + Na⁺] (Da)	Description
23.1	23	Na^+
39.1	35.5	Cl^-
117.2	116	HMDA
137	139	HMDA + Na^+
280	290	Cat
317	313	Cat + Na^+
344.9	344	3× HMDA
368.1	367	3 × HMDA + Na^+
399.1	404	Cat + HMDA
428.8	427	Cat + HMDA + Na^+
522.9	518	HMDA + Cat + HMDA
542.9	541	HMDA + Cat + HMDA + Na^+
576.9	572	5 × HMDA
702	692	Cat + HMDA + Cat
811.9	806	Cat + HMDA + Cat + HMDA
895	889	Cat + Cat + Cat + Na^+
919	922	HMDA + Cat + HMDA + Cat + HMDA
1033.2	1028	9 × HMDA

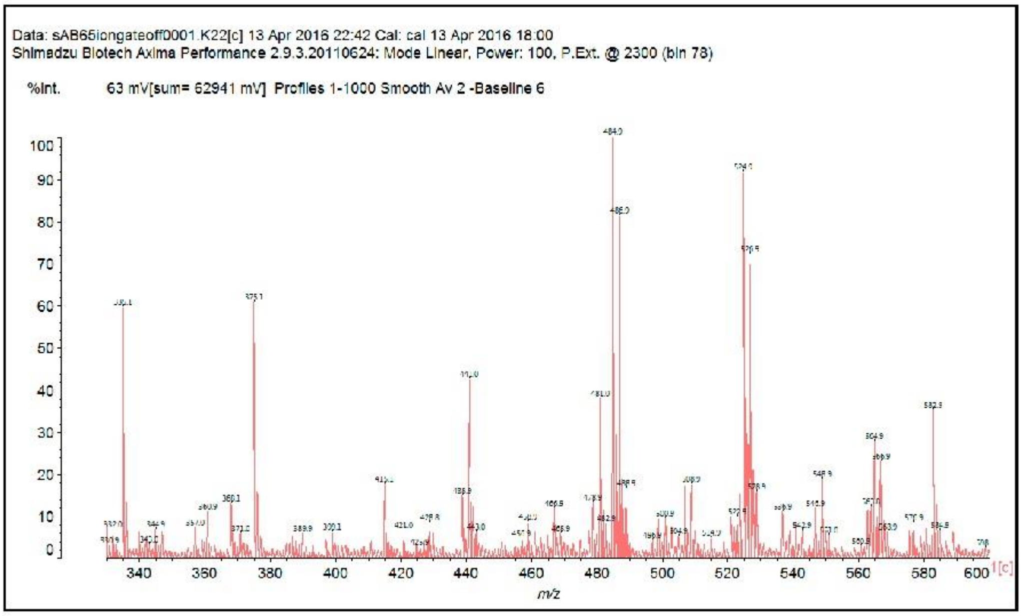

Figure S16. MALDI ToF spectrum of the uncatalysed reaction of catechin monomer + hexamethylenediamine at 65 °C; 330–600 Da range.

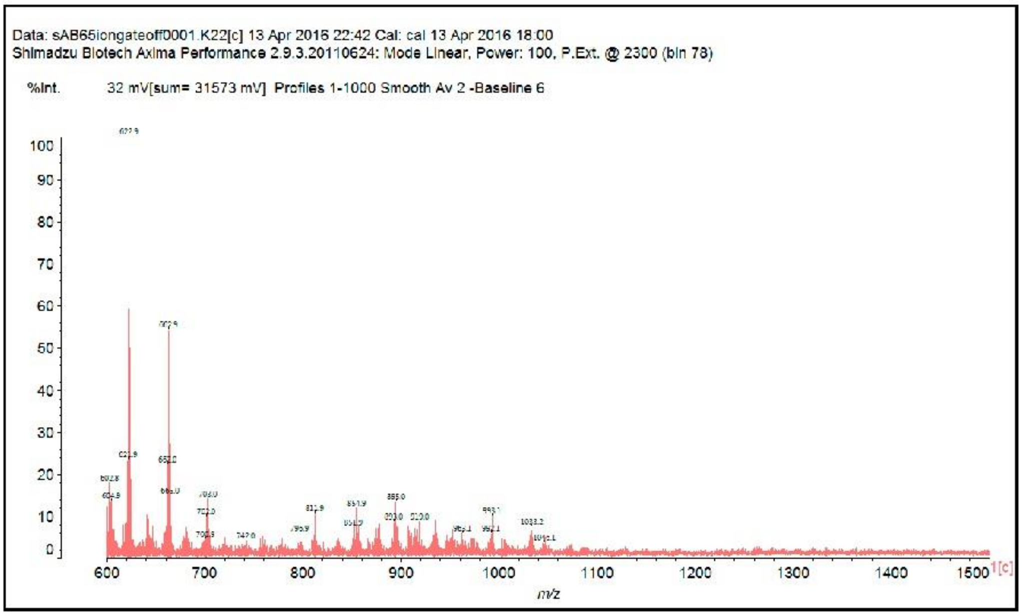

Figure S17. MALDI ToF spectrum of the uncatalysed reaction of catechin monomer + hexamethylenediamine at 65 °C; 600–1500 Da range.

B180

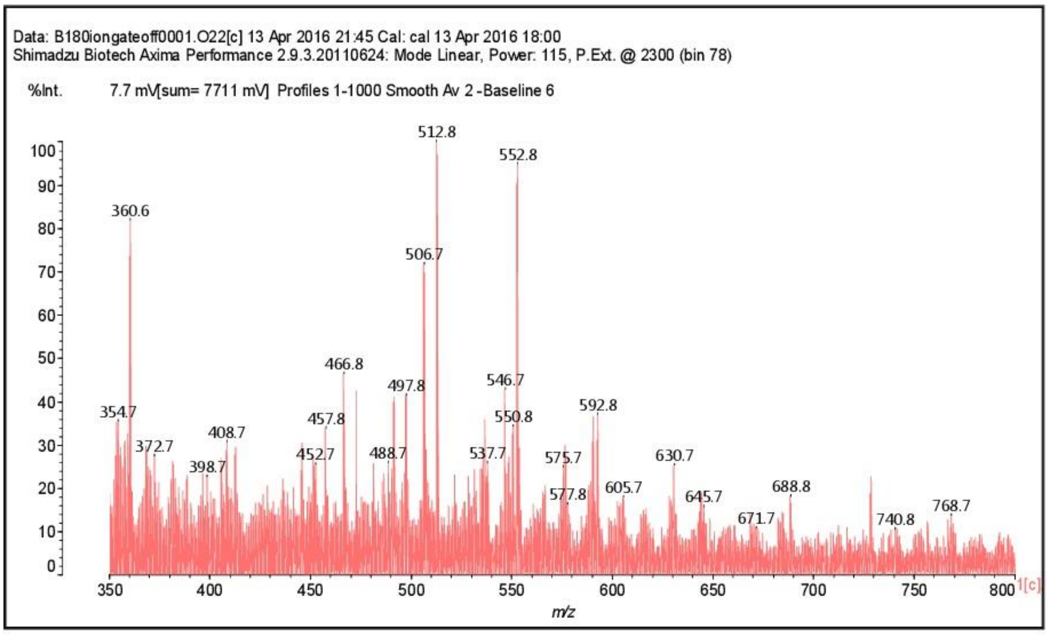

Figure S18. MALDI ToF spectrum of the reaction of catechin monomer + hexamethylenediamine + NaOH at 185 °C; 350–800 Da range.

B180

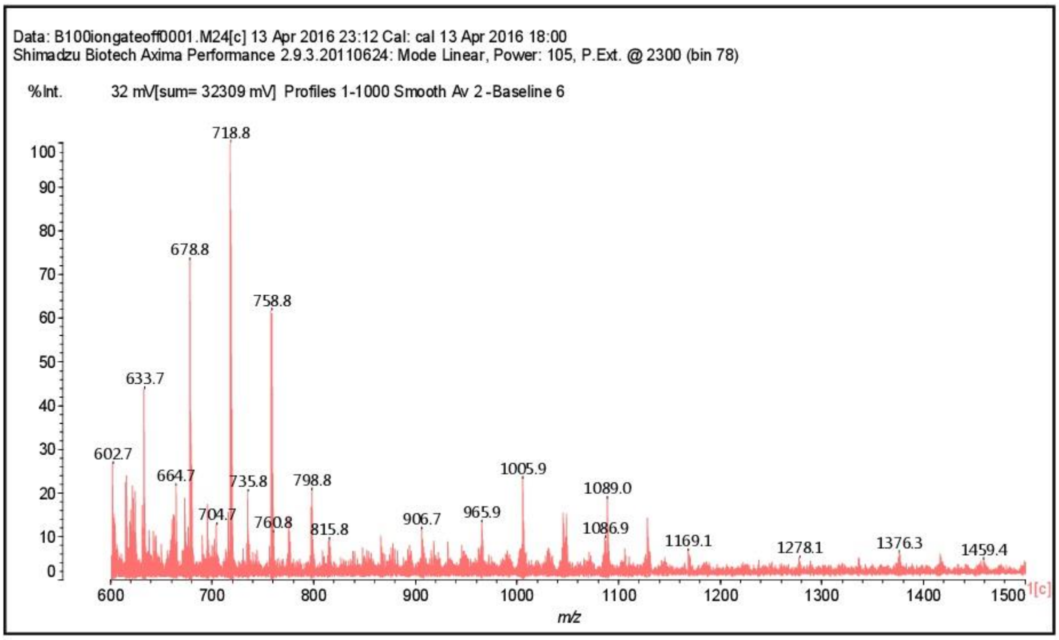

Figure S19. MALDI ToF spectrum of the reaction of catechin monomer + hexamethylenediamine + NaOH at 185 °C; 600-1500 Da range.

B100

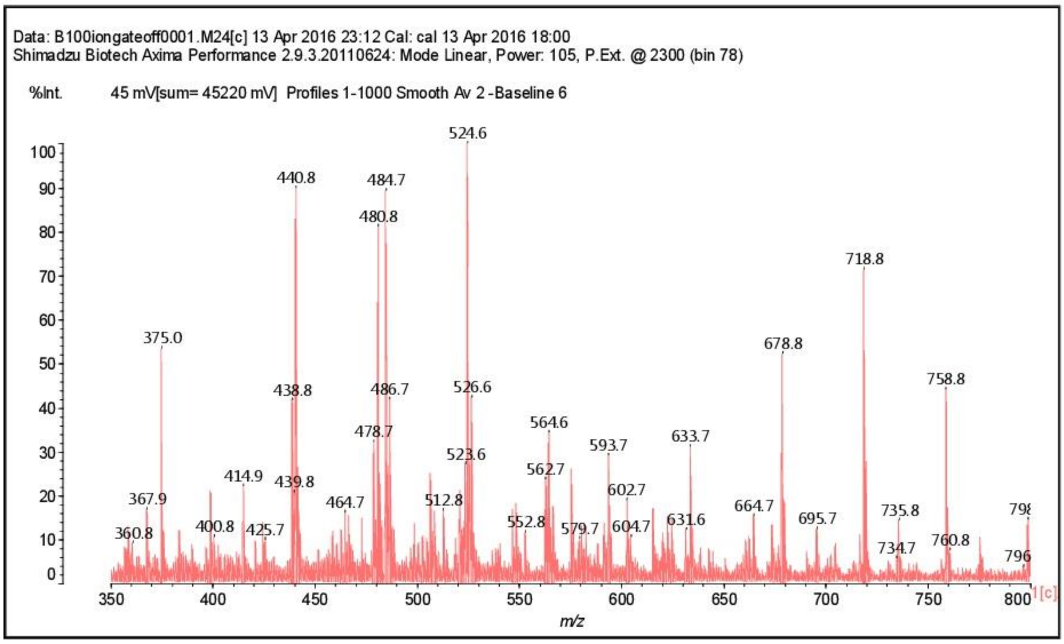

Figure S20. MALDI ToF spectrum of the reaction of catechin monomer + hexamethylenediamine + NaOH at 100 °C; 350–800 Da range.

B100

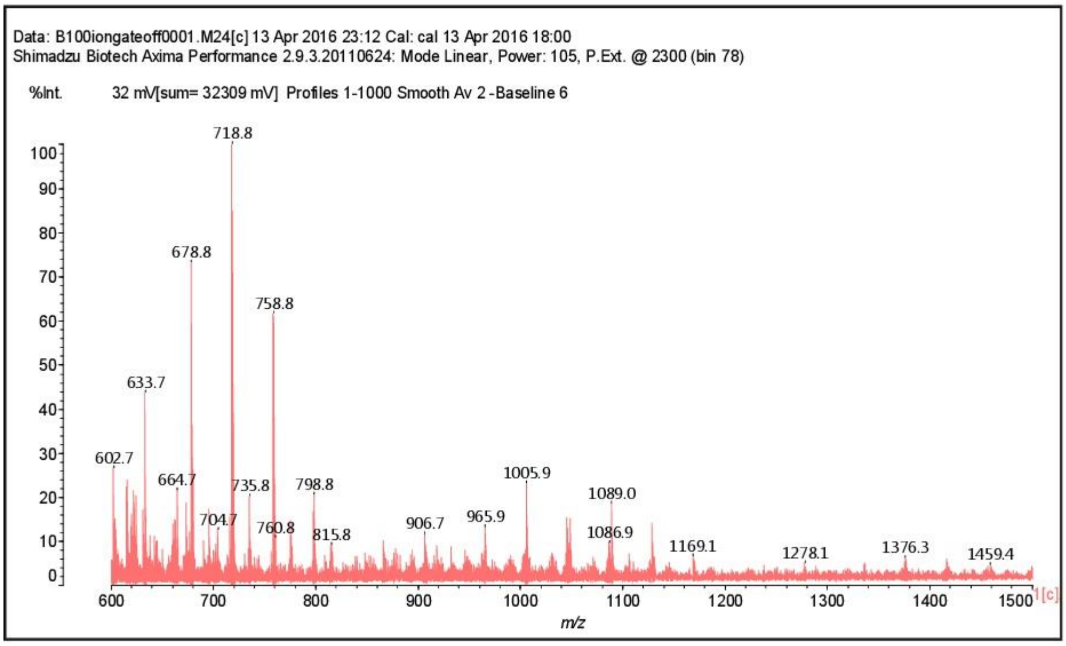

Figure S21. MALDI ToF spectrum of the reaction of catechin monomer + hexamethylenediamine + NaOH at 100 °C; 600 – 1500 Da range.

B65

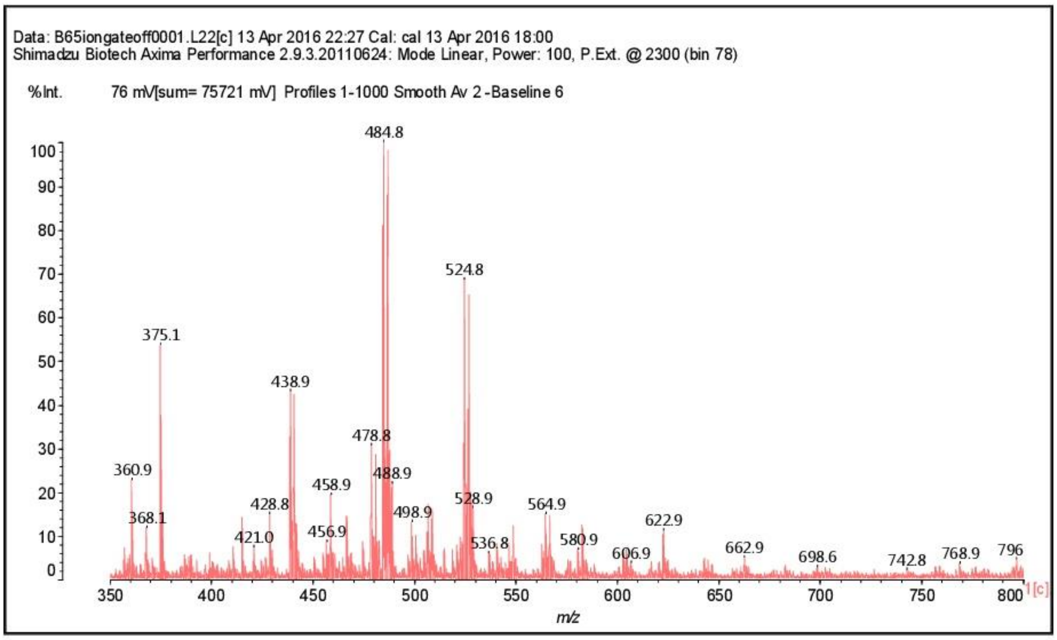

Figure S22. MALDI ToF spectrum of the reaction of catechin monomer + hexamethylenediamine + NaOH at 65 °C; 350–800Da range.

B65

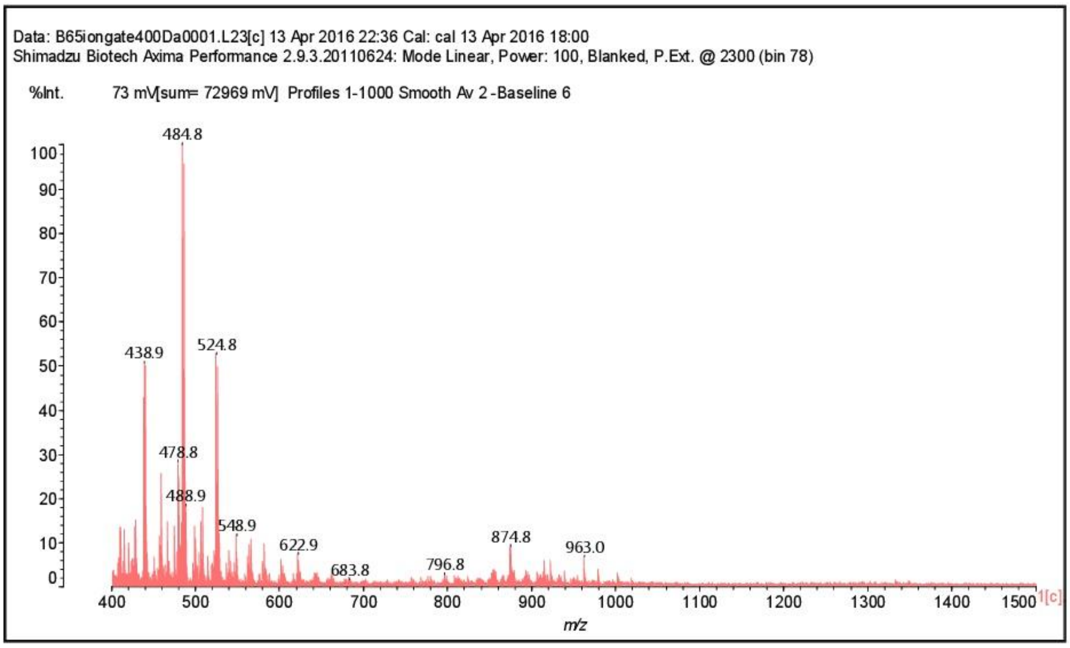

Figure S23. MALDI ToF spectrum of the reaction of catechin monomer + hexamethylenediamine + NaOH at 65 °C; 600–1500 Da range.

A180

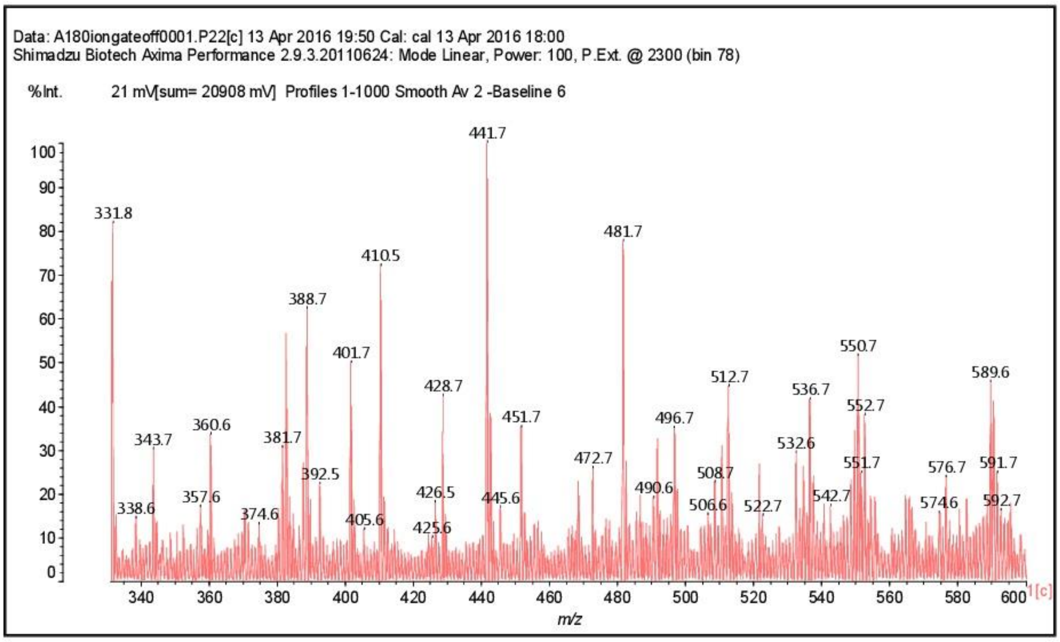

Figure S24. MALDI ToF spectrum of the reaction of catechin monomer + hexamethylenediamine + pTSA at 185 °C; 350-800 Da range.

Polymers **2017**, *9*, 37; doi:10.3390/polym9020037

A100

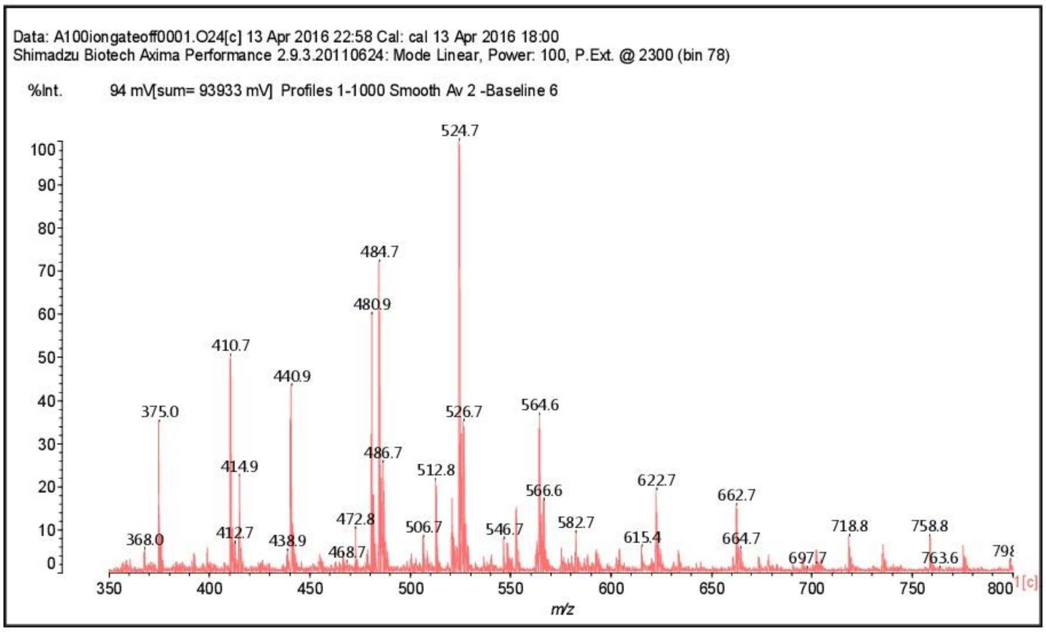

Figure S25. MALDI ToF spectrum of the reaction of catechin monomer + hexamethylenediamine + pTSA at 100 °C. 350–800 Da range.

A100

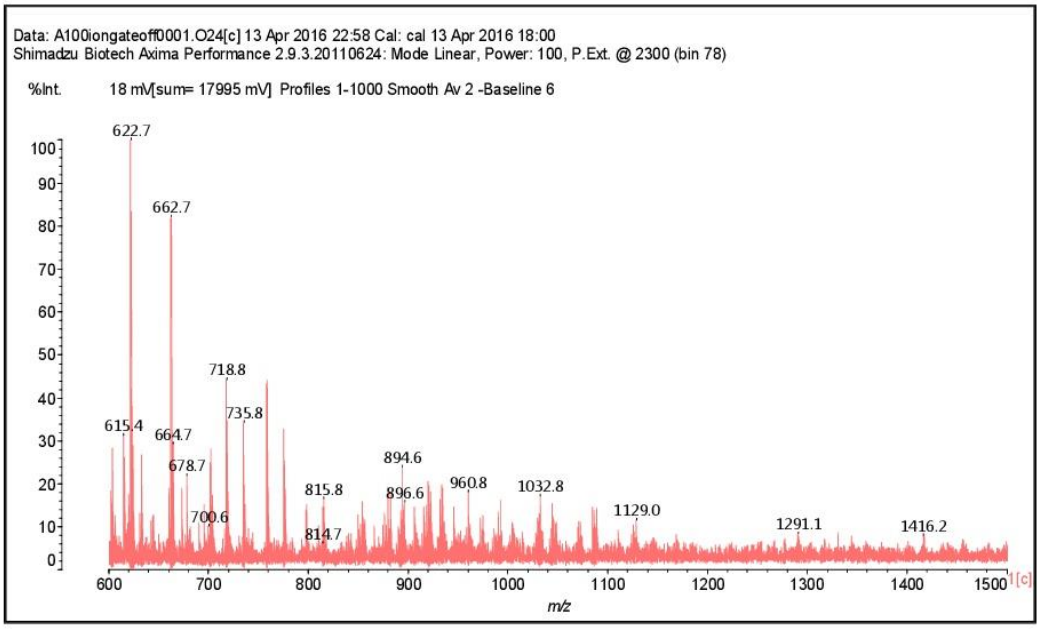

Figure S26. MALDI ToF spectrum of the reaction of catechin monomer + hexamethylenediamine + pTSA at 100 °C; 600–1500 Da range.

A65

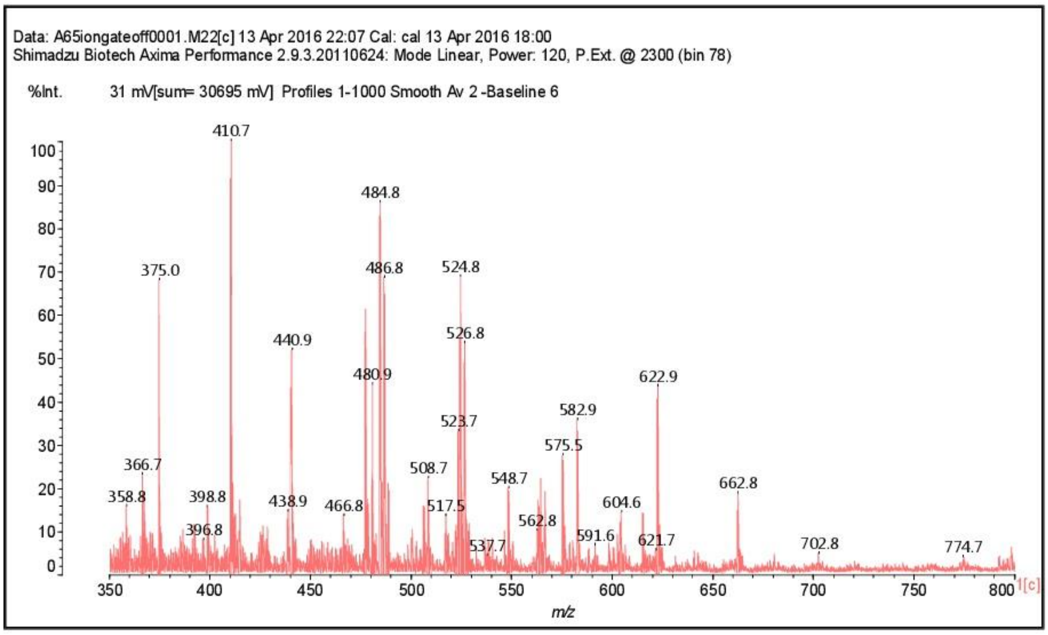

Figure S27. MALDI ToF spectrum of the reaction of catechin monomer + hexamethylenediamine + pTSA at 65 °C; 350–800 Da range.

A65

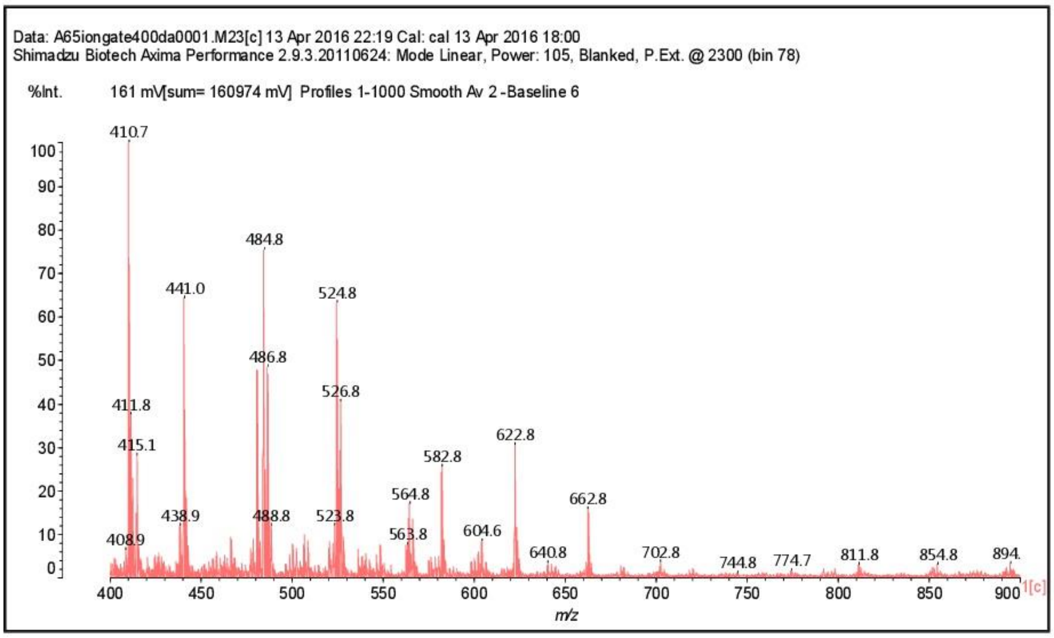

Figure S28. MALDI ToF spectrum of the reaction of catechin monomer + hexamethylenediamine + pTSA at 65 °C; 400–900 Da range.

CP MAS ^{13}C NMR
Catechin A180

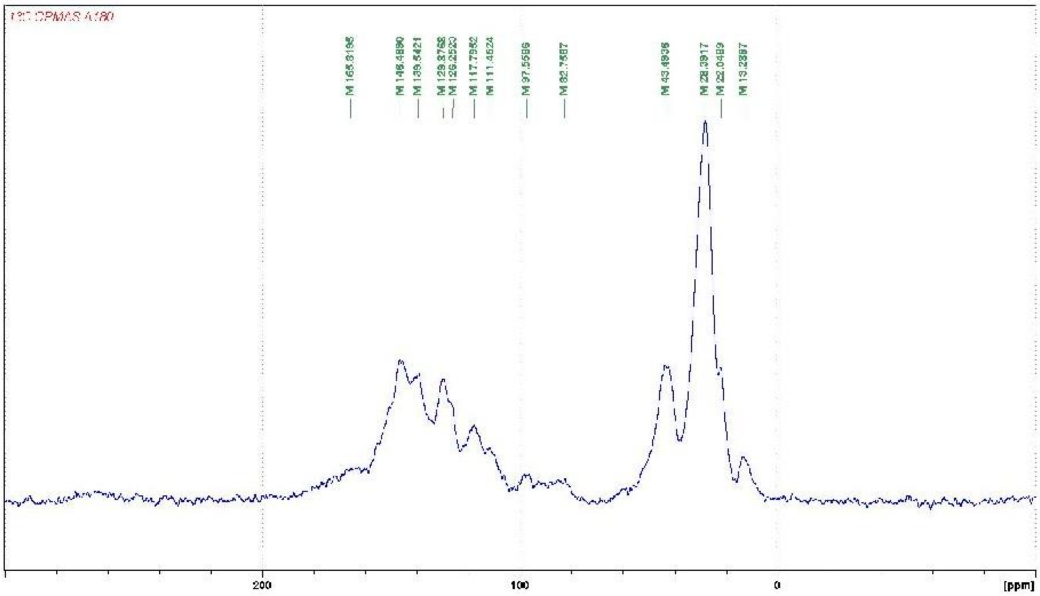

Figure S29. CP MAS ^{13}C NMR spectrum of the reaction of catechin monomer + hexamethylenediamine + pTSA at 185 °C.

Catechin A 100

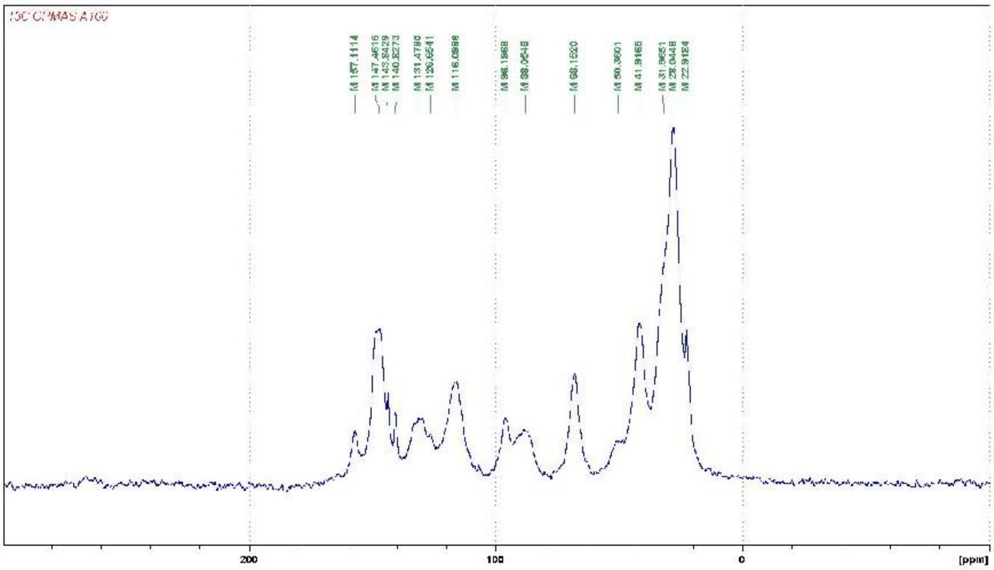

Figure S30. CP MAS ^{13}C NMR spectrum of the reaction of catechin monomer + hexamethylenediamine + pTSA at 100 °C.

Catechin B180

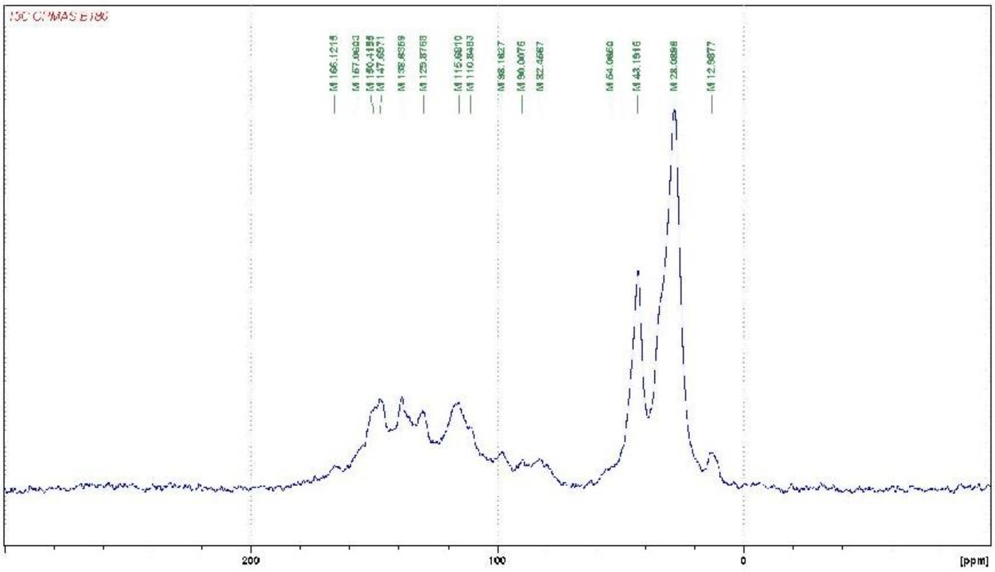

Figure S31. CP MAS [13]C NMR spectrum of the reaction of catechin monomer + hexamethylenediamine + NaOH at 185 °C.

Catechin B100

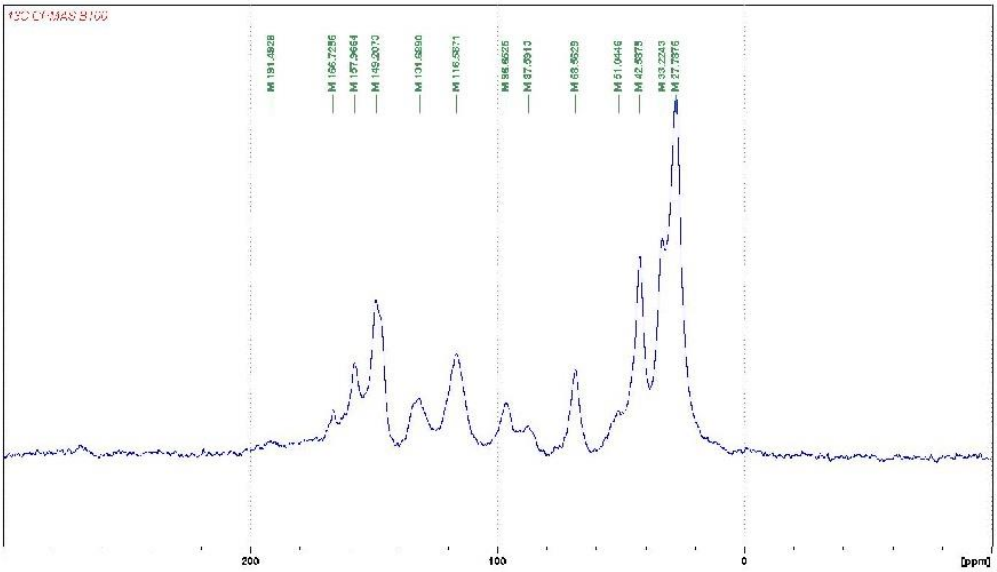

Figure S32. CP MAS [13]C NMR spectrum of the reaction of catechin monomer + hexamethylenediamine + NaOH at 100 °C.

Catechin SAB 180

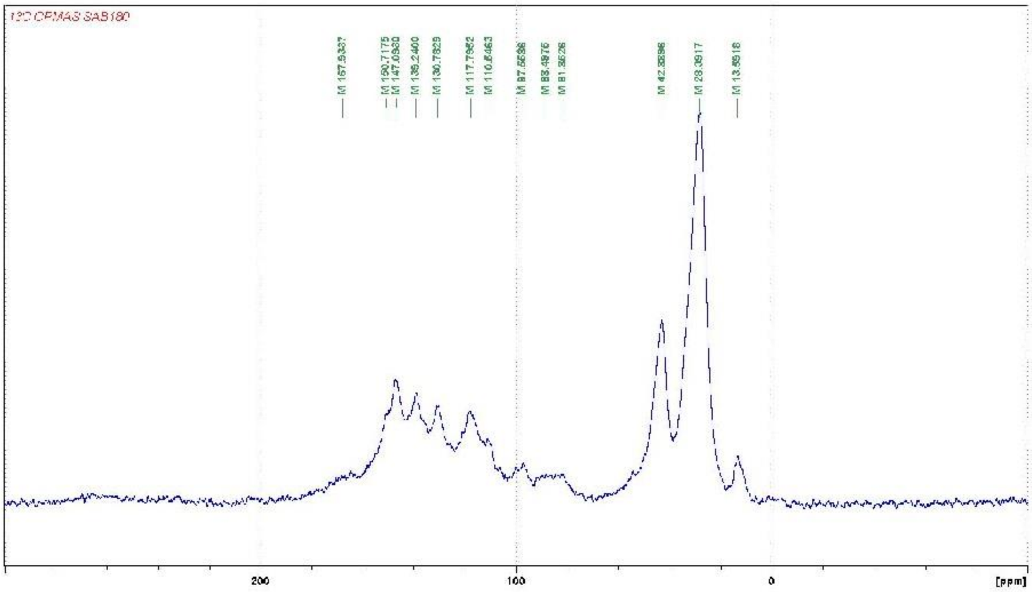

Figure S33. CP MAS ^{13}C NMR spectrum of the uncatalysed reaction of catechin monomer + hexamethylenediamin at 185 °C.

Catechin SAB100

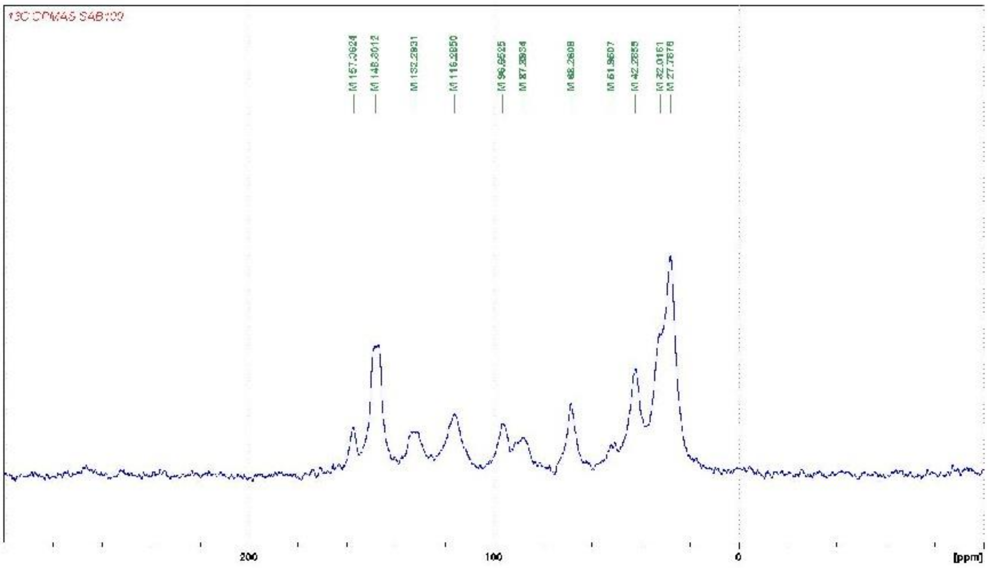

Figure S34. CP MAS ^{13}C NMR spectrum of the uncatalysed reaction of catechin monomer + hexamethylenediamin at 100 °C.

3 « Polycondensation resins by lignin reaction with (poly)amines »

Auteurs: F.J. Santiago-Medina[1], A. Pizzi[1,2], M.C. Basso[1], L. Delmotte[3] et S. Abdalla[2]

[1] LERMAB, University of Lorraine, ENSTIB, 27 rue Philippe Seguin, 88000 Epinal, France

[2] Department of Physics, King Abdulaziz University, Jeddah, Saudi Arabia

[3] IS2M, Institut de Science des Matériaux de Mulhouse, CNRS LRC 7228; 15, rue Jean Starcky, BP 2488, 68057 Mulhouse, France

Résumé :

La réaction d'une lignine kraft désulfurée avec de l'hexaméthylènediamine comme modèle d'une polyamine a été étudiée. À cette fin, le guaiacol a également été utilisé comme composé modèle de lignine et traité dans les mêmes conditions. Les études de spectroscopie RMN-13C NMR, FTIR et MALDI-TOF ont révélé que des composés de polycondensation conduisant à des résines ont été obtenus par réaction des amines avec les groupes hydroxy phénoliques et aliphatiques de lignine. Simultanément, une deuxième réaction conduisant à la formation de liaisons ioniques entre les mêmes groupes s'est produite. Ces nouvelles réactions ont clairement démontré qu'elles impliquaient plusieurs groupes hydroxyle phénolique et alcoolique, ainsi que l'oligomérisation des unités de lignine, pour former des résines durcies.

Published by *Journal of Renewable Materials*

Scrivener First

Polycondensation Resins by Lignin Reaction with (Poly) amines

F. J. Santiago-Medina[1], A. Pizzi[1, 2]*, M. C. Basso[1], L. Delmotte[3] and S. Abdalla[2]

[1]LERMAB, University of Lorraine, ENSTIB, 27 rue Philippe Seguin, 88000 Epinal, France
[2]Department of Physics, King Abdulaziz University, Jeddah, Saudi Arabia
[3]IS2M, Institut de Science des Matériaux de Mulhouse, CNRS LRC 7228; 15, rue Jean Starcky, BP 2488, 68057 Mulhouse, France

Received March 06, 2017; Accepted April 13, 2017

ABSTRACT: The reaction of a desulphurized kraft lignin with hexamethylene diamine as a model of a polyamine has been investigated. For this purpose, guaiacol was also used as a lignin model compound and treated under similar conditions. Solid state CP-MAS ^{13}C NMR, FTIR and MALDI-TOF spectroscopy studies revealed that polycondensation compounds leading to resins were obtained by the reaction of the amines with the phenolic and aliphatic hydroxy groups of lignin. Simultaneously a second reaction leading to the formation of ionic bonds between the same groups occurred. These new reactions have been clearly shown to involve several phenolic and alcohol hydroxyl groups, as well as lignin units oligomerization, to form hardened resins.

KEYWORDS: Lignin-amine reactions, lignin-amine condensation, oligomer distribution, resins, MALDI-TOF, CP-MAS ^{13}C NMR, FTIR

1 INTRODUCTION

The abundance of different types of lignin as a waste product in wood pulp mills has made these materials an attractive proposition for the preparation of resins and adhesives ever since the pulping of wood to produce paper. There is a very large amount of literature on the use of lignin in the preparation of adhesives and resins and some good reviews exist for some of the relevant fields of application [1]. Contrary to the abundance of articles in the literature on this subject the corresponding industrial applications of these materials are rather scant. There are well-documented cases of the industrial utilization of lignin in adhesives for wood [1, 2] as well as in other fields, but all of these were generally discontinued after only short periods of industrial use for one reason or other. Most of these serious attempts to utilize lignin as an adhesive or a resin were based on its reaction with formaldehyde, other aldehydes, aldehyde-based resins such as phenol-formaldehyde (PF), urea-formaldehyde (UF), tannin-aldehyde, and on isocyanate resins [3–9]. Processes based on the self-coagulation of lignin [1, 5, 10], peroxide-induced gelling [1, 11] and others, although of definite interest, have always had some inherent disadvantages regarding their industrial application. One of the most evident disadvantages ever has been the low reactivity of lignin with aldehydes, aldehyde-yielding compounds and aldehyde-based resins. This was first partially overcome for some applications (i) by pre-reacting lignin with an aldehyde before adding it to a traditional resin such as a PF or UF resin [12–14], this process having been used industrially for plywood for a couple of decades in North America: and then (ii) by supporting this further by recurring crosslinking reactions not based on just the reaction of an aldehyde with phenolic nuclei of lignin but also with an isocyanate. This latter approach formed mixed networks based on methylene and urethane bridges [3, 4, 8, 9].

In the latter approach the main drawback for the use of lignin in different resins was overcome by using the alternative reaction of isocyanates with the groups formed on an aldehyde-pre-reacted lignin [3, 4, 8, 9, 15]. This indicated that to overcome the traditional low reactivity and poor crosslinking drawbacks of lignin its application must pass by reactions that are not based on the classical phenols-aldehyde approach. Polymeric isocyanates served such a purpose well, but as they are now also considered partially toxic before being neutralized in their crosslinked state, they have also become less accepted for possible use.

*Corresponding author: antonio.pizzi@enstib.uhp-nancy.fr

It is on the basis of this background that the recent development to crosslink other polyphenols, such as tannins, by alternate polycondensation reactions [16, 17] has led to check the possibility of applying these same reactions to obtain new, hardened, crosslinked polycondensation resins based on lignin. One of these approaches and the results obtained, namely the reaction with diamines, and by inference with polyamines, of a commercial, desulfurized kraft lignin to form a hardened resin is described in this study. The reaction presented is of particular interest when applied for the rapidity of initial reaction, rendering it of interest for the preparation of non-drip coatings and for quick initial immobilization of pressure projected insulation foams.

Reactions of lignin with amines are found in the literature through the intermediate of aldehydes, particularly in formaldehyde, for example, to form asphalt emulsifiers [18, 19], or of reaction of lignin with an amine and epichloridrin [20]. However, there does not appear to be any record of direct reaction of diamines or other polyamines with lignin to form hardened crosslinked resins. Thus, in this study the reaction with diamines with lignin was investigated, first by using guaiacol as a simple model compound, followed by the same reactions on a kraft lignin by extensive MALDI-TOF spectroscopy, FTIR and solid-state CP-MAS ^{13}C NMR studies. The findings are presented in this article.

2 MATERIALS AND METHODS

2.1 Materials and Reactions

Guaiacol (purity > 98%, HPLC quality) as a simple model compound of lignin was supplied by Sigma-Aldrich. The commercial lignin used was a desulphurized softwood kraft lignin, namely Biochoice kraft lignin supplied by Domtar Inc. (Montreal, Quebec, Canada) from their Plymouth, North Carolina mill (USA).

From these two chemicals, the following experiments have been carried out. The samples were prepared as follows:

1. 0.5 g of guaiacol was mixed in equimolar amount with 0.67 g of hexamethylenediamine (HDMA) (70% solution in water) catalyzed by the addition of 1 g NaOH 33% solution in water. The sample was prepared with the proportions above, then reacted in an oven at 100 °C during 18 h.
2. 4 g of 50% water solution of Biochoice lignin at pH > 10 was mixed with 2 g of hexamethylene diamine (HMDA) (70% solution in water) + 0.8 g of NaOH 33% solution in water. Two samples were prepared with the proportions above and they were reacted in an oven at 100 °C and 180 °C during 18 h, respectively.
3. 4 g of 50% water solution of Biochoice lignin at pH > 10 was mixed with 2 g of hexamethylene diamine (HMDA) (70% solution in water) + 2 g of NaOH 33% solution in water. Two samples were prepared with the proportions above and they were reacted in an oven at 100 °C and 180 °C during 18 h, respectively.

All reactions were carried out in an oven not blanketed with inert gas using the temperatures indicated for each case and inside open containers.

Before reaction the samples were liquid solutions. After the reaction in the oven, the samples prepared from lignin at 100 °C were a paste and at 180 °C became a dry, hardened solid, while the samples prepared from guaiacol at 100 °C became a viscous liquid.

2.2 Matrix-Assisted Laser Desorption Ionization Time-of-Flight (MALDI-TOF) Mass Spectrometry Analysis

The spectra were recorded on a KRATOS Kompact MALDI AXIMA TOF 2 instrument. The irradiation source was a pulsed nitrogen laser with a wavelength of 337 nm. The time period of a laser pulse was 3 ns. The measurements were carried out using the following conditions: polarity-positive, flight path-linear, mass-high (20 kV acceleration voltage), 100–150 pulses per spectrum. The delayed extraction technique was used by applying delay times of 200–800 ns.

2.3 CP-MAS ^{13}C NMR

Solid-state CP-MAS (cross-polarization/magic angle spinning) ^{13}C NMR spectra of the aforementioned oven-dried solids were recorded on a Bruker MSL 300 spectrometer at a frequency of 75.47 MHz. Chemical shifts were calculated relative to tetramethyl silane (TMS). The rotor was spun at 4 kHz on a double-bearing 7 mm Bruker probe. The spectra were acquired with 5 s recycle delays, a 90° pulse of 5 ms and a contact time of 1 ms. The number of transients was 3000.

2.4 Fourier Transform Infrared (FTIR) Spectroscopy

A PerkinElmer Frontier ATR (attenuated total reflection) spectrophotometer equipped with a diamond/ZnSe crystal was used to analyze the lignin and the reaction products. About 150 mg of sample was placed on the crystal and the contact was obtained with 32 scans with the resolution of 4 cm^{-1} from 4000 to 600 cm^{-1}.

Additional samples were prepared without HMDA under the same conditions that the samples prepared in points 2 and 3 in the samples preparation section to analyze the influence of thermal degradation on the samples. The results have been presented in the supplementary material.

3 RESULTS AND DISCUSSION

3.1 MALDI-TOF

The physical state of the sample obtained by reaction of guaiacol with hexamethylene diamine (HMDA) catalyzed by NaOH was a viscous liquid. The interpretation of the peaks of the MALDI-TOF spectrum shown in Figures 1a,b and the assignment of species formed

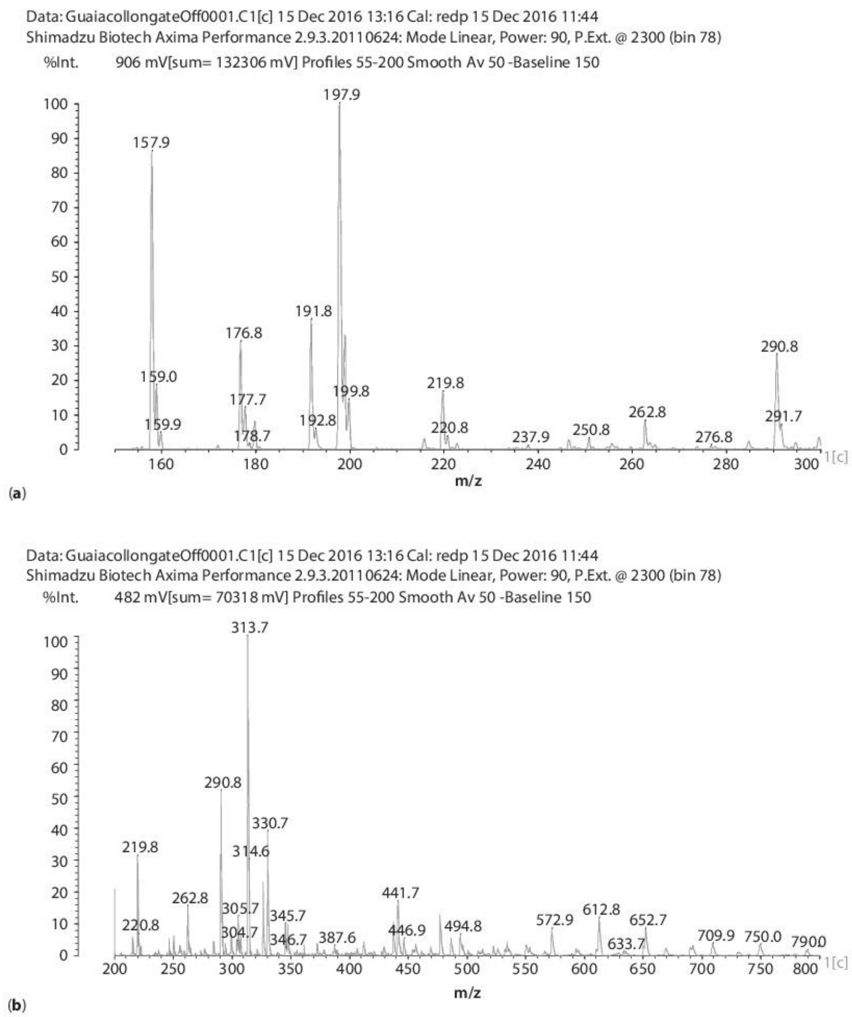

Figure 1 MALDI-TOF spectrum of the products obtained by the reaction of guaiacol with HMDA: (**a**) 50 Da–300 Da range and (**b**) 200 Da–800 Da range.

Table 1 MALDI-TOF peaks interpretation. NaOH-catalyzed reaction of guaiacol and hexamethylenediamine at 100 °C. Legend: "-" = covalent bond, "(+)(-)" = ionic bond, and "(+)(-) Na" = Na^+ linked to flavonoid units phenolic –OHs as $–O^-Na^+$.

Experimental	Calculated	Oligomer
157 Da		2,5-dihydroxybenzoic acid (DHB) (Matrix with 154 Da MW))
177 Da	177 Da	2,5-dihydroxybenzoic+Na^+
198 Da	200	2,5-dihydroxybenzoic+2x Na^+
219 Da	221 Da	Guaiacol-HMDA
246 Da	241 Da	Guaiacol-HMDA+Na^+
251 Da	251 Da	DHB-HMDA, Reaction of the amine with the matrix
263 Da	263 Da	Guaiacol(+)(-)HMDA+Na^+ Salt formation
326 Da	326 Da	Guaiacol-HMDA-Guaiacol
347 Da	349 Da	Guaiacol-HMDA-Guaiacol+ Na^+
372 Da	371 Da	HMDA-DHB-HMDA+Na^+
387 Da	387 Da	Guaiacol(+)(-)HMDA(-)(+) Guaiacol+Na^+ Double salt
446 Da	445 Da	DHB-3×HMDA
477 Da	476 Da	HMDA-DHB-HMDA-Guaiacol+Na+
495 Da	495 Da	HMDA-DHB-HMDA(-)(+) Guaiacol+Na+
572 Da	573 Da	DHB-3×HMDA-Guaiacol+Na+
653 Da	654 Da	DHB-3×HMDA-2×Guaiacol

are shown Table 1. Two types of reactions appear to occur from the calculation of the MALDI masses found, namely 1) the formation of secondary amines by reaction of the hexamethylene diamine on the free –OH groups of the guaicol units, and 2) the formation of $–O^-$ NH_3^+-ionic salt bonds between guaiacol and diamine. Thus, structures of type 1 at 347 Da such as

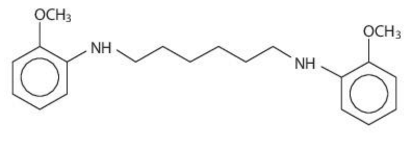

are present alongside structures of type 2 such as the one at 387 Da

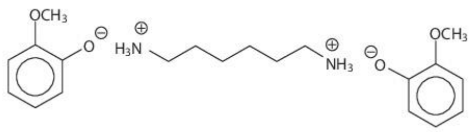

These two types of bonds are the same that have been found in the reactions of flavonoid monomers and flavonoid tannins with diamine under the same reaction conditions [17].

The samples obtained by reaction of lignin with HMDA at 100 °C were pastes, while those reacted at 180 °C were hardened solids.

Some of the masses found in the lignin-HMDA MALDI-TOF spectra also belong to unreacted lignin units or oligomers. The products obtained in the reactions at 100 °C with 0.8 g NaOH catalyst are shown in Figure 2a–c and in Table 2. Those obtained in the reaction at 180 °C with 0.8 g and at 100 °C and 180 °C with 2 g NaOH catalyst are shown in the figures and spectra in the Supplementary Material.

In Table 2 and Figure 2a are shown the results of the NaOH-catalyzed reaction at 100 °C. It can be seen that 5 fragments of lignin units occur as follows:

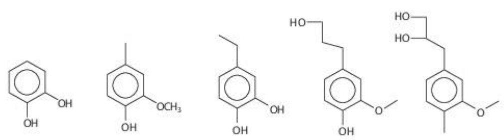

I II III IV V

at 110 Da, 138.2 Da, 13.2 Da, 179.7 Da and 197.8 Da, respectively, and react and combine with HMDA to form a number of different oligomers (Table 2). Table 2 shows oligomers in which covalent bonds between the HMDA and lignin units are formed, such as those of the peaks at 205 Da, 235 Da, 441 Da, 461 Da, 463 Da, 501 Da, 541 Da, 610 Da, 685 Da, 698 Da, 712 Da and 789 Da, thus corresponding to structures of the type at 441 Da

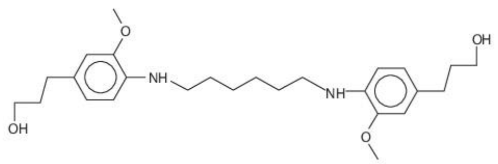

This type of oligomer arrives at trimers of lignin reacted with HMDA (698 Da and 712 Da, Table 2).

Ionic-type salt bond species are also present as the species represented by the peaks at 255 Da and 345 Da corresponding to the structure such as the one at 345 Da shown below.

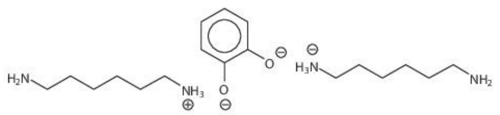

Mixed species in which HMDA moieties are linked to lignin units both by covalent and ionic bonds also

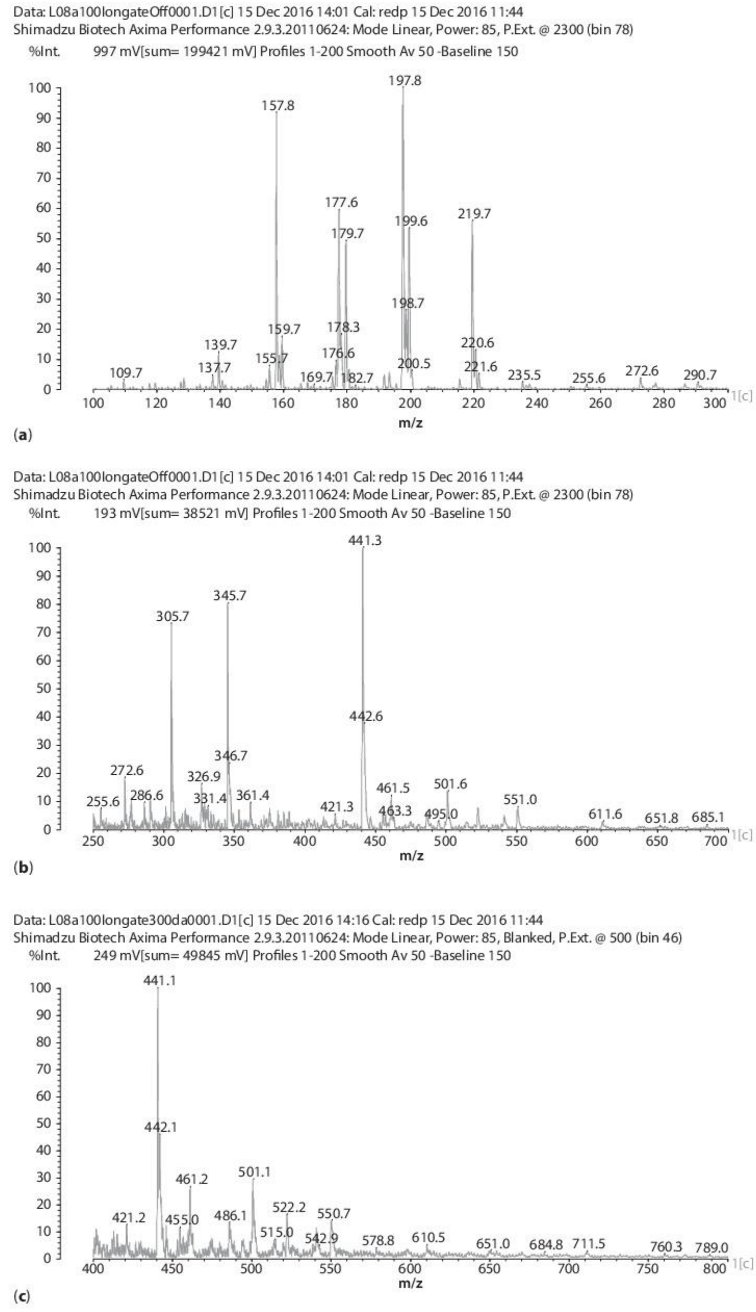

Figure 2 MALDI-TOF spectrum of the products obtained by the reaction of lignin with HMDA catalyzed by 0.8 g NaOH at 100 °C: (**a**) 100 Da–300 Da range, (**b**) 250 Da–700 Da range and (**c**) 400 Da–800 Da range.

Table 2 MALDI-TOF peaks interpretation. NaOH-catalyzed reaction of kraft Biochoice lignin and hexamethylenediamine at 100 °C catalyzed with 0.8 g NaOH solution. Legend: "-" = covalent bond and "(+)(-)" = ionic bond.

Experimental	Oligomer type
109 Da	Lignin fragment I
139 Da	HMDA+Na$^+$ Or lignin fragments II and III
179.7 Da	Lignin unit of type (IV)
197.8 Da	Lignin unit of type (V)
205 Da	Lignin fragment I-HMDA, 1 covalent bond
219.7 Da	Lignin unit V + Na$^+$
235 Da	Lignin fragment II or III-HMDA, 1 covalent bond
255 Da	Lignin fragment II or III(-)(+)HMDA, formation of salt bond
345 Da	HMDA(+)(-)(Lignin fragment III)(-)(+) HMDA, two ionic bonds
389 Da	HMDA(+)(-)Lignin unit IV-HMDA, one ionic bond and one covalent bond
441–442 Da	Lignin unit IV-(HMDA)-Lignin unit IV
461 Da	Lignin unit V-(HMDA)-Lignin unit IV
463 Da	Lignin unit IV-(HMDA)-Lignin unit V + Na$^+$
501 Da	Lignin unit V-(HMDA)-Lignin unit V + Na$^+$
539–541 Da	Lignin unit IV-(HMDA)-Lignin unit IV-(HMDA)
555.8 Da	Lignin unit IV-(HMDA)-Lignin unit IV(-)(+)HMDA, 2 covalent, 1 salt bonds
610–611 Da	Lignin unit IV-(HMDA)-Lignin unit IV-Lignin unit IV
685 Da	Lignin unit IV-(HMDA)-(Lignin unit IV)$_2$-HMDA
698–702 Da	Lignin unit IV-(HMDA)-Lignin unit IV-(HMDA)-Lignin unit IV
712 Da	Lignin unit V-(HMDA)-Lignin unit IV-(HMDA)-Lignin unit IV
789 Da	Lignin unit IV-(HMDA)-(Lignin unit IV)$_3$
959 Da	Lignin unit VI(-)(+)HMDA(+)(-)Lignin unit VI (-)(+)HMDA(+)(-)Lignin unit VI

occur, such as the peaks at 389 Da and 555.8 Da. These present two possibilities as illustrated by the chemical species at 389Da

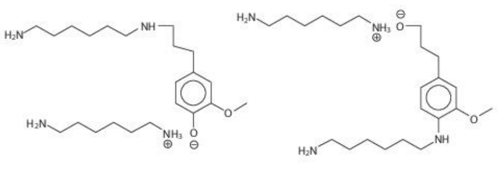

in which the ionic salt bond can be either on the phenolic oxygen or on the alcoholic oxygen of the lignin unit. While it would appear logical that the first possibility be the most likely due to the more definite negative charge on the oxygen, the second structure is surprisingly also possible if one considers the structure of the chemical species at 555.8 Da where both types of structure definitely exist.

It must be pointed out that even higher oligomers exist, as attested by the hardened 180 °C reaction products, these species being of too high a molecular weight to be easily detected by MALDI. The species formed in the other experiments were of the same nature as described above, all the results being reported in the Supplementary Material. The higher molecular weight oligomer found was in the case of the 2 g NaOH-catalyzed at 180 °C, where an oligomer at 959 Da was detected, the species being a trimer of a lignin unit of 244 molecular weight linked through two HMDAs. Two possible structures (VI) of 244 Da molecular weight, both present in the original lignin, can possibly participate to this trimer, namely,

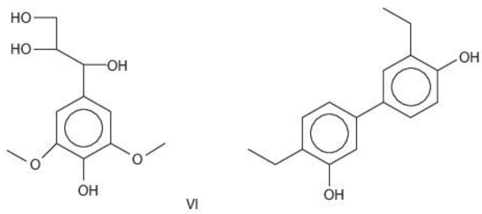

VI

forming an ionic salt bonded oligomer of the type Lignin(-)(+)HMDA(+)(-)Lignin(-)(+)HMDA(+)(-) Lignin (See Supplementary Material).

3.2 Fourier Transform Infrared (FTIR)

Guaiacol + HMDA

In the FTIR spectrum of the reaction product of guaiacol with HMDA one can notice the absence of the band corresponding to O-H stretching bond (Figure 4). This means that reaction has occurred involving the phenolic hydroxyl group of guaiacol and HMDA. Furthermore, there are two bands at 3353 and 3290 cm^{-1} belonging to the N-H stretching bond in aliphatic primary amines, confirming that reaction has occurred. As the sample was prepared in equimolar amount, there are two amine groups for each hydroxyl group. Thus, at least half of the amine groups (primary amines) are unreacted. The first band at 3353 cm^{-1} is most probably due to the overlap of the band belonging to the aromatic secondary amine and the band corresponding to the first signal for the aliphatic primary

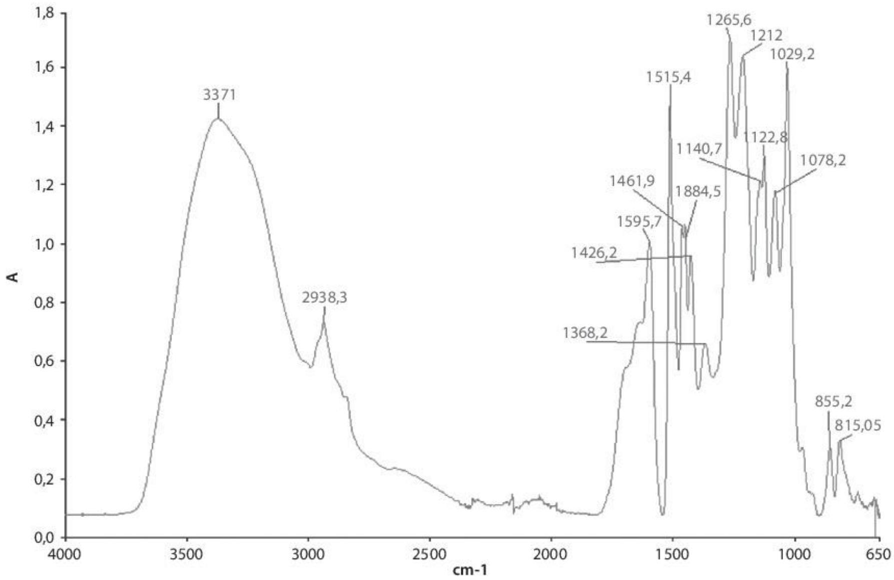

Figure 3 FTIR spectrum of unreacted lignin.

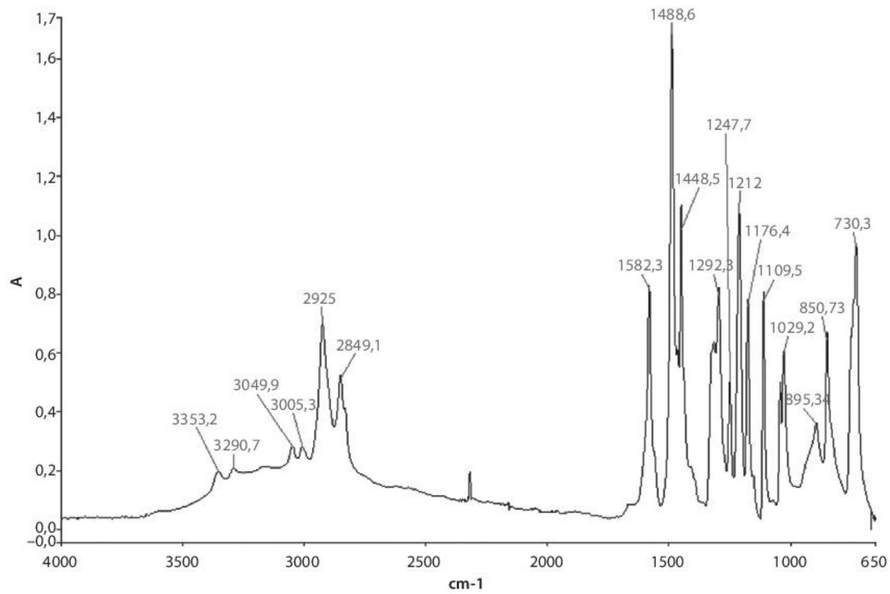

Figure 4 FTIR spectrum of the products obtained by the reaction of guaiacol with HMDA at 100 °C.

amine. The band at 1292 cm^{-1} belongs to the aromatic secondary amine. It means that substitution of the hydroxyl group on the aromatic ring by the amine group has occurred (Table 3, Figure 4).

Lignin + HMDA

The preparation of the samples under a non-inert atmosphere leads to thermal degradation of the lignin, as can be observed in the samples with and without HMDA (Figure 5 and Supplementary Material). The air oxidation effect on the lignin is especially shown in the range 1300–1000 cm^{-1} of the spectra when compared to the non-heated, unreacted lignin [21, 22]. It is also possible to observe the increase in the size of the peak at 1595 cm^{-1} due to the increase in temperature, higher than that for the non-heated, unreacted lignin. This is so because the more elevated is the temperature applied, the more significant is the effect when HMDA is added. According to Kotilainen *et al.* [23] and Li *et al.* [21] this increase should belong to the air oxidation of a major portion of the lignin content. Conversely, the shoulders next to the peak at 1595 cm^{-1} in the lignin spectrum suggest that there should be a small proportion of structures with a ketone group in the lignin. These shoulders decrease in intensity until practically disappearing. This is true especially when the HMDA is used and when a temperature increase is used.

Table 3 FTIR assignments for the NaOH-catalyzed reaction of guaiacol with HMDA at 100 °C.

Band (cm^{-1})	Assigment
3353+3290	N-H stretching (aromatic secondary and aliphatic primary NH)
3049	C-H stretching (aromatic CH)
3005	C-H stretching (aromatic CH)
2925	C-H stretching (methylene CH asymmetric stretch)
2849	C-H stretching (methylene CH symmetric stretch and O-CH_3)
1582	C=C-C stretching (aromatic skeleton)
1488	C=C-C stretching (aromatic skeleton)
1448	C=C-C stretching (aromatic skeleton) with C-H bond in methylene
1292	C-N stretching (aromatic secondary CN)
1212	C-O-Ar (aromatic ether)
1176	C-H in-plane deformation (aromatic ring)
1109	C-H in-plane deformation (aromatic ring)
1029	C-O-C stretching (CO in ether)
895	C-H out-of-plane (aromatic ring)
850	C-H out-of-plane (aromatic ring)
730	Methylene –$(CH_2)_n$– rocking (n>3)

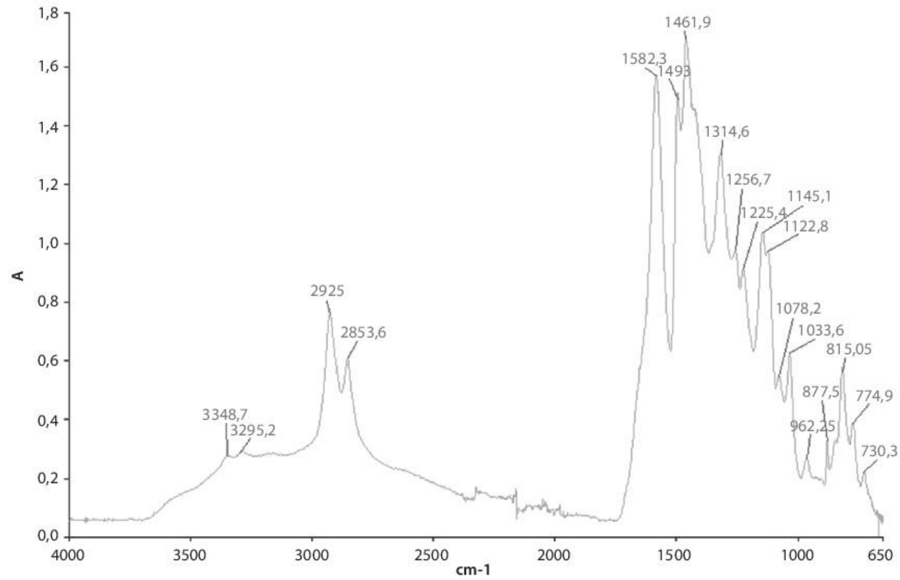

Figure 5 FTIR spectrum of the products obtained by the reaction of lignin with HMDA catalyzed by 2 g NaOH at 180 °C.

Table 4 FTIR assignments for the product of the NaOH-catalyzed reaction of lignin with HMDA at 100 °C and 180 °C [21, 24–27].

Band (cm^{-1})	Assigments	Band location (cm^{-1})		
		Lignin	Reaction at 100 °C	Reaction at 180 °C
3400		3371	–	–
~3380 + ~3325	N-H stretching (aromatic secondary and aliphatic primary NH)	–	3349+3287	3345+3282
~3130	C-H stretching (aromatic CH)	–	3167	–
2960-2925	C-H stretching (methylene CH asymmetric stretch)	2938	2922	2922
2850-2840	C-H stretching (methylene CH symmetric stretch and O-CH_3)	–	2850	2855
~1600	C=C-C stretching (aromatic skeleton) and C=O streching	1595	1590	1581
1513	C=C-C stretching (aromatic skeleton)	1515	1496	
1460	C-H deformation (asymmetric in –CH_2 and –CH_3)	1461	1460	1460
1445	C=C-C stretching (aromatic skeleton)	1448	-	–
1425	C=C-C stretching (aromatic skeleton) with C-H bond in methylene	1426	1421	–
1370-1365	Aliphatic C-H stretching in CH_3 and phenol OH	1368	–	–
1350-1280	C-N stretching (aromatic secondary CN)	–	1304	1318
1265	C-O stretching of guaiacyl unit	1265	1260	1255
~1220	C-OH+C-O-Ar (phenolic OH and ether in syringli and guaiacyl)	1212	1224	1224
1190-1130	C-N stretching (secondary amine CN)	1140	1144	1144
1115	C-H in-plane deformation (aromatic ring)	1122	1126	1122
1075	C-H in-plane deformation (aromatic ring) and C-O deformation in secondary alcohols and aliphatic ethers	1078	1077	1077
1035-1030	C-O-C stretching (CO in ether and aliphatic primary alcohol) and C-H deformation in-plane	1029	1037	1033
900-860	C-H out-of-plane (aromatic ring)	855	921	881
810-750	C-H out-of-plane (aromatic ring)	810	819	814
750-720	Methylene –$(CH_2)_n$– rocking (n>3)	–	725	725

This could suggest that there is reaction between keto group and diamine.

Conversely, no major differences appear to occur between the spectra due to either the difference in reaction temperature or the differences in the NaOH catalyst concentration (see Supplementary Material).

In the FTIR spectra of the reaction of lignin with HMDA the characteristic bands due to the amine reaction are several (Table 4, Figure 5). The double band at 3348 and 3295 cm^{-1} belongs to N-H stretching in aliphatic primary amines. Probably, the first band at 3348 cm^{-1} is most likely the overlap of the band belonging to the aromatic secondary amine and the band corresponding to the first signal for the aliphatic primary amine. Again, as for guaiacol, the band corresponding to O-H stretching is absent. The peak at 1515 cm^{-1} in unreacted lignin shifts to 1493-7 cm^{-1} after the reaction. Its size decreases when the temperature and the amount of catalyst increase, until being practically included in the band at 1461 cm^{-1}. The latter increases masking the peak at 1493-7 cm^{-1} for the opposite trend. Both peaks refer to the structure of the aromatic rings, thus these variations could pertain to the reaction of diamine with the aromatic rings of lignin. There are bands at 1305 cm^{-1} for the samples prepared at 100 °C and at 1314 cm^{-1} for samples prepared at 180 °C. These bands belong to the C-N bond in aromatic secondary amines. Thus, this is a further confirmation of the existence of a reaction between the aromatic ring in lignin and the amine. In addition, these bands are absent in the unreacted lignin spectrum. Moreover, the band at 1145 cm^{-1} increases its intensity with respect to the band at 1122–1126 cm^{-1}, while the opposite happens in the spectrum of unreacted lignin. The band at 1145 cm^{-1} belongs to the C-N stretch in aliphatic secondary amines; thus, it means that there is also reaction of substitution by the amine of the alcohol groups in the aliphatic chain of lignin. This confirms what was already inferred by MALDI-TOF where structures in which the alcohol hydroxyl group of the lignin units side chain have also reacted covalently with HMDA to form a secondary amine, as illustrated above for the 398 Da structure. Furthermore, the band at 1145 cm^{-1}, as the band between 1126–1122 cm^{-1}, has practically disappeared in the spectra of lignin + NaOH (see Supplementary Material), indicating that these bands show: (i) the thermal degradation suffered by the lignin, but also (ii) that their increase when HMDA is present occurs due to the interaction between the amine and the lignin.

3.3 CP MAS ^{13}CNMR

Lignin + HMDA

From the NMR spectra the reactions occurring appear to be more advanced when the temperature is higher. The corresponding CP MAS ^{13}C NMR spectrum of lignin + HMDA (case 3, see experimental part) is shown in Figure 6. The superposition of this spectrum with the spectrum of the original unaltered lignin is shown in Figure 7.

In Figure 6, first of all the aliphatic carbon in position alpha to an -NH of the diamine reacted covalently with the lignin must have a shift of 43–44 ppm while the same for an unreacted aliphatic amine should have a calculated shift of 41–42 ppm. Looking at the spectra it can be noticed that the shift is at 43.6 ppm, indicating that the amine has reacted covalently. This is confirmed by other indications. The shift for the C in β of the covalently reacted diamine should be at 30 ppm while the unreacted one is at 37 ppm and the one of the ionic salt formed one should be at 33–34 ppm. The 30 ppm peak is not visible at all as it is covered totally by the strong peak at 27–28 ppm. The 37 ppm peak has disappeared, indicating that for the lignin + HMDA + 2g NaOH at 180 °C the reaction is completed. However, a clear peak does appear at 34.8 ppm, indicating that the formation of the ionic-type salt is also significant in the reaction of the diamine with lignin.

The other clear indication of the formation of covalent and ionic bonds between the amine and the lignin –OH groups is the disappearance of the peak at 147 ppm, indicating that the lignin C4 aromatic carbons carrying the phenolic –OH groups have reacted. The species formed by this reaction are defined by the appearance of two new peaks: one at 151 ppm, characteristic of the covalent bond in which NH has substituted the phenolic –OH, and one at 43.6 ppm, characteristic of a positively charged primary amine as present in the ionic salt. These peaks belong to the

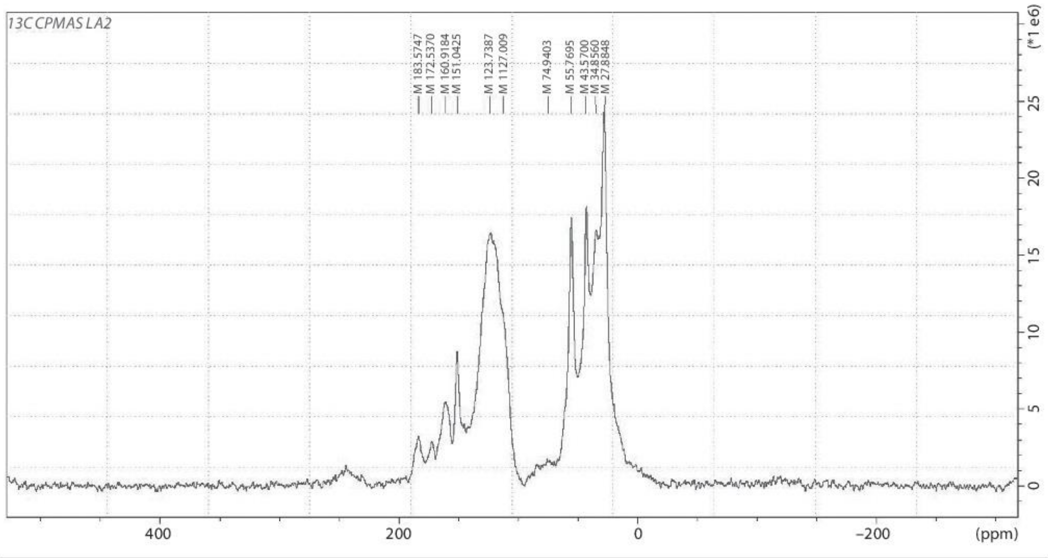

Figure 6 CP MAS ^{13}C NMR spectrum of the products obtained by the reaction of lignin with HMDA catalyzed by 2 g NaOH at 180 °C.

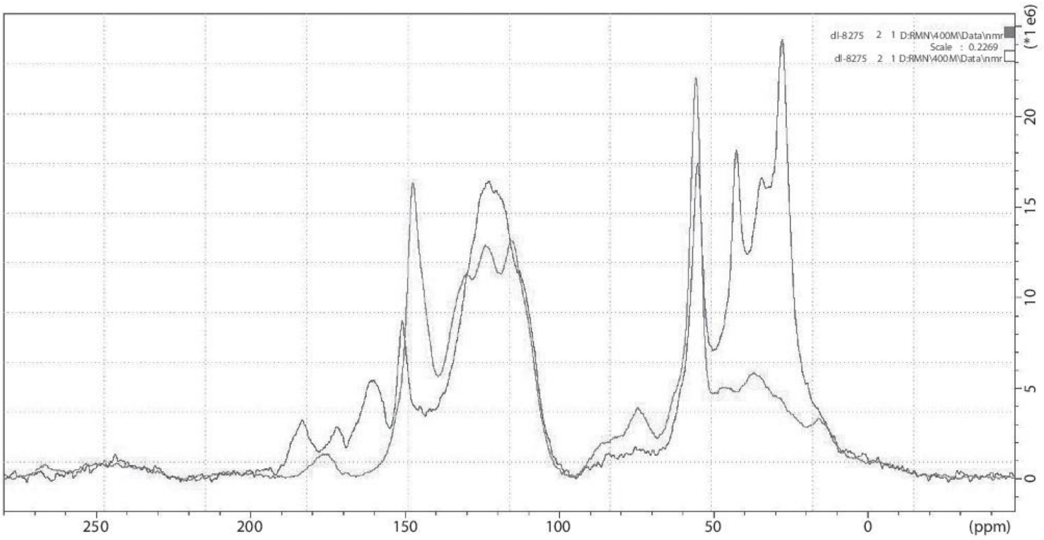

Figure 7 Superposition of the CP MAS ^{13}C NMR spectra of the unreacted lignin and of the products obtained by the reaction of lignin with HMDA catalyzed by 2 g NaOH at 180 °C.

lignin's C4 that has reacted with an amine both covalently and forming a salt. This confirms the interpretation given to the MALDI spectra

The total disappearance in the spectra of the lignin C peaks of the lignin unit's aliphatic side chains at 75 ppm and 86 ppm indicates that even the alcoholic –OH on the lignin side chain has reacted with the amine, either covalently or to form a salt, which is not evident from the spectra.

Finally, the strong peak at 27.8 ppm belongs to diamine linked either covalently or as totally ionized salts to the lignin. The unreacted diamine should present this shift at 33.8 ppm. This may be confused with the 34.8 ppm peak that is instead an indication of the shift for the amine β carbons when ionic bonds are formed.

4 CONCLUSIONS

1. Covalent bonds are formed by reaction between the amine and the aromatic rings of lignin by substitution of the lignin phenolic –OH groups.
2. Covalent bonds are formed by reaction between the amine and the aliphatic side chain of lignin by substitution of the lignin alcohol –OH groups of the lignin side chain.
3. At 180 °C and 100 °C there is a proportion of ionic bonds formed between the amine and the –OH groups both on the aromatic rings and on the aliphatic side chain of lignin units.
4. At 180 °C and to a lesser extent also at 100 °C, lignin reacted with hexamethylene diamine forms hard, condensed solids.

AKNOWLEDGMENTS

The LERMAB is supported by a grant overseen by the French National Research Agency (ANR) as part of the "Investissements d'Avenir" program (ANR-11-LABX-0002-01, Lab of Excellence ARBRE). This paper was also partially funded by King Abdulaziz University (KAU) under grant No (4-130-37-RG). The second and fifth authors acknowledge the support of KAU.

REFERENCES

1. H.H. Nimz, Lignin-based wood adhesives, in *Wood Adhesives Chemistry and Technology*, A. Pizzi (Ed.), pp. 247–288, Marcel Dekker, New York, NY (1983).
2. K.J. Forss and A. Fuhrman, Karatex – the lignin based adhesive for plywood, particleboard and fiberboard. *Paperi ja Puu* **11**, 817–824 (1976).
3. N.-E. El Mansouri, A. Pizzi, and J. Salvadó, Lignin-based wood panel adhesives without formaldehyde. *Holz Roh Werkstoff* **65**(1), 65–70 (2007).

4. N.-E. El Mansouri, A. Pizzi, and J. Salvadó, Lignin-based polycondensation resins for wood adhesives. *J. Appl. Polymer Sci.* **103**, 1690–1699 (2007).
5. A. Pizzi, *Wood Adhesives Chemistry and Technology*, Marcel Dekker, New York, NY (1983).
6. H. Younesi-Kordkheili and A. Pizzi, Properties of plywood panels bonded with ionic liquid-modified lignin–phenol–formaldehyde resin. *J. Adhesion*. (2016). DOI: 10.1080/00218464.2016.1263945
7. H. Younesi-Kordkheili and A. Pizzi, Improving properties of ionic liquid-treated lignin-urea-formaldehyde resins by small addition of isocyanate for wood adhesive. *J. Adhesion* (2017). DOI: 10.1080/00218464.2017.1282350
8. A. Pizzi and A. Stephanou, Rapid curing lignins-based exterior wood adhesives, Part 1: Diisocyanates reaction mechanisms and application to panel products. *Holzforschung* **47**, 439–445 (1993).
9. A. Pizzi and A. Stephanou, Rapid curing lignins-based exterior wood adhesives, Part 2: Acceleration mechanisms and application to panel products. *Holzforschung* **47**, 501–506 (1993).
10. K.C. Shen, Spent sulphite liquor binders for exterior waferboard. *Forest Prod. J.* **27**(5), 32–38 (1977).
11. H.H. Nimz and G.Hitze, The application of spent sulphite liquor as an adhesive for particleboard. *Cellulose Chem. Technol.* **24**, 371–382 (1980).
12. L. Calvé, Industrial application of phenolic-lignin adhesives. Paper presented at the XIX IUFRO World Congress, Montreal, Canada (1990).
13. D. Atkinson, Advancement in NAF adhesives technology. Presented at International Conference on Wood Adhesives, Forest Products Society, Toronto, Canada (2015).
14. T. Sellers Jr., Modification of phenolic resins with organosolv lignins and evaluation of strandboard made by the resin as binder. PhD thesis, University of Tokyo, Japan, 148 p. (1993).
15. M.C. Basso, A. Pizzi, C. Lacoste, L. Delmotte, F.A. Al-Marzouki, S. Abdalla, and A. Celzard, MALDI-TOF and ^{13}C NMR analysis of tannin–furanic–polyurethane foams adapted for industrial continuous lines application. *Polymers* **6**, 2985–3004 (2014).
16. M.C. Basso, A. Pizzi, J. Polesel-Maris, L. Delmotte, B. Colin, and Y. Rogaume, MALDI-TOF and ^{13}C NMR analysis of the cross-linking reaction of condensed tannins by triethyl phosphate. *Ind. Crops Prod.* (2016). DOI: 10.1016/j.indcrop.2016.11.031
17. F.J. Santiago-Medina, A. Pizzi, M.C. Basso, L. Delmotte, and A. Celzard, Polycondensation resins by flavonoid tannins reaction with amines. *Polymers* **9**(2), 37 (2017). DOI: 10.3390/polym9020037
18. X. Tao, L.S. Shi, M.J. Sun, and N. Li, Synthesis of lignin amine asphalt emulsifier and its investigation by online FTIR spectrophotometry. *Adv. Mater. Res.* **909**, 72–76 (2014).
19. P. Dilling and S. Falkehag, Process for producing cationic lignin amines, US Patent 3718639 A, assigned to Westwaco Corp. (1973).
20. J.B. Doughty, Lignin amines as asphalt emulsifiers, US Patent 3871893 A, assigned to Westwaco Corp. (1975).
21. J. Li, B. Li, and X. Zhang, Comparative studies of thermal degradation between larch lignin and Manchurian ash lignin. *Polym. Degrad. Stab.* **78**, 279–285 (2002).
22. D.W. Rutherford, R.L. Wershaw, and L.G. Cox, Changes in composition and porosity occurring during the thermal degradation of wood and wood components, Scientic investigations report No. 2004-2592, U.S. Department of the Interior, U.S. Geological Survey, Reston, Virginia, USA (2005).
23. R.A. Kotilainen, T.J. Toivanen, and R.J. Alén, FTIR monitoring of chemical changes in softwood during heating. *J. Wood Chem. Technol.* **20**, 307–320 (2000).
24. A. Mancera, V. Fierro, A. Pizzi, S. Dumarçay, P. Gérardin, J. Velásquez, G. Quintana, and A. Celzard, Physicochemical characterization of sugar cane bagasse lignin oxided by hydrogen peroxide. *Polym. Degrad. Stab.* **95**, 470–476 (2010).
25. O. Faix, Classification of lignin from different botanical origins by FT-IR spectroscopy. *Holzforschung* **45**, 21–27 (1991).
26. N.-E. El Mansouri, Q. Yuan, and F. Huang, Characterization of alkaline lignins for use in phenol-formaldehyde and epoxy resisns. *Biosources* **6**, 2647–2662 (2011).
27. B. Esteves, A. Velez-Marques, I. Domingos, and H. Pereira, Chemical changes of heat treated pine and eucalypt wood monitored by FTIR. *Maderas: Cienc. Tecnol.* **15**, 245–258 (2013).

Supplementary Document Available Online

http://www.scrivenerpublishing.com/journalsuppl/jrm/JRM-2017-0021/jrm_JRM-2017-0021_supp1.docx

3.1 Matériel supplémentaire de « Polycondensation resins by lignin reaction with (poly)amines »

SUPPLEMENTARY MATERIAL

BIOCHOICE LIGNIN : MALDI-TOF IDENTIFIED I SPECIES

137.8 Da= 138 Da calculated

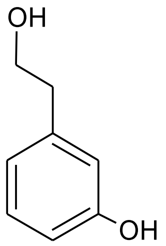

154-156 Da = 154 Da calculated

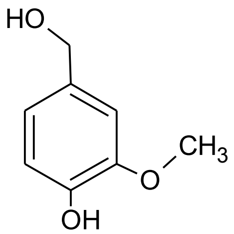

179.7 Da

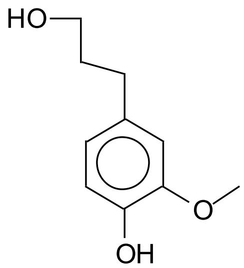

198.2 Da

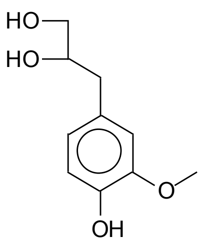

177.8 Da = see above without Na+

198.7-199.7 Da = see above, without Na+

200.6 Da = 201 (Calc) = 177.8+23, with Na+

242 Da = 242 Da calculated

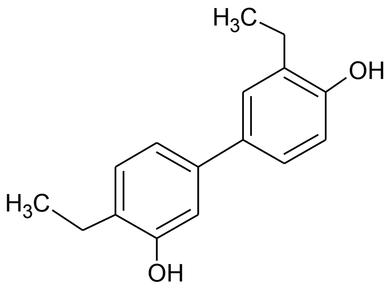

OR

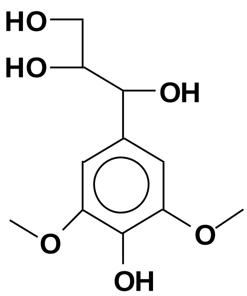

272.5-273.5 Da = 274.3 Calculated (178 +94)

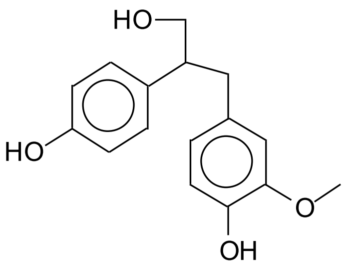

326.7-327.6 Da = 327.3 calculated, with Na+

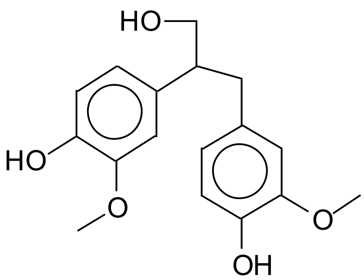

397.4 Da = 401, deprotonated 400 calculated = 178+198+23

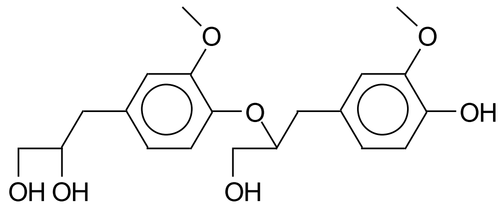

420.2 Da = 1 × deprotonated, without Na+

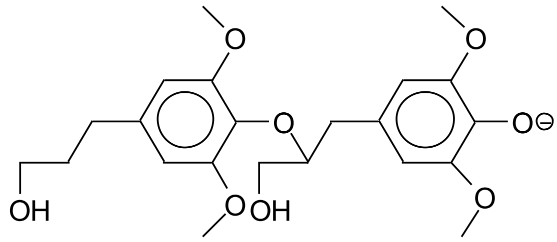

441-443 Da = 445 Da calculated, deprotonated = 444 Da with Na+

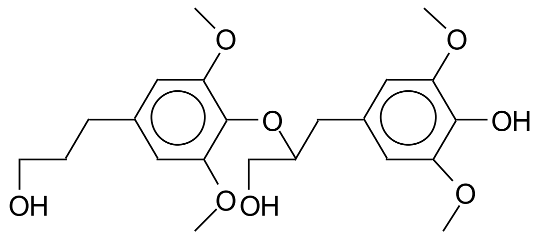

If it would have the possibility to find a double bond, as in the next structure, it could be another alternative for 443 Da mass peak.

Alternative for 441-443 Da = 443 Da calculated, with Na+

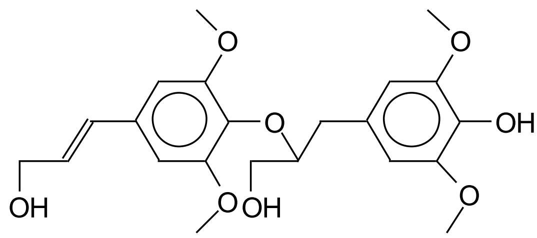

536.8 Da = 537.2 Da calculated, with Na+

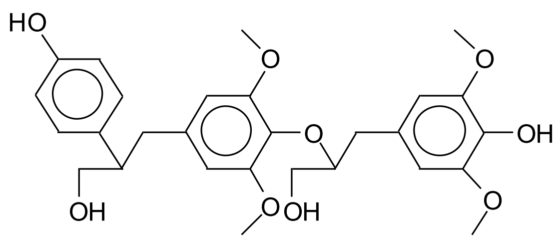

OR

536 Da = 178 × 3 = 542 Da Lignin trimer (calculated) deprotonated without Na+

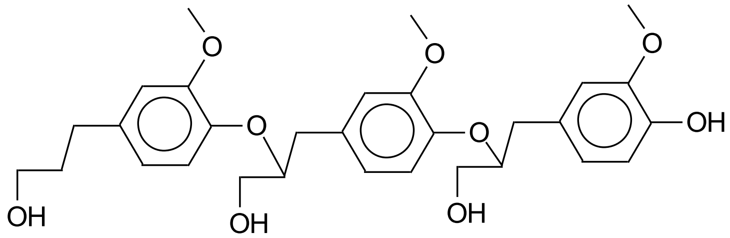

552 Da = first more probable, without Na+

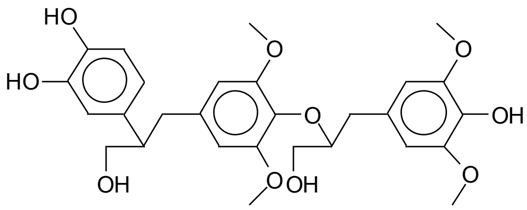

OR

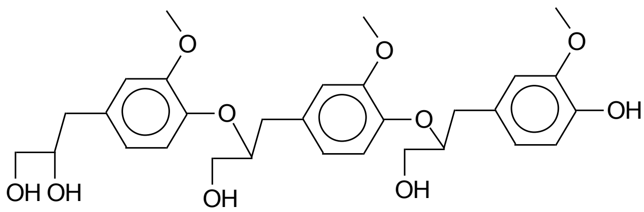

575 Da = 552+23, thus with Na+

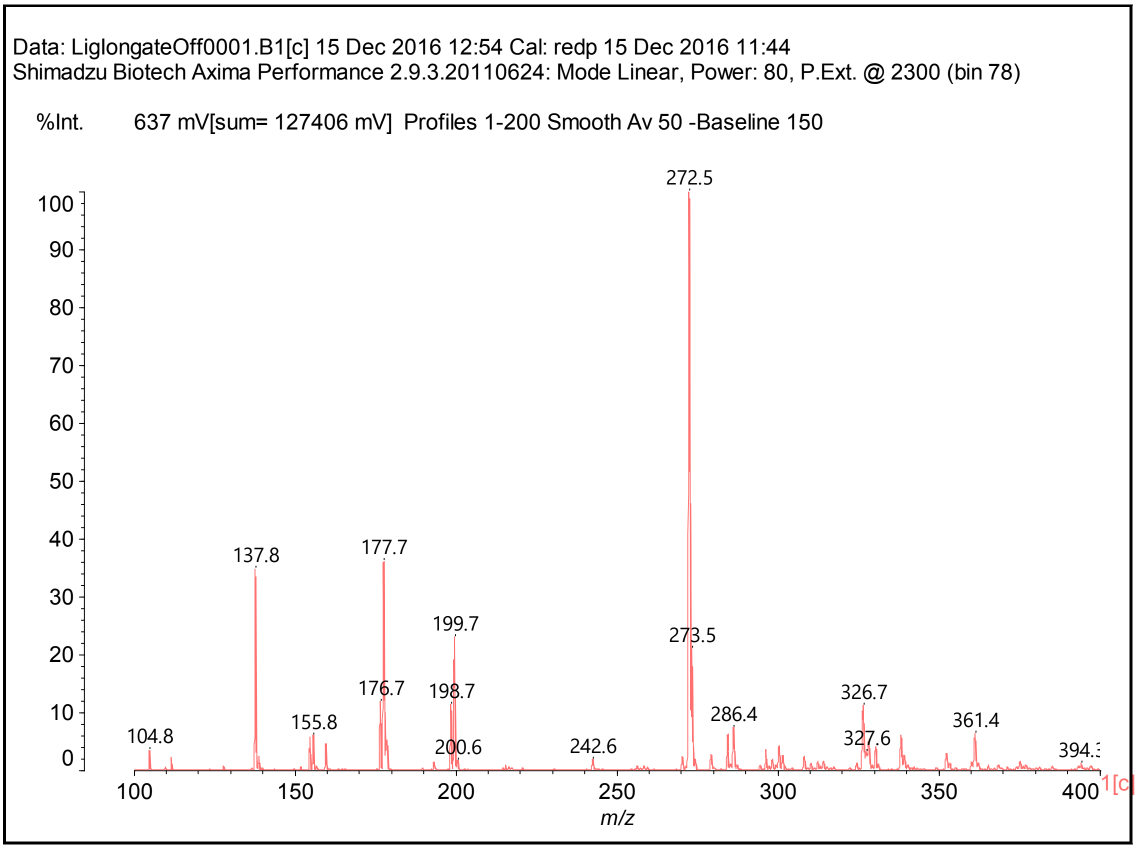

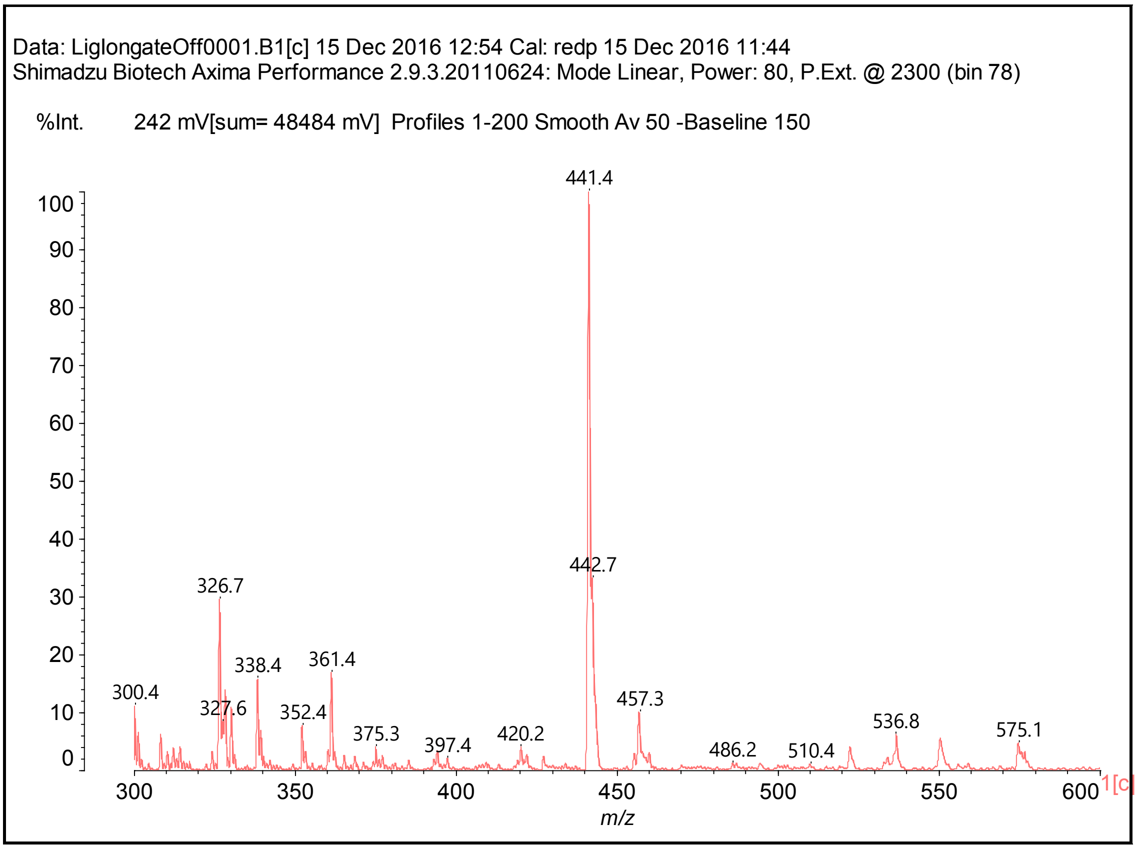

Maldi-ToF spectra of unreacted lignin: 100-400 Da and 300-600 Da range.

Lignin 0.8 g NaOH catalyzed at 180 °C : MALDI-TOF interpretation

This sample was prepared by mixing 4 g of 50% of lignin in water at pH > 10 with 2 g of hexamethylenediamine at 70% in water and 0.8 g of NaOH at 33% in water, as catalyst. The mixture was reacted in an oven overnight at 180 °C.

Legend:

HMDA = Hexamethylenediamine

“-” = covalent bond

“+-” = ionic bond

Experimental Peak (Da)	Oligomer	alculated ɾalue (Da)	Number Ionic bonds	Number covalent bonds
104	Lignin			
137,8	Lignin			
198	Lignin			
235,5	138Lig-HMDA	236		1
272,6	Lignin			
	156Lig+-HMDA	272	1	
276-8	138Lig+-HMDA +Na	277	1	
	156Lig-HMDA +Na	277		1
	180Lig-HMDA	278		1
305-306	104Lig+-HMDA-104Lig	306	1	1
318	180Lig+-HMDA +Na	319	1	
	198Lig-HMDA +Na	319		1
335	HMDA+-104Lig+-HMDA	336	2	
	HMDA-138Lig-HMDA	334		2
345	104Lig-HMDA-138Lig +Na	345		2
358	HMDA-138Lig-HMDA +Na	357		2
	242Lig+-HMDA	358	1	
375,5	HMDA-180Lig-HMDA	376		2
440-443	Lignin			
	180Lig-HMDA-180Lig	440		2
461	HMDA-242Lig-HMDA +Na	461		2
463	180Lig-HMDA-180Lig +Na	463		2
526-9	104Lig+-HMDA+-104Lig+-HMDA-104Lig	526	3	1
	HMDA+-272+-HMDA +Na	527	2	
551	HMDA-138Lig-HMDA-138Lig-HMDA	552		4
555,8	180Lig-HMDA-180Lig+-HMDA	556	1	2
	HMDA+-104Lig+-HMDA+-104Lig+-HMDA	556	4	
	180Lig-HMDA-180Lig+-HMDA	556	1	2
578,8	180Lig-HMDA-180Lig+-HMDA +Na	579	1	2

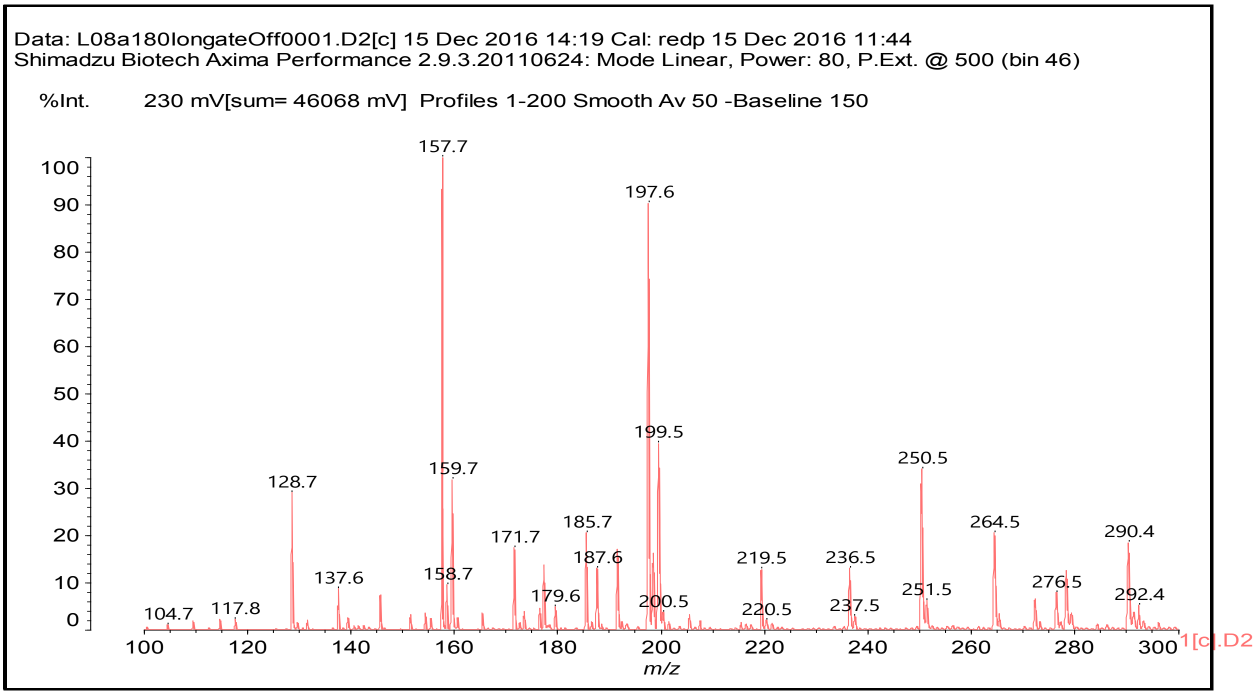
Data: L08a180longateOff0001.D2[c] 15 Dec 2016 14:19 Cal: redp 15 Dec 2016 11:44
Shimadzu Biotech Axima Performance 2.9.3.20110624: Mode Linear, Power: 80, P.Ext. @ 500 (bin 46)
%Int.
230 mV[sum= 46068 mV] Profiles 1-200 Smooth Av 50 -Baseline 150
157.7
197.6
199.5
250.5
159.7
128.7
185.7
264.5
290.4
171.7
187.6
219.5
236.5
137.6
158.7
251.5
276.5
179.6
292.4
200.5
237.5
220.5
104.7
117.8
m/z
1[c].D2

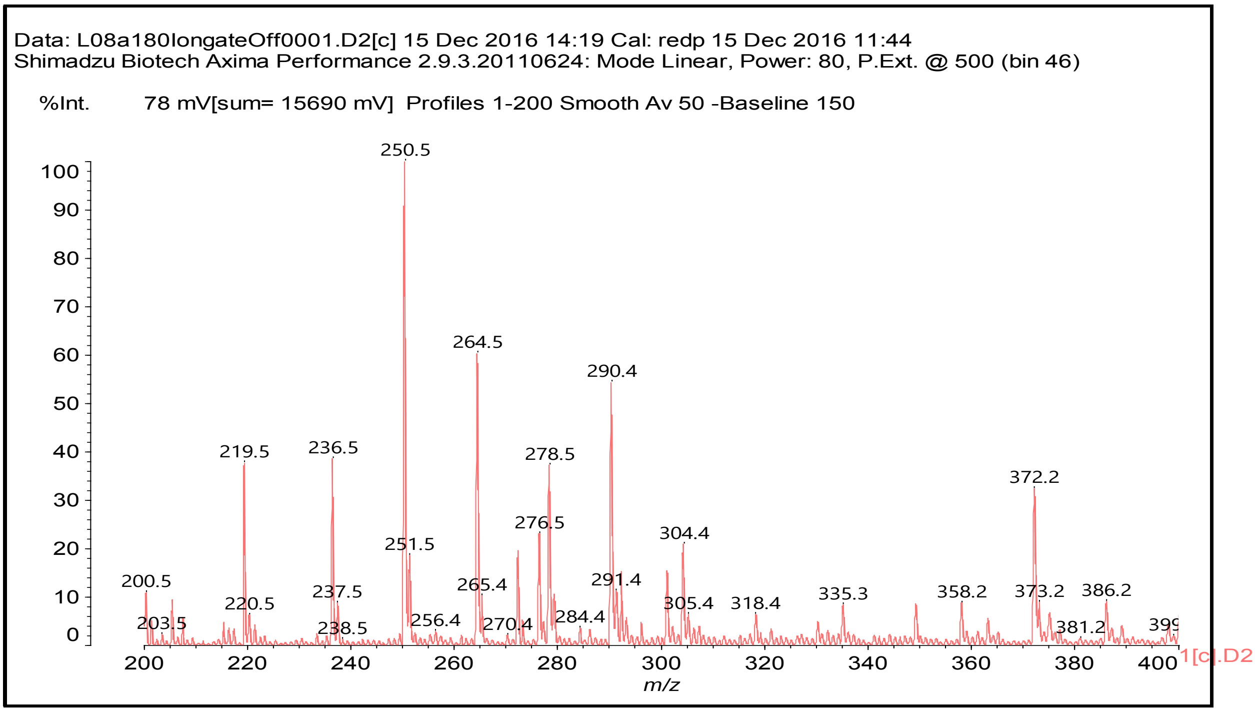
Data: L08a180longateOff0001.D2[c] 15 Dec 2016 14:19 Cal: redp 15 Dec 2016 11:44
Shimadzu Biotech Axima Performance 2.9.3.20110624: Mode Linear, Power: 80, P.Ext. @ 500 (bin 46)
%Int.
78 mV[sum= 15690 mV] Profiles 1-200 Smooth Av 50 -Baseline 150
250.5
264.5
290.4
219.5
236.5
278.5
372.2
276.5
304.4
251.5
200.5
265.4
291.4
220.5
237.5
305.4
318.4
335.3
358.2
373.2
386.2
203.5
238.5
256.4
270.4
284.4
381.2
m/z
1[c].D2

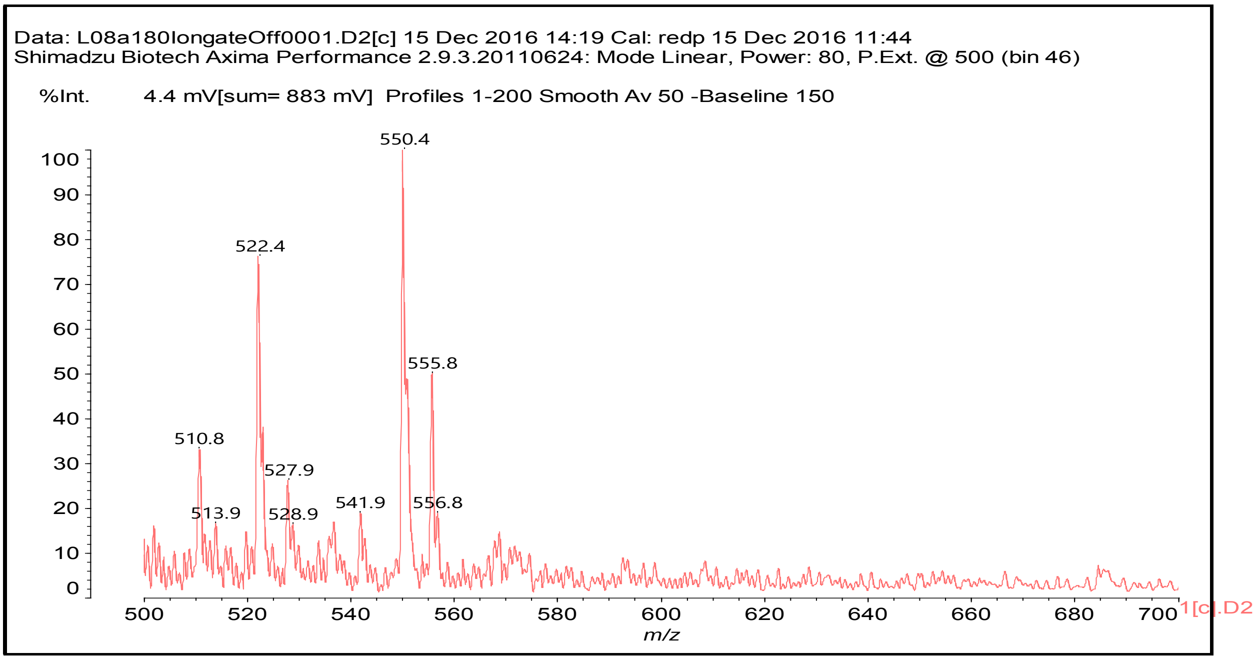

Maldi-ToF spectrum of the product obtained by the reaction of lignin with HMDA catalyzed by 0.8 g NaOH at 180ºC: 100-300 Da, 200-400 Da and 500-700 Da range.

Lignin 2 g NaOH catalyzed at 100 °C: MALDI-TOF interpretation

This sample was prepared by mixing 4 g of 50% of lignin in water at pH > 0 with 2 g of hexamethylenediamine at 70% in water and 2 g of NaOH at 33% in water, as catalyst. The mixture was reacted in an oven overnight at 100 °C.

Legend:

HMDA = Hexamethylenediamine

"-" = covalent bond

"+-" = ionic bond

Experimental peak (Da)	Oligomer	Calculated value (Da)	Number Ionic bonds	Number covalent bonds
198	Lignin			
235,5	138Lig-HMDA	236		1
255	138Lig+-HMDA	254	1	
272,6	Lignin			
	156Lig+-HMDA	272	1	
305-306	104Lig+-HMDA-104Lig	306	1	1
345	104Lig-HMDA-138Lig+Na	345		2
375,5	HMDA-180Lig-HMDA	376		2
389	HMDA+-156Lig+-HMDA	388	2	
440-443	Lignin			
	180Lig-HMDA-180Lig	440		2
461	HMDA-242Lig-HMDA+Na	461		2
463	180Lig-HMDA-180Lig+Na	463		2
495	198Lig-HMDA+-198Lig	494	1	1
	198Lig+-HMDA+-180Lig	494	2	
	156Lig-HMDAx2-156Lig+Na	495		4
501	180Lig+-HMDA+-180Lig+Na	499	2	
	198Lig-HMDA-198Lig+Na	499		2
	198Lig+-HMDA-180Lig+Na	499	1	1
551	HMDA-138Lig-HMDA-138Lig-HMDA	552		4
555,8	180Lig-HMDA-180Lig-O-+HMDA	556	1	2
	HMDA+-104Lig+-HMDA+-104Lig+-HMDA	556	4	
	180Lig-HMDA-180Lig+-HMDA	556	1	2
578,8	180Lig-HMDA-180Lig+-HMDA+Na	579	1	2
654	HMDA+-180Lig-HMDA-180Lig-HMDA	654	1	3

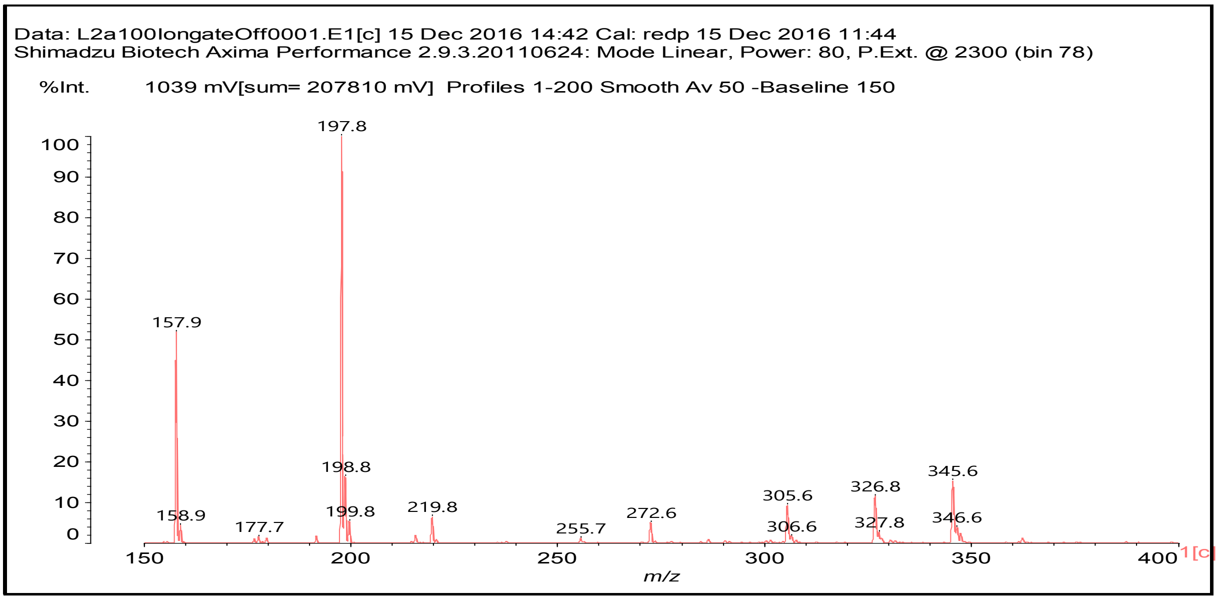

Data: L2a100IongateOff0001.E1[c] 15 Dec 2016 14:42 Cal: redp 15 Dec 2016 11:44
Shimadzu Biotech Axima Performance 2.9.3.20110624: Mode Linear, Power: 80, P.Ext. @ 2300 (bin 78)
%Int.
1039 mV[sum= 207810 mV] Profiles 1-200 Smooth Av 50 -Baseline 150
197.8
157.9
198.8
345.6
326.8
305.6
158.9
177.7
199.8
219.8
255.7
272.6
306.6
327.8
346.6
m/z
1[c].E1

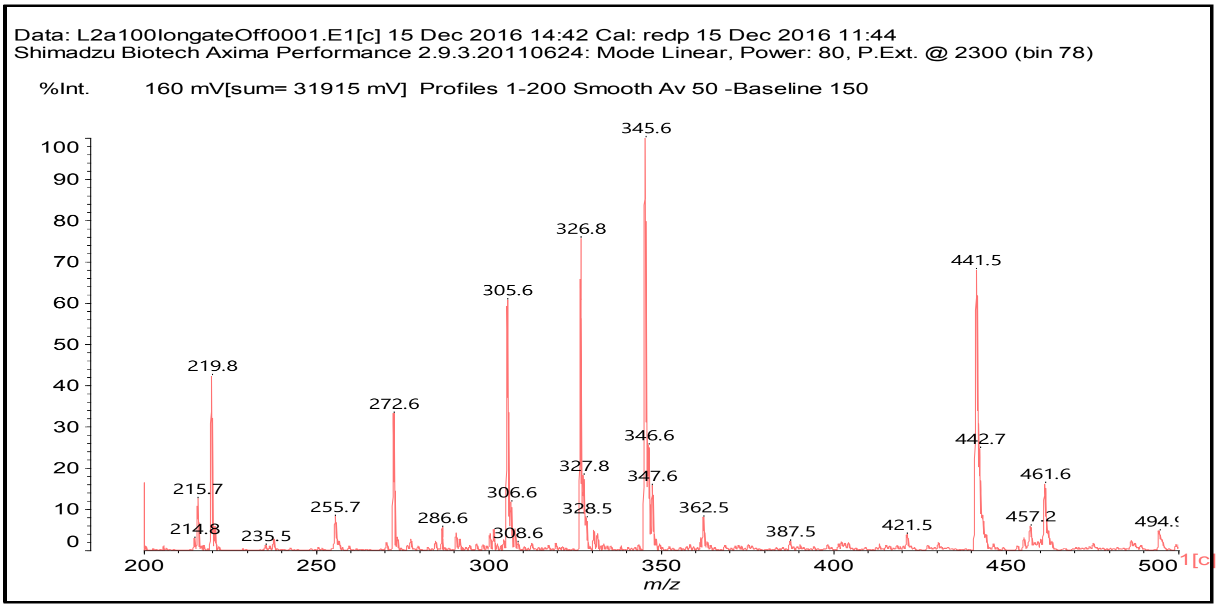

Data: L2a100IongateOff0001.E1[c] 15 Dec 2016 14:42 Cal: redp 15 Dec 2016 11:44
Shimadzu Biotech Axima Performance 2.9.3.20110624: Mode Linear, Power: 80, P.Ext. @ 2300 (bin 78)
%Int.
160 mV[sum= 31915 mV] Profiles 1-200 Smooth Av 50 -Baseline 150
345.6
326.8
441.5
305.6
219.8
272.6
346.6
442.7
327.8
347.6
461.6
215.7
306.6
255.7
362.5
286.6
328.5
457.2
214.8
308.6
387.5
421.5
235.5
m/z
1[c].E1

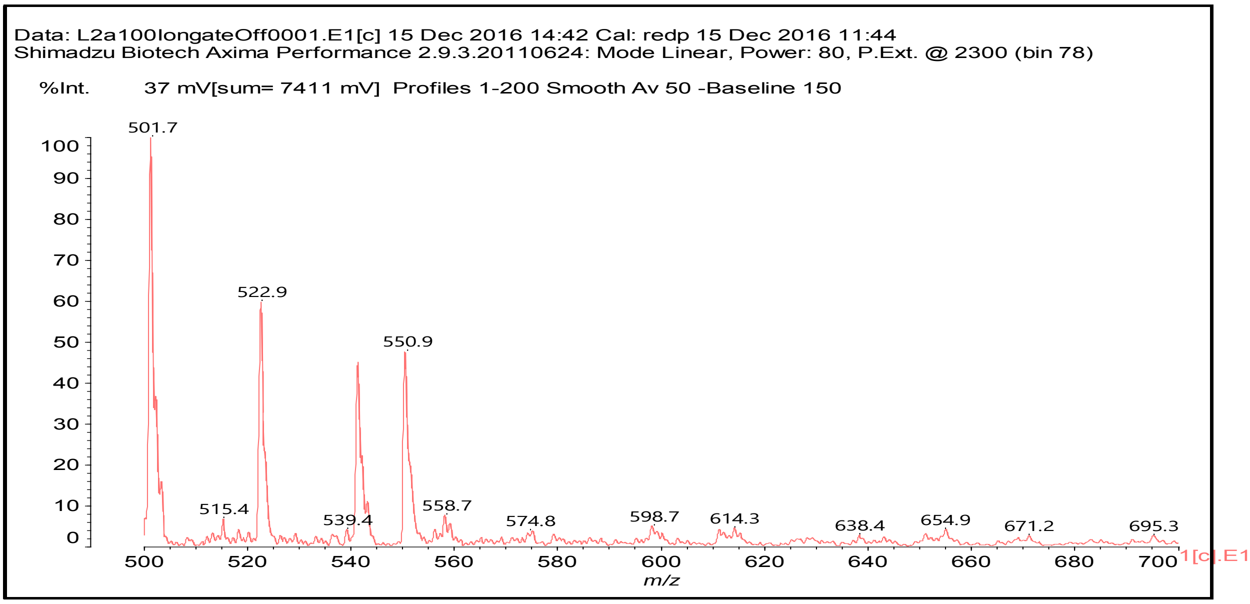

Maldi-ToF spectrum of the product obtained by the reaction of lignin with HMDA catalyzed by 2 g NaOH at 100ºC: 150-400 Da, 200-500 Da and 500-700 Da range.

Lignin 2 g NaOH catalyzed at 180 °C: MALDI-TOF interpretation

This sample was prepared by mixing 4 g of 50% of lignin in water at pH > 10 with 2 g of hexamethylenediamine at 70% in water and 2 g of NaOH at 33% in water, as catalyst. The mixture was reacted in an oven overnight at 100 °C.

Legend:

HMDA = Hexamethylenediamine

"-" = covalent bond

"+-" = ionic bond

Experimental peak (Da)	Oligomer	Calculated value (Da)	Number Ionic bonds	Number covalent bonds
104	Lignin			
138	Lignin			
198	Lignin			
235,5	138Lig-HMDA	236		1
272,6	Lignin			
	156Lig+-HMDA	272	1	
305-306	104Lig+-HMDA-104Lig	306	1	1
345	104Lig-HMDA-138Lig+Na	345		2
375,5	HMDA-180Lig-HMDA	376		2
440-443	Lignin			
	180Lig-HMDA-180Lig	440		2
461	HMDA-242Lig-HMDA+Na	461		2
463	180Lig-HMDA-180Lig+Na	463		2
495	198Lig-HMDA+-198Lig	494	1	1

	198Lig+-HMDA+-180Lig	494	2	
	156Lig-HMDAx2-156Lig+Na	495		4
501	180Lig+-HMDA+-180Lig+Na	499	2	
	198Lig-HMDA-198Lig+Na	499		2
	198Lig+-HMDA-180Lig+Na	499	1	1
526-9	104Lig+-HMDA+-104Lig+-HMDA-104Lig	526	3	1
	HMDA+-272+-HMDA+Na	527	2	
551	HMDA-138Lig-HMDA-138Lig-HMDA	552		4
555,8	180Lig-HMDA-180Lig-O-+HMDA	556	1	2
	HMDA+-104Lig+-HMDA+-104Lig+-HMDA	556	4	
	180Lig-HMDA-180Lig+-HMDA	556	1	2
588	HMDA+-138Lig-HMDA-138Lig+-HMDA	588	2	2
	242Lig-HMDA-242Lig+Na	587		2
610,5	198Lig+-HMDA+-198Lig-HMDA	610	2	1
	198Lig+-HMDA+-180Lig+-HMDA	610	3	
	HMDA-156Lig-HMDA-156Lig-HMDA+Na	611		4
	HMDA+-138Lig-HMDA-138Lig+-HMDA+Na	611	2	2
651	198Lig+-HMDA+-198Lig+-HMDA+Na	651	3	
	156Lig-HMDA-156Lig-HMDA-156Lig+Na	651		4
	138Lig+-HMDA+-138Lig+-HMDA-138Lig+Na	651	3	1
774	HMDA-180Lig-HMDA-156Lig-HMDA-180Lig-HMDA	774		6
836	HMDA-242Lig-HMDA-198Lig-HMDAx2+Na	837		5
898	HMDA+-242Lig-HMDA-242Lig-HMDAx2+Na	899	1	4
959	242Lig+-HMDA+-242Lig+-HMDA+-242Lig	958	4	

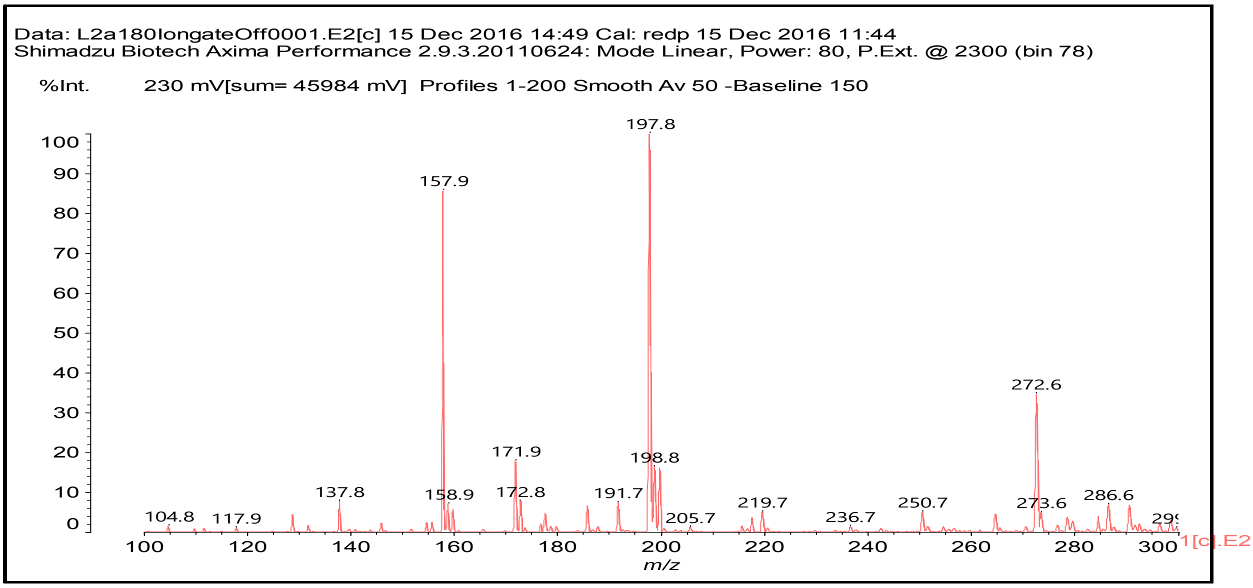
Data: L2a180IongateOff0001.E2[c] 15 Dec 2016 14:49 Cal: redp 15 Dec 2016 11:44
Shimadzu Biotech Axima Performance 2.9.3.20110624: Mode Linear, Power: 80, P.Ext. @ 2300 (bin 78)
%Int.
230 mV[sum= 45984 mV] Profiles 1-200 Smooth Av 50 -Baseline 150
197.8
157.9
272.6
171.9
198.8
137.8
158.9
172.8
191.7
219.7
250.7
273.6
286.6
104.8
117.9
205.7
236.7
m/z

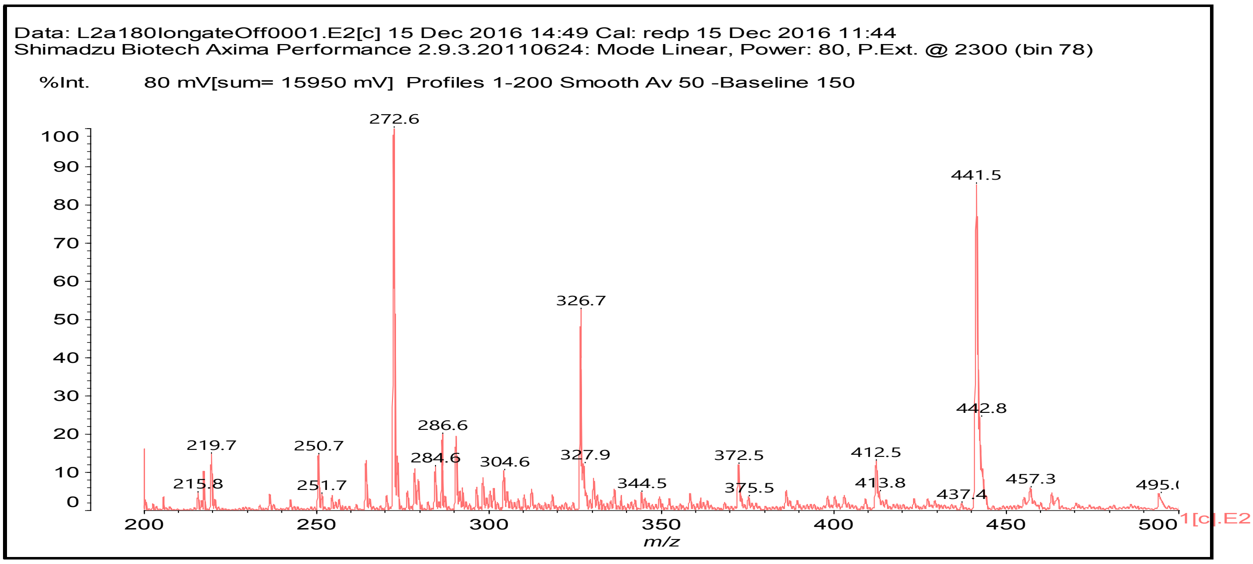
Data: L2a180IongateOff0001.E2[c] 15 Dec 2016 14:49 Cal: redp 15 Dec 2016 11:44
Shimadzu Biotech Axima Performance 2.9.3.20110624: Mode Linear, Power: 80, P.Ext. @ 2300 (bin 78)
%Int.
80 mV[sum= 15950 mV] Profiles 1-200 Smooth Av 50 -Baseline 150
272.6
441.5
326.7
442.8
286.6
219.7
250.7
284.6
304.6
327.9
372.5
412.5
215.8
251.7
344.5
375.5
413.8
437.4
457.3
m/z

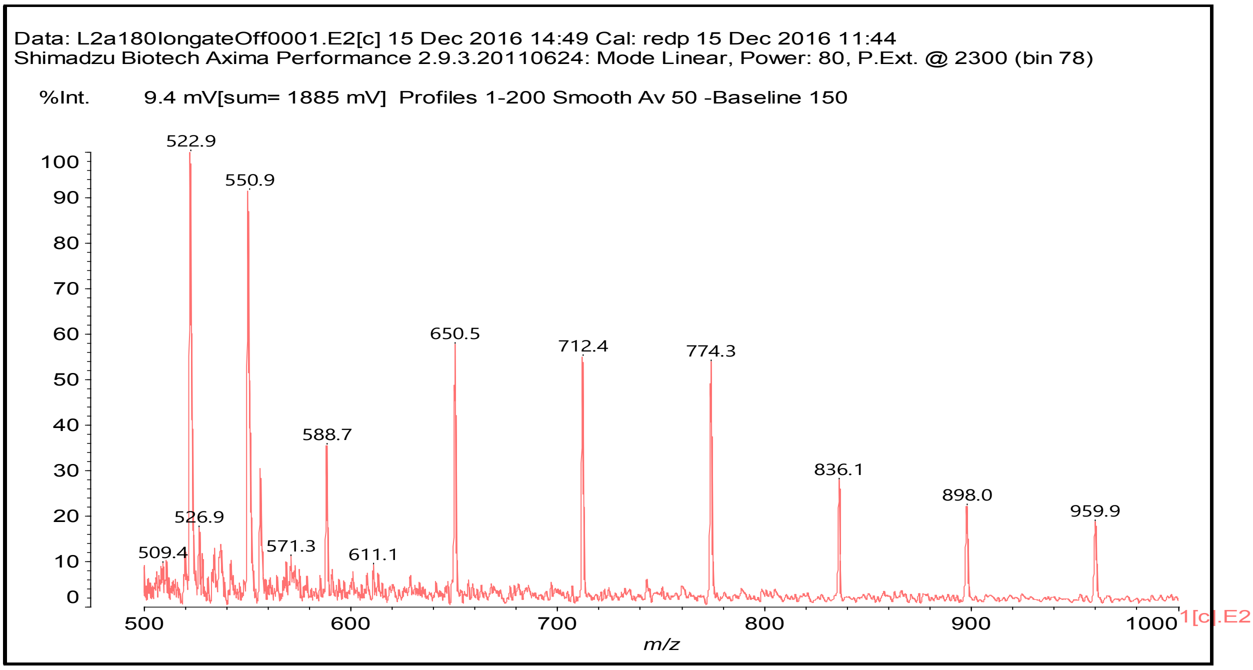

Maldi-ToF spectrum of the product obtained by the reaction of lignin with HMDA catalyzed by 2 g NaOH at 180ºC: 100-300 Da, 200-500 Da and 500-1000 Da range.

FTIR

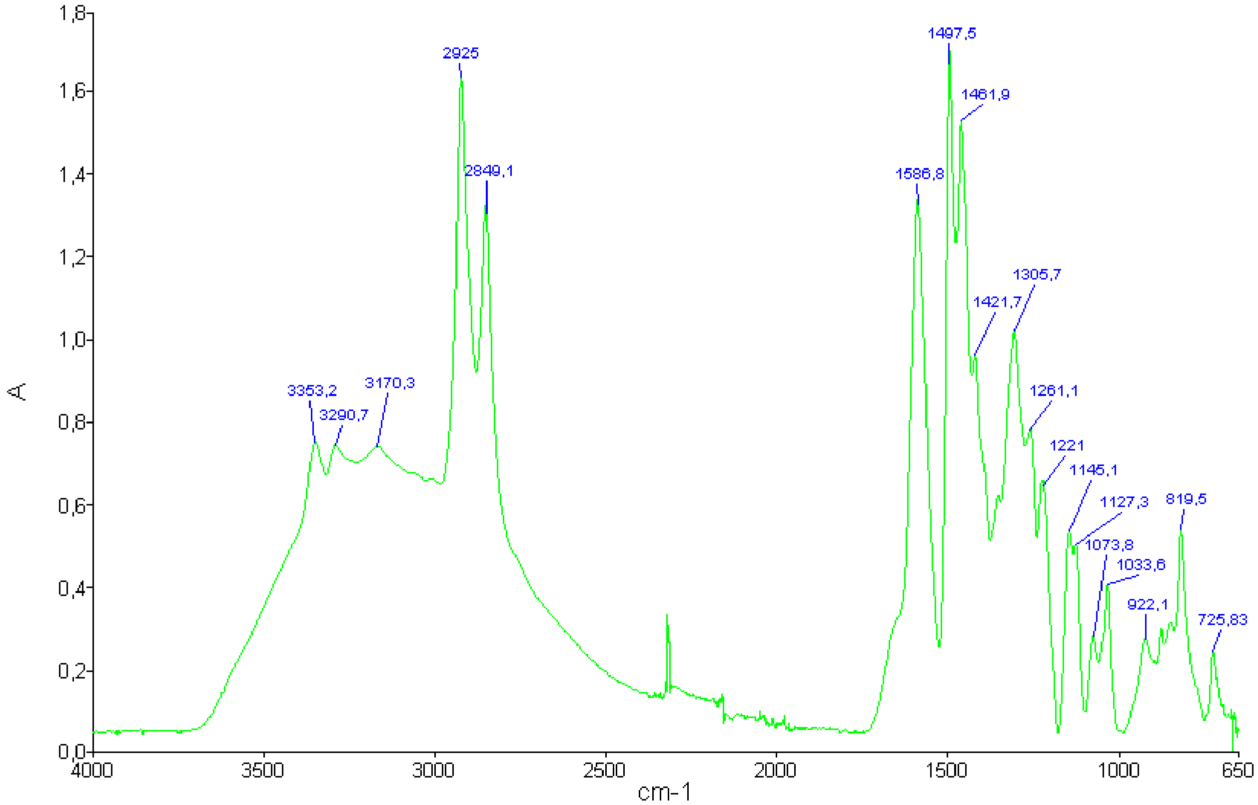

Lignin + HMDA 0.8 g NaOH catalyzed at 100 °C

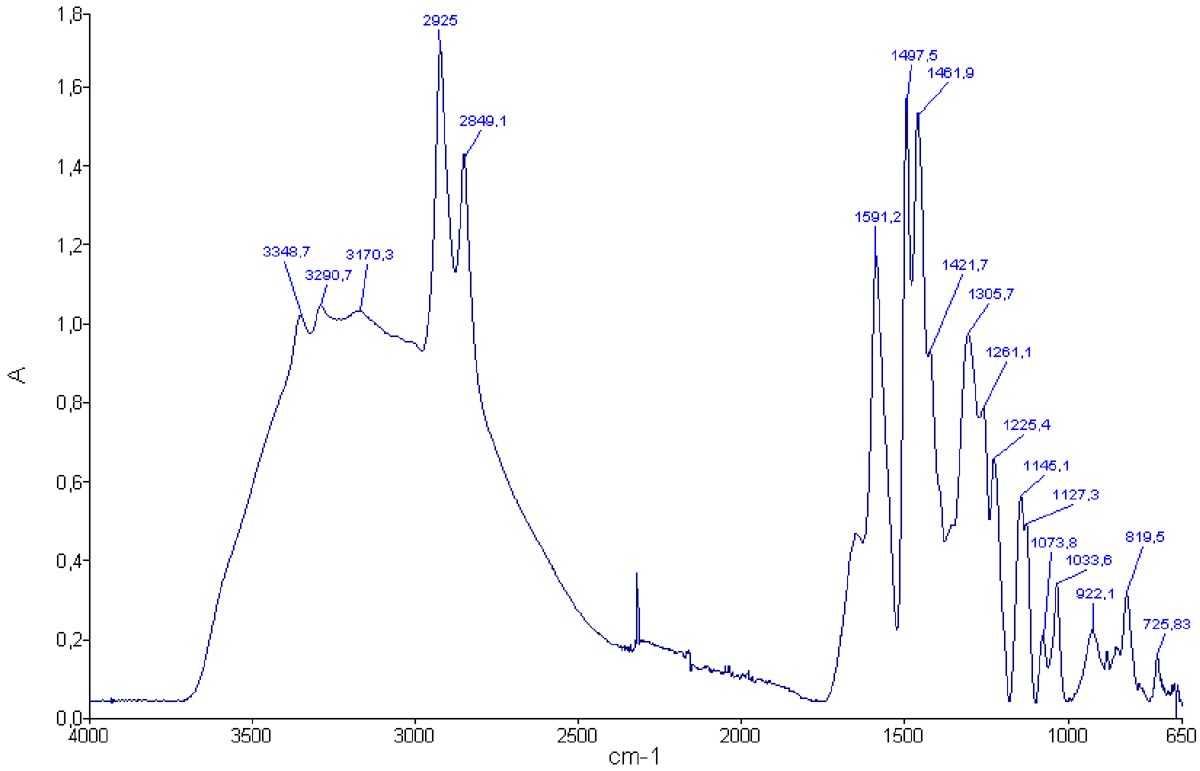

Lignin + HMDA 2 g NaOH catalyzed at 100 °C

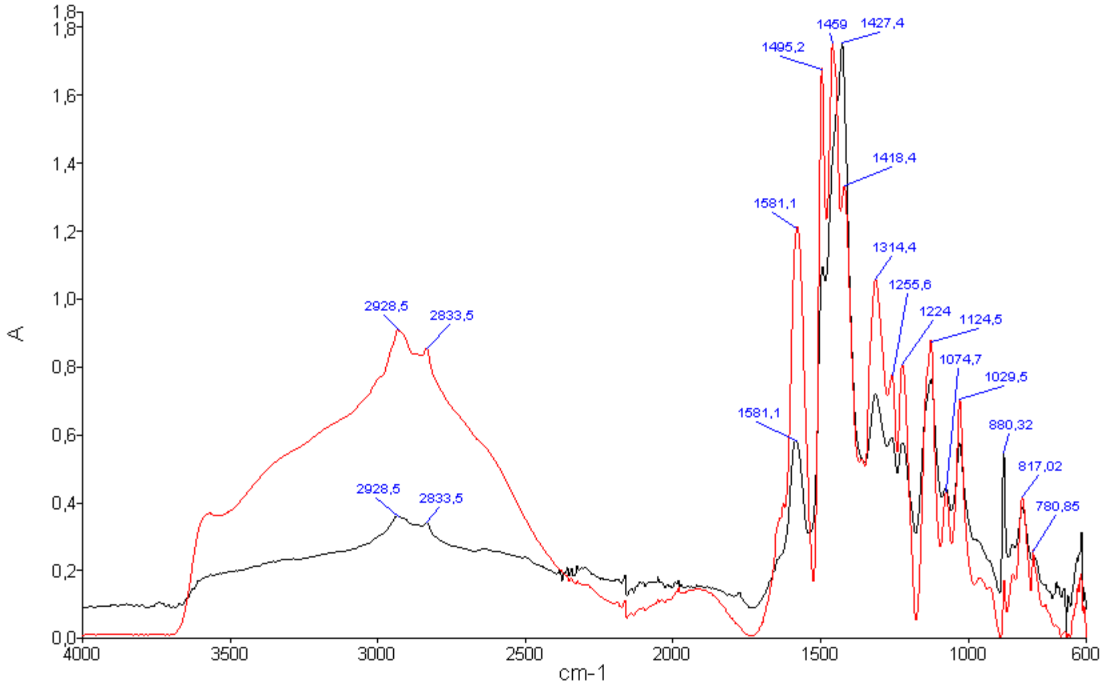

Lignin + 0.8 g NaOH (black) and lignin + 2 g NaOH (red) at 100 °C

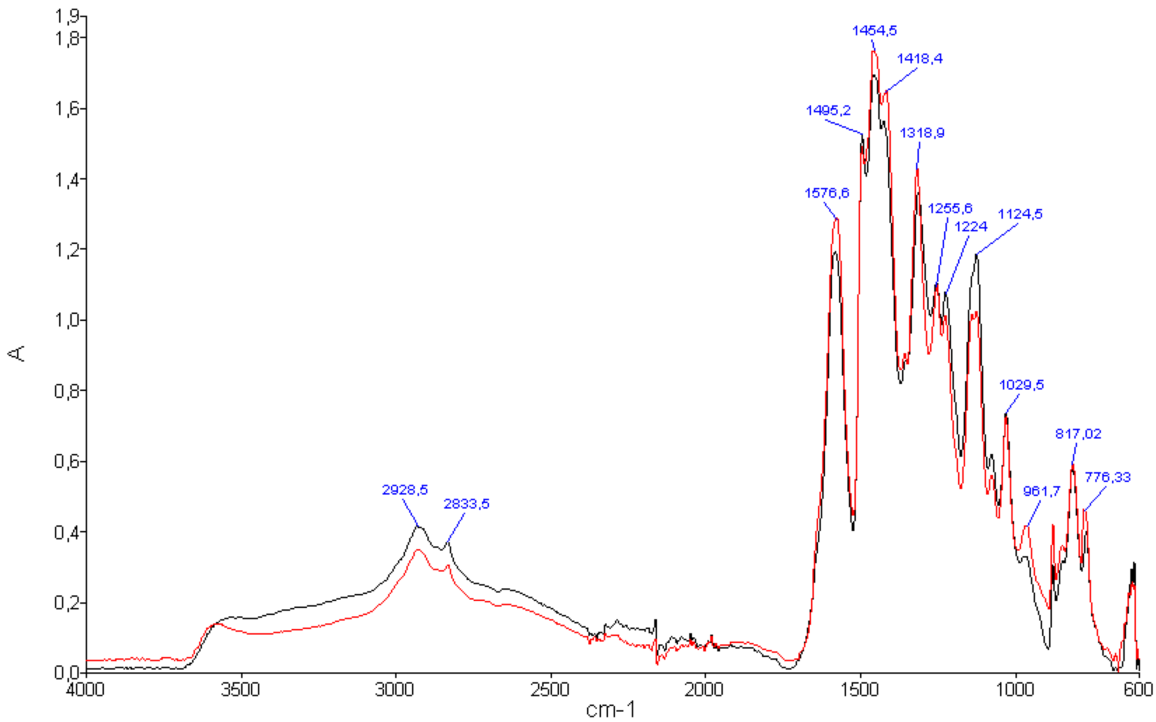

Lignin + 0.8 g NaOH (black) and lignin + 2 g NaOH (red) at 180 °C

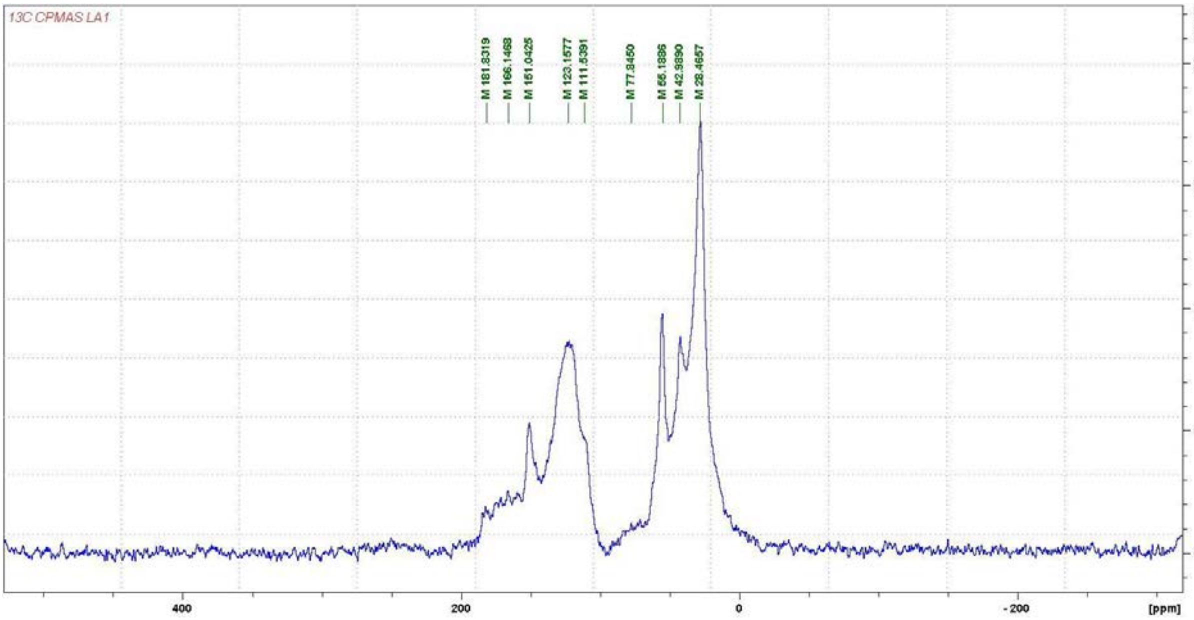

CP MAS ^{13}C NMR of Lignin + HMDA 0.8 g NaOH catalyzed at 180 °C

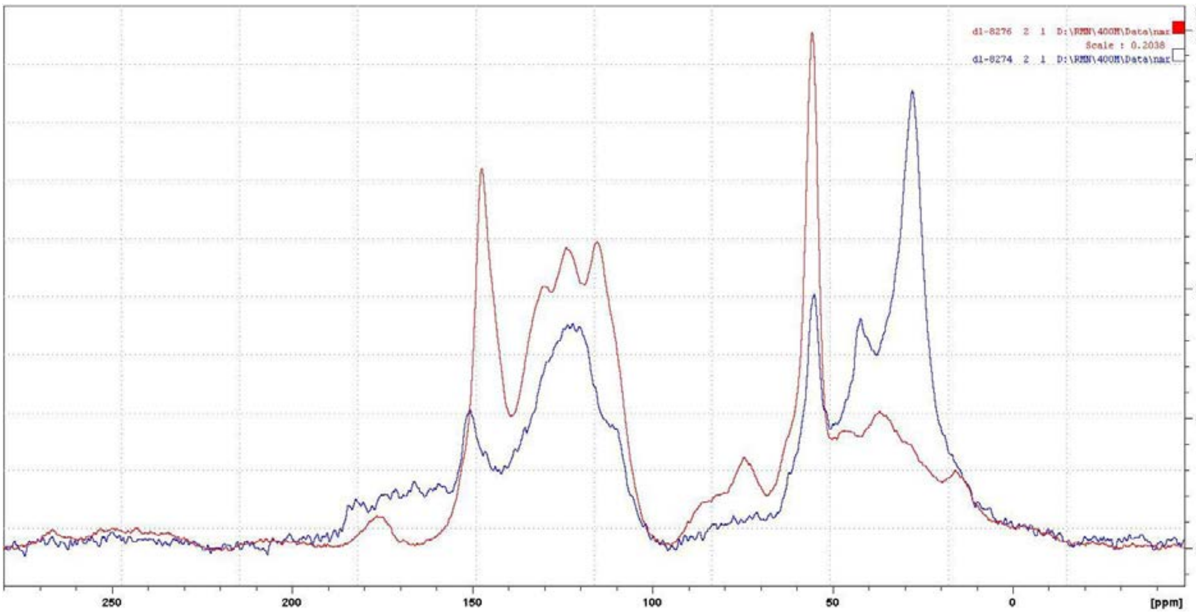

CP MAS ^{13}C NMR spectra superposition of original unreacted lignin and of Lignin + HMDA 0.8 g NaOH catalyzed at 180 °C

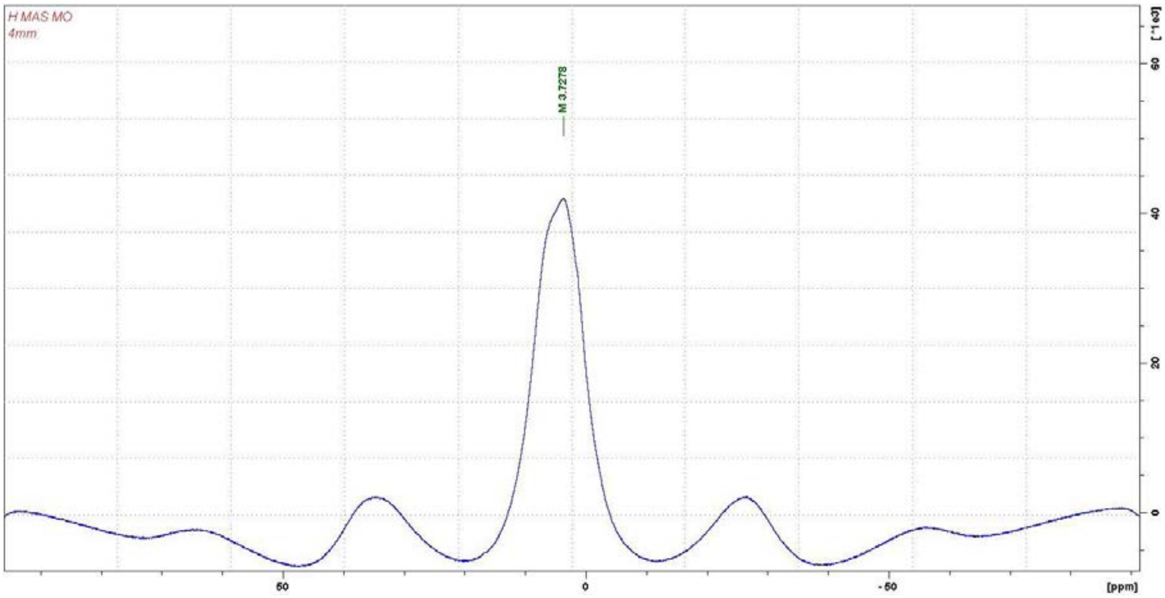

H NMR original lignin

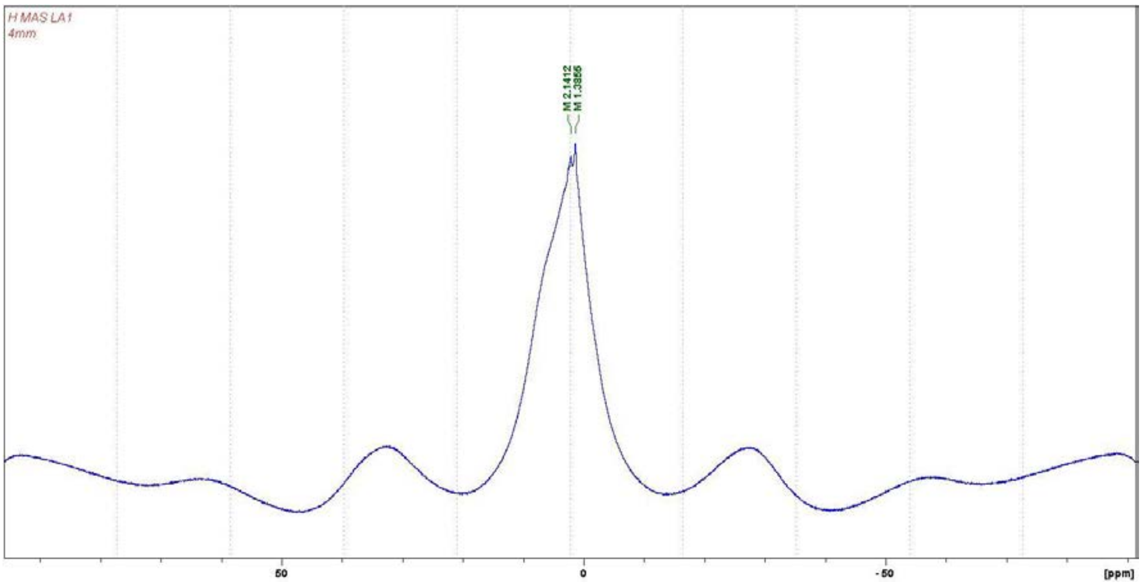

Lignin + HMDA + 0.8 g NaOH at 180 °C

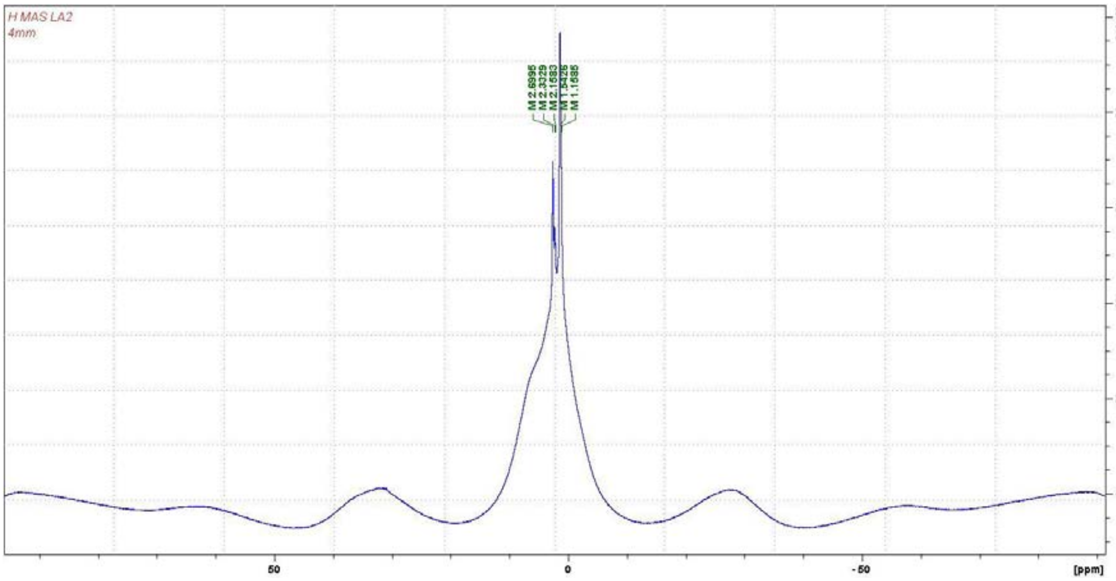

Lignin + HMDA + 2 g NaOH at 180 °C

4 « Isocyanate-free polyurethanes by coreaction of condensed tannins with aminated tannins ».

Auteurs: M. Thébault[1,2], A. Pizzi[1,3], F.J. Santiago-Medina[1], F.M. Al-Marzouki[3] et S. Abdalla[3]

[1] Laboratory of Studies and Research on Wood Material (LERMAB), University of Lorraine, 88000 Epinal, France

[2] Kompetenzzentrum Holz (WoodKPlus), 9300 Sankt Veit-an-der-Glan, Austria

[3] Department of Physics, King Abdulaziz University, Jeddah, Saudi Arabia

Résumé:

Des résines de polyuréthane biosourcedées exemptes d'isocyanates à un niveau de pourcentage très élevé ont été préparées par réaction d'extrait de tanin mimosa aminé pré-préparé avec du carbonate de diméthyle. La réaction a eu lieu avec facilité à température ambiante. Les indications étaient que les polyuréthanes obtenus formaient un film dur lorsqu'ils sont durcis à une température supérieure à 100 ° C. En outre, la fraction de carbohydrates de l'extrait de tanin semblait également être carbonée et réagie pour générer des liaisons de polyuréthane sans isocyanate avec les tanins aminés. Cela a indiqué que non seulement la fraction polyphénolique de l'extrait de tanin, mais aussi son autre composant majeur, peut être utilisée pour préparer des résines de polyuréthane. Les monomères de flavonoïdes et les oligomères carbonatés à différents niveaux, tous les deux n'ayant pas réagi et liés à l'uréthane aux monomères et oligomères de flavonoïdes aminés, ont été identifiés par la spectrométrie FTIR et MALDI-TOF.

Published by *Journal of Renewable Materials*

Scrivener First

Isocyanate-Free Polyurethanes by Coreaction of Condensed Tannins with Aminated Tannins

M. Thébault[1,2], A. Pizzi[1,3]*, F.J. Santiago-Medina[1], F.M. Al-Marzouki[3] and S. Abdalla[3]

[1]*Laboratory of Studies and Research on Wood Material (LERMAB), University of Lorraine, 88000 Epinal, France*
[2]*Kompetenzzentrum Holz (WoodKPlus), 9300 Sankt Veit-an-der-Glan, Austria*
[3]*Department of Physics, King Abdulaziz University, Jeddah, Saudi Arabia*

Received May 06, 2016; Accepted May 25, 2016

ABSTRACT: Isocyanate-free polyurethane resins biosourced to a very high percentage level were prepared by the reaction of aminated mimosa tannin extract with commercial mimosa tannin extract prereacted with dimethyl carbonate. The reaction took place with ease at ambient temperature. Indications were that the polyurethanes obtained formed a hard film when cured at a temperature higher than 100 °C. Furthermore, the carbohydrate fraction of the tannin extract also appeared to be carbonated and reacted to generate isocyanate-free polyurethane linkages with the aminated tannins. This indicated that not only the polyphenolic fraction of the tannin extract, but also its other major component, can be used to prepare polyurethane resins. Flavonoid monomers and oligomers carbonated at different levels, both unreacted and urethane-linked to aminated flavonoid monomers and oligomers, were identified by FTIR and MALDI-TOF spectrometry.

KEYWORDS: Flavonoid tannins, non-isocyanate polyurethanes, MALDI-TOF, FTIR, aminated tannins, carbohydrate polyurethanes

1 INTRODUCTION

The strong research trend on resins, adhesives and plastics derived for renewable, biosourced materials has being gaining momentum as interest in such materials continues to grow. In the case of polyurethanes (PUR), considerable literature now exists on the use of biosourced polyols, this approach leading to PURs partially biosourced up to around 50% [1–6]. This approach works well but its shortcoming is the severe limit in biosourced materials which can be used. In reality, it is not the number of eligible biosourced polyols that are lacking, but an adequate alternative to the use of the other major and essential reagents, namely reactive isocyanates. Isocyanates are the materials which have rendered possible the dominance of polyurethanes in many fields today. However, they are now classified as toxic, thus under pressure by new and upcoming government regulations. Moreover, isocyanates are mainly synthesized in industry through the phosgene ($COCl_2$) route, a hazardous route that needs specific precautions [7]. Some research was carried out several decades ago to synthesize new kinds of isocyanates by using fatty acids in vegetable oils [8–9] and furan derivatives [10–12]. These chemicals, however, are still isocyanates, thus potentially toxic materials, and in part are not issued from biosourced materials.

An alternative approach to the preparation of polyurethanes without any use of isocyanates does exist [13–15]. In a first step, a synthetic polyol, generally propylene glycol, is reacted with either a cyclic carbonate [16] or dimethyl carbonate [17]. This is followed by a second step where the carbonated polyol is reacted with a diamine, generally hexamethylene diamine, to form the isocyanate-free polyurethane. This approach has again relied on the use of synthetic, non-biosourced materials [18] or the use of vegetable oils as polyol reagents [14, 19]. Recently, this same approach was used to prepare isocyanate-free urethanes based on hydrolyzable and condensed tannins [20, 21], these materials being biosourced forestry waste. These polyurethanes, however, although being biosourced up to 45–50%, contained as reagents not only the biosourced tannin extracts, but also a synthetic diamine, the latter being the second major reagent involved. Thus, to have an isocyanate-free urethane of much higher biosourced origin, it would be necessary to substitute a biosourced

Corresponding author: antonio.pizzi@univ-lorraine.fr

material for one of the other two main reagents, namely the diamine [3, 4, 13, 18, 20, 21].

2 MATERIALS AND METHODS

2.1 Materials

Mimosa (*Acacia mearnsii* formerly *mollissima,* de Wildt) bark tannin extract was provided by Silvachimica (San Michele Mondovi, Italy). It contained 80–82% actual flavonoid monomers and oligomers, 1% of amino and imino acids, the balance being composed mainly of oligomeric carbohydrates, mainly hemicellulose fragments, and some carbohydrate monomers.

The majority of the flavonoid part of mimosa tannin extract is composed of robinetinidin and fisetinidin but also includes 10–15% of catechin and delphinidin (Figure 1), each of these monomers forming the repeating units of the tannin, the units being respectively linked by C4-C6 or C4-C8 [22]. The tannins enchainments formed by these units are respectively called prorobinetinidin, profisetinidin, procyanidin and prodelphinidin. The average number of units varies from monomers to octamers with an average DPn between 4 and 5 [23] which are otherwise too difficult to determine by other techniques. It has been possible to determine by MALDI-TOF for the two major industrial polyflavonoid tannins which exist, namely mimosa and quebracho tannins, and some of their modified derivatives that: (i. Dimethyl carbonate (99%) was purchased at Acros Organics (Geel, Belgium) and the ammonium hydroxide solution (28%) from Sigma-Aldrich (St. Louis, Missouri).

2.2 Procedure

Five grams of tannins were reacted with 5,6 g of a 28% ammonia hydroxide water solution for approximately ten minutes at ambient temperature (22–23 °C). The solution became viscous rather rapidly due to the alkaline condition brought by the ammonia solution. This type of solution, after stirring for 1 h at ambient temperature, tends to increase in viscosity if left at ambient temperature for up to 1 day, due to further tannin condensation under basic conditions and formation of =N- bridges between flavonoids [24].

The reactions were carried out at ambient temperature. First, 5 g Mimosa tannin extract were added to 10.5 g dimethyl carbonate and mixed under mechanical stirring for two h [21]. At this stage, tannins are only solvated into the carbonate solvent; the pH then being around 5. This was added to the aminated tannins and stirred vigorously for a few minutes. Carboxymethylation of phenolic hydroxyl groups by dimethyl carbonate group, which is generally observed at temperatures around 90 °C for phenol, has been reported to be a bimolecular nucleophilic substitution, acyl-cleaving in basic catalysis ($B_{AC}2$) [17]. Due to the basic conditions of the aminated tannins mixture, a condensation reaction is expected to occur according to the following mechanism (Figure 2):

The reaction mixture so obtained was left to gel at ambient temperature (between 20 and 25 °C) for at least 24 h. Under these conditions, only oligomers of urethanes could be expected. Their solubility in a solvent such as acetone/water rendered possible their characterization by MALDI-TOF. To verify these can cure into a thermoset resin if heated at high temperature, a part of this material was placed in an oven at

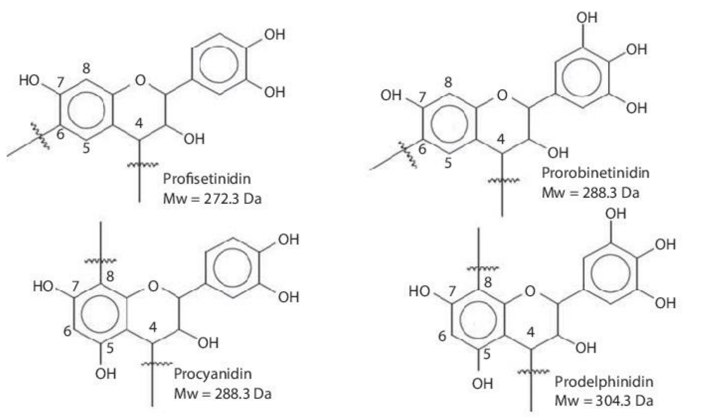

Figure 1 The four main structures in commercial flavonoid tannins.

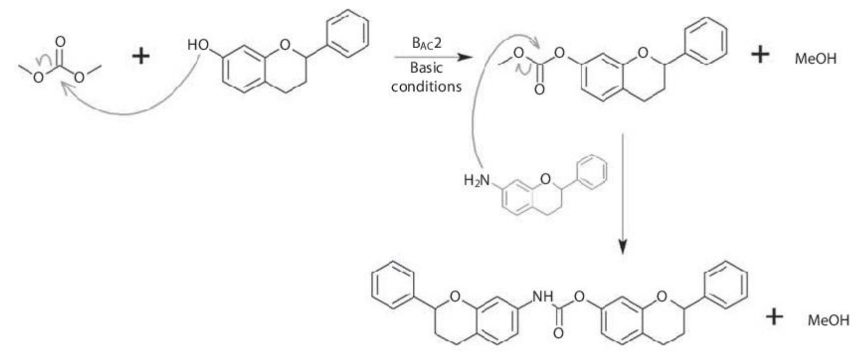

Figure 2 Bimolecular nucleophilic substitution, acyl-cleaving in basic catalysis ($B_{AC}2$) mechanism between dimethyl carbonate and a flavonoid tannin molecule.

103 °C for 24 h. A hard solid, insoluble in acetone/water, was then obtained.

2.3 Analysis

2.3.1 *Fourier Transform Infrared (FTIR) Analysis*

To confirm the presence of urethane structures, Fourier transform infrared (FTIR) analysis was carried out using a Shimadzu IRAffinity-1 spectrophotometer (Shimadzu France, Marne-la Vallée, France). A blank sample tablet of potassium bromide, ACS reagent from Acros Organics (Geel, Belgium), was prepared for the reference spectrum. A similar tablet was prepared by mixing potassium bromide with 5% w/w of the sample powder to analyze. The spectrum was obtained in absorbance measurement by combining 32 scans with a resolution of 2.0.

2.3.2 *MALDI-TOF Analysis*

Matrix-assisted laser desorption/ionization with time-of-flight (MALDI-TOF) characterization is a high resolution mass spectrometry technique which can analyze oligomers and pre-polymers distribution. The samples to analyze are mixed with a matrix consisting of crystallized molecules such as 2,5-dihydroxy benzoic acid (DHB). For this reason, they must be dissolved in a solvent in order to be efficiently associated with the matrix.

Samples for MALDI-TOF analysis were prepared by first dissolving 5 mg of sample powder in 1 mL of a 50:50 v/v acetone/water solution. Then 10 mg of this solution is added to 10 µL of the 2,5-dihydroxy benzoic acid (DHB) matrix. The locations dedicated to the samples on the analysis plaque were first covered with 2 µL of a NaCl solution 0.1M in 2:1 v/v methanol/water, and predried. Then 1 µL of the sample solution was placed on its dedicated location and the plaque was dried again. MALDI-TOF spectra were obtained using an Axima-Performance mass spectrometer from Shimadzu Biotech (Kratos Analytical, Shimadzu Europe Ltd., Manchester, UK) using a linear polarity-positive tuning mode after calibrating the instrument with red phosphorous standard. The measurements were carried out making 1000 profiles per sample with 2 shots accumulated per profile. The spectrum precision is of +1Da.

3 RESULTS AND DISCUSSION

3.1 Fourier Transform Infrared Spectrometry (FTIR) Analysis

Figure 3 shows the FTIR spectra of the original mimosa tannins extracts (a), these tannin extracts reacted with an ammonia solution (b), and the product obtained by reaction of the carbonated mimosa tannin extract with the aminated tannin extract (c).

Actually, several peaks in the reaction material spectrum (c) could be relevant for the presence of urethane linkages, namely at 3400 cm^{-1}, 1700 cm^{-1}, 1507 cm^{-1}, 1296 cm^{-1} (the urethane peak being generally in the range of 1200–1300 cm^{-1}), and 1072 cm^{-1}. However, these peaks can also be relevant for other linkage types present in (a) and (b), such as C-O and C-N respectively. The characteristic bands of aromatic nuclei at 1600 cm^{-1}, 1500 cm^{-1} and 1460 cm^{-1} are present in the three materials spectra, although two of them seem to be covered by a large band at 1630 cm^{-1}, relevant for $-NH_2$ and/or C=N deformation. Aromatic moieties remain dominant in reaction

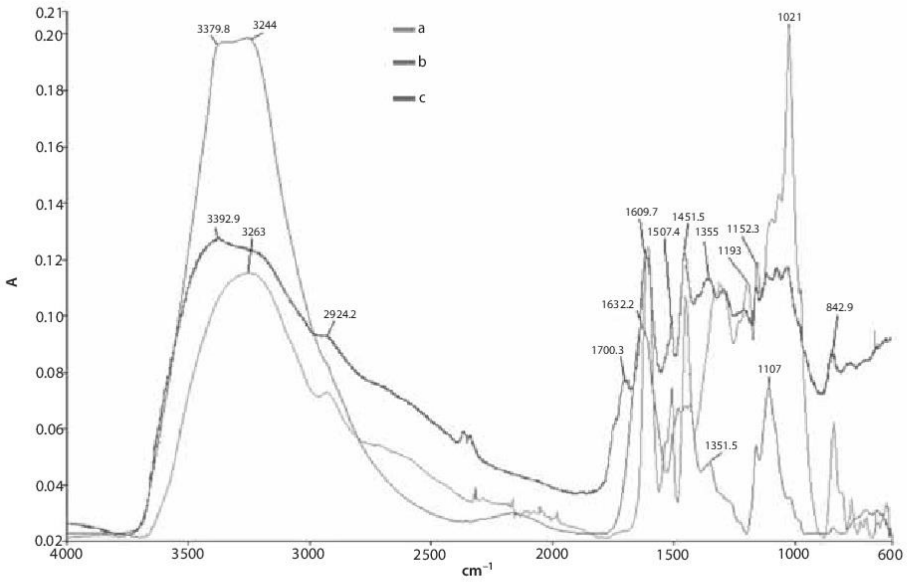

Figure 3 FTIR spectra of (**a**) Mimosa tannins extract; (**b**) Mimosa tannins extract reacted with an ammonia solution; (**c**) the product mixture obtained by reaction of mimosa tannin extract in dimethyl carbonate with the aminated tannin extract.

material (c), meaning that urethane bonds would not be significant enough compared to flavonoids polyphenolic structures. There are, however, some clues that let us suppose that some urethane bonds could have been actually formed in the reaction material (c).

In the original tannin extracts spectrum (a), a major peak at 1020 cm^{-1} can be attributed to the C-O-C ether of the heterocyclic ring of the flavonoid. This is small in (c), indicating opening of the heterocyclic ring, a fairly common occurrence in flavonoids. Alternatively, it could be assigned to either a carbohydrate primary hydroxyl stretching or, alternatively, to the C-O stretching of the only alcohol –OH on the C3 site of the flavonoid. In either of these last two cases its decrease in (c) would indicate that either the –OH in C3 of the flavonoids has reacted and/or that –OH groups on the carbohydrates have also reacted.

In the aminated tannins material (b), two bands between 3240 and 3400 cm^{-1} attest to the presence of primary amines, and the width of the band between 3500 and 3000 cm^{-1} shows that not all the hydroxyl groups have been aminated. The major peak at 1632 cm^{-1} is relevant for $–NH_2$ and/or C=N deformation. The presence of –C=N- groups has been demonstrated by ^{13}C NMR in aminated tannins obtained in the manner described here [24]. However, in the reaction material (c), this peak is less represented as it is probably covered by the more dominant band at 1610 cm^{-1} of aromatic nuclei. However, a major band at 3340 cm^{-1} remains in the spectrum, relevant for secondary amines, partly masked by the wide –OH peak. This is due to the tannin residual hydroxyl groups, the methanol produced during carbonatation, or possible residual water.

In the aminated tannins (b), the most relevant peak for the amine groups is at 3380 cm^{-1}, whereas it is situated at 3340 cm^{-1} in (c) due to a greater level of substitution on the carbons in alpha positions: for instance, the C=O of urethane bond. Concerning the remaining phenolic –OH groups, their vibrational band is usually approximately situated between 3700 and 3125 cm^{-1}. However, for tannin extracts alone (a), this band is rather symmetric and centered at 3250 cm^{-1}. This is typical of the intermolecular interactions of the -OH groups (between 3400 and 3200 cm^{-1}), this being common between flavonoid monomer units. Concerning the -NH vibration, the bands are generally narrower, which on spectra is characterized by particular peaks besides the large vibration of the remaining –OH groups [(b) and (c)]. Finally, the appearance of the 1700 cm^{-1} band in (c) is characteristic of urethanes, this when it is coupled with the 1220–1230 cm^{-1} band (with the caution that this could also be interpreted as the C-O stretching of phenolic groups) and the small band at 1020–1035 cm^{-1} (also described above for other possible interpretations).

3.2 MALDI-TOF Analysis

At this early stage of reaction, the material prepared at ambient temperature is not expected to be a fully crosslinked network. However, the pre-polymerized moieties soluble in acetone/water and likely to contain some urethane linkages could be characterized by MALDI-TOF spectrometry. In this way, possible urethane/polyurethane moieties could be compared in molecular weight to the main peaks and patterns that were obtained in the spectrum in the range of 400–1500 Da.

The MALDI spectrum of the material prepared at ambient temperature is presented in Figure 4(c) to compare it with the original mimosa tannins extract (a) and the aminated mimosa tannins extracts (b). Interpretations of these last two spectra were already done in previous works on mimosa tannins chemistry [23–25] prorobinetinidin (PR and tannins reacted with ammonia [24]. A first assessment that can be made, comparing these three spectra, is that the main signals and repeating patterns are different. It indicates, on the one hand, that the basic monomer unit of the reaction material (c) is not the same as in either the raw material or in the initial materials. Thus, the mass difference between the main signal of 889 Da in the original tannins (a), which can correspond to a procyanidin trimer for instance, and the main signal of 1113 Da in the reaction material (c), is of 224 Da, which is lower than a flavonoid unit. This is probably due to a complex combination of carbonation with dimethyl carbonate and formation of urethane linkages. Conversely, while the main repeating patterns of the original tannin (a) are separated by a mass differential of 288 Da, the reaction material's (c) are of approximately 286 ± 2Da, which supposes that the additional monomers are tannins original units in which some hydroxyl groups have been substituted by amine groups, resulting in the slight loss of mass observed.

Thus, a list of possible oligomers interpreted from Figure 4 is shown in Table 1. In the reacted mix, one can find multicarbonated flavonoid oligomers, several carbonated at different levels, and carbonated and aminated flavonoid monomers and oligomers linked by urethane linkages. Aminated flavonoid species reacted through a urethane bridge with carbohydrate monomers contained in the extract are also present. First, it must be pointed out that the identical molecular weight of catechin and robinetinidin does not allow distinguishing which of the two structures is present. Thus, in the discussion that follows and in Table 1 wherever catechin is indicated it can be robinetinidin instead, and vice versa. While in the type of tannin used (mimosa), where robinetinidin is in the majority, the higher potential reactivity of catechin could indicate that in the structure described below both exist with the two types of flavonoid.

Examples of urethane-linked flavonoids are those at 796 Da, 812 Da, 827 Da, 861 Da, 1084 Da, 1100 Da, 1112 Da, 1117 Da, 1130 Da, 1381 Da, 1397 Da and 1413 Da. It is possible that these types of species have structures of the type observed for the 861 Da peak, for instance, namely:

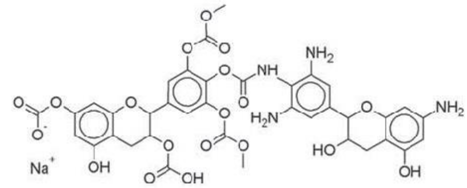

with a variable number of carbonated and aminated flavonoids.

One can observe species in which two flavonoid monomers are linked by a urethane such as those represented by the peaks at 796 Da, 812 Da and 861 Da, and species in which flavonoid oligomers are linked through a single urethane bridge to a flavonoid monomer or oligomers such as the peaks at 1084 Da, 1100 Da, 1112 Da, 1130 Da, 1381 Da, 1397 Da and 1413 Da, such as one of the representations of the peak at 1413 Da:

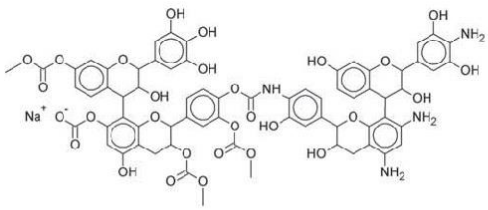

And the peak at 1397 Da which can be represented as:

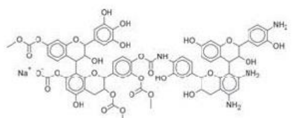

On top of these species there are species where flavonoid monomers are linked through a urethane bridge to a carbohydrate monomer such as the peaks

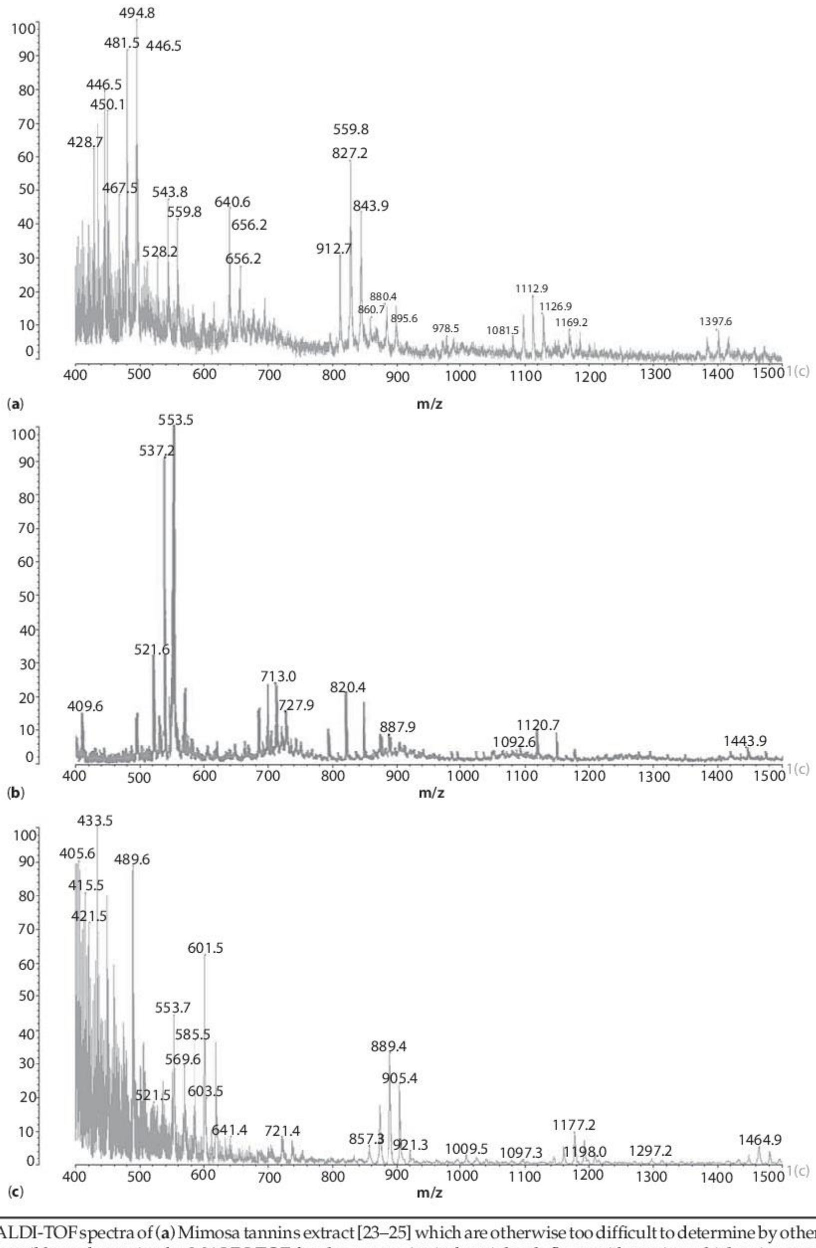

Figure 4 MALDI-TOF spectra of (**a**) Mimosa tannins extract [23–25] which are otherwise too difficult to determine by other techniques. It has been possible to determine by MALDI-TOF for the two major industrial polyflavonoid tannins which exist, namely mimosa and quebracho tannins, and some of their modified derivatives that: (i; (**b**) Mimosa tannins extract reacted with an ammonia solution [24]; (**c**) the product mixture obtained by reaction of mimosa tannin extract in dimethyl carbonate with the aminated tannin extract.

Table 1 Interpreted possible oligomer species identified by MALDI-TOF for the mixture of carbonated mimosa tannin extract reacted at ambient temperature with aminated mimosa tannin extract. The urethane linkage between flavonoid units is indicated as "URETHANE."

Moiety	Corresponding description possibilities
481 Da	Urethane aminated fisetinidin-carbohydrate monomer
495-496 Da	Urethane aminated catechin-carbohydrate monomer (or robinetinidin-sugar)
529 Da	Fisetinidin tetracarbonated, sodium
543 Da	Catechine and/or robinetinidin tetracarbonated OR unprotonated monocarbonated carbohydrate monomer-URETHANE-diaminated fisetinidin
559 Da	Delphinidin tetracarbonated OR unprotonated monocarbonated carbohydrate monomer-URETHANE-triaminated robinetinidin
640 Da	Monocarbonated catechin/robinetinidin dimer OR unprotonated monocarbonated fisetinidin-URETHANE-fisetinidin
655 Da	Monocarbonated delphinidin dimer OR unprotonated monocarbonated robinetinidin-URETHANE-fisetinidin
796 Da	Unprotonated tricarbonated catechin-URETHANE-tetraamminated catechin OR diaminated catechin-URETHANE-carbohydrate monomer-URETHANE-protonated triaminated fisetinidin
812-813 Da	Unprotonated tricarbonated catechin-URETHANE-pentaaminated delphinidin OR protonated catechin-URETHANE-carbohydrate monomer-URETHANE-protonated robinetinidin
827-830 Da	Unprotonated tetracarbonated robinetinidin-URETHANE-triaminated delphinidin
843 Da	Unprotonated tetracarbonated delphinidin dimer OR unprotonated tetracarbonated catechin-URETHANE-tetraaminated delphinidin
861 Da	Unprotonated tetratacarbonated delphinidin-URETHANE-triaminated delphinidin
880 Da	Diaminated [(robinetinidin)$_2$ delphinidin] trimer
895 Da	Triaminated [(delphinidin)$_2$-robinetinidin] trimer
1081 Da	Tricarbonated (catechin)$_2$ dimer-URETHANE-triaminated delphinidin
1097 Da	Tricarbonated catechin-delphinidin dimer-URETHANE-triaminated delphinidin
1113 Da	Unprotonated tetracarbonated (catechin)$_2$ dimer-URETHANE-pentaaminated delphinidin OR triaminated robinetinidin-URETHANE-unprotonated tricarbonated delphinidin-URETHANE-triaminated robinetinidin
1126 Da	Pentaaminated delphinidin-URETHANE-unprotonated tricarbonated delphinidin-URETHANE-tetraaminated robinetinidin
1381 Da	Tetracarbonated monoaminated fisetinidin-catechin dimer-URETHANE-monoaminated fisetinid-robinet dimer
1397 Da	Unprotonated tetracarbonated robinetinidin-catechin dimer-URETHANE-triaminated fisetinidin-catechin dimer
1413 Da	Unprotonated tetracarbonated robinetinidin-catechin dimer-URETHANE-triaminated robinetinidin-catechin dimer

at 481 Da, 496 Da, such as the 481 Da peak represented as:

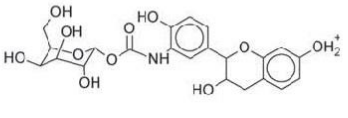

And even species in which two urethane bridges link a monomeric carbohydrate to two different flavonoid monomers such as for the peaks at 796 Da and 813 Da, for example:

796Da

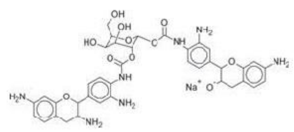

And
813 Da

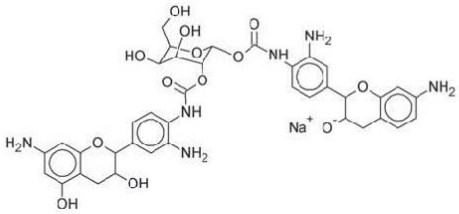

The presence of these two species implies that in carbonating the polyphenolic part of the tannin extract, the carbohydrate monomers, and possibly also carbohydrate oligomers, present in the commercial extract can get carbonated as well. This then renders possible their reaction with aminated flavonoids to form species like those belonging to the 796 Da and 813 Da peaks. Reaction of carbohydrates with dimethyl carbonate and the reaction which follows with aminated compounds were already observed in the case of the reaction of hydrolyzable tannins with hexamethylenediamine to form urethanes [20].

4 CONCLUSION

- The preparation of more than 70% biosourced isocyanate-free polyurethane resins for adhesives and surface finishes obtained by the reaction of carbonated condensed flavonoid tannin extracts by reaction with aminated tannin extracts of the same nature seems to be possible.
- The reaction to obtain the intermediate resins in solution, finally applicable and curable at 103 °C, occurs with ease at ambient temperature. Furthermore, if dimethyl carbonate is also considered as biosourced, then the composition of these polyurethanes is well over 80–90% biosourced.
- The carbohydrate fraction of the tannin extracts can also be carbonated and reacted to generate isocyanate-free polyurethane linkages with aminated tannins. The carbohydrates in tannin extracts are in general either carbohydrate monomers or short carbohydrate oligomers, both originating from hydrolysis of hemicelluloses during tannin extraction.

These findings show that the entire tannin extract and not only its polyphenolic components can be used to prepare polyurethanes. It opens up the possibility of producing the same starting exclusively from carbohydrates, a possibility that must still be checked.

Aknowledgments

The first and second authors thank the LERMAB. LERMAB is supported by a grant overseen by the French National Research Agency (ANR) as part of the "Investissements d'Avenir" program (ANR-11-LABX-0002-01, Lab of Excellence ARBRE). This paper was partially funded by King Abdulaziz University (KAU) under grant No (4-130-37-RG). The second, fourth and fifth authors, acknowledge the support of KAU.

REFERENCES

1. Y. Peng, Z. Zheng, P. Sun, X. Wang, and T. Zhang, Synthesis and characterization of polyphenol-based polyurethane. *New J. Chem.* **37**, 729–734 (2013).
2. J.-J. Ge, X. Shi, M. Cai, R. Wu, and M. Wang, A novel biodegradable antimicrobial PU foam from wattle tannin. *J. Appl. Polym. Sci.* **90**, 2756–2763 (2003).
3. J.-J. Ge and K. Sakai, Decomposition of polyurethane foams derived from condensed tannin II: Hydrolysis and aminolysis of polyurethane foams. *J. Wood Sci.* **44**, 103–105 (1998).
4. J.-J. Ge and K. Sakai, Compressive properties and biodegradabilities of polyurethane foams derived from condensed tannins. *Mokuzai Gakkaishi* **39**, 801–806 (1993).
5. M.C. Basso, A. Pizzi, C. Lacoste, L. Delmotte, F.A. Al-Marzouki, S. Abdalla, and A. Celzard, MALDI-TOF and ^{13}C NMR analysis of tannin–furanic–polyurethane foams adapted for industrial continuous lines application. *Polymers* **6**, 2985–3004 (2014).
6. M.C. Basso, S. Giovando, A. Pizzi, H. Pasch, N. Pretorius, L. Delmotte, and A. Celzard, Flexible-elastic copolymerized polyurethane-tannin foams. *J. Appl. Polym. Sci.* **131**, 40499–40505 (2014).
7. C. Six and F. Richter, Isocyanates, organic, in: *Ullmann's Encyclopedia of Industrial Chemistry*, Wiley-VCH Verlag, Weinheim, Germany (2003).
8. L. Hojabri, X. Kong, and S.S. Narine, Fatty acid-derived diisocyanate and biobased polyurethane produced from vegetable oil: Synthesis, polymerization, and characterization. *Biomacromol.* **10**, 884–891 (2009).
9. S.S. Washburne and W.R. Peterson, Isocyanates derived from fatty acids by the trimethylsilyl azide modification of the Curtius rearrangement. *J. Am. Oil Chem. Soc.* **49**, 694–695 (1972).
10. J. Nowakowski, Isocyanate intermediates. II. Trichloromethyl chloroformate – a convenient reagent for the preparation of diisocyanates with benzene or furan rings. *J. für Prakt. Chemie/Chemiker-Zeitung* **334**, 187–189 (1992).
11. J.D. Gather, Furfuryl isocyanates, US Patent 3049552 A, assigned to Merck & Co Inc (August14, 1962).

12. S. Boufi, N. Belgacem, M.N. Quillerou, and A. Gandini, Urethanes and polyurethanes bearing furan moieties. 4. Synthesis, kinetics, and characterization of linear polymers. *Macromolecules* **26**, 6706–6717 (1993).
13. G. Rokicki and A. Piotrowska, A new route to polyurethanes from ethylene carbonate, diamines and diols. *Polymer* **43**, 2927–2935 (2002).
14. B. Nohra, L. Candy, J.-F. Blanco, C. Guerin, Y. Raoul, and Z. Mouloungui, From petrochemical polyurethanes to biobased polyhydroxyurethanes, a review. *Macromolecules* **46**, 3771–3792 (2013).
15. H. Blattmann, M. Fleischer, M. Bähr, and R. Mülhaupt, Isocyanate- and phosgene-free routes to polyfunctional cyclic carbonates and green polyurethanes by fixation of carbon dioxide. *Macromol. Rapid Commun.* **35**, 1238–1254 (2014).
16. V. Besse, F. Camara, C. Voirin, R. Auvergne, S. Caillol, and B. Boutevin, Synthesis and applications of unsaturated cyclocarbonates. *Polym. Chem.* **4**, 4545–4561 (2013).
17. P. Tundo and M. Selva, The chemistry of dimethyl carbonate. *Acc. Chem. Res.* **9**, 706–716 (2002).
18. F. Camara, S. Benyahya, V. Besse, G. Boutevin, R. Auvergne, B. Boutevin, and S. Caillol, Reactivity of secondary amines for the synthesis of nonisocyanate polyurethanes. *Eur. Polym. J.* **55**, 17–26 (2014).
19. M. Thebault, A. Pizzi, S. Dumarcay, P. Gerardin, E. Fredon, and L. Delmotte, Polyurethanes from hydrolysable tannins obtained without using isocyanates. *Ind. Crops Prod.* **59**, 329–336 (2014).
20. M. Desroches, S. Benyahya, V. Besse, R. Auvergne, B. Boutevin, and S. Caillol, Synthesis of bio-based building blocks from vegetable oils: a platform chemicals approach. *Lipid Technol.* **26**, 35–38 (2014).
21. M. Thebault, A. Pizzi, H. Essawy, A. Baroum, and G. Van Assche, Isocyanate free condensed tannin-based polyurethanes. *Eur. Polym. J.* **67**, 513–526 (2015).
22. A. Pizzi, *Wood Adhesives Chemistry and Technology*, Marcel Dekker, New York, NY (1983).
23. H. Pasch, A. Pizzi, and K. Rode, MALDI-TOF mass spectrometry of polyflavonoid tannins. *Polymer* **42**, 7531–7539 (2001).
24. F. Braghiroli, V. Fierro, A. Celzard, A. Pizzi, K. Rode, W. Radke, L. Delmotte, and J. Parmentier, Reaction of condensed tannins with ammonia. *Ind. Crops Prod.* **44**, 330–335 (2013).
25. Y. Ishida, K. Kitagawa, K. Goto, and H. Ohtani, Solid sampling technique for direct detection of condensed tannins in bark by matrix-assisted laser desorption/ionization mass spectrometry. *Rapid Commun. Mass Spectrom.* **19**, 706–710 (2005).

5 « Polyurethanes from kraft lignin without using isocyanates »

Auteurs: F.J. Santiago-Medina[1], M.C.Basso[1], A.Pizzi[1,2], L.Delmotte[3]

[1] LERMAB, University of Lorraine, 27 rue Philippe Seguin, 88000 Epinal, France

[2] Dept. of Physics, King Abdulaziz University, Jeddah, Saudi Arabia

[3] Material Science Institute of Mulhouse, UMR CNRS 7361, University of Haute Alsace, 15 rue Jean Starcky, BP 2488, 68057 Mulhouse Cedex, France

Résumé:

La réaction d'une lignine kraft désulfurée avec de l'hexaméthylène diamine et du carbonate de diméthyle a permis de développer des résines de polyuréthane exemptes d'isocyanate. Le présent travail de recherche repose sur des études antérieures réalisées avec des tanins hydrolysables et des tanins condensés, mais en profitant du nombre élevé de groupes hydroxyle présents dans la lignine et de leur caractère différent, aromatique ou aliphatique. Les matériaux obtenus ont été analysés par spectrométrie à infrarouge de transformée de Fournier (FTIR), par spectrométrie de masse à ionisation de désorption laser assistée matricielle (MALDI-TOF) et par polarisation croisée à l'état solide / centrifugation par angle magique CP MAS 13C RMN, qui a révélé la présence de fonctions uréthane. L'interprétation des résultats a montré un plus grand nombre d'espèces que lorsque des tanins ont été utilisés et a indiqué la présence de deux types de liaison dans les nouvelles molécules formées: les liaisons ioniques et covalentes dans les hydroxylés aromatiques et aliphatiques.

Accepted to Journal of Renewable Materials

POLYURETHANES FROM KRAFT LIGNIN WITHOUT USING ISOCYANATES

F.J.Santiago-Medina[1], M.C.Basso[1], A.Pizzi[1,2]*, L.Delmotte[3]

[1]LERMAB, University of Lorraine, 27 rue Philippe Seguin, 88000 Epinal, France

[2]Dept. of Physics, King Abdulaziz University, Jeddah, Saudi Arabia

[3]Material Science Institute of Mulhouse, UMR CNRS 7361, University of Haute Alsace, 15 rue Jean Starcky, BP 2488, 68057 Mulhouse Cedex, France

*Corresponding author: Anotnio Pizzi (antonio.pizzi@univ-lorraine.fr) LERMAB, University of Lorraine.

ABSTRACT

The reaction of a desulphurized kraft lignin with hexamethylene diamine and dimethyl carbonate has allowed to develop isocyanate-free polyurethane resins. The present research work is based in previous studies made with hydrolysables and condensed tannins but taking in advantage the higher number of hydroxyl groups present in the lignin. The obtained materials were analyzed by Fournier transform infrared (FTIR) spectroscopy, matrix assisted laser desorption ionization time of flight (MALDI-TOF) mass spectrometry and solid state cross-polarization/magic angle spinning CP MAS 13C NMR, which have revealed the presence of urethane functions. The interpretation of the results has shown a larger number of species than when tannins were used and has indicated the presence of two types of bond in the new molecules formed: ionic and covalent bonds.

Keywords: Lignin, urethanes, non-isocyanate polyurethanes, MALDI-TOF, FTIR

INTRODUCTION

Polyurethanes can be prepared from a great variety of biorenewable polyols, such as tannin [1–7] and lignin [8–11]. However, reaction of these biosourced polyols with polymeric isocyanates is still necessary to prepare polyurethanes. Alternate chemical routes to prepare non-isocyanate based polyurethanes exist. These were pioneered by Rokicki et Piotrowska [12] and may involve vegetable oil derived materials as polyols derived from renewable resources [13]. However, the use of vegetable oils in resins has been shown to present an unfavorable environmental balance, while the environmental balance of tannin-derived resins has been shown to be favorable [14].

Recently, polyurethanes without isocyanates based on hydrolysable and condensed tannins have been prepared [15–17]. Tannins, mostly composed of natural polyphenolics, were reacted with dimethyl carbonate and hexamethylenediamine to prepare non-isocyanate polyurethanes. In this paper, the same approach to form polyurethane bridges is applied to kraft lignin. The lignin is a very different polyphenolic material than tannin. The basic unit of lignin is a phenylpropane unit, which contains both aromatic and aliphatic hydroxyl groups instead of only aromatic hydroxyl groups as tannin. The aliphatic hydroxyl group is bonded to a saturated (sp3) carbon in a chain, while the aromatic hydroxyl is bonded to an unsaturated (sp2) carbon in the benzene ring. The benzene ring can stabilizes a possible negative charge of the phenoxide ion through resonance due to it is formed by sp2 carbons, something more difficult in an aliphatic chain. This can lead to different behavior between aromatic and aliphatic hydroxyls in the preparation of isocyanate-free polyurethanes with kraft lignin.

EXPERIMENTAL

Samples preparation

The commercial lignin used was a desulphurised softwood kraft lignin, namely Biochoice kraft lignin supplied by Domtar Inc (Montreal, Quebec, Canada) from their Plymouth, North Carolina mill (USA). Dimethyl carbonate 99% (DMC) was obtained from by Acros organics (Geel, Belgium), and hexamethylenediamine tech. 70% (HMDA) by Aldrich Chemical Company Inc. (Milwaukee, USA).

The samples were prepared as follow, without applying any purification step to any of the reagents:

1. 10g of lignin powder were mixed and stirred during two hours with 22g of dimethyl carbonate (DMC) at room temperature. Then, 8g of hexamethylenediamine (HMDA) was added to the mixture and stirred. The mixture was divided into four samples, which were kept at room temperature and at 80ºC, 103ºC and 180ºC in an oven during 24 hours. These samples have been called LDH-X, where X is the temperature at which the sample was reacted.
2. 8g of lignin powder and 8 g of HMDA were mixed and placed in an oven at 60ºC during 18 hours. The mixture was then divided into four parts. To each part, half of its weight was added as weight of DMC. The samples were placed at room temperature and in ovens at 80ºC, 103ºC and 180ºC during 24 hours. These samples have been called LHDWpH-X, where X is the temperature at which the sample was reacted.
3. 8g of lignin powder and 8 g of HMDA, which was previously mixed with 1.5g of 33% NaOH in water, were mixed and placed in an oven at 60ºC during 18 hours. The mixture was then divided into four parts. To each part, half of its weight was added as weight of DMC. The samples were placed at room temperature and in ovens at 80ºC, 103ºC and 180ºC during 24 hours. The samples have been called as LHDpH-X, where X is the temperature of the sample.

All the samples were prepared in open containers and in a no-neutral-gas-blanked oven. The samples were then stored in eppendorf sealed with parafilm inside of a desiccator. The samples were characterized as formed.

The samples obtained by reacting at 180ºC were solids, and the samples obtained by reacting at 103ºC were hard pastes and the remaining ones were viscous liquids.

Coating samples

The samples of lignin based urethanes have been tested for coating application on the surface of beech wood. The samples were prepared as described in the experimental part. However, after the addition of HMDA in the LDH formulation and the addition of DMC for the formulations of LHDWpH and LHDpH, the samples were heated one hour in an oven at 60ºC to obtain a homogeneous viscous liquids, which become quickly pastes as the temperature decreased. The viscous liquids were then spread over the wood surfaces with a spatula, to a load of around 1-2 kg/m^2. The coated wood samples were put in an oven preheated at 180ºC and were covered with a silicone sheet. A metal plate was placed over the samples with 3 kg of weight over it to apply pressure. The coated wood were left one hour at 180ºC before cooling.

Analysis

FTIR

To confirm the presence of urethane structures, a Fourier Transform Infra-Red (FTIR) analysis was carried out using a Shimadzu IRAffinity-1 spectrophotometer. A blank sample tablet of potassium bromide, ACS reagent from ACROS Organics, was prepared for the reference spectrum. A similar tablet was prepared by mixing potassium bromide with 5% w/w of the sample powder to analyze. The spectrum was obtained in absorbance measurement by combining 32 scans with a resolution of 2.0. The reference DMC spectrum can be obtained [18].

MALDI-TOF analysis

Samples for Matrix assisted laser desorption ionization time-of-flight (MALDI-TOF) analysis were prepared first dissolving 5mg of sample powder in 1mL of a 50:50 v/v acetone/water solution. Then 10 mg of this solution is added to 10µL of a 2,5-dihydroxy benzoic acid (DHB) matrix. The locations dedicated to the samples on the analysis plaque were first covered with 2µL of a NaCl solution 0.1M in 2:1 v/v methanol/water, and predried. Then 1µL of the sample solution was placed on its dedicated location and the plaque is dried again. MALDI-TOF spectra were obtained using an Axima-Performance mass spectrometer from Shimadzu Biotech (Kratos Analytical Shimadzu Europe Ltd., Manchester, UK) using a linear polarity-positive tuning mode. The measurements were carried out making 1000 profiles per sample with 2 shots accumulated per profile. The spectrum precision is of +1Da.

CP-MAS ^{13}C NMR

Solid-state CP-MAS (cross-polarization/magic angle spinning) ^{13}C NMR spectra of the solid samples obtained by the different methods at 180 ºC were recorded on a Bruker MSL 300 spectrometer at a frequency of 75.47 MHz. Chemical shifts were calculated relative to tetramethyl silane (TMS). The rotor was spun at 4 kHz on a double-bearing 7 mm Bruker probe. The spectra were acquired with 5 s recycle delays, a 90º pulse of 5 ms and a contact time of 1 ms. The number of transients was 3000.

Contact angle

The contact angle of the treated surfaces at one minute from the water drop being placed on it with a syringe were measured using an EasyDrop contact angle apparatus, with the Drop Shape Analysis software (Krüs GmbH, Hamburg, Germany). Untreated wood was used as control.

RESULTS AND DISCUSSION

MALDI-TOF

In Tables 1, 2 and 3 are shown the interpretation of the peaks of the MALDI-TOF analysis of the reaction products obtained for the LDH, LHDWpH and LHDpH at 180°C, thus for the cases in which the reaction was more complete. A number of species are noticeable but what is of interest is the presence of urethane linkages obtained by the different reactions occurring. Thus, chemical species formed by the reaction of the diamine with the aliphatic hydroxyl group of a lignin unit according to a reaction already described [19] have then reacted with dimethylcarbonate to form a urethane group between this latter and the diamine. This is shown by the peak at 361 Da from the LHDWpH spectrum at 180°C , as follows:

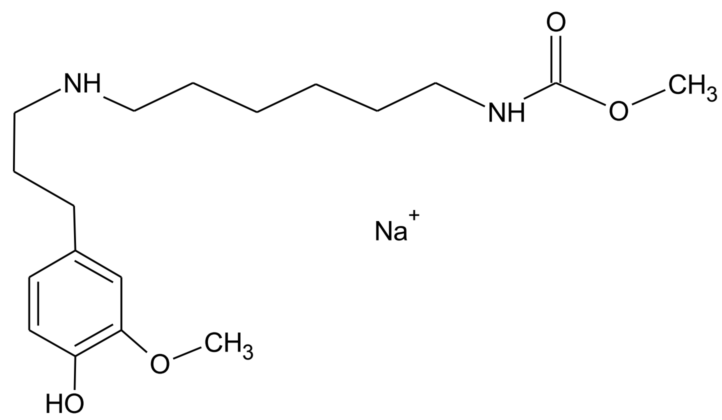

361Da

Similar species of urethane linkages between diamine and dimethyl carbonate but where an ionic bond has formed between one of the amino groups of the diamine and an aliphatic hydroxyl group of a lignin unit also occur as the peak at 441 Da from LHDWpH at 103°C, as follows:

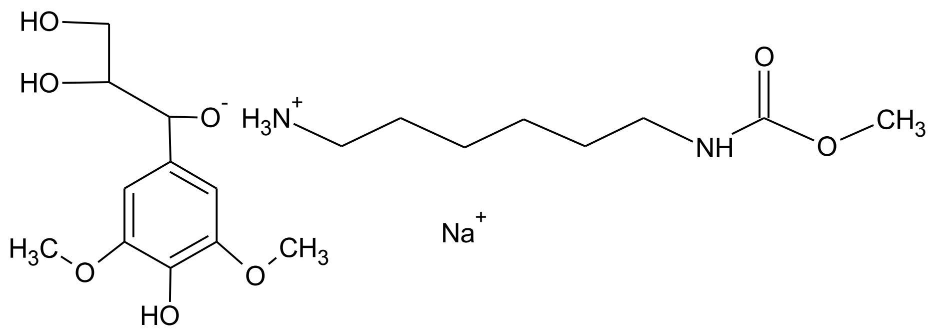

441 Da

The more significant types of compounds are, however, those where the urethane linkages are formed between the carbonate prereacted on lignin units and the diamine leading to oligomers and cross-linking in this manner between lignin chains. An example of this type of urethane linkages is shown by the peak at 555 Da from LDH at 180°C.

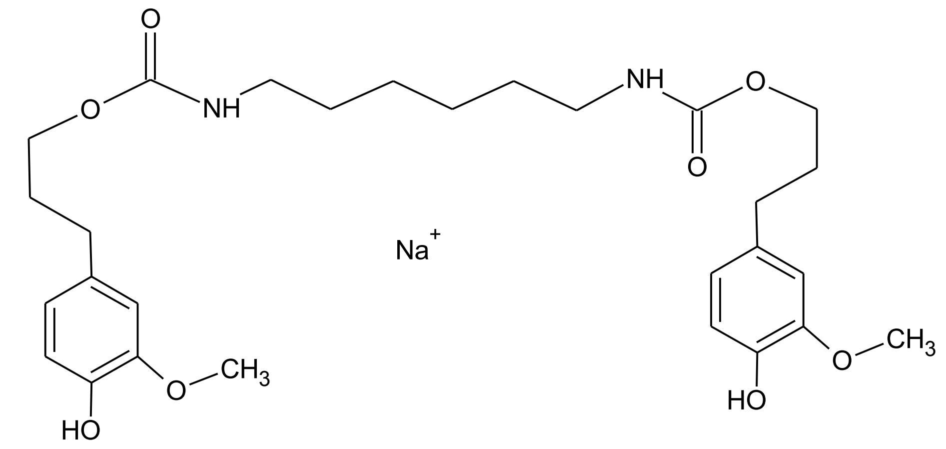

555 Da

Equally urethane linkages in chemical species formed by reaction of the diamine with the dimethyl carbonate prereacted with the phenolic hydroxyl groups of lignin units do occur, as indicated by the peak at 361 Da from the spectrum of LDH at 180ºC.

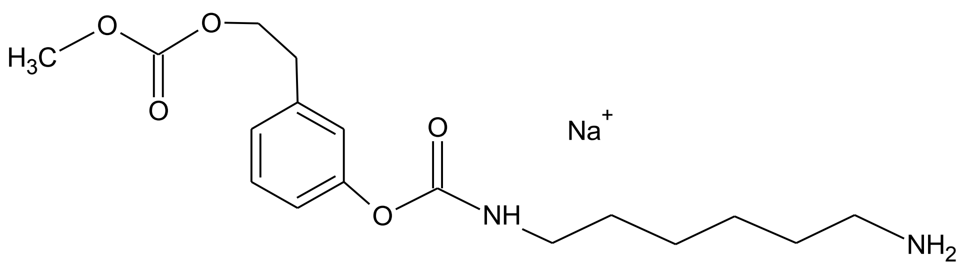

361 Da

FT-IR

Fig. 2 shows the FT-IR spectrum of the unmodified, unreacted, original lignin, and Fig. 3 shows the product of the reaction of lignin with DMC at ambient temperature. On these two figures can be seen [20]:

- The band at 1745 cm^{-1} belonging to C=O stretching in the ester group of dimethylcarbonate (DMC) (Fig. 3).
- The band at 1645 cm^{-1} belonging to the C=O stretching in lignin, this peak appearing as one of the shoulders of the peak at 1595 cm^{-1} peak in unreacted lignin (Fig. 2).
- The band at 1451 cm^{-1} belonging to the asymmetric C-H deformation in $–CH_3$ and $–CH_2$, and the aromatic skeleton plus the C-H deformation in CH_3 from DMC (Fig. 3).
- The band at 1274 cm^{-1} belonging to C-O stretching in the ester group of both DMC and DMC reacted with lignin (Fig. 3).
- The band at 1030 cm^{-1} reduces clearly its intensity when comparing Figs. 2 and 3. This peak belongs to the aromatic C-H vibration in plane, but also to the C-O in primary alcohols. Thus, its reduction should be due to the decrease in the proportion of primary alcohols as these have reacted with DMC.
- The bands at 1745, 1451 and 1274 cm^{-1} are practically the same and with a similar trend than the peaks found in the DMC spectrum.

Then, there are several clear trends noticeable when comparing the samples prepared at 103ºC and 180ºC (Figs. 4 and 5). While the spectra at 103ºC show well-defined peaks, the spectra of the samples at 180ºC show broad bands. This trend at 180°C is due to two reasons: the higher degree of polymerization and cross-linking of the samples at 180°C which causes a marked broadening of the bands, and possibly indicating some thermal degradation of the material.

The peaks at 3334, 1686, and 1532 cm^{-1} are guide values of the presence of urethanes bond in the samples prepared by the three methods used [16,21]. These peaks are very marked in all the three type of preparation of samples and they are absent in the spectrum of unreacted lignin.

Conversely, in the reaction between lignin and diamines, without DMC, two peaks (between 3380 and 3290 cm^{-1}) belonging to N-H stretching are observed, typically of primary amines [19,22]. In the spectra analyzed here, only one peak is found (3334 cm^{-1}) corresponding to N-H stretching (Fig. 4). This means that most of the amines present in these samples are secondary amines, thus showing that there was reaction with the amine to form a urethane bond.

The C=O bond in amides appears at lower wavelength than in ester bonds. This explains that the value of C=O in the spectrum of LDH at 103ºC has been displaced to 1686 cm^{-1} (from 1780 cm^{-1}), due to the reaction between the DMC and HMDA. However, there are two bands in the spectrum of LDH at 180ºC within the C=O range (1763 and 1636 cm^{-1}) (Fig. 5). This should mean that the amount of reacted amine with DMC is lower at 180°C than at 103ºC. It can be interpreted as the new species formed give their peak at 1636 cm^{-1}, while the peak at 1763 cm^{-1} belongs to the remaining esters from DMC. This should be because in the case of the reaction being conducted at 180°C, the temperature used is higher than the boiling point of HMDA, leading to its evaporation before its reaction with either DMC or lignin, or both. Conversely, Radice et al. [23] found that the band around 1690 cm^{-1} belongs to the carbonyl stretching vibration in associated urethane bonds.

The peak around 1530 cm^{-1} belongs to C=O and N-H deformation in the amide groups of urethane bonds but also it should be influenced by the aromatic skeleton of the lignin. The peak around 1460 cm^{-1} correspond to the CH_2 scissoring and CH_3 deformations.

The peaks at 1300 cm^{-1} and lower are difficult to assign to one definite bond movement as they involve cooperative motions such as C-C stretching or C-O-C antisymmetric stretching. Within this range it us worth taking note of the peak at 1265-1256 cm^{-1}, which should be influenced by several bond movements, especially from the C-O stretching from the different reagents, from the lignin and from the ester group from the reaction with DMC, but also from C-N elongation.

13C NMR

Fig. 6 shows the ^{13}C NMR spectrum of the sample LHDWpH at 180ºC, the spectra for the other samples and for the unreacted lignin are in the Supplementary material document. Looking at the spectrum of the sample LHDWpH and a spectrum of unreacted lignin, several differences can be noticed. The peaks at 75 and 86 ppm, indicating the aliphatic chain of the lignin, have practically disappeared for all the products obtained by the different methods. Also, the peak at 145-147 ppm (carbon in the aromatic ring of lignin linked with the hydroxyl group) is decreased but still presents in the samples spectra. These fact indicate that there both the aromatic and the aliphatic hydroxyl groups of the lignin fragments do react to form covalent or ionic bonds. In addition, the shift at 37 ppm belonging to the C in β has disappeared, also indicating that there is reaction with the lignin. Nevertheless, their presence (145 ppm and 74 ppm) in the spectra of the products obtained seems to indicate that the reaction may not be completed.

Conversely, the unreacted DMC should show two peaks, at 156 ppm for the ester carbon and at 54 ppm for the carbon in the methyl groups. The complete absence of the first one (156 ppm) is one evidence that the DMC reacted to form urethane bond with the HMDA or to react with the lignin. The samples show also a shift at 59 ppm, which can be attributed to the variation in the resonance of the residual methyl groups in reacted DMC. Conversely, the unreacted aliphatic HMDA should present a peak at 42 ppm. The spectra show peaks at 40-41 ppm, this suggesting that there is still unreacted HMDA.

Finally, the shift at 27 ppm belong to diamine linked either covalently or as totally ionized salts to the lignin. This shift shows a different resonance depending on the method used to prepare the samples, being 27 ppm for LDH and 28 ppm for the other two methods.

Contact angle

The product obtained from the reaction of the lignin with both dymethylcarbonate and hexemethyldiamine has been applied on the surface of beech wood. When, this product has been used as formed and left to harden at ambient temperature (20ºC), the hardening of the samples was not completed. However, when pressure was applied, as described in the experimental part, a homogeneous hard film was obtained on the wood surface. Table 4 shows the results obtained in the contact angle test. The clear increase of the values of the contact angle when compared to that of uncoated wood indicates that the application of these coatings lignin-based are effective because they increase the hydrophobicity of the wood.

CONCLUSIONS

- The work presented demonstrates that non-isocyanate based polyurethanes can be prepared using kraft lignin.
- A larger number of species were observed respect to previous works done with tannins.
- The reaction of the lignin with the hexamethylenediamine allows to obtain molecules of polyurethane where there are ionic bonds, covalent bonds or both.
- The reaction is more complete at 180ºC than at 103ºC, but certain degree of degradation of the samples is already observed due to the high temperature as indicated in the FTIR spectrum.

REFERENCES

[1] Y. Peng, Z. Zheng, P. Sun, X. Wang, and T. Zhang, "Synthesis and characterization of polyphenol-based polyurethane," *New J. Chem.* **37**, 729 (2013).

[2] J. Ge, X. Shi, M. Cai, R. Wu, and M. Wang, "A novel biodegradable antimicrobial PU foam from wattle tannin," *J. Appl. Polym. Sci.* **90**, 2756–2763 (2003).

[3] J.-J. Ge and K. Sakai, "Decomposition of polyurethane foams derived from condensed tannin II: Hydrolysis and aminolysis of polyurethane foams," *J. Wood Sci.* **44**, 103–105 (1998).

[4] J.-J. Ge and K. Sakai, "Compressive properties and biodegradabilities of polyurethane foams derived from condensed tannin," *Mokuzai Gakkaishi* **39**, 801–806 (1993).

[5] A. Pizzi, "Tannin-based polyurethane adhesives," *J. Appl. Polym. Sci.* **23**, 1889–1891 (1979).

[6] M. C. Basso, S. Giovando, A. Pizzi, H. Pasch, N. Pretorius, L. Delmotte, and A. Celzard, "Flexible-elastic copolymerized polyurethane-tannin foams," *J. Appl. Polym. Sci.* **131**, 40499 (2014).

[7] D. E. García, W. G. Glasser, A. Pizzi, A. Osorio-Madrazo, and M.-P. Laborie, "Hydroxypropyl tannin derivatives from Pinus pinaster (Ait.) bark," *Ind. Crops Prod.* **49**, 730–739 (2013).

[8] O. Faruk and M. Sain, "Continuous Extrusion Foaming of Lignin Enhanced Thermoplastic Polyurethane (TPU)," *J. Biobased Mater. Bioenergy* **7**, 309–314 (2013).

[9] H. Hatakeyama and T. Hatakeyama, "Advances of Polyurethane Foams Derived from Lignin," *J. Renew. Mater.* **1**, 113–123 (2013).

[10] J. Liu, H.-F. Liu, L. Deng, B. Liao, and Q.-X. Guo, "Improving aging resistance and mechanical properties of waterborne polyurethanes modified by lignin amines," *J. Appl. Polym. Sci.* **130**, 1736–1742 (2013).

[11] Z. Wang, S. Xu, W. Hu, and Y. Xie, "Fractionation of the Biopolyols from Lignocellulosic Biomass for the Production of Rigid Foams," *BioEnergy Res.* **6**, 896–902 (2013).

[12] G. Rokicki and A. Piotrowska, "A new route to polyurethanes from ethylene carbonate, diamines and diols," *Polymer* **43**, 2927–2935 (2002).

[13] B. Nohra, L. Candy, J.-F. Blanco, C. Guerin, Y. Raoul, and Z. Mouloungui, "From Petrochemical Polyurethanes to Biobased Polyhydroxyurethanes," *Macromolecules* **46**, 3771–3792 (2013).

[14] "Project BEMA (Bois Eco Matériaux Aquitaine)," FCBA, Mont de Marsan, Aquitaine, France, 2012.

[15] M. Thébault, A. Pizzi, S. Dumarçay, P. Gerardin, E. Fredon, and L. Delmotte, "Polyurethanes from hydrolysable tannins obtained without using isocyanates," *Ind. Crops Prod.* **59**, 329–336 (2014).

[16] M. Thébault, A. Pizzi, H. A. Essawy, A. Barhoum, and G. Van Assche, "Isocyanate free condensed tannin-based polyurethanes," *Eur. Polym. J.* **67**, 513–526 (2015).

[17] M. Thébault, A. Pizzi, F. J. Santiago-Medina, F. M. Al-Marzouki, and S. Abdalla, "Isocyanate-Free Polyurethanes by Coreaction of Condensed Tannins with Aminated Tannins," *J. Renew. Mater.* **5**, 21–29 (2017).

[18] "FTIR spectrum of dimethylcarbonate," http://www.chemspider.com/Chemical-Structure.11526.html?rid=e5727503-3442-42a1-b39c-9e6fee59f3db (2017).

[19] F. J. Santiago-Medina, A. Pizzi, M. C. Basso, L. Delmotte, and S. Abdalla, "Polycondensation Resins by Lignin Reaction with (Poly)amines," *J. Renew. Mater.* (2017).

[20] J. E. Katon and M. D. Cohen, "The Vibrational Spectra and Structure of Dimethyl Carbonate and its Conformational Behavior," *Can. J. Chem.* **53**, 1378–1386 (1975).

[21] C. Bonini, M. D'Auria, L. Emanuele, R. Ferri, R. Pucciariello, and A. R. Sabia, "Polyurethanes and polyesters from lignin," *J. Appl. Polym. Sci.* **98**, 1451–1456 (2005).

[22] F.-J. Santiago-Medina, A. Pizzi, M. Basso, L. Delmotte, and A. Celzard, "Polycondensation Resins by Flavonoid Tannins Reaction with Amines," *Polymers* **9**, 37 (2017).

[23] S. Radice, S. Turri, and M. Scicchitano, "Fourier Transform Infrared Studies on Deblocking and Crosslinking Mechanisms of Some Fluorine Containing Monocomponent Polyurethanes," *Appl. Spectrosc.* **58**, 535–542 (2004).

Table 1. MALDI-ToF analysis of oligomer species formed in the reaction of kraft lignin with dimethyl carbonate and hexamethylenediamine at 180°C. Case LDH.

U = urethane linkage; DMC= dimethyl carbonate; HMDA = hexamethylenediamine; 138 lignin = lignin fragment of 138 molecular weight; 198 lignin= lignin fragment of 198 molecular weight

Peak in Spectrum (Da)	Oligomer type	Calculated Peak (Da)
137,6	Lignin	
255,5	DMC-138Lig-DMC	254
	198Lig-DMC	256
301,6	138Lig-DMC-138Lig	302
327,7	138Lig=DMCx2=138Lig	328
339,5	198Lig-DMC-U-HMDA	340
358,7	DMC-274Lig=DMC	358
360,5	DMC-138Lig-DMC-138Lig	360
361,5	DMC-138Lig-DMC-U-HMDA+Na	361
	138Lig-DMC-198Lig	362
366,7	138Lig-DMC-179Lig+Na	366
376,4	138Lig-DMC-154Lig-DMC	376
386,7	305Lig-DMC+23	386
413,5	DMC-274Lig-DMC+Na	413
441,7	HMDA-U-DMC-274Lig=DMC	442
443,7	DMC-198Lig-DMC-U-HMDA+Nax2	444
	HMDA-U-DMC-138Lig-DMC-138Lig	444
465,7	HMDA-U-DMC-182Lig-DMC-U-HMDA	466
	HMDA-U-DMC-274Lig=DMC+Na	465
479,7	HMDA-U-DMC-198Lig-DMCx2+Nax2	479
493,8	305Lig-DMC-U-HMDA+Nax2	493
537,4	154Lig-DMC-154Lig-DMC-154Lig+Na	537
538,3	DMC-198Lig-DMC-198Lig-DMC	538
543,6	154Lig-DMC-U-HMDA-U-DMC-180Lig+Na	543
	178Lig-DMC-U-HMDA-U-DMC-198Lig	544
551,3	198Lig-DMC-305Lig+Na	552
556,6	182Lig-DMC-U-HMDA-U-DMC-182Lig+Na	555
	154Lig-DMC-138Lig-DMC-154Lig-DMC	556
573,4	DMC-138Lig-DMC-138Lig-DMC-138Lig-DMC+Na	573
	274Lig-DMC-274Lig	574
593,8	154Lig-DMC-U-HMDA-U-DMC-272Lig	594
608	198Lig-DMC-U-HMDA-U-DMC-242Lig	608
621,8	DMC-198Lig-DMC-198Lig-DMC-U-HMDA	622
639,4	HMDA-U-DMC-274Lig-(DMC)-DMC-U-HMDA+Na	639
	154Lig-DMC-138Lig-DMC-154Lig-DMC-U-HMDA	640

673,2	180Lig-DMC-U-HMDA-U-DMC-326Lig	674
713,2	DMC-274Lig-DMC-274Lig-DMC+Na	713
	138Lig-DMC-179Lig-DMC-179Lig-DMC-U-HMDA+Na	713
	272Lig-DMC-U-HMDA-U-DMC-272Lig	712
735,3	138Lig-DMC-179Lig-DMC-179Lig-DMC-U-HMDA+Nax2	736
763,5	HMDA-U-DMC-138Lig-DMC-138Lig-DMC-138Lig-DMC-U-HMDA+Nax2	764

Table 2. MALDI-ToF analysis of oligomer species formed in the reaction of kraft lignin with dimethyl carbonate and hexamethylenediamine at 180°C. Case LHDWpH.

U = urethane linkage; DMC= dimethyl carbonate; HMDA = hexamethylenediamine; 104, 138, 154, 178, 182, 198, 326 lignin = lignin fragments of respectively 104, 138, 154, 178, 182, 198, 326 molecular weight.

Peak in Spectrum (Da)	Oligomer type	Calculated Peak (Da)
137,8	Lignin	
198	Lignin	
279,6	182Lig-HMDA	280
316,8	138Lig-HMDA-U-DMC+Na	317
335	HMDA+-104+-HMDA	336
333,7	HMDA-138-HMDA	334
335,7	138Lig+-HMDA-U-DMC+Na	335
	138Lig+-HMDA-U-DMC+Na	335
	156Lig-HMDA-U-DMC+Na	335
338,8	182Lig-HMDA-U-DMC	338
344,8	104Lig-HMDA-138Lig+Na	345
352,8	156Lig+-HMDA-U-DMC+Na	353
357,7	HMDA-138Lig-HMDA+Na	357
358,8	242Lig+-HMDA	358
	138Lig+-HMDA-U-DMC+Nax2	358
	156Lig-HMDA-U-DMC+Nax2	358
361,6	182Lig-HMDA-U-DMC+Na	361
378	HMDA-182Lig-HMDA	378
392,8	HMDA-138-HMDA-U-DMC	392
400	198Lig-HMDA-U-DMC+Nax2	400
414,9	HMDA-138-HMDA-U-DMC+Na	415
	HMDA-138Lig-HMDA-U-DMC+Na	415
443,8	Lignin	
	182Lig-HMDA-182Lig	444
	244Lig+-HMDA-U-DMC+Na	441
450,8	DMC-U-HMDA-138-HMDA-U-DMC	450
451,9	DMC-U-HMDA+-104+-HMDA-U-DMC	452
458	HMDA-182Lig-HMDA-U-DMC+Na	459
475,8	DMC-U-HMDA+-104+-HMDA-U-DMC+Na	475
495	198Lig-HMDA+-198Lig	494
537,5	138Lig-HMDA-U-DMC-U-HMDA-154Lig+Na	537
	138Lig-HMDA-U-DMC-U-HMDA-178Lig	538
543,9	HMDA-242Lig-HMDA-U-DMC+Nax2	542
551	HMDA-138Lig-HMDA-138Lig-HMDA	552
556,8	HMDA+-104Lig+-HMDA+-104Lig+-HMDA	556
559,6	154Lig-HMDA-U-DMC-U-HMDA-182Lig	558

	182Lig-HMDA-182Lig-O-+HMDA	560
	182Lig-HMDA-182Lig+-HMDA	560
576,9	178Lig-HMDA-U-DMC-U-HMDA-154Lig+Na	577
	DMC-U-HMDA-242Lig-HMDA-U-DMC+Na	577
600,2	242Lig+-HMDA+-242Lig	600
	DMC-U-HMDA-242Lig-HMDA-U-DMC+Nax2	600
602,9	182Lig-HMDA-U-DMC-U-HMDA-198Lig	602
608	HMDA+-272+-HMDA-U-DMC+Na	608
610	198Lig+-HMDA+-198Lig-HMDA	610
	198Lig+-HMDA+-180Lig+-HMDA	610
	HMDA-138Lig-HMDA-138Lig-HMDA-U-DMC	610
622	178Lig-HMDA-U-DMC-U-HMDA-198Lig+Na	621
636,1	180Lig-HMDA-180Lig-O-+HMDA-U-DMC+Na	637
	HMDA+-104Lig+-HMDA+-104Lig+-HMDA-U-DMC+Na	637
	180Lig-HMDA-180Lig+-HMDA-U-DMC+Na	637
	180Lig-HMDA-180Lig+-HMDA-U-DMC+Na	637
713,3	HMDA+-180Lig-HMDA-180Lig-HMDA	712
735,2	HMDA+-180Lig-HMDA-180Lig-HMDA	735
764,2	DMC-U-HMDA+-138Lig+-HMDA+-138Lig+-HMDA-U-DMC+Na	763
875,4	DMC-U-HMDA-242Lig-HMDA-242Lig-HMDA-U-DMC	876
	326Lig-HMDA-U-DMC-U-HMDA-326Lig	874
891,7	DMC-U-HMDA-180Lig-HMDA-156Lig-HMDA-180Lig-HMDA-U-DMC	890

Table 3. MALDI-ToF analysis of oligomer species formed in the reaction of kraft lignin with dimethyl carbonate and hexamethylenediamine at 180°C. Case LHDpH.

U = urethane linkage; DMC= dimethyl carbonate; HMDA = hexamethylenediamine; 138, 156, 178, 182, 198, 242 lignin = lignin fragments of respectively 138, 156, 178, 182, 198, 242 molecular weight.

Peak in Spectrum (Da)	Oligomer type	Calculated Peak (Da)
137,8	Lignin	
198	Lignin	
278,7	138Lig+-HMDA+Na	277
	156Lig-HMDA+Na	277
279,6	182Lig-HMDA	280
316,7	138Lig-HMDA-U-DMC+Na	317
330,7	156Lig+-HMDA-U-DMC	330
358,7	HMDA-138Lig-HMDA+Na	357
	242Lig+-HMDA	358
	138Lig+-HMDA-U-DMC+Nax2	358
	156Lig-HMDA-U-DMC+Nax2	358
361,6	182Lig-HMDA-U-DMC+Na	361
379,6	HMDA-182Lig-HMDA	378
400,6	180Lig+-HMDA-U-DMC+Nax2	400
	198Lig-HMDA-U-DMC+Nax2	400
441,7	244Lig+-HMDA-U-DMC+Na	441
443,8	182Lig-HMDA-182Lig	444
451	DMC-U-HMDA-138-HMDA-U-DMC	450
	DMC-U-HMDA+-104+-HMDA-U-DMC	452
457,7	HMDA-180Lig-HMDA-U-DMC+Na	457
469,7	HMDA+-156Lig+-HMDA-U-DMC+Na	469
472,8	DMC-U-HMDA-138-HMDA-U-DMC+Na	473
	DMC-U-HMDA-138Lig-HMDA-U-DMC+Na	473
494,7	DMC-U-HMDA-182Lig-HMDA-U-DMC	494
494,7	198Lig-HMDA+-198Lig	494
	156Lig-HMDAx2-156Lig+Na	495
537,4	138Lig-HMDA-U-DMC-U-HMDA-154Lig+Na	537
	138Lig-HMDA-U-DMC-U-HMDA-178Lig	538
551	HMDA-138Lig-HMDA-138Lig-HMDA	552
	DMC-U-HMDA-242Lig-HMDA-U-DMC+Na	577
602,8	138Lig-HMDA-U-DMC-U-HMDA-242Lig	602
	178Lig-HMDA-U-DMC-U-HMDA-180Lig+Na	603
607,8	HMDA+-272+-HMDA-U-DMC+Nax2	608
613,9	180Lig-HMDA-180Lig-O-+HMDA-U-DMC	614
	HMDA+-104Lig+-HMDA+-104Lig+-HMDA-U-DMC	614
	180Lig-HMDA-180Lig+-HMDA-U-DMC	614

621,8	178Lig-HMDA-U-DMC-U-HMDA-198Lig+Na	621
633,8	HMDA-138Lig-HMDA-138Lig-HMDA-U-DMC+Na	633
642,8	DMC-U-HMDA+-272+-HMDA-U-DMC+Na	643
	178Lig-HMDA-U-DMC-U-HMDA-242Lig	642
647,8	272Lig-HMDA-U-DMC-U-HMDA-154Lig	648
704	DMC-U-HMDA+-138Lig-HMDA-138Lig+-HMDA-U-DMC	704
727,7	DMC-U-HMDA+-138Lig-HMDA-138Lig+-HMDA-U-DMC+Na	727
	DMC-U-HMDA-156Lig-HMDA-156Lig-HMDA-U-DMC+Na	727
	DMC-U-HMDA+-138Lig-HMDA-138Lig+-HMDA-U-DMC+Na	727
735	HMDA+-180Lig-HMDA-180Lig-HMDA-U-DMC+Na	735
741	DMC-U-HMDA+-138Lig+-HMDA+-138Lig+-HMDA-U-DMC	740
763,9	DMC-U-HMDA+-138Lig+-HMDA+-138Lig+-HMDA-U-DMC+Na	763
789,9	198Lig+-HMDA-198Lig-HMDA+-198Lig	790
	198Lig-HMDA+-180Lig+-HMDA+-198Lig	790
	HMDA+-180Lig+-HMDA+-180Lig+-HMDA-U-DMC+Na	789
	HMDA-198Lig+-HMDA+-198Lig-HMDA-U-DMC+Na	789
	HMDA+-198Lig+-HMDA+-180Lig+-HMDA-U-DMC+Na	789
	272Lig-HMDA-U-DMC-U-HMDA-272Lig+Na	789
	242Lig-HMDA-U-DMC-U-HMDA-326Lig	790
829,7	DMC-U-HMDA+-180Lig+-HMDA-180Lig-HMDA-U-DMC+Na	829
	DMC-U-HMDA-198Lig-HMDA-198Lig+-HMDA-U-DMC+Na	829
	DMC-U-HMDA+-198Lig-HMDA-180Lig+-HMDA-U-DMC+Na	829

Table 4. Contact angle results obtained from the coating experiences.

Coating samples	Contact angle with water (º)
Untreated wood	34º
LHDWpH formulation	96º
LHDpH formulation	78º
LDH formulation	88º

FIGURE LEGENDS

Fig. 1: MALDI-ToF of the reaction products for the reaction LDH at 180°C of lignin to form non-isocyanate polyurethanes. (a) 10 Da – 1000 Da range. (b) 1000 Da – 2000 Da range.

Fig.2. FT-IR of unreacted lignin.

Fig. 3. FT-IR of the reaction of lignin with dimethyl carbonate at ambient temperature.

Fig. 4. FT-IR of the reaction LDH of lignin with dimethyl carbonate and hexamethylene diamine according to preparation method 1 at 103ºC.

Fig. 5. FT-IR of the reaction LDH of lignin with dimethyl carbonate and hexamethylene diamine according to preparation method 1 at 180ºC

Fig. 6. 13C NMR spectrum of LHDWpH at 180ºC

Fig. 7. Left. Sample left to harden at ambient temperature. Right. Sample of LHDWpH after heated at 180ºC during one hour covered with a silicone sheet.

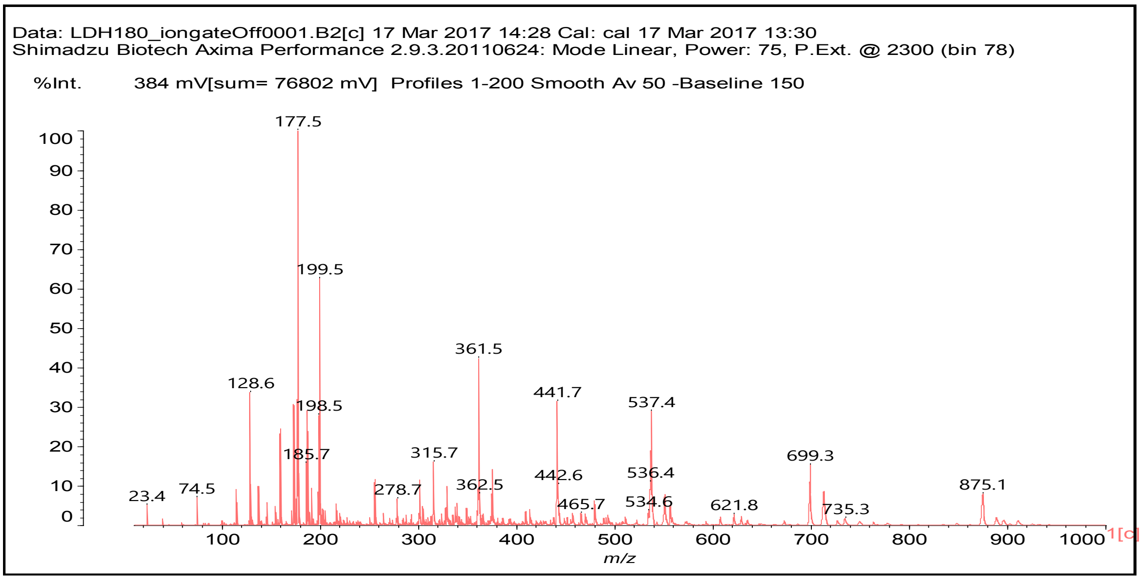

Fig. 1a: 180°C LDH

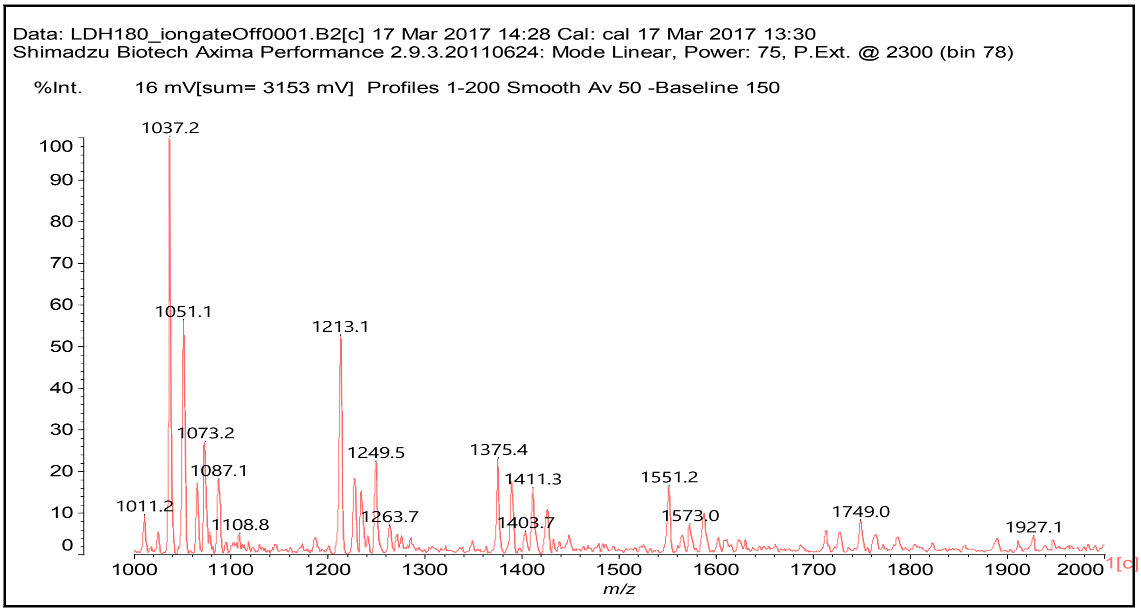

Fig. 1b: 180°C LDH

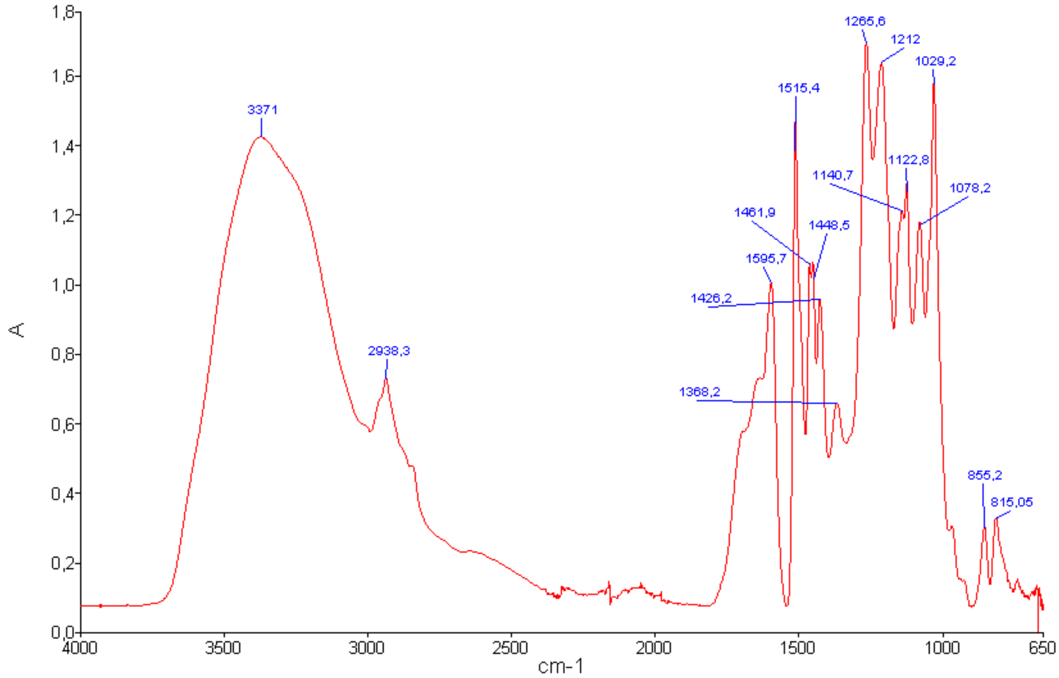

Fig.2 FT-IR of unreacted lignin

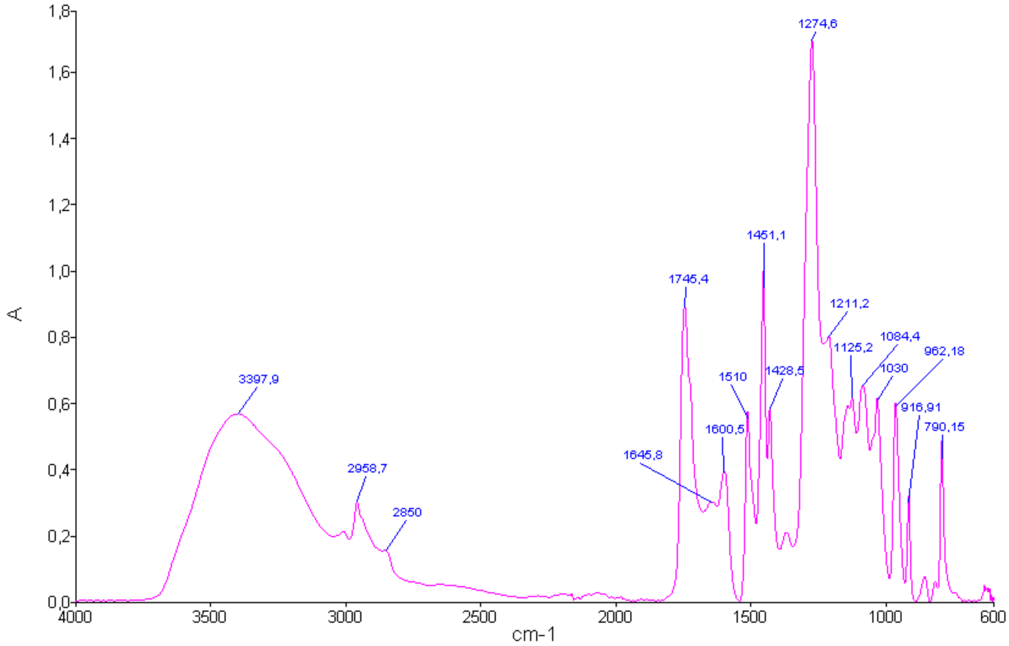

Fig. 3. Lignin + DMC at ambient temperature.

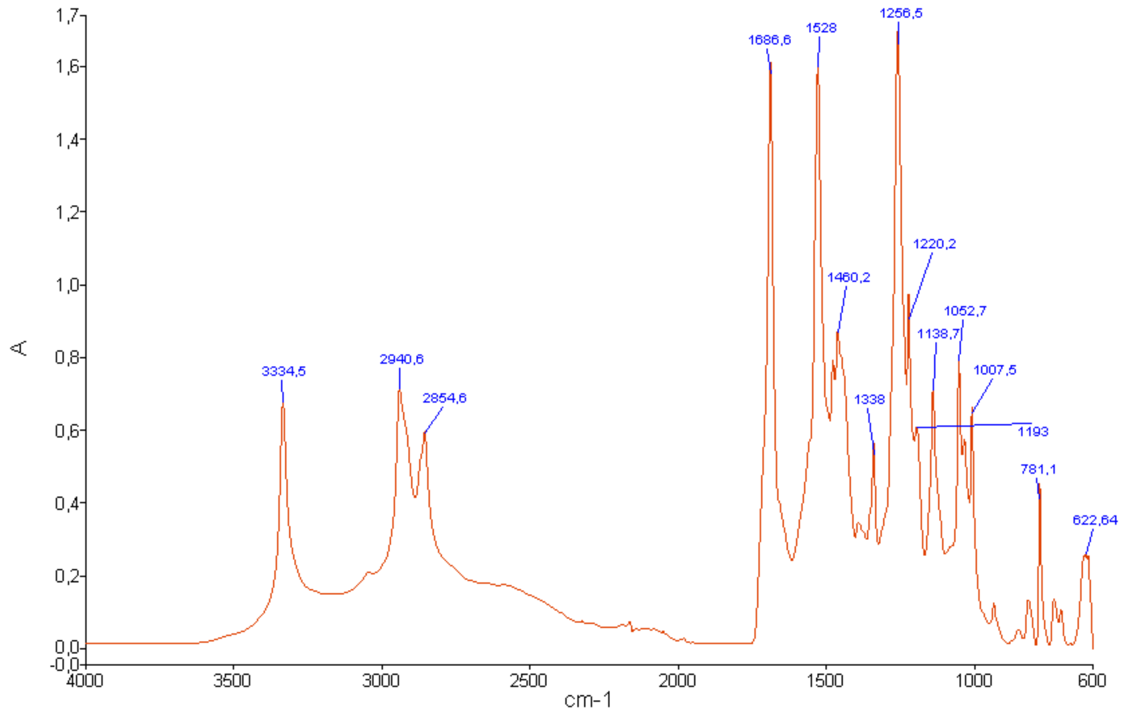

Fig. 4. LDH 103ºC: Preparation methods 1 at 103ºC

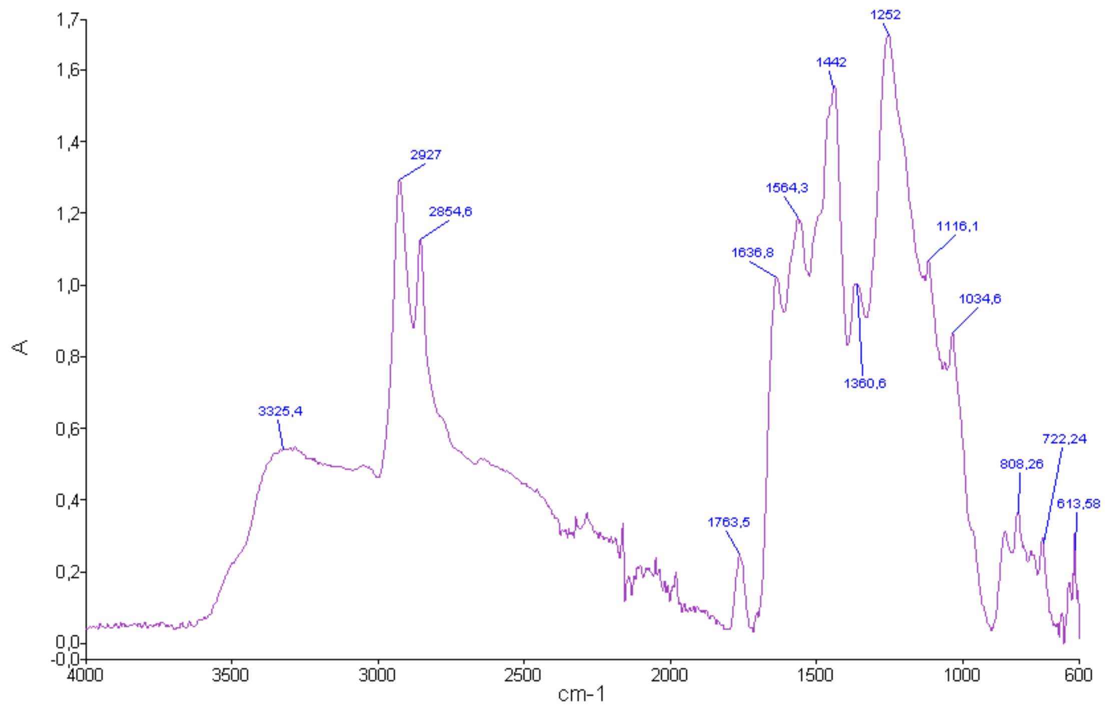

Fig. 5. LDH 180ºC: Preparation methods 1 at 180ºC

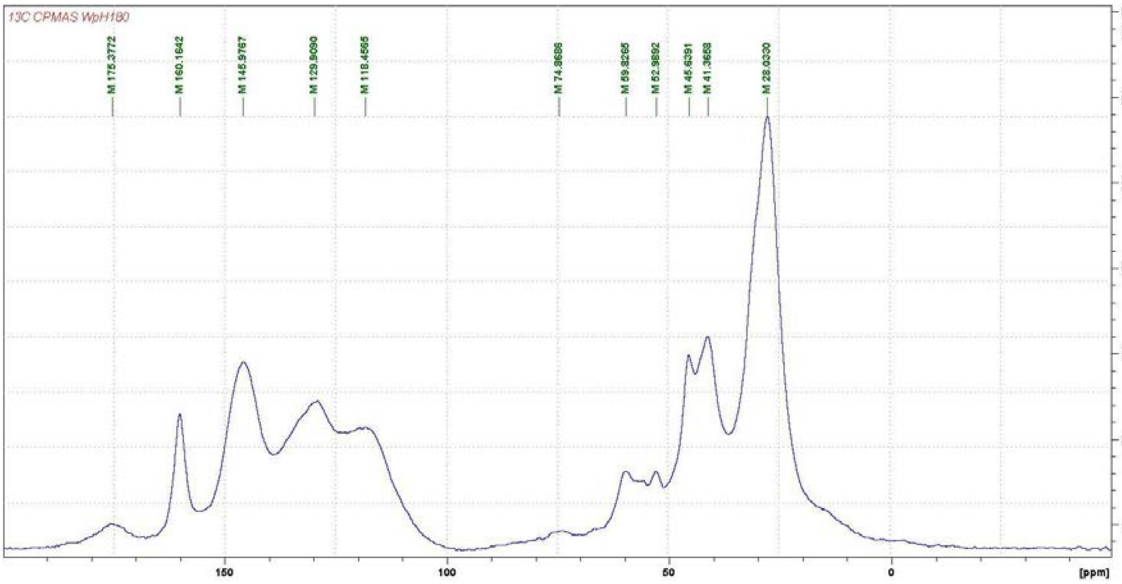

Fig. 6. 13C NMR spectrum for LHDWpH at 180ºC

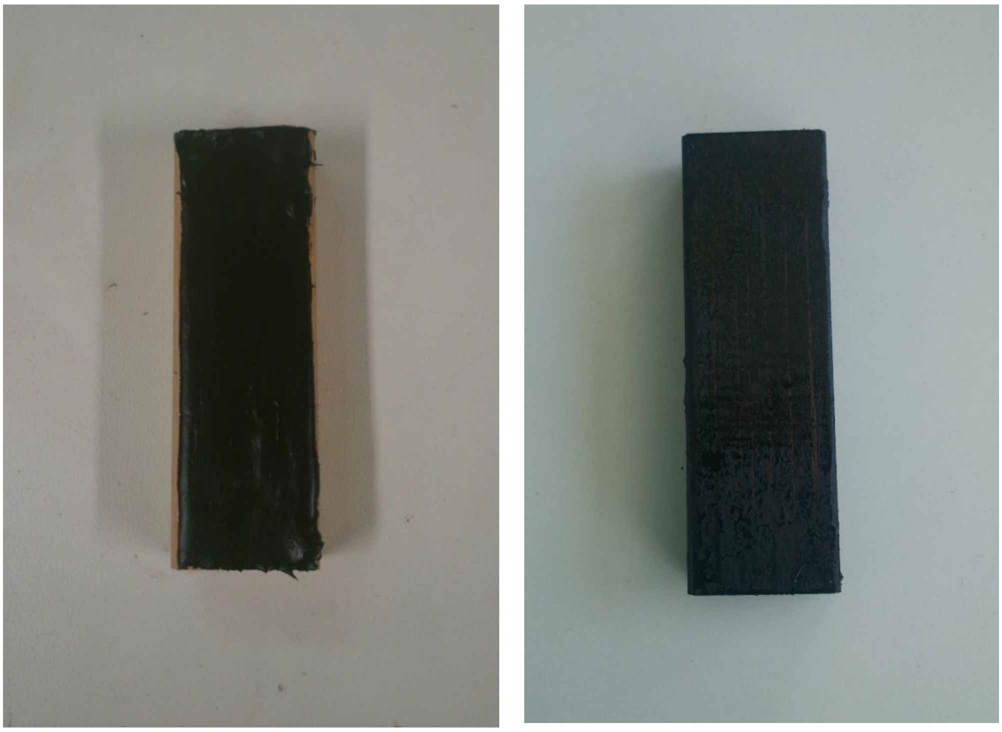

Fig. 7. Samples of coating.

5.1 Matériel supplémentaire de « Polyurethanes from kraft lignin without using isocyanates »

SUPPLEMENARY MATERIAL

CP-MAS 13C NMR

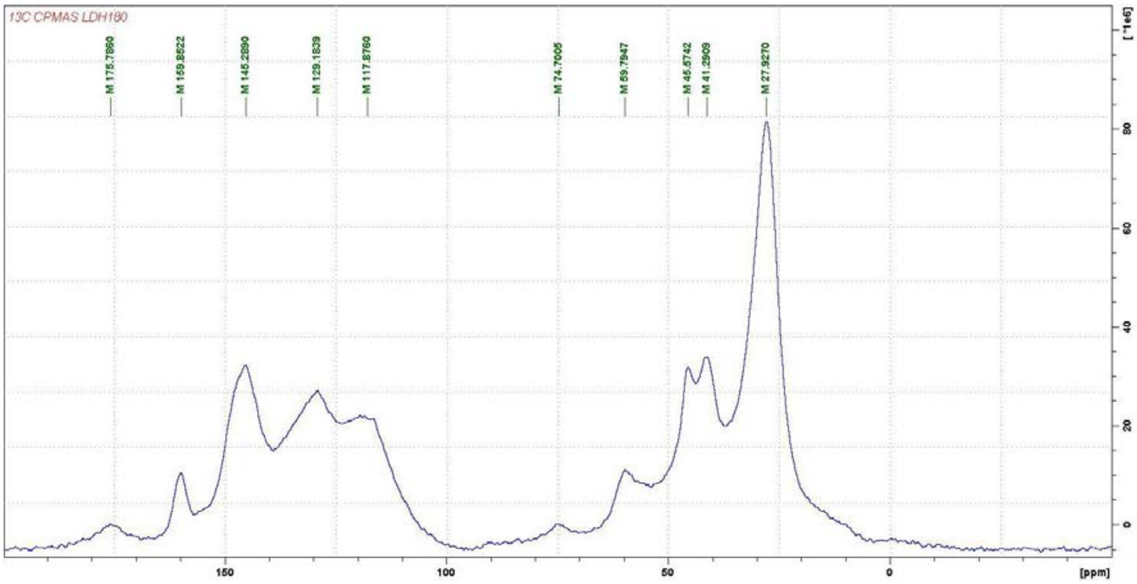

Fig. S1. 13C NMR spectrum of LDH at 180ºC

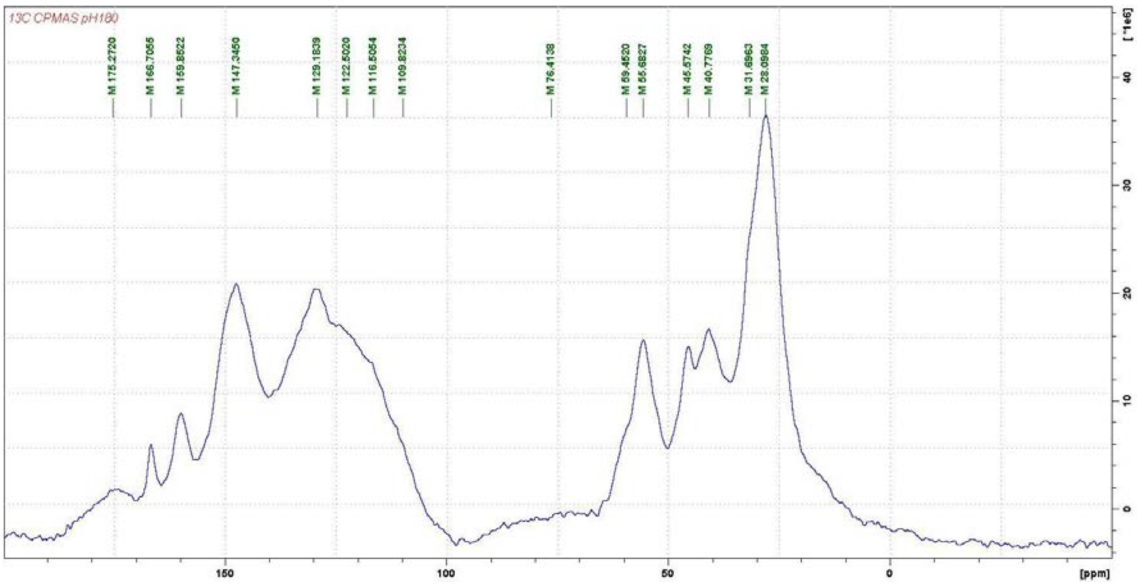

Fig. S2. 13C NMR spectrum of LHDpH at 180ºC

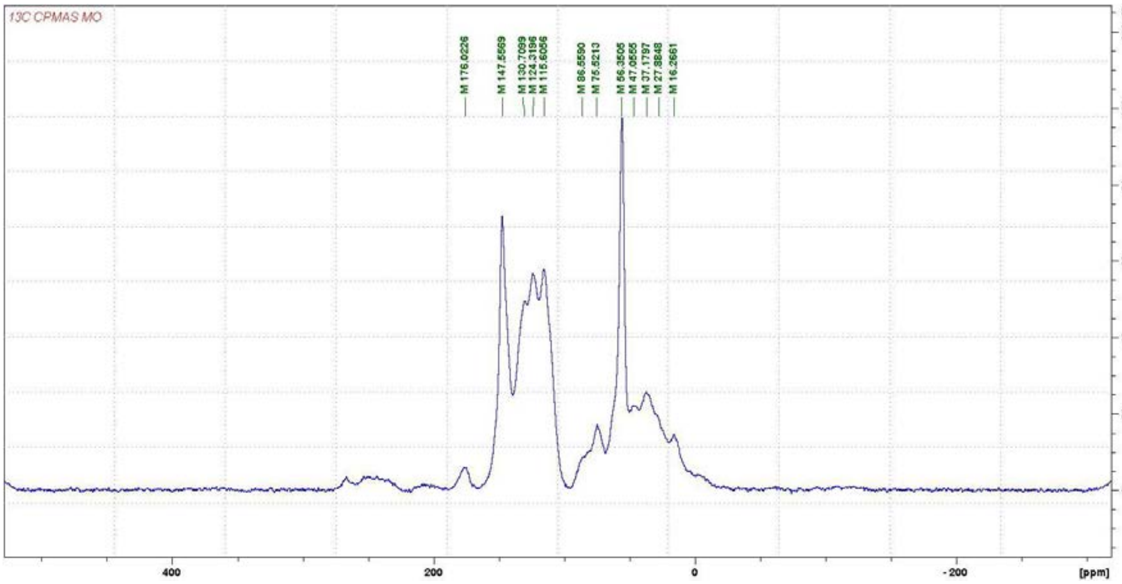

Fig. S3. 13C NMR spectrum of unreacted lignin

FTIR

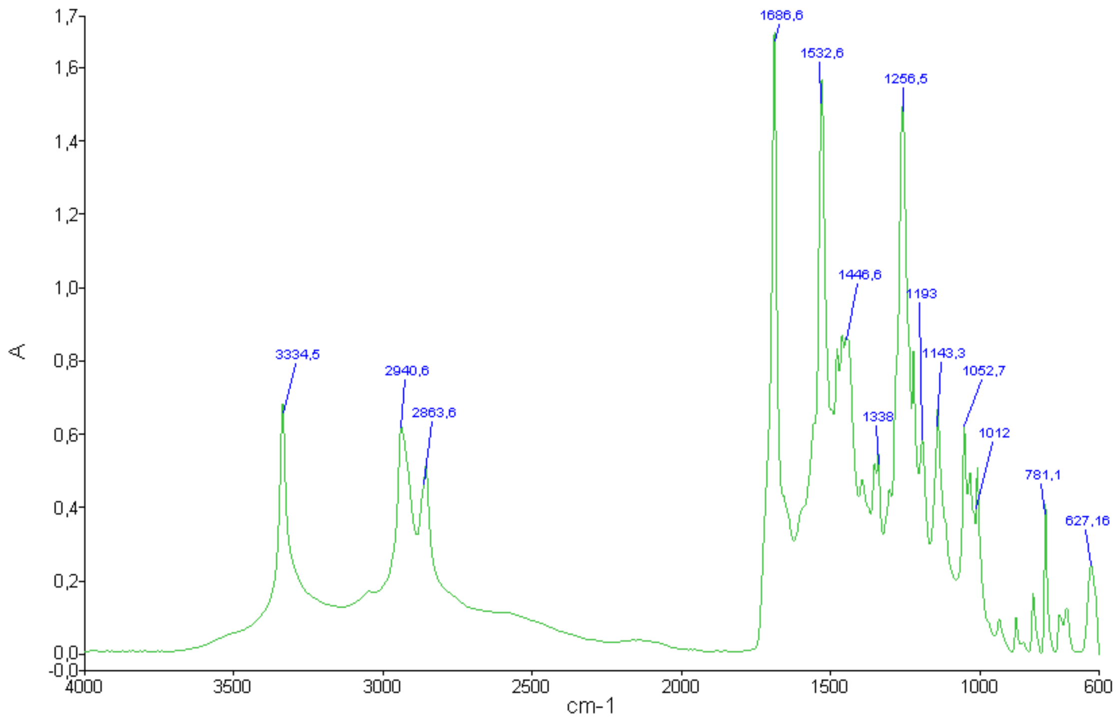

Fig. S4. FT-IR of the reaction LHDpH of lignin with dimethyl carbonate and hexamethylene diamine according to preparation method 3 at 103ºC.

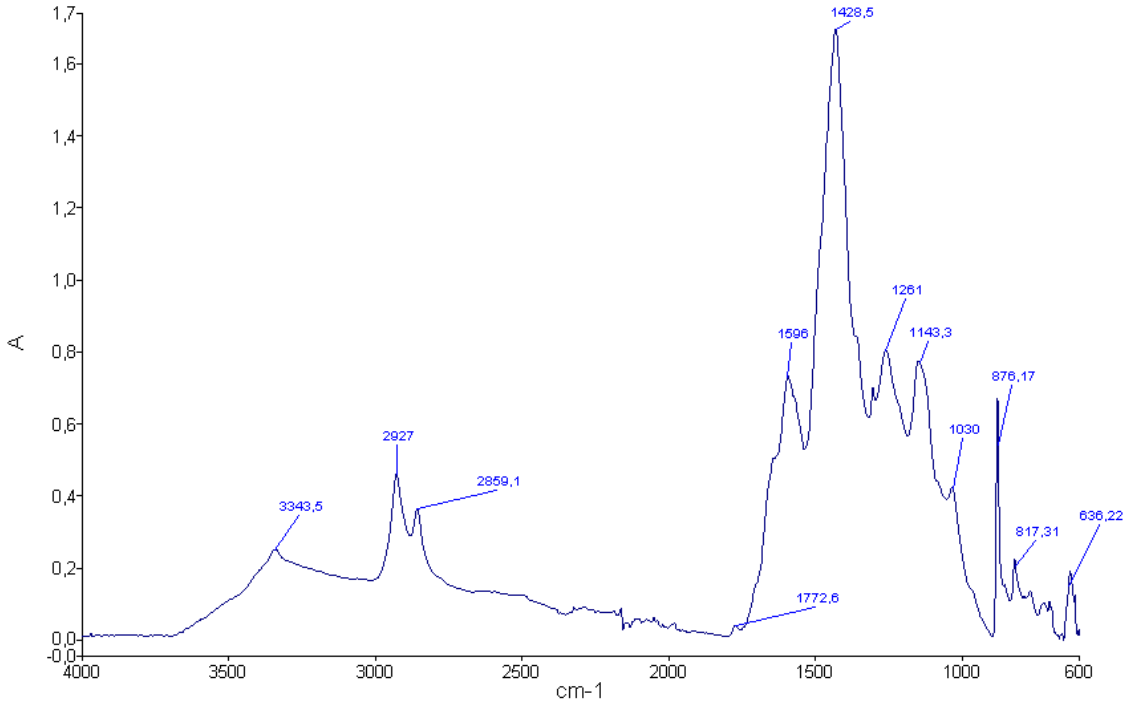

Fig. S5. FT-IR of the reaction LHDpH of lignin with dimethyl carbonate and hexamethylene diamine according to preparation method 3 at 180ºC.

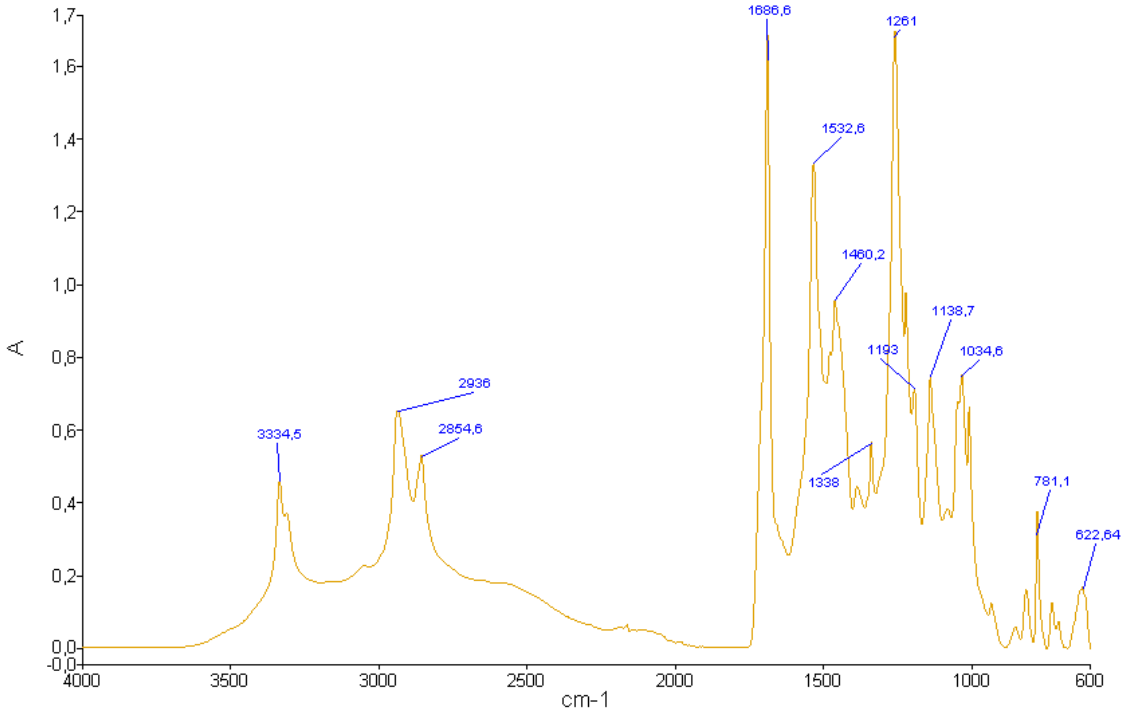

Fig. S6. FT-IR of the reaction LHDWpH of lignin with dimethyl carbonate and hexamethylene diamine according to preparation method 2 at 103ºC.

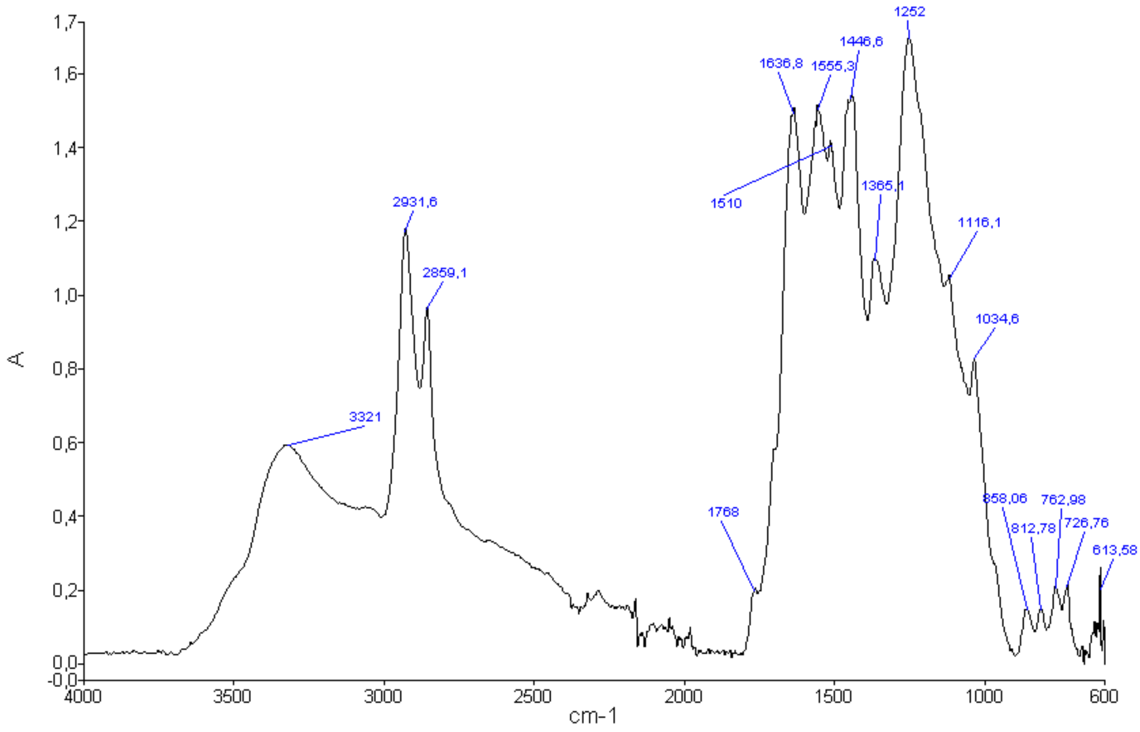

Fig. S7. FT-IR of the reaction LHDWpH of lignin with dimethyl carbonate and hexamethylene diamine according to preparation method 2 at 180ºC.

MALDI ToF

Table S1. MALDI-ToF analysis of oligomer species formed in the reaction of kraft lignin with dimethyl carbonate and hexamethylenediamine at room temperature. Case LDH.

U = urethane linkage; DMC= dimethyl carbonate; HMDA = hexamethylenediamine; 104, 138, 154, 178, 182, 198, 326 lignin = lignin fragments of respectively 104, 138, 154, 178, 182, 198, 326 molecular weight.

Peak in Spectrum (Da)	Oligomer type	Calculated Peak (Da)
137,6	Lignin	
255,5	DMC-138Lig-DMC	254
	198Lig-DMC	256
300,4	242Lig-DMC	300
	274Lig=DMC	300
301,5	138Lig-DMC-138Lig	302
314,5	DMC-198Lig-DMC	314
328,4	138Lig=DMCx2=138Lig	328
338,7	DMC-198Lig-DMC+Na	337
	DMC-138Lig-DMC-U-HMDA	338
357,5	154Lig-DMC-154Lig+Na	357
	DMC-274Lig=DMC	358
361,5	DMC-138Lig-DMC-138Lig	360
365,6	138Lig-DMC-179Lig+Na	366
376,4	138Lig-DMC-154Lig-DMC	376
398	DMC-198Lig-DMC-U-HMDA	398
406,8	242Lig-DMC-U-HMDA+Na	407
413,5	DMC-274Lig-DMC+Na	413
429,4	138Lig-DMC-242Lig+Na	429
443,7	DMC-198Lig-DMC-U-HMDA+Nax2	444
443,7	138Lig-DMC-U-HMDA-U-DMC-138Lig	444
457,3	DMC-138Lig-DMC-154Lig-DMC+Na	457
480,7	HMDA-U-DMC-198Lig-DMCx2+Nax2	479
522,9	154Lig-DMC-U-HMDA-U-DMC-178Lig+Na	523
537,4	154Lig-DMC-154Lig-DMC-154Lig+Na	537
	DMC-198Lig-DMC-198Lig-DMC	538
551,2	198Lig-DMC-305Lig+Na	552
	180Lig-DMC-U-HMDA-U-DMC-180Lig+Na	551
570,8	138Lig-DMC-U-HMDA-U-DMC-242Lig+Na	571
572	154Lig-DMC-154Lig-DMC-154Lig-DMC	572
573,4	DMC-138Lig-DMC-138Lig-DMC-138Lig-DMC+Na	573
602,8	138Lig-DMC-138Lig-DMC-274Lig	602
626,8	DMC-242Lig-DMC-242Lig-DMC	626

	DMC=274Lig-DMC-274Lig=DMC	626
628,8	138Lig-DMC-179Lig-DMC-179Lig-DMC+Na	629
713,4	DMC-274Lig-DMC-274Lig-DMC+Na	713
	138Lig-DMC-179Lig-DMC-179Lig-DMC-U-HMDA+Na	713
809,9	138Lig-DMC-198Lig-DMC-198Lig-DMC-198Lig	810

Table S2. MALDI-ToF analysis of oligomer species formed in the reaction of kraft lignin with dimethyl carbonate and hexamethylenediamine at 80°C. Case LDH.

U = urethane linkage; DMC= dimethyl carbonate; HMDA = hexamethylenediamine; 104, 138, 154, 178, 182, 198, 326 lignin = lignin fragments of respectively 104, 138, 154, 178, 182, 198, 326 molecular weight.

Peak in Spectrum (Da)	Oligomer type	Calculated Peak (Da)
255,5	DMC-138Lig-DMC	254
	198Lig-DMC	256
300,4	242Lig-DMC	300
	274Lig=DMC	300
314,5	DMC-198Lig-DMC	314
328,7	138Lig=DMCx2=138Lig	328
336,7	DMC-198Lig-DMC+Na	337
338,7	DMC-138Lig-DMC-U-HMDA	338
339,7	198Lig-DMC-U-HMDA	340
357,5	154Lig-DMC-154-Lig+Na	357
	DMC-274Lig=DMC	358
365,6	138Lig-DMC-179Lig+Na	366
372	198Lig-DMCx3+Na	372
379,8	DMC-180Lig-DMC-U-HMDA	380
398	DMC-198Lig-DMC-U-HMDA	398
407,8	242Lig-DMC-U-HMDA+Na	407
441,7	HMDA-U-DMC-274Lig=DMC	442
464,8	HMDA-U-DMC-182Lig-DMC-U-HMDA	466
	HMDA-U-DMC-274Lig=DMC	465
480,7	HMDA-U-DMC-198Lig-DMCx2+Nax2	479
507,8	138Lig-DMC-U-HMDA-U-DMC-178Lig+Na	507
520,7	DMC-274Lig-DMC-U-HMDA+Nax2	520
	154Lig-DMC-U-HMDA-U-DMC-198Lig	520
522,9	154Lig-DMC-U-HMDA-U-DMC-178Lig+Na	523
537,4	154Lig-DMC-154Lig-DMC-154Lig+Na	537
	DMC-198Lig-DMC-198Lig-DMC	538
553,6	198Lig-DMC-305Lig+Na	552
572,8	154Lig-DMC-154Lig-DMC-154Lig-DMC	572
	DMC-138Lig-DMC-138Lig-DMC-138Lig-DMC+Na	573

626,8	DMC-242Lig-DMC-242Lig-DMC	626
	DMC=274Lig-DMC-274Lig=DMC	626
628,8	138Lig-DMC-179Lig-DMC-179Lig-DMC+Na	629

Table S3. MALDI-ToF analysis of oligomer species formed in the reaction of kraft lignin with dimethyl carbonate and hexamethylenediamine at 103°C. Case LDH.

U = urethane linkage; DMC= dimethyl carbonate; HMDA = hexamethylenediamine; 104, 138, 154, 178, 182, 198, 326 lignin = lignin fragments of respectively 104, 138, 154, 178, 182, 198, 326 molecular weight.

Peak in Spectrum (Da)	Oligomer type	Calculated Peak (Da)
137,6	Lignin	
255,8	DMC-138Lig-DMC	254
	198Lig-DMC	256
300,4	242Lig-DMC	300
	274Lig=DMC	300
328,4	138Lig=DMCx2=138Lig	328
339,9	198Lig-DMC-U-HMDA	340
357,9	154Lig-DMC-154-Lig+Na	357
358,8	DMC-274Lig=DMC	358
359,7	DMC-138Lig-DMC-138Lig	360
363,8	198Lig-DMC-U-HMDA+Na	363
366,8	138Lig-DMC-179Lig+Na	366
372,7	198Lig-DMCx3+Na	372
375,8	138Lig-DMC-154Lig-DMC	376
382,9	DMC-182Lig-DMC-U-HMDA	382
397,8	DMC-198Lig-DMC-U-HMDA	398
406,8	242Lig-DMC-U-HMDA+Na	407
457,8	DMC-138Lig-DMC-154Lig-DMC+Na	457
465,9	HMDA-U-DMC-182Lig-DMC-U-HMDA	466
	HMDA-U-DMC-274Lig=DMC+Na	465
481,9	HMDA-U-DMC-198Lig-DMC-U-HMDA	482
497	DMC-274Lig-DMC-U-HMDA+Na	497
504,9	HMDA-U-DMC-198Lig-DMC-U-HMDA+Na	505
	HMDA-U-DMC-198Lig-DMC-U-HMDA+Na	505
504,9	138Lig-DMC-U-HMDA-U-DMC-198Lig	504
520,8	DMC-274Lig-DMC-U-HMDA+Na	520
522,9	154Lig-DMC-U-HMDA-U-DMC-178Lig+Na	523
537,8	154Lig-DMC-154Lig-DMC-154Lig+Na	537
	DMC-198Lig-DMC-198Lig-DMC	538
539,9	DMC-138Lig-DMC-242Lig-DMC-U-HMDA+Na	539
	198Lig-DMCx3-(U-HMDA)x2+Na	540

548,9	138Lig-DMC-U-HMDA-U-DMC-242Lig	548
	178Lig-DMC-U-HMDA-U-DMC-180Lig+Na	549
562,8	DMC-138Lig-DMC-242Lig-DMC-U-HMDA+Nax2	562
	198Lig-DMCx3-(U-HMDA)x2+Nax2	563
567,4	DMC-242Lig-DMC-242Lig	568
580,9	HMDA-U-DMC-274Lig-DMC-U-HMDA+Na	581
587,9	178Lig-DMC-U-HMDA-U-DMC-242Lig	588
604,9	HMDA-U-DMC-274Lig-DMC-U-HMDA+Nax2	604
615,9	242Lig-DMC-U-HMDA-U-DMC-182Lig+Na	615
620,9	272Lig-DMC-U-HMDA-U-DMC-180Lig	620
638,9	HMDA-U-DMC-274Lig-DMCx2+Nax2	639
655,9	154Lig-DMC-154Lig-DMC-154Lig-DMC-U-HMDA	656
655,9	138Lig-DMC-U-HMDA-U-DMC-326Lig+Na	655
662,9	HMDA-U-DMC-274Lig-(DMC)-DMC-U-HMDA+Na	662
	154Lig-DMC-138Lig-DMC-154Lig-DMC-U-HMDA+Na	663
675	HMDA-U-DMC-242Lig-DMC-242Lig+Na	675
680,9	DMC-138Lig-DMC-138Lig-DMC-138Lig-DMC-U-HMDA+Nax2	680
695,9	178Lig-DMC-U-HMDA-U-DMC-326Lig+Na	695
809,9	138Lig-DMC-198Lig-DMC-198Lig-DMC-198Lig	810

Table S4. MALDI-ToF analysis of oligomer species formed in the reaction of kraft lignin with dimethyl carbonate and hexamethylenediamine at room temperature. Case LHDpH.

U = urethane linkage; DMC= dimethyl carbonate; HMDA = hexamethylenediamine; 104, 138, 154, 178, 182, 198, 326 lignin = lignin fragments of respectively 104, 138, 154, 178, 182, 198, 326 molecular weight.

Peak in Spectrum (Da)	Oligomer type	Calculated Peak (Da)
137,8	Lignin	
198	Lignin	
255	138Lig+-HMDA	254
358,5	HMDA-138Lig-HMDA+Na	357
	242Lig+-HMDA	358
	138Lig+-HMDA-U-DMC+Nax2	358
	156Lig-HMDA-U-DMC+Nax2	358
361,4	182Lig-HMDA-U-DMC+Na	361
378	HMDA-182Lig-HMDA	378
392,6	HMDA-138-HMDA-U-DMC	392
441,5	Lignin	
	244Lig+-HMDA-U-DMC+Na	441
457	HMDA-180Lig-HMDA-U-DMC+Na	457
494,8	198Lig-HMDA+-198Lig	494

	198Lig+-HMDA+-180Lig	494
	156Lig-HMDAx2-156Lig+Na	495
537,2	138Lig-HMDA-U-DMC-U-HMDA-154Lig+Na	537
	138Lig-HMDA-U-DMC-U-HMDA-178Lig	538
551	HMDA-138Lig-HMDA-138Lig-HMDA	552
602,7	178Lig-HMDA-U-DMC-U-HMDA-180Lig+Na	603

Table S5. MALDI-ToF analysis of oligomer species formed in the reaction of kraft lignin with dimethyl carbonate and hexamethylenediamine at 80°C. Case LHDpH.

U = urethane linkage; DMC= dimethyl carbonate; HMDA = hexamethylenediamine; 104, 138, 154, 178, 182, 198, 326 lignin = lignin fragments of respectively 104, 138, 154, 178, 182, 198, 326 molecular weight.

Peak in Spectrum (Da)	Oligomer type	Calculated Peak (Da)
137,8	Lignin	
198	Lignin	
236,7	138Lig-HMDA	236
255,7	138Lig+-HMDA	254
276,7	138Lig+-HMDA+Na	277
	156Lig-HMDA+Na	277
305,7	104Lig+-HMDA-104Lig	306
312,7	138Lig+-HMDA-U-DMC	312
330,7	156Lig+-HMDA-U-DMC	330
336	HMDA+-104+-HMDA	336
338,6	182Lig-HMDA-U-DMC	338
358,7	242Lig+-HMDA	358
	138Lig+-HMDA-U-DMC+Nax2	358
	156Lig-HMDA-U-DMC+Nax2	358
361	182Lig-HMDA-U-DMC+Na	361
375,6	HMDA-180Lig-HMDA	376
388,7	HMDA+-156Lig+-HMDA	388
394	HMDA+-104+-HMDA-U-DMC	394
416,7	242Lig+-HMDA-U-DMC	416
	HMDA+-104+-HMDA-U-DMC+Na	417
441,8	Lignin	
	244Lig+-HMDA-U-DMC+Na	441
457,5	HMDA-182Lig-HMDA-U-DMC+Na	459
495,7	156Lig-HMDAx2-156Lig+Na	495
	DMC-UHMDA-138Lig-HMDA-U-DMC+Nax2	496
513,5	138Lig-HMDA-U-DMC-U-HMDA-154Lig	514

520,8	138Lig-HMDA-U-DMC-U-HMDA-138Lig+Na	521
537,7	138Lig-HMDA-U-DMC-U-HMDA-154Lig+Na	537
	138Lig-HMDA-U-DMC-U-HMDA-178Lig	538
551,7	HMDA-138Lig-HMDA-138Lig-HMDA	552
577,8	DMC-U-HMDA-242Lig-HMDA-U-DMC+Na	577
	178Lig-HMDA-U-DMC-U-HMDA-154Lig+Na	577
	178Lig-HMDA-U-DMC-U-HMDA-178Lig	578

Table S6. MALDI-ToF analysis of oligomer species formed in the reaction of kraft lignin with dimethyl carbonate and hexamethylenediamine at 103°C. Case LHDpH.

U = urethane linkage; DMC= dimethyl carbonate; HMDA = hexamethylenediamine; 104, 138, 154, 178, 182, 198, 326 lignin = lignin fragments of respectively 104, 138, 154, 178, 182, 198, 326 molecular weight.

Peak in Spectrum (Da)	Oligomer type	Calculated Peak (Da)
137,8	Lignin	
198	Lignin	
235,5	138Lig-HMDA	236
272,6	Lignin	
	156Lig+-HMDA	272
305,7	104Lig+-HMDA-104Lig	306
255	138Lig+-HMDA-U-DMC	312
330,8	156Lig+-HMDA-U-DMC	330
358,7	HMDA-138Lig-HMDA+Na	357
	242Lig+-HMDA	358
	138Lig+-HMDA-U-DMC+Nax2	358
	156Lig-HMDA-U-DMC+Nax2	358
363,7	182Lig-HMDA-U-DMC+Na	361
388,7	HMDA+-156Lig+-HMDA	388
446,8	HMDA+-156Lig+-HMDA-U-DMC+Na	446
495,7	156Lig-HMDAx2-156Lig+Na	495
	DMC-U-HMDA-138Lig-HMDA-U-DMC+Nax2	496
537,8	138Lig-HMDA-U-DMC-U-HMDA-154Lig+Na	537
	138Lig-HMDA-U-DMC-U-HMDA-178Lig	538
551,8	HMDA-138Lig-HMDA-138Lig-HMDA	552
579	180Lig-HMDA-180Lig+-HMDA+Na	579
580,8	180Lig-HMDA-U-DMC-U-HMDA-178Lig	580
602,9	138Lig-HMDA-U-DMC-U-HMDA-242Lig	602
	178Lig-HMDA-U-DMC-U-HMDA-180Lig+Na	603
620,8	178Lig-HMDA-U-DMC-U-HMDA-198Lig+Na	621
638,8	180Lig-HMDA-180Lig+-HMDA-U-DMC+Na	637

	180Lig-HMDA-180Lig-O-+HMDA--U-DMC+Na	637
	HMDA+-104Lig+-HMDA+-104Lig+-HMDA-U-DMC+Na	637
	180Lig-HMDA-180Lig+-HMDA-U-DMC+Na	637
650,9	198Lig+-HMDA+-198Lig+-HMDA+Na	651
	156Lig-HMDA-156Lig-HMDA-156Lig+Na	651
	138Lig+-HMDA+-138Lig+-HMDA-138Lig+Na	651
654	HMDA+-180Lig-HMDA-180Lig-HMDA	654
684,5	198Lig-HMDA-U-DMC-U-HMDA-242Lig+Na	685
694,9	272Lig-HMDA-U-DMC-U-HMDA-178Lig+Na	695
	DMC-U-180Lig-HMDA-180Lig-O-+HMDA-U-DMC+Na	695
	DMC-U-HMDA+-104Lig+-HMDA+-104Lig+-HMDA-U-DMC+Na	695
738	HMDA+-182Lig-HMDA-182Lig-HMDA-U-DMC+Na	739
751,9	DMC-U-HMDA-156Lig-HMDA-156Lig-HMDA-U-DMC+Nax2	750
	DMC-U-HMDA+-138Lig-HMDA-138Lig+-HMDA-U-DMC+Nax2	750
770	DMC-U-HMDA+-180Lig-HMDA-180Lig-HMDA-U-DMC	770
828	DMC-U-HMDA+-180Lig+-HMDA-180Lig-HMDA-U-DMC+Na	829
	DMC-U-HMDA-198Lig-HMDA-198Lig+-HMDA-U-DMC+Na	829
	DMC-U-HMDA+-198Lig-HMDA-180Lig+-HMDA-U-DMC+Na	829
912,2	DMC-U-HMDA-180Lig-HMDA-156Lig-HMDA-180Lig-HMDA-U-DMC+Na	913

Table S7. MALDI-ToF analysis of oligomer species formed in the reaction of kraft lignin with dimethyl carbonate and hexamethylenediamine at room temperature. Case LHDWpH.

U = urethane linkage; DMC= dimethyl carbonate; HMDA = hexamethylenediamine; 104, 138, 154, 178, 182, 198, 326 lignin = lignin fragments of respectively 104, 138, 154, 178, 182, 198, 326 molecular weight.

Peak in Spectrum (Da)	Oligomer type	Calculated Peak (Da)
137,8	Lignin	
197,7	Lignin	
236,7	138Lig-HMDA	236
255,6	138Lig+-HMDA	254
272,5	Lignin	
	156Lig+-HMDA	272
358,6	HMDA-138Lig-HMDA+Na	357
	242Lig+-HMDA	358
	138Lig+-HMDA-U-DMC+Nax2	358
	156Lig-HMDA-U-DMC+Nax2	358
	180Lig-HMDA-U-DMC+Na	359
416,6	HMDA-138-HMDA-U-DMC+Na	415
	HMDA-138Lig-HMDA-U-DMC+Na	415

	242Lig+-HMDA-U-DMC	416
	HMDA+-104+-HMDA-U-DMC+Na	417
441,7	Lignin	
	244Lig+-HMDA-U-DMC+Na	441
453,8	DMC-U-HMDA+-104+-HMDA-U-DMC	452
474,7	DMC-U-HMDA+-104+-HMDA-U-DMC+Na	475
494,8	198Lig-HMDA+-198Lig	494
	198Lig+-HMDA+-180Lig	494
	156Lig-HMDAx2-156Lig+Na	495
513,5	138Lig-HMDA-U-DMC-U-HMDA-154Lig	514
514,6	DMC-U-HMDA-180Lig-HMDA-U-DMC+Na	515
537,5	138Lig-HMDA-U-DMC-U-HMDA-154Lig+Na	537
	138Lig-HMDA-U-DMC-U-HMDA-178Lig	538
551	HMDA-138Lig-HMDA-138Lig-HMDA	552
603	178Lig-HMDA-U-DMC-U-HMDA-180Lig+Na	603

Table S8. MALDI-ToF analysis of oligomer species formed in the reaction of kraft lignin with dimethyl carbonate and hexamethylenediamine at 80ºC. Case LHDWpH.

U = urethane linkage; DMC= dimethyl carbonate; HMDA = hexamethylenediamine; 104, 138, 154, 178, 182, 198, 326 lignin = lignin fragments of respectively 104, 138, 154, 178, 182, 198, 326 molecular weight.

Peak in Spectrum (Da)	**Oligomer type**	**Calculated Peak (Da)**
137,8	Lignin	
198	Lignin	
235,5	138Lig-HMDA	236
255	138Lig+-HMDA	254
272,6	Lignin	
	156Lig+-HMDA	272
	156Lig+-HMDA-U-DMC	330
345	104Lig-HMDA-138Lig+Na	345
353,7	156Lig+-HMDA-U-DMC+Na	353
358,6	242Lig+-HMDA	358
	138Lig+-HMDA-U-DMC+Nax2	358
	156Lig-HMDA-u-DMc+Nax2	358
363,7	182Lig-HMDA-U-DMC+Na	361
388,7	HMDA+-156Lig+-HMDA	388
416	HMDA-138Lig-HMDA-U-DMC+Na	415
	HMDA-138-HMDA-U-DMC+Na	415
	242Lig+-HMDA-U-DMC	416

	HMDA+-104+-HMDA-U-DMC+Na	417
438,7	DMC-U-HMDA-138Lig-HMDA+Nax2	438
	242Lig+-HMDA-U-DMC+Na	439
451,7	DMC-U-HMDA+-104+-HMDA-U-DMC	452
495,7	156Lig-HMDAx2-156Lig+Na	495
496,6	DMC-U-HMDA-138Lig-HMDA-U-DMC+Nax2	496
520,7	138Lig-HMDA-U-DMC-U-HMDA-138Lig+Na	521
537,7	138Lig-HMDA-U-DMC-U-HMDA-154Lig+Na	537
	138Lig-HMDA-U-DMC-U-HMDA-178Lig	538
540,7	138Lig-HMDA-U-DMC-U-HMDA-180Lig	540
562,7	138Lig-HMDA-U-DMC-U-HMDA-180Lig+Na	563
578,7	180Lig-HMDA-U-DMC-U-HMDA-154Lig+Na	579
580,7	180Lig-HMDA-180Lig+-HMDA+Na	579
	180Lig-HMDA-U-DMC-U-HMDA-178Lig	580
581,6	138Lig-HMDA-U-DMC-U-HMDA-198Lig+Na	581
	180Lig-HMDA-U-DMC-U-HMDA-180Lig	582
597	154Lig-HMDA-U-DMC-U-HMDA-198Lig+Na	597
	198Lig-HMDA-U-DMC-U-HMDA-178Lig	598
602,8	138Lig-HMDA-U-DMC-U-HMDA-242Lig	602
	178Lig-HMDA-U-DMC-U-HMDA-180Lig+Na	603
613,7	HMDA+-104Lig+-HMDA+-104Lig+-HMDA-U-DMC	614
620,7	182Lig-HMDA-182Lig-O-+HMDA-U-DMC	618
	182Lig-HMDA-182Lig+-HMDA-U-DMC	618
	178Lig-HMDA-U-DMC-U-HMDA-198Lig+Na	621
638,7	180Lig-HMDA-180Lig-O-+HMDA-U-DMC+Na	637
	HMDA+-104Lig+-HMDA+-104Lig+-HMDA-U-DMC+Na	637
	180Lig-HMDA-180Lig+-HMDA-U-DMC+Na	637
	180Lig-HMDA-180Lig+-HMDA-U-DMC+Na	637
644,8	180Lig-HMDA-U-DMC-U-HMDA-242Lig	644
648,8	272Lig-HMDA-U-DMC-U-HMDA-154Lig	648
654	HMDA+-180Lig-HMDA-180Lig-HMDA	654
655,7	138Lig-HMDA-U-DMC-U-HMDA-272Lig+Na	655
674,7	180Lig-HMDA-U-DMC-U-HMDA-272Lig	674
706,8	242Lig-HMDA-U-DMC-U-HMDA-242Lig	706
731,7	HMDA+-180Lig+-HMDA+-180Lig+-HMDA-Na	731
	HMDA-198Lig+-HMDA+-198Lig-HMDA+Na	731
	HMDA+-198Lig+-HMDA+-180Lig+-HMDA+Na	731
	198Lig+-HMDA+-198Lig+-HMDA-U-DMC+Nax2	732
764,8	DMC-U-HMDA+-138Lig+-HMDA+-138Lig+-HMDA-U-DMC+Na	763
793,6	DMC-U-HMDA+-180Lig-HMDA-180Lig-HMDA-U-DMC+Na	793
820,8	272Lig-HMDA-U-DMC-U-HMDA-326Lig	820
890,6	DMC-U-HMDA-180Lig-HMDA-156Lig-HMDA-180Lig-HMDA-U-DMC	890
957,5	DMC-U-HMDA+-242Lig-HMDA-242Lig-HMDAx2+Na	957
	242Lig+-HMDA+-242Lig+-HMDA+-242Lig	958

Table S9. MALDI-ToF analysis of oligomer species formed in the reaction of kraft lignin with dimethyl carbonate and hexamethylenediamine at 103°C. Case LHDWpH.

U = urethane linkage; DMC= dimethyl carbonate; HMDA = hexamethylenediamine; 104, 138, 154, 178, 182, 198, 326 lignin = lignin fragments of respectively 104, 138, 154, 178, 182, 198, 326 molecular weight.

Peak in Spectrum (Da)	Oligomer type	Calculated Peak (Da)
137,8	Lignin	
198	Lignin	
235,5	138Lig-HMDA	236
255	138Lig+-HMDA	254
272,6	Lignin	
	156Lig+-HMDA	272
330,7	156Lig+-HMDA-U-DMC	330
354,7	156Lig+-HMDA-U-DMC+Na	353
358,7	HMDA-138Lig-HMDA+Na	357
	242Lig+-HMDA	358
	138Lig+-HMDA-U-DMC+Nax2	358
	156Lig-HMDA-U-DMC+Nax2	358
363,7	182Lig-HMDA-U-DMC+Na	361
388,7	HMDA+-156Lig+-HMDA	388
417	242Lig+-HMDA-U-DMC	416
	HMDA+-104+-HMDA-U-DMC+Na	417
437,7	HMDA-138Lig-HMDA-U-DMC+Na	438
441	244Lig+-HMDA-U-DMC+Na	441
451,7	DMC-U-HMDA-138-HMDA-U-DMC	450
	DMC-U-HMDA+-104+-HMDA-U-DMC	452
462,7	HMDA-242Lig-HMDA+Na	461
495,7	198Lig-HMDA+-198Lig	494
	198Lig+-HMDA+-180Lig	494
	156Lig-HMDAx2-156Lig+Na	495
	DMC-U-HMDA-138Lig-HMDA-U-DMC+Nax2	496
538,7	138Lig-HMDA-U-DMC-U-HMDA-178Lig	538
580,8	182Lig-HMDA-U-DMC-U-HMDA-178Lig	582
	138Lig-HMDA-U-DMC-U-HMDA-198Lig+Na	581
597	154Lig-HMDA-U-DMC-U-HMDA-198Lig+Na	597
	198Lig-HMDA-U-DMC-U-HMDA-178Lig	598
638,8	180Lig-HMDA-180Lig-O-+HMDA-U-DMC+Na	637
	HMDA+-104Lig+-HMDA+-104Lig+-HMDA-U-DMC+Na	637
	180Lig-HMDA-180Lig+-HMDA-U-DMC+Na	637
	180Lig-HMDA-180Lig+-HMDA-U-DMC+Na	637
655,8	138Lig-HMDA-U-DMC-U-HMDA-272Lig+Na	655

828,1	DMC-U-HMDA+-180Lig+-HMDA-180Lig-HMDA-U-DMC+Na	829
	DMC-U-HMDA-198Lig-HMDA-198Lig+-HMDA-U-DMC+Na	829
	DMC-U-HMDA+-198Lig-HMDA-180Lig+-HMDA-U-DMC+Na	829

6 « Lignin-derived non-toxic aldehydes for ecofriendly tannin adhesives for wood panels »

Auteurs: F.J. Santiago-Medina[1], G.Foyer[2,3], A.Pizzi[1,4], S.Calliol[2] et L.Delmotte[5]

[1] LERMAB, University of Lorraine, Epinal, France

[2] ICGM (UMR 5253 – CNRS, UM, ENSCM), Ecole Nationale Superieure de Chimie de Montpellier (ENSCM), Montpellier, France

[3] Safran-Herakles, France

[4] Dept. of Physics, King Abdulaziz University, Jeddah, Saudi Arabia

[5] IS2M, Institut de Science des Matériaux de Mulhouse, CNRS LRC 7228, University of Haute Alsace, Mulhouse, France

Résumé:

Un adhésif basé sur la réaction d'un tanin condensé de type procyanidine à réaction très rapide, à savoir le tanin de pin purifié, et les aldéhydes non toxiques de qualité alimentaire dérivés de la lignine ont montré qu'ils satisfaisaient bien les normes pertinentes pour les panneaux de particules de bois. La vanilline et un dérivé dialdéhyde de la vanilline étaient les aldéhydes utilisés. Les oligomères obtenues et leur distribution ont été déterminées par spectroscopie de masse de l'ionisation de désorption par laser assistée par matrice (MALDI-ToF) pour les réactions avec la catéchine utilisée comme composé modèle et avec le tanin de pin lui-même et par résonance magnétique nucléaire (CP MAS ^{13}C RMN) pour la réaction avec le tanin de pin.

Published by *International Journal of Adhesion and Adhesives*

LIGNIN-DERIVED NON-TOXIC ALDEHYDES FOR ECOFRIENDLY TANNIN ADHESIVES FOR WOOD PANELS

F.Santiago-Medina[1], G.Foyer[2,3], A.Pizzi[1,4]*, S.Calliol[2], L.Delmotte[5]
[1]LERMAB, University of Lorraine, Epinal, France
[2]ICGM (UMR 5253 – CNRS, UM, ENSCM), Ecole Nationale Superieure de Chimie de Montpellier (ENSCM), Montpellier, France
[3]Safran-Herakles, France
[4]Dept. of Physics, King Abdulaziz University, Jeddah, Saudi Arabia
[5]IS2M, Institut de Science des Matériaux de Mulhouse, CNRS LRC 7228, University of Haute Alsace, Mulhouse, France
**Correspondence to*: antonio.pizzi@univ-lorraine.fr

ABSTRACT

An adhesive based on the reaction of a very fast reacting procyanidin-type condensed tannin, namely purified pine bark tannin, and food-grade non-toxic slow-reacting aldehydes derived from lignin was shown to satisfy well the relevant standards for bonding wood particleboard. Vanillin and a dialdehyde derivative of vanillin were the aldehydes used. The oligomers obtained and their distribution have been determined by matrix assisted laser ionization desorption time-of-flight (MALDI-TOF) mass spectrometry for the reactions with catechin used as a model compound and with the pine tannin itself, and by cross polarization magic angle spinning ^{13}C nuclear magnetic resonance (CP MAS ^{13}C NMR) for the reaction with pine tannin.

Keywords: Particleboard bonding, ecofriendly adhesives, tannin.

INTRODUCTION

Tannin adhesives have now been around for a long time, a considerable amount of research on them has been published [1,2] and they have also been used industrially in a number of different countries [3-5]. However, the older industrially-used technology already in operation from the early 1970s still relies on the use of paraformaldehyde [1,3]. The proportion of formaldehyde used for these adhesives is anyhow only about 1/10th of the one used in equivalent synthetic adhesives. Nonetheless, there is now intense pressure to diminish or even eliminate formaldehyde from wood adhesives as it has been classified Carcinogenic Mutagenic Reprotoxic (CMR) [6]. In the case of tannin adhesives some substitutes have been tested [1,7,8] but three have dominated research on formaldehyde alternatives, namely hexamethylenetetramine (hexamine) [4,9-11], glyoxal [12], glyoxalated lignin [13] and furanic materials such as furfural and furfuryl alcohol [1,13]. Two of these approaches have been tried industrially [3-5]. Hexamine on the basis that, in presence of a fast reacting condensed flavonoid tannin, it does not decompose to formaldehyde but to extremely reactive intermediate compounds cross-linking without elimination of formaldehyde [9-11]. Glyoxal has been promoted and used for the more reactive procyanidin-type tannins such as pine bark tannin and other similar tannins [12]. Notwithstanding this, and the demonstrated advantages (and disadvantages) of hexamine and the limitation of glyoxal to the more reactive condensed tannin types, the search is still on for a compound capable to cross-link some tannins and being totally environment friendly.

Formaldehyde reacts with tannins to produce polymerization through methylene bridge linkages at reactive positions on the flavonoid molecules, mainly the A rings. Other aldehydes react also in the same manner as formaldehyde, but are less reactive [1]. The phloroglucinol-like A rings of procyanidin-type tannins, such as pine bark tannin, show reactivity toward formaldehyde comparable to that of phloroglucinol [15-17]. Assuming the reactivity with formaldehyde of phenol to be 1 and that of phloroglucinol to be 100, the A rings of pine tannins, as all procyanidin-type tannins, have a reactivity of around 40 [1,18]. They are thus far more reactive than phenol itself. Tannins present minimal reactivity at pHs around 3.5-4.5 and their reactivity progressively increases as the pH increases to eventually almost stabilize at around pH 10 and higher. Thus, if an aldehyde of lower reactivity needs to be used, such as glyoxal, or even less reactive, to ensure that a thermoset cross-linked resin is obtained, a very reactive tannin, such as a procyanidin type tannin needs to be chosen, as well as a range of pH in which the cross-linking reaction is relatively fast. In commercial mimosa tannin adhesives for wood particleboard panels when using formaldehyde, the gel time at 100°C at which the resin is set to obtain optimal results is around 110-130 seconds [1,3]. Conversely the much slower gelling synthetic phenol formaldehyde resins gel in anything between 9 and 40 minutes at 100°C according to the presence or not of accelerators in the glue-mix.

First of all it is necessary to remind that flavonoid and hydrolysable tannins have been certified as non-toxic in their REACH evaluation [19,20]. Thus, to maintain a totally environment friendly, non-toxic classification of wood adhesives based on these materials nothing short than a cross-linker both non-toxic and environment friendly and derived from a natural material would be acceptable to further improve them. It is evident that a material, an aldehyde for example, used commercially for food purposes, without being itself a foodstuff would be ideal for such a purpose. Industrial vanillin is produced worldwide in large quantities from lignin as a byproduct of the pulp and paper industry for flavouring industrial ice-creams and other foodstuff [21]. It is purified to a high grade for human nutrition, thus it is relatively expensive for this reason and because the world production for this application can be satisfied by the equivalent of the output of a single pulp mill. This means that the quantities produced can be easily increased more than 1000-fold with a marked decrease in costs, especially if its need of extensive purification is waived due to a non nutritional use as is the case of wood adhesives.

Recently, phenol has been shown to be too little reactive to prepare phenolic resins if reacted with vanillin [22]. However, phenolic resins have recently been successfully prepared by overcoming this problem by reaction of phenol with biobased vanillin-derived difunctional aldehydes [22]. The problem of the reactivity of phenol with aldehydes much less reactive than formaldehyde can however be overcome by using a much more reactive phenol. Thus, this article, describes (i) the reaction of a purified procyanidin-type tannin, namely pine bark tannin, with both vanillin and one experimental biobased vanillin-derived difunctional aldehyde, and (ii) to test the wood adhesives so formed for their bonding capability directly in wood panels while identifying the oligomers formed and their distribution to explain the results obtained.

EXPERIMENTAL

1.1 Materials

Purified maritime pine (*Pinus pinaster*) bark tannin extract (Phenopyn) was obtained by DRT (Derives Resiniques et Terpeniques, Dax, France). It is a commercial product purified for use as a food additive where the carbohydrates have been eliminated leaving exclusively the polyphenolic part of the flavonoid, procyanidin-type tannin [23]. Catechin was obtained from Sigma-Aldrich. Vanillin 99% was obtained from Sigma-Aldrich. 4-phenoxybenzaldehyde (Hyd-BzAld) of formula

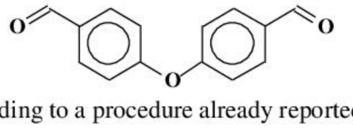

was prepared from vanillin according to a procedure already reported [22].

1.2 Gel time

For tannin adhesives the gel test is generally performed as follows: 10 g of a 45% (w/w) tannins/water solution and 5% of powdered paraformaldehyde on a dry and solid tannin matter

content basis are added to a test tube and placed in a water bath, which is maintained at boiling temperature (100ºC) at normal atmospheric pressure. A wire spring is inserted in the test tube and rapidly moved up and down and the time to gelling is measured by a stopwatch. The test is done in duplicate and the average value is reported.
For the vanillin and the experimental Hyd-BzAld the gel time was done on the following solutions under the following conditions:

1. purified maritime pine tannin dissolved in water/ethanol 50/50 by weight at 40%-45% solids + 20% vanillin at pH 3.2, thus with no correction of pH.
2. purified maritime pine tannin dissolved in water/ethanol 50/50 by weight at 40%-45% solids + 20% vanillin but after correcting the pH of the pine tannin solution (before adding vanillin) to pH 9.5.
3. purified maritime pine tannin dissolved in water/ethanol 50/50 by weight at 40%-45% solids + 20% Hyd-BzAld but after correcting the pH of the pine tannin solution (before adding vanillin) to pH 9.5.

The test had to be done in a water/ethanol solution due to the low viscosity of vanillin in water. The vanillin was predissolved in ethanol at ambient temperature. Furthermore, Hyd-BzAld had to be predissolved in ethanol at 40°C to form a 20% solution by weight. The solution remained stable after cooling.
The pH of tannins solution was adjusted using a 33% NaOH water solution. This test is a standard FESYP (European Federation of Panels Manufacturers) test and is used extensively in Europe for wood adhesives [24].

1.3 MALDI-TOF analysis

1.3.1 MALDI-TOF mass spectrometry

The spectra were recorded on a KRATOS AXIMA Performance mass spectrometer from Shimadzu Biotech (Kratos Analytical, Shimadzu Europe Ltd., Manchester, UK). The irradiation source was a pulsed nitrogen laser with a wavelength of 337 nm. The length of one laser pulse was 3 ns. Measurements were carried out using the following conditions: polarity-positive, flight path-linear, 20 kV acceleration voltages, 100-150 pulses per spectrum. The delayed extraction technique was used applying delay times of 200-800 ns. The software Maldi-MS was used for the data treatment.

1.3.2 MALDI-TOF sample preparation

The samples were dissolved in a solution of water/acetone (1:1) up to 7.5 mg/ml. For the enhancement of ion formation NaCl solution was added and placed on the MALDI target. The solutions of the samples and the matrix were mixed in equal amounts and 1.5 µl of the resulting solution was placed on the MALDI target. As the matrix, 2,5-dihydroxy benzoic acid was used. Red phosphorous was used as reference for spectrum calibration. Finally, after evaporation of the solvent, the MALDI target was introduced into the spectrometer. Due to the addition of sodium salt in the positive mode, the majority of the mass peaks correspond to $[M+Na^+]$. In order to obtain the molecular weight of the chemical species of the peak, 23 Da for sodium must be subtracted were indicated in the Tables.

1.4 CP MAS ^{13}C NMR

Solid state CP-MAS (cross-polarisation/magic angle spinning) ^{13}C NMR spectra of the fine powders obtained were recorded on a Bruker AVANCE II 400 MHz spectrometer at a sample spin of 12 kHz. Chemical shifts were calculated relative to tetramethyl silane (TMS). The rotor was spun at 4 kHz on a double-bearing 7 mm Bruker probe. The spectra were acquired with 5 s recycle delays, a 90° pulse of 5 micro s and a contact time of 1 ms. The number of transients was 3000.

1.5 Thermomechanical Analysis (TMA)

The experimental pine tannin/vanillin and pine tannin/Hyd-BzAld adhesive systems were tested by thermomechanical analysis. The samples were prepared by applying each resin system between two beech wood plies in a layer of 350 µm, for total sample dimensions of 21x6x1.1 mm. These beech-resin-beech specimens were tested in non-isothermal mode between 40°C and 220°C at a heating rate of 10°C/minute with a Mettler Toledo 40 TMA equipment in three-point bending on a span of 18 mm exercising a force cycle of 0.1/0.5 N on the specimens, with each force cycle of 12 seconds (6s/6s). The classical mechanics relationship between force and deflection

$$E = [L^3/(4bh^3)][\Delta F/(\Delta f_{wood} - \Delta f_{adhesive})]$$

allows the calculation of the Young's modulus E for each case tested. Such a measuring system has been introduced and is used to follow the progressive hardening of the adhesive with the increase of temperature and to indicate comparatively if an adhesive system is faster or slower hardening and if it gives stronger joints than another one [25-28].

1.6 Wood particleboard preparation and testing.

Five identical monolayer particleboard were prepared using the following glue mix: to 100 g of purified maritime pine (Pinus pinaster) tannin dissolved in water/ethanol 50/50 by weight to yield a concentration of 40%-45% solids. The pH was corrected to 9.5 with NaOH solution at 33% concentration. To this were added 20g (20% solids on solids) vanillin in ethanol. The glue mix was applied at a level of 10% solids on dry industrial wood chips and the panels hot pressed at 220°C, for 7.5 minutes with a pressure cycle of 28 kg cm^{-3}/15 kg cm^{-3}/5 kg cm^{-3} for 2 min/2.5 min/3 min. After cooling each panel was cut and 5 samples for each were tested for dry internal bond (IB) strength according to European Norm EN319 (1993) [29].

RESULTS AND DISCUSSION

The first parameter to be checked to determine the suitability for wood adhesives of a tannin-aldehyde system is its reactivity, hence its gel time at 100°C, under different reaction conditions. Table 1 shows the gel times obtained with maritime pine (*Pinus pinaster*) bark tannin with both vanillin and with Hyd-BzAld. These are compared to controls based on the same tannin tested with formaldehyde as hardener, and on a commercial mimosa-formaldehyde tannin adhesive also hardened with formaldehyde.

The results in Table 1 show that to obtain for maritime pine/vanillin and a maritime pine/Hyd-BzAld adhesive systems a gel time comparable to a commercial mimosa tannin adhesive it is necessary to increase the pH of the system to 10. At this pH the gel times obtained, within the 2 min to 4 min range, are within a range of gel time values acceptable for board-making. Equally, within the range of minimum reactivity of the pine tannin, at pH 3.2, the gel time obtained is well within the interval of gel times considered useful for synthetic phenol-formaldehyde resins. Such encouraging results indicate two things: (i) that the maritime pine/vanillin and a maritime pine/Hyd-BzAld adhesive systems actually react and cross-link, and (ii) that they cross-link under given conditions in an industrially suitable time.

It is necessary then to define what type of oligomer structures are formed by the reaction of tannin with vanillin and with Hyd-BzAld. To study such reactions, at first pure catechin monomer was reacted with vanillin and the products obtained determined by matrix assisted laser desorption ionization time-of-flight (MALDI-ToF) mass spectrometry. The results are shown in Figs.1-3 and Table 2. Adducts obtained by addition of one vanillin onto one catechin such as those represented by the peaks at 440-442 Da and 465 Da are formed, as well as adducts of two vanillin reacted onto a single catechin (618 Da). Oligomers are clearly formed by vanillin linking two or more catechin molecules through benzyl bridges, such as the peaks at 735 Da, 1025 Da, 1159 Da, 1449 Da 1584 Da and 1873 Da. These have the general structure -[-vanillin-catechin-]$_n$- repeating a number of times, in the spectra in Figs. 1-3 up to tetramers. Catechin dimerisation is also evident with the 601 Da peak, such dimerisation having partially contributed also to the oligomers represented by the peaks at 1025 Da, 1449 Da and 1873 Da (Table 2).

Second, the reaction with vanillin was repeated under the same conditions but using maritime pine tannin, thus a mix of polyflavonoid oligomer species. The results obtained by MALDI-ToF are shown in Table 3 and Fig. 4. Indication that vanillin and tannin have reacted are shown by the peaks at 440-486 Da indicating the formation of vanillin-catechin monomer adducts, at 639 Da indicating reaction of two vanillins onto a catechin monomer and also dimers at 681-684 Da and 700 Da, obtained by the introduction of vanillin-derived benzyl bridges between two flavonoids, two fisetinidins the former and a catechin and a fisetinidin the latter. These later compounds are confirmed by CP MAS ^{13}C NMR. Thus the CP MAS ^{13}C NMR in Fig. 5 shows all the peaks characteristic of a condensed flavonoid tannin [2] but with some variations. As the tannin was a purified one there are no carbohydrates present. The variations observed are a decrease of the C2 peak at 81 ppm, indicating that some of the flavonoid units heterocyclic ring has opened [2,30,31]. Furthermore, a very marked decrease of the free C6 site at 96-98 ppm indicates that a high number of C6 sites have reacted. The doublet of peaks at 58 ppm and 55 ppm belong respectively to the vanillin methoxy group and to the benzyl linkage of a vanillin molecule linking two flavonoid oligomers. This indicates that the structures detected by NMR are of the type

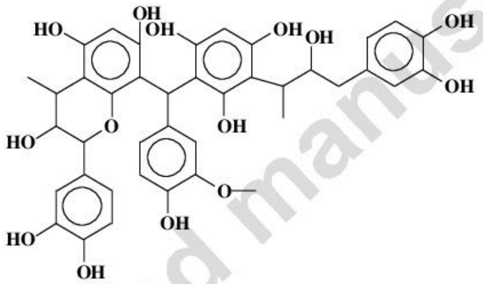

The NMR spectra shown can be compared with the equivalent NMR spectra of pure tannin in a number of relevant references [2,30,31].

Third, the reaction of maritime pine tannin with the experimental biosourced, vanillin-structure-derived difunctional aldehyde Hyd-BzAld was studied by MALDI-ToF.

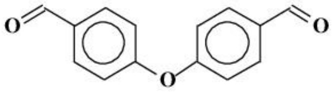

Hyd-BzAld

The reaction products obtained are shown in Figs. 6-8 and Table 4. Here too adducts of the catechin monomer of the tannin with the Hyd-BzAld are formed (535-539 Da) having structures of the type

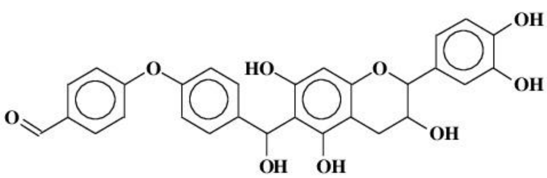

to the same series of which belong also the oligomers at 551 Da and 1037 Da.

Oligomer species in which the Hyd-BzAld forms bridges between two flavonoids are also present, for example the peak at 811-813 Da such as

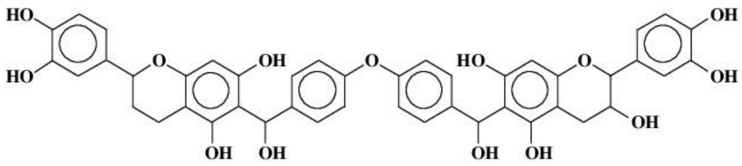

It must be noted that the Hyd-BzAld can be linked to either the C6 or C8 reactive sites of the flavonoids, the species depicted above being linked through the double aldehyde attached at the two C6 sites of the two flavonoid units, thus in brief C6-C6 (as in the figure), but equivalent species linked again through the double aldehyde C8-C8 or C6-C8 being also possible. Furthermore, for the same 811-813 Da peak, the two flavonoids can be linked in a different configuration by a benzyl bridge generated by just one of the two aldehyde groups of Hyd-BzAld, such as

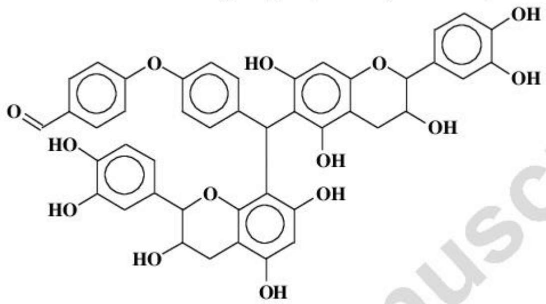

Oligomers as the 1326 Da peak formed by catechin-HydBzAld-catechin-HydBzAld-catechin are observed and belong to the series 811 Da, 826 Da, 842 Da, 1326 Da, 1342 Da, 1358 Da, 1374 Da, and a multitude of other peaks (cf. Fig. 8) among which are 1568 Da and 1857 Da.

After having determined that both the systems based on maritime pine tannin/vanillin and maritime pine tannin/Hyd-BzAld can react to form oligomers and cross-link to hardened resins under the conditions outlined it remained to test the bonds such resins are capable of forming. Thus, first thermomechanical analysis (TMA) was used to determine the potential strength of the hardened adhesive systems. In Figs. 9 and 10 are shown the TMA graphs of the two systems. In comparing them one can observe that the increase in MOE (thus in joint strength of the system [24-27] for the maritime pine tannin/vanillin adhesive is worse than for the maritime pine tannin/Hyd-BzAld one. This confirms previous work in which it was found that better performing synthetic phenolic resins can be prepared with vanillin-derived difunctional aldehydes [21] rather than with vanillin itself. In fact in Figs 8 and 9 it can be seen that the maximum MOE achieved by the pine tannin/Hyd-BzAld adhesive is 3000 MPa at 130°C while the MOE of the pine tannin/vanillin adhesive reached approximately 2000 MPa at 165°C.

To confirm the results obtained by TMA, five laboratory particleboard panels were prepared and tested according to European Norm EN319 (1993). The internal bond (IB) strength at a given density, generally between 0.670 to 0.700 g/cm^3, is the direct indication of how good is the adhesive bonding of the panel. The results obtained for dry internal bond strength are shown in Table 5. The average internal bond of the panels was of 0.47 MPa, that compares favourably with the 0.35 MPa required by EN319 (1993), thus confirming that a resin system totally non-toxic and biosourced based on polyflavonoid tannins and cross-linked with vanillin as hardener can satisfy the relevant requirements of international standards.

CONCLUSIONS

The preparation of phenolic resins obtained by the reaction of synthetic phenol with lignin-derived aldehydes has prompted the attempt to totally substitute the synthetic materials in such a type of resin. The reaction of a very fast reacting procyanidin-type tannin, namely purified pine bark tannin, with two slow-reacting lignin-derived aldehydes, both non-toxic and of foodstuff grade, namely vanillin and one of its dialdehyde derivatives, has shown that the preparation of adhesives capable of bonding wood particleboard satisfying the relevant European standards is possible without the use of any oil-derived materials. The demonstration of the reaction oligomers formed has passed (i) first through a MALDI-TOF mass spectrometry analysis of the reaction of the less reactive aldehyde, vanillin, with catechin monomer as a flavonoid tannin model compound, (ii) second through the same analysis supported by CP MAS ^{13}C NMR for its reaction with purified pine bark tannin and (iii) third through a MALDI-TOF mass spectrometry analysis of the reaction of the vanillin-derived dialdehyde with purified pine bark tannin. The oligomers distribution was also obtained. The adhesive so prepared is totally non-toxic, environment friendly and biosourced.

REFERENCES

[1] Pizzi A. Tannin based adhesives, chapter 4 in Wood Adhesives Chemistry and Technology Vol. 1 (A.Pizzi Ed.), Marcel Dekker, New York (1983)

[2] Pizzi A. Advanced Wood Adhesives Technology, Marcel Dekker, New York; (1994)

[3] A.Pizzi A. Wattle-based adhesives for exterior grade particleboard. Forest Prod J 1978; 28: 42-47.

[4] Pichelin F, Nakatani M, Pizzi A, Wieland S, Despres A, Rigolet S. Structural beams from Thick wood panels bonded industrially with formaldehyde free tannin adhesives. Forest Prod J 2006; 56: 31-36.

[5] Valenzuela J, von Leyser E, Pizzi A, Westermeyer C, Gorrini B. Industrial production of pine tannin-bonded particleboard and MDF. Eur J Wood Prod 2012; 70: 735-740

[6] European Chemicals Agency, CMR substances from Annex VI of the CLP (Classification, Labeling and Packaging) regulations, Registered under REACH (Registration, Evaluation, Authorisation and Restriction of Chemicals) regulations or notified under CLP, Helsinki, Finland , 2012

[7] Pizzi A, Rossouw DDu T, Daling GME. The role of aldehydes other than formaldehyde in tannin-based wood adhesives. Holzforschung Holzverwertung 1980; 32: 101-107.

[8] Böhm R, Hauptmann M, Pizzi A, Friederich C, Laborie M-P. The chemical, kinetic and mechanical characterization of tannin-based adhesives with different crosslinking systems Int J Adhesion Adhes 2016; 68: 1-8 DOI: 10.1016/j.ijadhadh.2016.01.006

[9] Kamoun C, Pizzi A. Mechanism of hexamine as a non-aldehyde polycondensation hardener, Part 1. Holzforschung Holzverwertung 2000a; 52: 16-19.

[10] Kamoun C, Pizzi A. Mechanism of hexamine as a non-aldehyde polycondensation hardener, Part 2: recomposition of intermediate reactive compound. Holzforschung Holzverwertung 2000b; 52: 66-67.

[11] Kamoun C, Pizzi A, Zanetti M. Upgrading of MUF resins by buffering additives – Part 1: hexamine sulphate effect and its limits. J Appl Polym Sci 2003; 90: 203-214.

[12] Ballerini A, Despres A, Pizzi A. Non-toxic, zero-emission tannin-glyoxal adhesives for wood panels. Holz Roh Werkst 2005; 63: 477-478.

[13] Navarrete P, Mansouri HR, Pizzi A, Tapin-Lingua S, Benjelloun-Llayah B, Rigolet S. Synthetic-resin-free wood panel adhesives from low molecular mass lignin and tannin, J Adh Sci Technol. 2010; 24: 1597-1610.

[14] Abdullah UHB, Pizzi A. Tannin-Furfuryl alcohol wood panel adhesives without formaldehyde. Eur J Wood Prod 2013; 71: 131-132.

[15] Pizzi A, Horak RM, Ferreira D, Roux DG. Condensates of phenol, resorcinol, phloroglucinol and pyrogallol, as flavonoids A- and B-rings model compounds with formaldehyde, Part 1. J Appl Polym Sci 1979; 24: 1571-1581.

[16] Pizzi A, Horak RM, Ferreira D, Roux DG. Condensates of phenol, resorcinol, phloroglucinol and pyrogallol, as flavonoids A- and B-rings model compounds with formaldehyde, Part 2. Cellulose Chem Techn 1979; 13: 753-764
[17] Rossouw DDuT, Pizzi A, McGillivray G. The kinetics of condensation of phenolic polyflavonoid tannins with aldehydes. J Polym Sci, Chem 1980; 18: 3323-3338.
[18] Pizzi A, Scharfetter H. The chemistry and development of tannin-based wood adhesives for exterior plywood. J Appl Polym Sci 1978; 22: 1745-1761.
[19] European Chemical Agency, REACH (Registration, Evaluation, Authorisation and Restriction of Chemicals) regulations, Helsinki, Finland (2006)
[20] Giovando S, Silva Chimica, REACH certificate of acceptance of tannin extracts as non-toxic, St.Michele Mondovi, Italy, 2010.
[21] Araujo JD, Grande CA, Rodrigues AE. Vanillin production from lignin oxidation in a batch reactor. Chem Eng Res Design 2010; 88: 1024-1032.
[22] Foyer G, Chanfi B-H, Boutevin B, Caillol S, David G. New method for the synthesis of formaldehyde-free phenolic resins from lignin-based aldehyde precursors. Eur Polym J 2016; 74: 296-309.
[23] Navarrete P, Pizzi A, Pasch H, Rode K, Delmotte L. Characterisation of two maritime pine tannins as wood adhesives, J Adh Sci Technol 2013; 27: 2462-2479.
[24] FESYP Methods, Federation europeenne des syndacats des fabricants de panneaux de particules, Brussels, Belgium 1979
[25] Laigle Y, Kamoun C, Pizzi A. Particleboard I.B. forecast by TMA bending in UF adhesives curing. Holz Roh Werkst 1998; 56: 154.
[26] Zhao C, Garnier S, Pizzi A. Particlebord dry and wet IB forecasting by gel time and dry TMA bending in PF wood adhesives. Holz Roh Werkst 1998; 56: 402.
[27] Garnier S, Huang Z, Pizzi A. Commercial tannin adhesives-bonded particleboard IB forecasting by TMA bending. Holz Roh Werkst 2001; 59: 46.
[28] Lecourt M, Humphrey P, Pizzi A. Comparison of TMA and ABES as forecasting systems of wood bonding effectiveness. Holz Roh Werkst 2003; 61: 75–76.
[29] European Norm EN 319 (1993) Perpendicular Tensile Strength of Particleboards and Fibreboards
[30] Pizzi A, Stephanou A. A ^{13}C NMR study of polyflavonoid tannin adhesives intermediates, Part 1: non-colloidal, performance-determining rearrangements. J Appl Polym Sci. 1994; 51: 2109-2124.
[31] Thompson D, Pizzi A. Simple ^{13}C NMR methods for the quantitative determination of polyflavonoid tannins characteristics. J Appl Polym Sci. 1995; 55: 107-112.

Table 1. Gel times of purified pinus pinaster condensed flavonoid tannin with vanillin and with Hyd-BzAld

Resin type	pH	Gel time
Commercial Mimosa tannin adhesive +formaldehyde control	6.8	2 minutes 10 seconds
Pinus pinaster+formaldehyde control	3.2	1 minute 30 seconds
Pinus pinaster + vanillin	3.2	15 minutes 12 seconds
Pinus pinaster + vanillin	10	2 minutes 47 seconds
Pinus pinaster + Hyd-BzAld	10	3 minutes 24 seconds

Table 2. MALDI-ToF oligomers species formed by the reaction of catechin with vanillin

290 Da = catechin without Na^+
312 – 313 Da = catechin with Na^+
440-442 Da = catechin-vanillin without Na^+

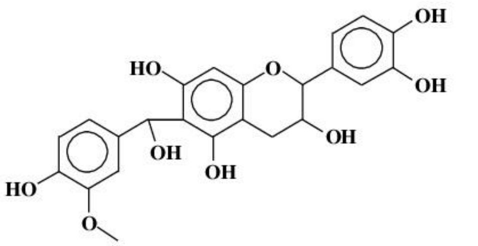

465 Da = catechin-vanillin with Na^+
601 Da = catechin-catechin dimer with Na^+
618 Da = vanillin-catechin-vanillin with Na^+
735 Da = catechin-van-catechin dimer with Na^+

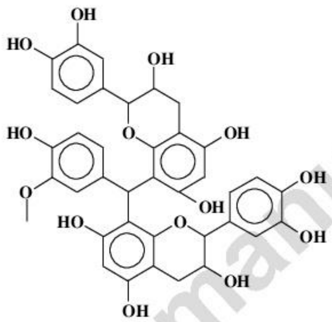

1025 Da = catechin-van-catechin-catechin with Na^+
1159 Da = catechin-van-catechin-van-catechin trimer with Na^+
1449 Da = catechin-van-catechin-van-catechin-catechin with Na^+
1584 Da = catechin-van-catechin-van-catechin-van-catechin tetramer with Na^+
1873 Da = catechin-van-catechin-van-catechin-van-catechin-catechin pentamer with Na^+

Table 3. MALDI-ToF oligomers species formed by the reaction of Pinus pinaster with vanillin

334 Da = gallocatechin multiprotonated with Na^+
440 Da = van-catechin without Na^+
465 Da = van-catechin with Na^+
486 Da = van-catechin multiprotonated with Na^+
532 Da = fisetinidin dimer having lost a –OH
617 Da = van-catechin-van with Na^+
639 Da = van-catechin-van multiprotonated with Na^+
681-684 Da = fisetinidin-van-fisetinidin without Na^+
700 Da = catechin-van-fisetinidin without Na^+

486 Da = 639 Da – 1x Vanillin
376 (380 calculated) Da = 532 – 1x vanillin

334 Da = 486 Da – 1xvanillin

Table 4. MALDI-ToF oligomers species formed by the reaction of Pinus pinaster with Hyd-BzAld

272.5 Da = fisetinidin without Na^+
226 Da = Hyd-BzAld without Na^+ thus:

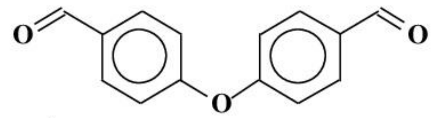

249 Da = Hyd-BzAld with Na^+
290 Da = catechin without Na^+
306 Da = gallocatechin without Na^+
313 Da = catechin with Na^+
316 Da = 313 Da triprotonated
535-539 Da =

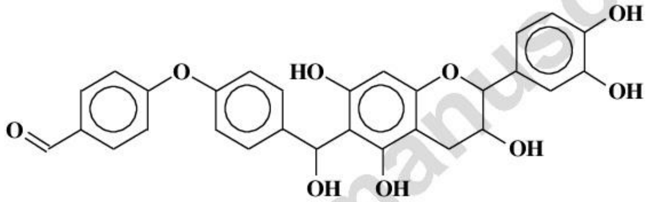

551 Da = gallocatechin-Hyd-BzAld (as 535 but gallocatechin)

811-813 Da = one of the following two structures, both catechin dimers :

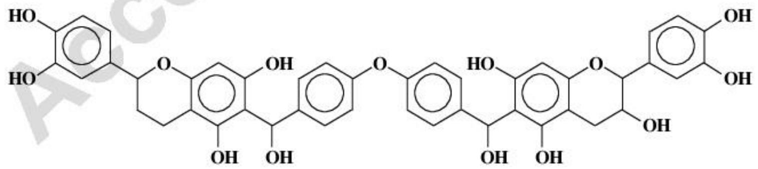

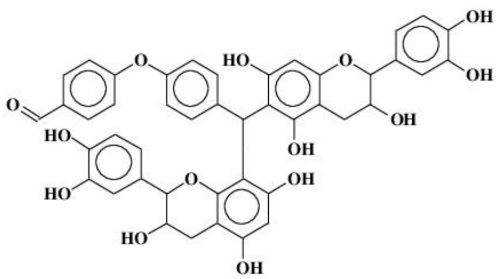

According to where the second flavonoid has reacted.

826 Da = the same as 811 but gallocatechin-HydBzAld-catechin, thus a dimer
842 Da = the same as 811 but gallocatechin-HydBzAld-gallocatechin, thus a dimer
1037 Da = 811 Da + 1x Hyd-BzAld, thus, catechin-HydBzAld-catechin-HydBzAld, still a dimer
1326 Da = 811 Da + 1x Hyd-BzAld + 1x Catechin, thus a trimer: catechin-HydBzAld-catechin-HydBzAld-catechin
1342 Da = 811 Da + 1x Hyd-BzAld + 1x Gallocatechin, thus a trimer: gallocatechin-HydBzAld-catechin-HydBzAld-catechin
1358 Da = gallocatechin-HydBzAld-gallocatechin-HydBzAld-catechin
1374 Da = gallocatechin-HydBzAld-gallocatechin-HydBzAld-gallocatechin
and so on to
1568 Da = gallocatechin-HydBzAld-catechin-HydBzAld-catechin-HydBzAld
and
1857 Da = gallocatechin-HydBzAld-catechin-HydBzAld-catechin-HydBzAld-catechin

Table 5. Particleboard internal bond (IB) strength results

	Density (g/cm^3)	IB strength Dry (MPa)
	0.669	0.45+0.02
	0.669	0.46+0.03
	0.662	0.46+0.02
	0.679	0.50+0.01
	0.674	0.49+0.01
Ave.	0.670	0.47
EN319 requirement		> 0.35

FIGURE LEGENDS

Fig. 1. MALDI-TOF mass spectrum of catechin-vanillin resin. Range 200 Da – 320 Da

Fig. 2. MALDI-TOF mass spectrum of catechin-vanillin resin. Range 340 Da – 800 Da

Fig. 3. MALDI-TOF mass spectrum of catechin-vanillin resin. Range 800 Da – 2000 Da

Fig. 4. MALDI-TOF mass spectrum of purified pine tannin-vanillin resin. Range 330 Da – 800 Da

Fig. 5. CP MAS ^{13}C NMR of purified pine tannin-vanillin resin

Fig. 6. MALDI-TOF mass spectrum of purified pine tannin-Hyd-BzAld resin. Range 200 Da – 320 Da

Fig. 7. MALDI-TOF mass spectrum of purified pine tannin-Hyd-BzAld resin. Range 340 Da – 800 Da

Fig. 8. MALDI-TOF mass spectrum of purified pine tannin-Hyd-BzAld resin.
Range 800 Da – 2000 Da

Fig. 9. Thermomechanical analysis (TMA) curve as a function of time and temperature of purified pine tannin-vanillin resin

Fig. 10. Thermomechanical analysis (TMA) curve as a function of time and temperature of purified pine tannin-Hyd-BzAld resin

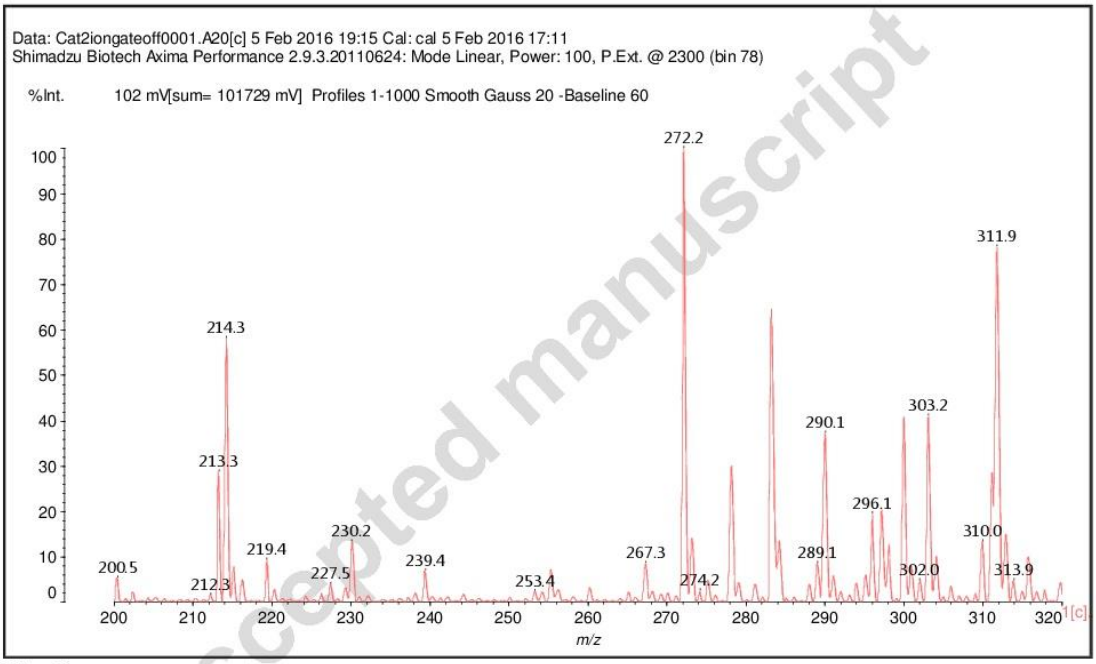

Fig. 1

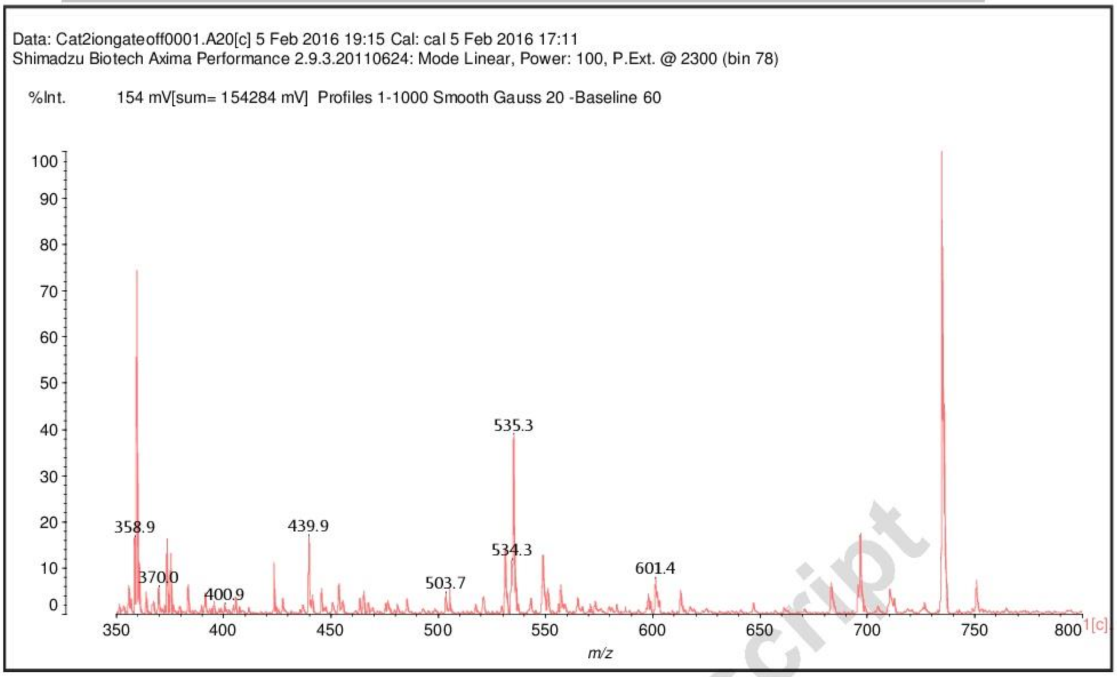
Data: Cat2iongateoff0001.A20[c] 5 Feb 2016 19:15 Cal: cal 5 Feb 2016 17:11
Shimadzu Biotech Axima Performance 2.9.3.20110624: Mode Linear, Power: 100, P.Ext. @ 2300 (bin 78)
%Int.
154 mV[sum= 154284 mV] Profiles 1-1000 Smooth Gauss 20 -Baseline 60
535.3
358.9
439.9
534.3
370.0
400.9
503.7
601.4
m/z

Fig. 2

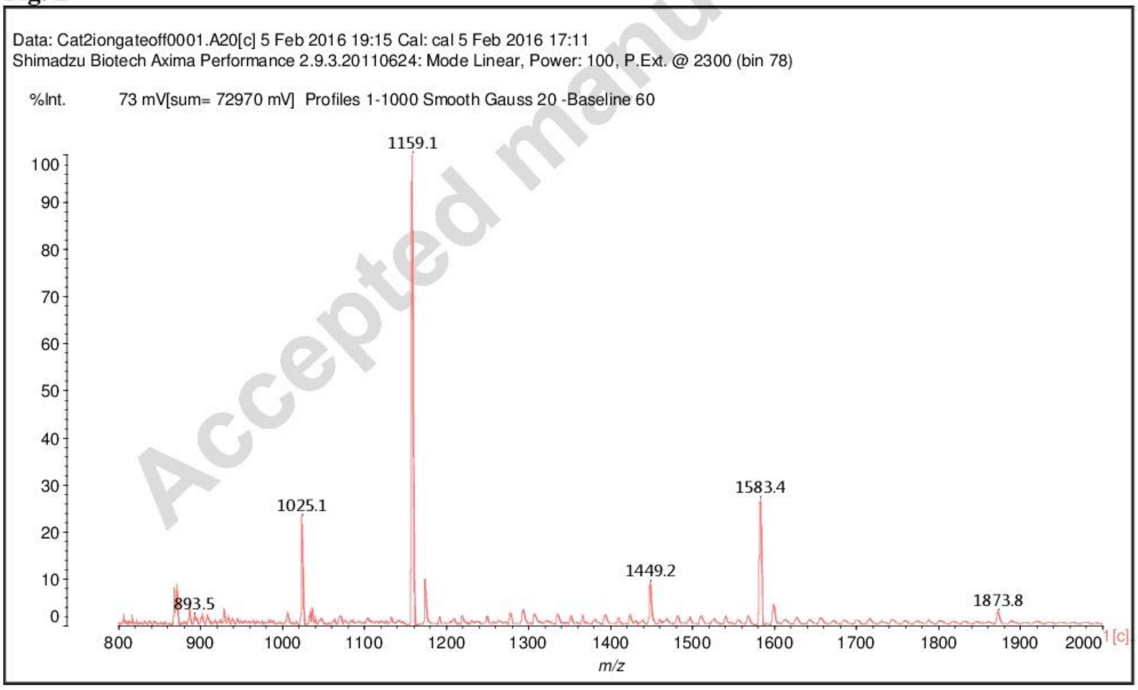
Data: Cat2iongateoff0001.A20[c] 5 Feb 2016 19:15 Cal: cal 5 Feb 2016 17:11
Shimadzu Biotech Axima Performance 2.9.3.20110624: Mode Linear, Power: 100, P.Ext. @ 2300 (bin 78)
%Int.
73 mV[sum= 72970 mV] Profiles 1-1000 Smooth Gauss 20 -Baseline 60
1159.1
1025.1
1583.4
1449.2
893.5
1873.8
m/z

Fig. 3.

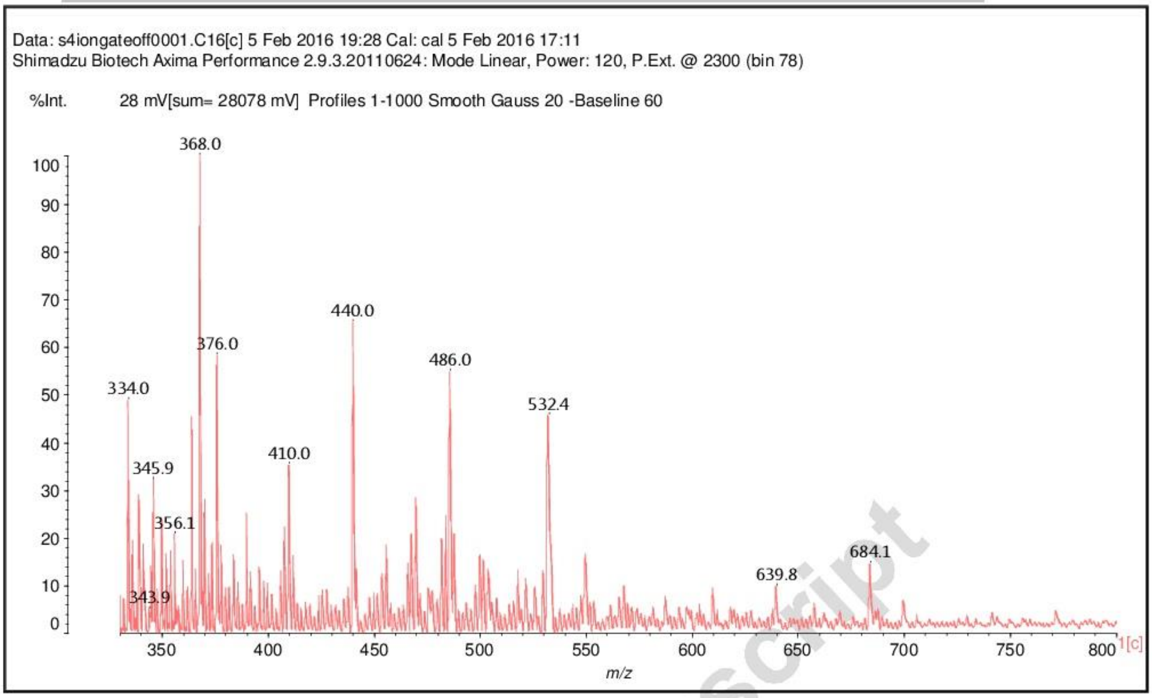
Data: s4iongateoff0001.C16[c] 5 Feb 2016 19:28 Cal: cal 5 Feb 2016 17:11
Shimadzu Biotech Axima Performance 2.9.3.20110624: Mode Linear, Power: 120, P.Ext. @ 2300 (bin 78)
%Int.
28 mV[sum= 28078 mV] Profiles 1-1000 Smooth Gauss 20 -Baseline 60
368.0
440.0
376.0
486.0
334.0
532.4
410.0
345.9
356.1
684.1
639.8
343.9
m/z
1[c]

Fig. 4.

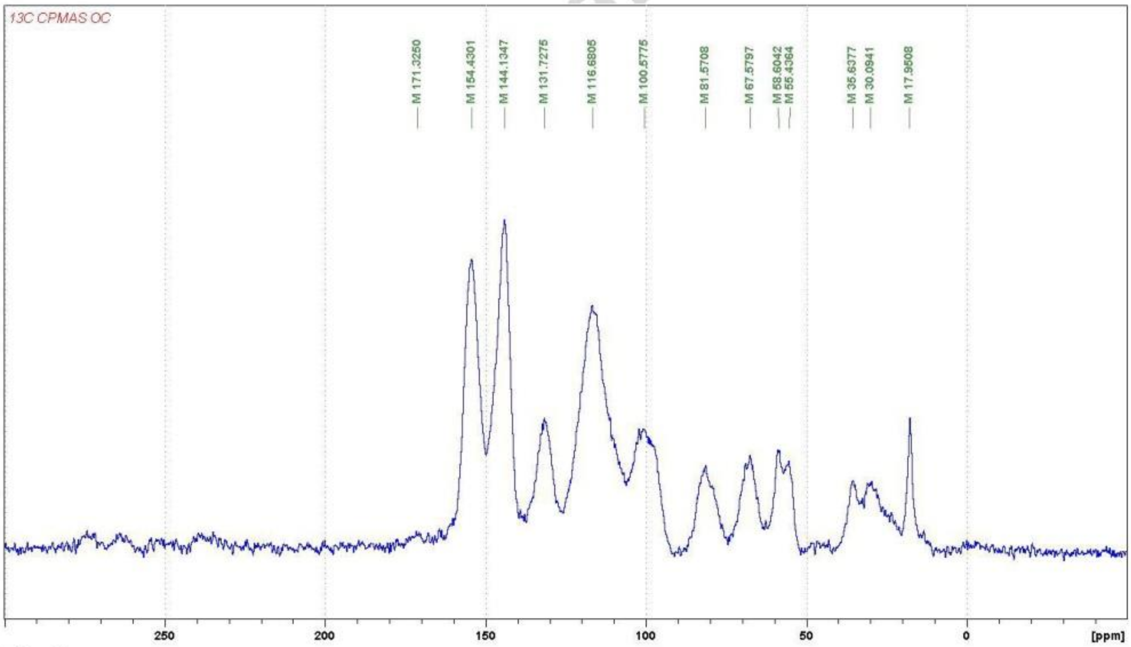
13C CPMAS OC
M 171.3250
M 154.4301
M 144.1347
M 131.7275
M 116.6805
M 100.5775
M 81.5708
M 67.5797
M 58.6042
M 55.4364
M 35.6377
M 30.0941
M 17.9508
[ppm]

Fig. 5.

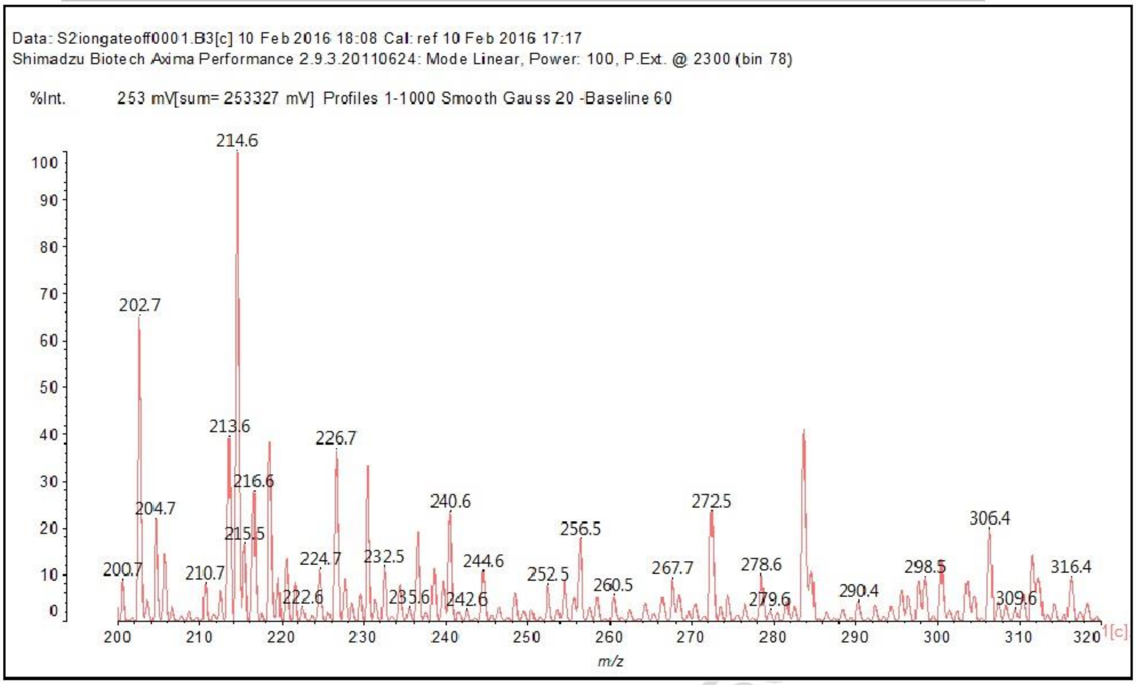
Data: S2iongateoff0001.B3[c] 10 Feb 2016 18:08 Cal: ref 10 Feb 2016 17:17
Shimadzu Biotech Axima Performance 2.9.3.20110624: Mode Linear, Power: 100, P.Ext. @ 2300 (bin 78)
%Int.
253 mV[sum= 253327 mV] Profiles 1-1000 Smooth Gauss 20 -Baseline 60
214.6
202.7
213.6
226.7
216.6
204.7
240.6
272.5
256.5
306.4
215.5
224.7
232.5
244.6
200.7
210.7
252.5
267.7
278.6
298.5
316.4
260.5
222.6
235.6
242.6
279.6
290.4
309.6
m/z
1[c]

Fig. 6.

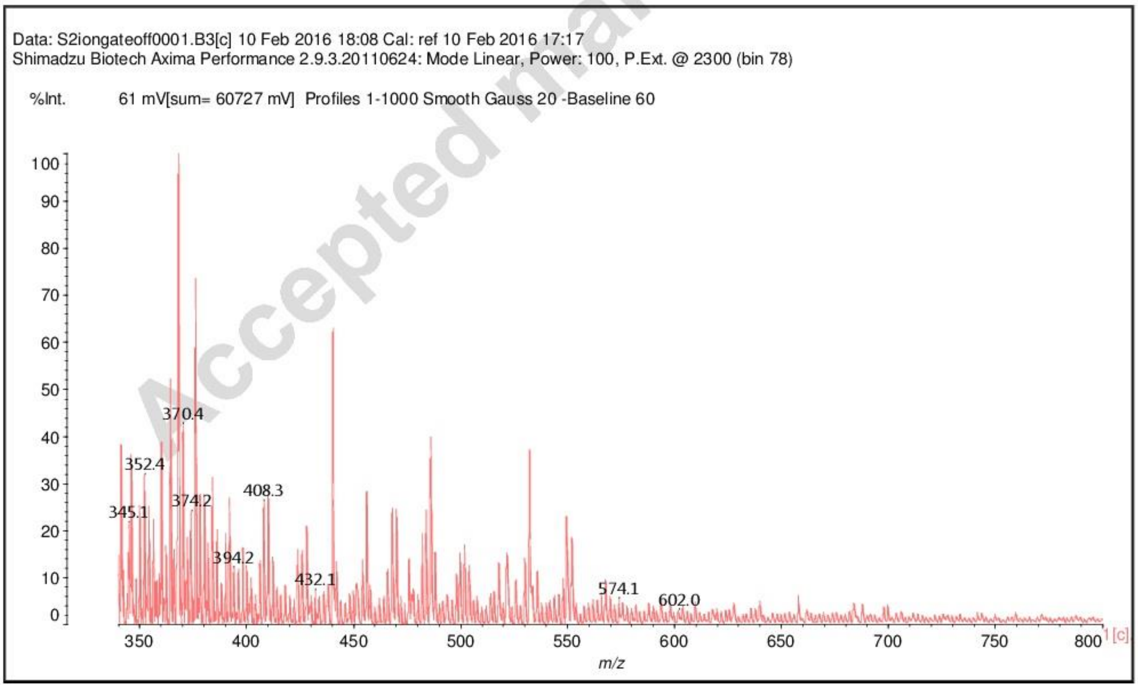
Data: S2iongateoff0001.B3[c] 10 Feb 2016 18:08 Cal: ref 10 Feb 2016 17:17
Shimadzu Biotech Axima Performance 2.9.3.20110624: Mode Linear, Power: 100, P.Ext. @ 2300 (bin 78)
%Int.
61 mV[sum= 60727 mV] Profiles 1-1000 Smooth Gauss 20 -Baseline 60
370.4
352.4
408.3
374.2
345.1
394.2
432.1
574.1
602.0
m/z
1[c]

Fig. 7.

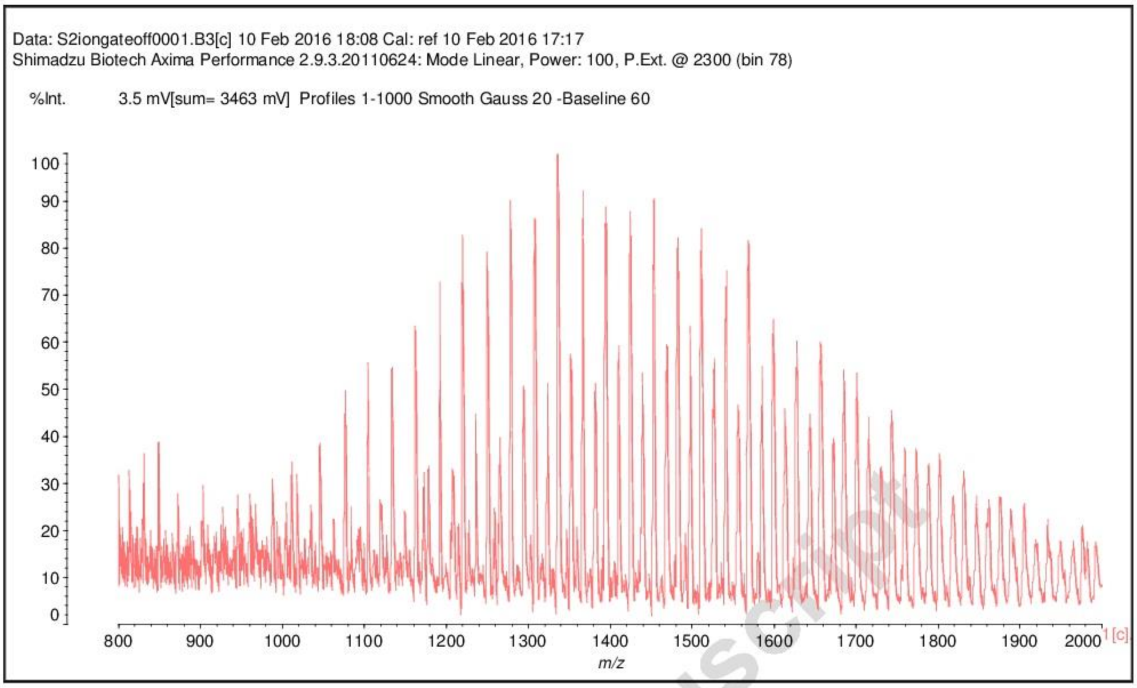
Data: S2iongateoff0001.B3[c] 10 Feb 2016 18:08 Cal: ref 10 Feb 2016 17:17
Shimadzu Biotech Axima Performance 2.9.3.20110624: Mode Linear, Power: 100, P.Ext. @ 2300 (bin 78)
%Int.
3.5 mV[sum= 3463 mV] Profiles 1-1000 Smooth Gauss 20 -Baseline 60
100
90
80
70
60
50
40
30
20
10
0
800
900
1000
1100
1200
1300
1400
1500
1600
1700
1800
1900
2000
m/z

Fig. 8.

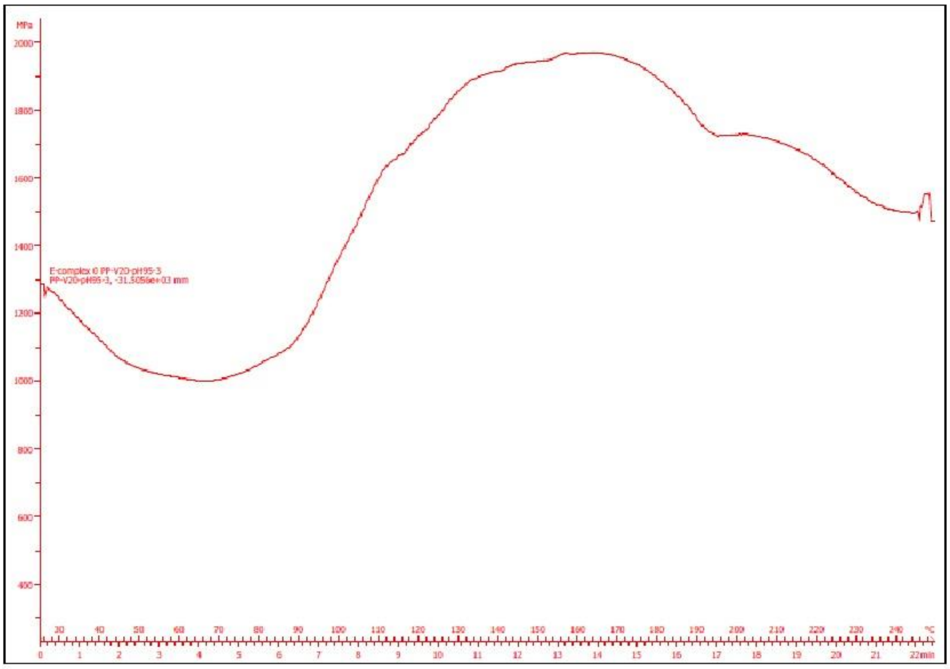
MPa
2000
1800
1600
1400
1200
1000
E-complex 0 PP-V20-pH95-3
PP-V20-pH95-3, -31.5056e+03 mm

Fig. 9.

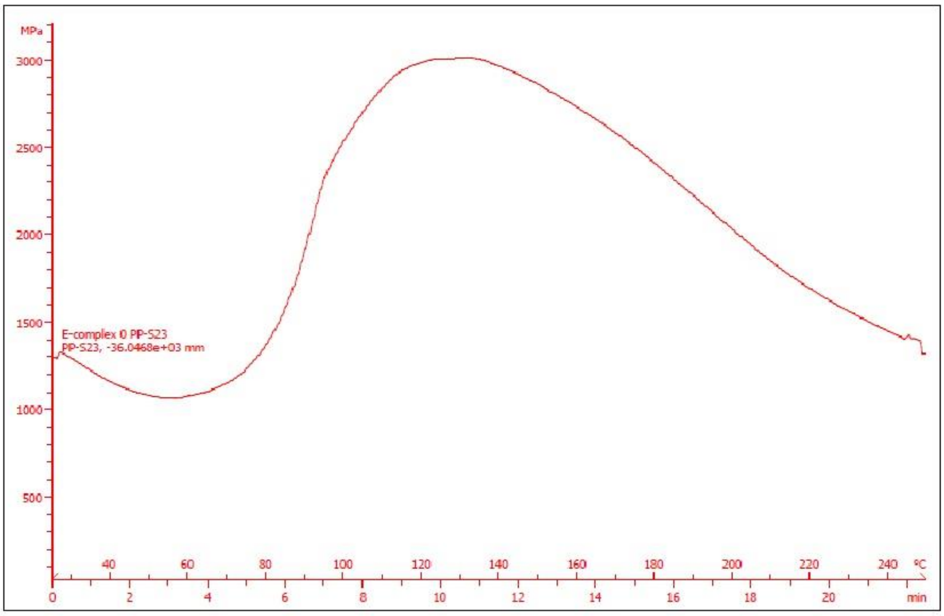
MPa
3000
2500
2000
1500
1000
500
E-complex 0 PP-S23
PP-S23, -36.0468e+03 mm
40
60
80
100
120
140
160
180
200
220
240
°C
0
2
4
6
8
10
12
14
16
18
20
min

Fig. 10.

7 « Mechanically blown wall-projected tannin-based foams »

Auteurs: F.J. Santiago-Medina[1], C. Delgado-Sánchez[2], M. C. Basso[1], A. Pizzi[1], V. Fierro[2] et A. Celzard[2]

[1] LERMAB, ENSTIB, University of Lorraine, 27 rue Philippe Séguin, BP 21042, 88051 Epinal cedex 9, France

[2] Institut Jean Lamour, UMR CNRS, University of Lorraine. ENSTIB, 27 rue Philippe Séguin, BP 21042, 88051 Epinal cedex 9, France

Résumé :

Les mousses à base de tanin condensées provenant de l'extrait de tanin de Quebracho ont été développées à l'aide d'une nouvelle méthode d'expansion à base de mousse de lutte contre l'incendie ou de tunnellisation, où un agente tensioactif forme une mousse liquide stable. Ce nouveau procédé mécanique d'expansion permet d'obtenir un matériau poreux solide après durcissement à température ambiante, à travers une mousse liquide formée par une résine de tanin et une solution aqueuse d'agent tensioactif. On rapporte la stabilité de la mousse liquide ainsi obtenue et l'influence de la quantité de catalyseur. L'utilisation de cette nouvelle approche pour la préparation de mousses rigides à base de tanin évite le problème du retrait présenté par de nombreuses autres formulations où le moussage physique ou chimique est utilisé. Des agents tensioactifs non ioniques ont également été utilisés dans la formulation pour obtenir des cellules plus petites et améliorer la structure du nouveau matériau. La densité granulométrique, les propriétés mécaniques et thermiques et l'aspect morphologique des mousses ont été caractérisés et rapportés.

Submitted to *Industrial Crops and Products*

MECHANICALLY BLOWN WALL-PROJECTED TANNIN-BASED FOAMS

F.J. Santiago-Medina[1,*], C. Delgado-Sánchez[2], M. C. Basso[1], A. Pizzi[1,*], V. Fierro[2], A. Celzard[2]

[1] LERMAB, ENSTIB, University of Lorraine, 27 rue Philippe Séguin, BP 21042, 88051 Epinal cedex 9, France
[2] Institut Jean Lamour, UMR CNRS, University of Lorraine. ENSTIB, 27 rue Philippe Séguin, BP 21042, 88051 Epinal cedex 9, France

[*] Corresponding author at LERMAB, University of Lorraine, 27 rue Philippe Seguin, BP 21042, 88051 Epinal cedex 9, France. Fax: +33 3 29 29 61 38.
E-mail address: francisco-jose.santiago-medina@univ-lorraine.fr (F.J. Santiago-Medina), antonio.pizzi@univ-lorraine.fr (A. Pizzi).

Abstract

Condensed flavonoid tannin-based foams from quebracho tannin extract have been developed using a new method of expansion based on fire-fighting or tunneling foams, where a foam concentrate forms a stable liquid foam. This new mechanical method of expansion allows obtaining a solid porous material after curing and hardening at room temperature, through a liquid foam formed by a tannin resin and an aqueous solution of surfactant. The stability of the as-obtained liquid foam and the influence of the amount of catalyst are reported. The use of this new approach for preparing tannin-based rigid foams avoids the problem of shrinkage presented by many other formulations where physical or chemical foaming is employed. Non-ionic surfactants have also been used in the formulation to obtain smaller cells and improve the structure of the new material. Bulk density, mechanical and thermal properties and morphological appearance of the foams have been characterised and reported.

Keywords

Tannin; Foams; Mechanical foaming; Foam concentrate; Thermal conductivity; Quebracho.

Introduction

A broad range of rigid foams is commercially available today, such as phenolic or polyurethane foams. These foams are used for a wide variety of applications, such as packaging in transportation, electronic applications, flower preservation, flame retardant or in building applications, e.g. for roofing, flooring or as insulation materials. However, as they are derived from petrochemical resources, their development from biosourced, renewable materials is gaining in importance.

Tannin-based foams are approximately 95% composed of natural raw materials and have shown potential as alternative to phenolic foams (Li et al., 2013; Tondi et al., 2009b; Zhao et al., 2010; Zhou et al., 2013). The main component of those foams is tannin, which is a nontoxic complex of polyflavonoids generally extracted from tree bark. This natural material has been shown to impart exceptional fire-resistant properties to the foams from it (Celzard et al., 2011). Moreover, tannin foams self-extinguish when the flame and the heat source are removed (Celzard et al., 2011). The second main component of these foams, at a 20% level by weight, is furfuryl alcohol. The latter is also a biosourced material, being obtained by catalytic reduction of furfural, a natural derivative obtained by carbohydrate hydrolysis from agricultural waste (Aguilar et al., 2002).

Tannin-based rigid foams prepared from mimosa bark extract (*Acacia mearnsii*) are known since 1994 (Meikleham and Pizzi, 1994). Most recently, similar materials have been developed to obtain relevant properties for different applications, such as floral preservation (Basso et al., 2016), and thermal (Tondi et al., 2008) or acoustic (Lacoste et al., 2015a) insulation. In addition, these foams could be prepared from condensed tannins extracted from different trees, such as mimosa (*Acacia mearnsii*, formerly *mollissima*, de Wildt) (Tondi et al., 2009b), quebracho (*Schinopsis lorentzii* and *balansae*) (Basso et al., 2015; Martinez de Yuso et al., 2014), as well as pine (*Pinus radiata* (Lacoste et al., 2013a) and *Pinus pinaster* (Lacoste et al., 2014b)). Many different formulations have already been developed, and the resultant materials have been prepared using different foaming methods. The most used methods are: chemical foaming (Basso et al., 2014b), physical foaming (Basso et al., 2015; Li et al., 2013), both of them together (Li et al., 2012; Li et al., 2012a) and even formulations without blowing agent (Basso et al., 2013a). Moreover, cellular tannin-based materials have been also obtained by a mechanical method (Szczurek et al., 2014). For improving the properties of the foams, different crosslinkers have been studied under acidic conditions, such as formaldehyde (Tondi et al., 2009b), other aldehydes (Lacoste et al., 2013b) or without any of them (Basso et al., 2011). Foams under alkaline conditions have also been developed (Basso et al., 2014a).

On the other hand, a firefighting foam is a stable mass of small bubbles used for fire suppression. It can extinguish a liquid fire by the combined mechanisms of cooling, separating the flame or the ignition source from the product surface, thus preventing its contact with oxygen resulting in the suppression of the combustive, and suppressing vapours and smothering the fire. Firefighting foams are classified in various types as a function of the kind of fire or risks incurred. Such foams are a combination of foam concentrate, water and air. The foam concentrate is a liquid foaming agent, which mixed with the recommended amount of water and air produces a foam. The mechanically-stirred foams, currently the most used for firefighting, are generated through a two-step process. In the first step, the foam concentrate is injected in the desired ratio into the water through the proportioning device. The foam proportioner, generally an eductor, works on the Venturi principle. The water flow through a reduced section creates then a pressure drop that picks up and introduces the foam concentrate from its tank into the water pipe. In the second step, the foam solution reaches the foam nozzle, within which air is injected into the foam solution. The foam solution and the air travel up to the outlet, where a properly expanded foam exits the nozzle.

The present work explains the preparation and the properties of tannin-based foams based on the firefighting or in-tunneling foams principle. For this new method, a tannin-furanic resin was mixed with an aqueous solution of foam concentrate and a catalyst. Through vigorous mechanical stirring, a large amount of air was then introduced into the mixture, leading to a fast expansion of the liquid foam. After curing at room temperature, a cellular material was obtained. This work is part of a research project dealing with tannin-based wall-projected foams.

Experimental

Materials

Quebracho (*Schinopsis lorentzii* and *Schinopsis balansae*) tannin extract, called Fintan T on the market, was provided by SilvaChimica (S. Michele Mondovi, Italy). Furfuryl alcohol, ethylene glycol and Kolliphor ELP were purchased from Sigma-Aldrich (France) and used as supplied. Phenolsulphonic acid 65% water solution was purchased at Capital Resin Corporation (Columbus, OH, USA). Ethoxylated tallow amine with the commercial name Noramox S11 was supplied by Arkema (Châteauroux, France) and the ethoxylated oleyl amine, OAM-10, was supplied by Saibaba Surfactants Ltd (Gujarat, India). The foaming agent used was SM2101-l, a proprietary product supplied by Condat (Chasse-sur-Rhone, France) mainly composed of alkyl glycols and modified fatty acid soaps.

Foam preparation

The new mechanically expanded tannin foams were prepared by vigorous stirring of a tannin resin solution with a solution of foam concentrate (SFC hereinafter). In a first step, a tannin resin containing 46.7 wt.% of tannin, 37.4 wt.% of furfuryl alcohol, 9.4 wt.% of water, 3.4 wt.% of ethylene glycol and 3.1 wt.% of ethoxylated castor oil was mixed by strong mechanical stirring until achieving a homogeneous mixture. This resin was prepared using a metallic paddle blade stirrer. Then, a 14 wt.% of foam concentrate in water was added to the prepared resin at a ratio SFC/resin of 0.6 and stirred at 2000 rpm for 5 min. Other resin to foaming surfactant ratios have been tried, giving a more unstable liquid foam (see below). For stirring and thus mechanically blowing the mixture into a foam, a special foaming blade stirrer (Fig. 1) was used. The unusual shape of this blade favours the incorporation of air in the mixture, decreasing the stirring time needed. In few seconds, after the stirring has begun, a liquid foam was formed increasing its volume progressively as more air was incorporated. Finally, the acid (14 g) was added under stirring, continued for 30 s more. After that, the foam was left to cure at room temperature. The stable liquid foam obtained just before the addition of acid and the final rigid foam are both shown in Fig. 2. The polycondensation between the different components was induced under acidic conditions by the exothermal self-condensation of the furfuryl alcohol in the mixture. Contrary to other foams formulation, in the present case there is not expansion due to the release of gasses during furfuryl alcohol self-condensation. The temperature in the foam increases while, simultaneously, the liquid foam hardens by crosslinking of the tannin-furfuryl alcohol system (Foo and Hemingway, 1985; Pizzi, 2016), turning the colour of the foam from light brown to black. This method has been used for a number of cases varying the quantity of acid as indicated in Table 1. Furthermore, three additional samples have been prepared using two non-ionic surfactants, an ethoxylated tallow amine (NSA3 and NSA6 formulations) and an ethoxylated oleyl amine (NSO formulation). All the formulations are detailed in Table 1.

Fig 1. Foaming blade.

Fig 2. Left. Liquid tannin foam. Right. Rigid tannin foam obtained with the new method.

Table 1. Formulations expressed in grams of each ingredient.

Sample name	Ac10	Ac14=NS	Ac20	Ac30	NSA3	NSA6	NSO
Quebracho tannin	16.4	16.4	16.4	16.4	16.4	16.4	16.4
Furfuryl alcohol	13	13	13	13	13	13	13
Water	3.3	3.3	3.3	3.3	3.3	3.3	3.3
Ethylene glycol	1.2	1.2	1.2	1.2	1.2	1.2	1.2
PEG-35 castor oil	1.1	1.1	1.1	1.1	1.1	1.1	1.1
Ethoxylated tallow amine	-	-	-	-	1.05	2.1	-
Ethoxylated oleyl amine	-	-	-	-	-	-	1.05
Aqueous foam concentrate solution (14% of surfactant)	21	21	21	21	21	21	21
Catalyst	10	14	20	30	14	14	14

Expansion and stability of the liquid foam

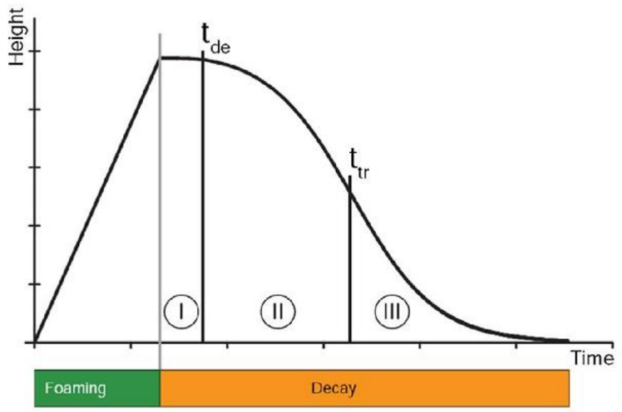

Fig. 3. Standard foam stability plot (Lunkenheimer et al., 2004; Rafati et al., 2016).

Liquid tannin foams are not stable for a too long period. In general, the lifetime of a foam can be split into two main regions, as shown in Fig. 3 (Lunkenheimer et al., 2004; Rafati et al., 2016). The first region corresponds to the foaming, where the liquid foam grows up progressively until the maximum volume. After stirring is stopped, the second region, the decay one, starts and the maximum volume is kept during a deviation time, t_{de}. When the deviation time is exceeded, the bubbles begin to collapse, while a liquid phase starts to drain and accumulates at the bottom of the vessel, separating the liquid foam in two well-defined phases. The destabilization events that can take place on a liquid tannin foam are explained more in detail elsewhere (Delgado-Sánchez et al., 2017). Drainage can be, therefore, used to study the stability of the foam through the transition time, t_{tr}, or half-life of the foam in respect to its maximum volume. Thus, the longer the transition time, the more stable is the liquid foam (Lunkenheimer et al., 2004; Rafati et al., 2016). However, taking the transition time as a reference is not the best option in our case. The objective is indeed obtaining homogeneous rigid foams before a significant decay takes place at the point at which liquid foams are already destabilized. Therefore, a "stability" time has been recorded between the end of stirring up to when only 20 mL of drained liquid was collected. This time was simply referred to as "stability" in the following: the longer such a time, the more stable the liquid foam.

Thus, liquid foams (LF1, LF2, LF3 and LF4) with a solution of foam concentrate at 14 wt.% in water and SFC/resin ratios of 0.4, 0.6 and 0.8 were prepared, together with another sample with a concentration in water of 21 wt.% of surfactant and an SFC/resin ratio of 0.8. Data of the growth of the liquid foam volume at regular intervals of time have been gathered during the stirring until a constant volume is achieved.

Amount of acid

Four samples (Ac10, Ac14, Ac20 and Ac30) with a concentration of foam concentrate of 14 wt.% in water and a ratio SFC/resin of 0.6 were prepared containing 10, 14, 20 and 30 g of phenolsulphonic acid, respectively.

Characterization of the rigid foams

Bulk density

After fully drying the samples, the latter were cut in 30 × 30 × 15 mm^3 specimens. Then, the bulk density, ρ_b, was calculated as the weight /volume ratio of each sample.

Thermal conductivity

Thermal conductivity measurements were carried out by the transient plane source method (Hot Disk TPS 2500S) (Hot Disk AB, Gothemburg, Sweden). The method to calculate the thermal conductivity is based on a transiently heated plane sensor, which acts both as a heat source and as a dynamic temperature sensor, and consisting of an electrically conducting pattern in the shape of a double spiral, which has been etched out of a thin nickel foil and sandwiched between two thin sheets of Kapton®. The plane sensor was fitted between two identical parallelepiped samples. The sensor used was C5501 with radius 6.403 mm. The conductivity was calculated by the Hot Disk 6.1 software.

Mechanical resistance

Compression tests were performed with a universal testing machine INSTRON 5944 (High Waycombe, UK) equipped with a 2 kN head. Samples of dimensions 30 × 30 × 15 mm^3 were compressed at 2 mm/min. During the tests, deformation and load were continuously recorded, and the corresponding curves presented the expected characteristics of cellular materials. The elastic modulus was defined as the slope of the first, linear region of the compression curve, and the compressive strength was defined as the height of the plateau region (Celzard et al., 2010).

Porous structure

The cellular morphologies of the foams were obtained by Hitachi S520 Scanning Electron Microscope (SEM, Tokyo, Japan). The cell size obtained from the average of five pictures for each sample was reported.

Foaming capacity

The catalyzed resin was poured into the chamber of a FOAMAT 281 foaming measuring equipment (Format Messtechnik GmbH, Karlsruhe, Germany). This equipment measures and records simultaneously the expansion, hardening, and temperature and pressure variation during the foaming process. The chamber is composed of a cardboard cylinder set on the manometer sensor. The pressure generated by the expansion is measured by the force applied to this metal plate sensor. A K-type thermocouple is immersed into the mixture and measures the temperature variation. The CMD (Curing Monitor Device) sensor measures the foam's dielectric properties during the transition from liquid to solid state. It is a dielectric polarization sensor composed of two interdigitated electrodes disposed on a printed circuit in such a manner as to form a type of flat capacitor at the bottom of the foaming chamber. Then, the contact is ensured by both (i) the blowing pressure right from the beginning and (ii) the direct correlation between the dielectric polarization negative slope and the rate of the molecular movements decrease in the resin due to the progress of cross-linking. The foam height is constantly monitored by an ultrasound sensor according to the pulse-echo method. The software "Mousse", version 3.80, was used to collect and process the data.

Results and discussion

Stability

Table 2 and Fig. 4 show the results of expansion and stability of the liquid foams. During the first seconds of stirring, the mixtures of resin + SFC undergo a large expansion corresponding to approximately 70% of the whole expansion, reaching volumes of more than 300 mL. After that initial expansion, the samples increase their volumes more or less progressively until they achieve their maximum volume. The large initial expansion of the resin and its final volume are strongly influenced by the ratio SFC/resin. Both increase with the latter, especially in the range of ratio from 0.6 to 0.8. Conversely, the stability of the liquid foam so formed decreases significantly when the SFC/resin ratio increases (Table 2). Besides, the increase in concentration of the SFC leads to more unstable liquid foams.

These results help to find a compromise between the final volume of the liquid foam and its stability as both characteristics are antagonistic. Foams with a large final volume are stable for too short a time before instability sets in. This causes that the liquid foam has not enough time to harden before its cells start to collapse. However, the foams presenting longer stability times are the ones with a low SFC/resin ratio and with a lower final volume of the liquid foam. This results in a final rigid foam of higher density. Because of this, choosing an intermediate SFC/resin ratio such as 0.6 seems necessary to achieve a compromise between both properties. A concentration of SFC of 14 wt.% was chosen as being preferable to prepare the other samples because at 21 wt.% concentration the foam becomes unstable too quickly.

Table 2. Maximum volume and calculated time of stability for each test for different concentrations of SFC in water solution and for different SFC/resin ratios.

Sample	Concentration of SFS in water (%)	Ratio SFS/resin	Max. Expansion (mL)	Instability (s)
LF1	14	0.4	425	240
LF2	14	0.6	550	180
LF3	14	0.8	570	60
LF4	21	0.8	600	40

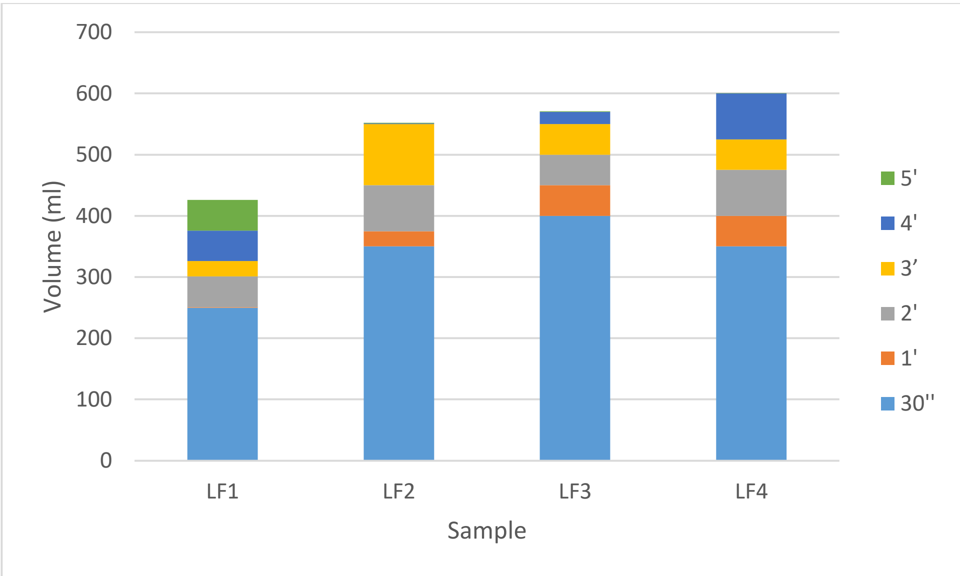

Fig 4. Increase in volume for each interval of time during stirring.

Effect of the amount of acid

The proportion of acid in the formulation must be high enough for the self-condensation of furfuryl alcohol to occur sufficiently fast and yield some degree of hardening in the liquid foam before the time of instability is reached. Fig. 5 shows the results obtained by the Foamat device where four different amounts of acid were tested. The dielectric polarization curve indicates the foam curing level. This curve shows a maximum coinciding with the maximum of temperature, indicating the moment of maximum molecular mobility. After this point, the resin molecular mobility decreases progressively as a consequence of the progress of the polymerization.

In the preparation of foams with 14 wt.% of SFC and 0.6 of SFC/resin ratio it is necessary that the polymerization begins before 180s to avoid foam destabilization. Fig. 5 shows clearly how the samples with an amount of acid higher than 14 g achieve a crosslinked structure before the bubbles/cells start to collapse and the resin drains. In addition, these samples (Ac14, Ac20 and Ac30) also show a faster curing than the samples where less than 14 g was used.

Characterization of the process of formation of a rigid tannin foam

The typical FOAMAT parameters that describe the formation of a rigid foam prepared with the new mechanical method of foaming is shown for the Ac14 = NS sample (Fig. 5). The temperature of the foam rises quickly until it reaches its maximum and afterwards decreases progressively during curing and cooling. This trend is similar to that of other tannin-based foams prepared by other methods such as tannin foams with blowing agent and formaldehyde (Basso et al., 2013a) or without both of them (Basso et al., 2013b). However, the maximum peak of temperature reached in the new method shows values between 15 and 25 ºC lower than in previous formulations of tannin foams (Basso et al., 2013b, 2013a; Čop et al., 2015; Lacoste et al., 2015b). This is probably due to the presence of a greater amount of water, which acts as a cooling agent, in the formulation. Such a difference in the peak of temperature results in a polymerization as fast as in the other methods mentioned above, but avoids the expansion due to the releasing of water and solvents. This prevents shrinkage, which always affects negatively the structure and properties of the foam. Fig. 5c shows the height of the NS foam. Only the height of NS formulation is shown because the trend was the same for the others formulations. This parameter remained constant (the same was observed as for the diameter of the foam) all through the measurement, proving that there is no shrinkage. Fig. 5b shows the variation of the dielectric polarization curve as a function of time. The curve increases until a maximum, which coincides with the maximum of temperature, reflecting the increase of the molecular mobility. Afterwards, the dielectric polarization curve drops because the molecular mobility is lower because hardening occurs in the liquid foam. Then, when the curing of the foam has finished, the curve becomes constant.

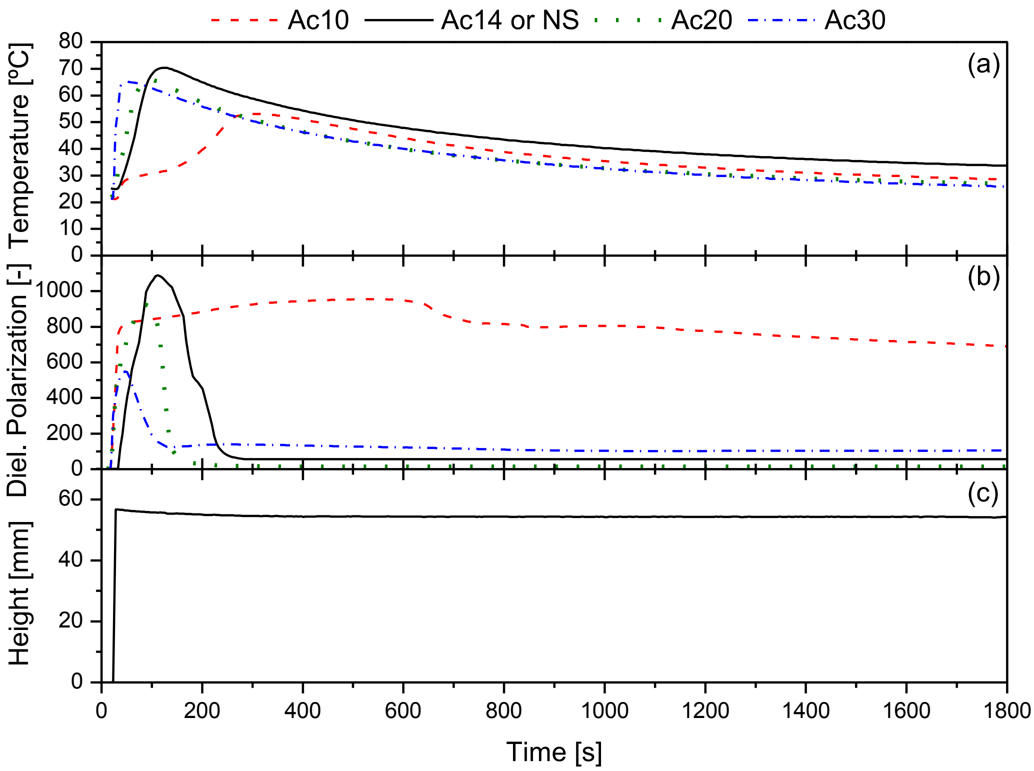

Fig. 5. Foamat results for the samples with different amounts of acid: (a) temperature as a function of time; (b) dielectric polarization as a function of time; and (c) height of the NS formulation during the time of analysis.

Structural and physical properties

The results of density, thermal conductivity and mechanical properties for each formulation are shown in Table 3. As expected for cellular materials, their thermal properties values directly depend on their density. The foams prepared with the new system show thermal conductivities comparable with those from the literature for other tannin-based foams with similar densities (Basso et al., 2011, 2013a, 2014b; Basso et al., 2015; Li et al., 2012c; Szczurek et al., 2014). Thermal conductivities below 0.05 W m^{-1} K^{-1} always correspond to materials with good insulating properties.

Table 3. Results of foams' characterization.

	NS	NSA3	NSA6	NSO
Density (g/cm^3)	0.076	0.073	0.080	0.069
Thermal conductivity (W/(m·K))	0.047	0.045	0.046	0.046
Average cell size (µm)	349	329	384	287
Compressive strength (MPa)	0.034	0.082	0.130	0.056
Elastic modulus (MPa)	0.49	1.19	1.33	0.59

The samples show the typical mechanical behaviour of cellular materials submitted to compression, i.e., with three consecutive regions, see Fig. 6. First a linear part at low strain, followed by a plateau region corresponding to the collapse of the cell layers and finally, the densification where all cell layers are compressed. All the mechanical properties values obtained are shown in Table 3. The weakest point of the foams formulated with the new method could be their mechanical properties. At similar density, both the compressive strength and the modulus of these foams are lower than those of others tannin foam formulations made by a frothing technique such as meringue foams (Szczurek et al., 2014), or free of formaldehyde (Basso et al., 2011, 2013a). They present even lower mechanical properties than tannin rigid foam made by chemical foaming (by blowing agent) hardened with formaldehyde (Celzard et al., 2010; Tondi et al., 2009b) or with additives, such as hyperbranched polymers (Li et al., 2012c) or isocyanates (Li et al., 2012b). This is expected because the present formulations do not contain those components, most of them toxic that increase crosslinking or reinforce the structure of the material. This will be a point to work further in the future.

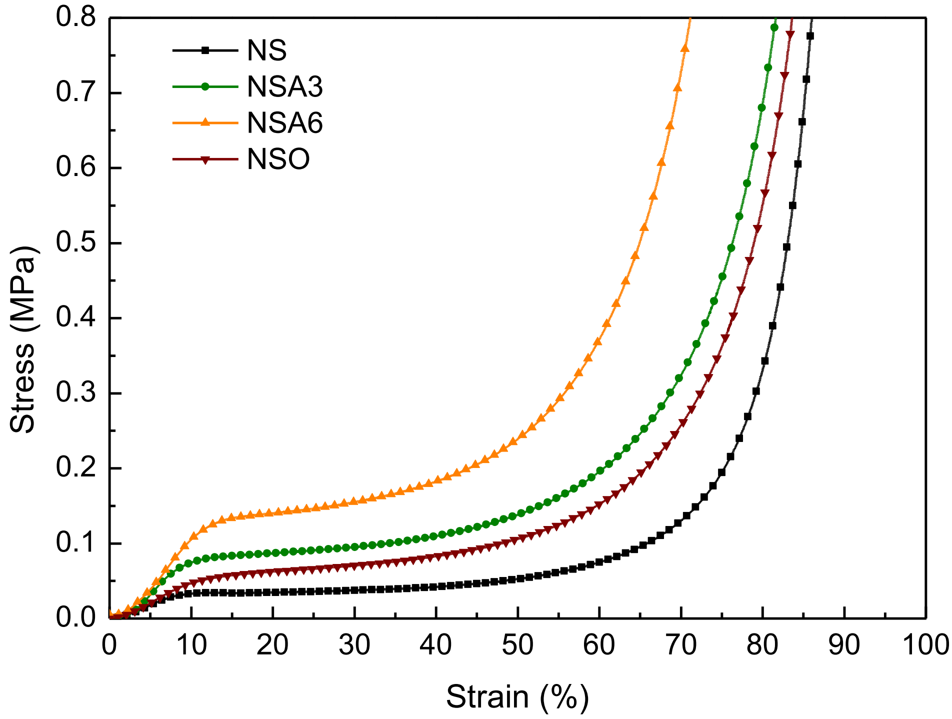

Fig. 6. Stress-strain curves of the four rigid foams listed in Table 3 submitted to compression.

Fig. 7 shows the SEM pictures of the structure of the samples NS, NSA3, NSA6 and NSO. All of them evidence isotropic, even, and open porosity, in which each cell is connected with its neighbours through circular windows. The use of an additional surfactant further improves foam's uniformity, yielding smaller cells and increasing the height of the plateau in the mechanical properties curves (see Fig 6 and Table 3). This occurs because the surfactant decreases the surface tension of the liquid phase, thus allowing smaller bubbles and thinner bubble walls. The surfactant also delays the collapse of the foam during foaming and until the first step of curing, when the foam is still liquid or semi-liquid (Basso, M.C. et al., 2015; Gardziella et al., 2000; Landrock, 1995; Zhang et al., 1999). However, an increase in the surfactant amount (NSA6) leads to it acting as a plasticizer (Basso, M.C. et al., 2015; Gardziella et al., 2000), increasing slightly the density of the foam and, curiously, also the cell size.

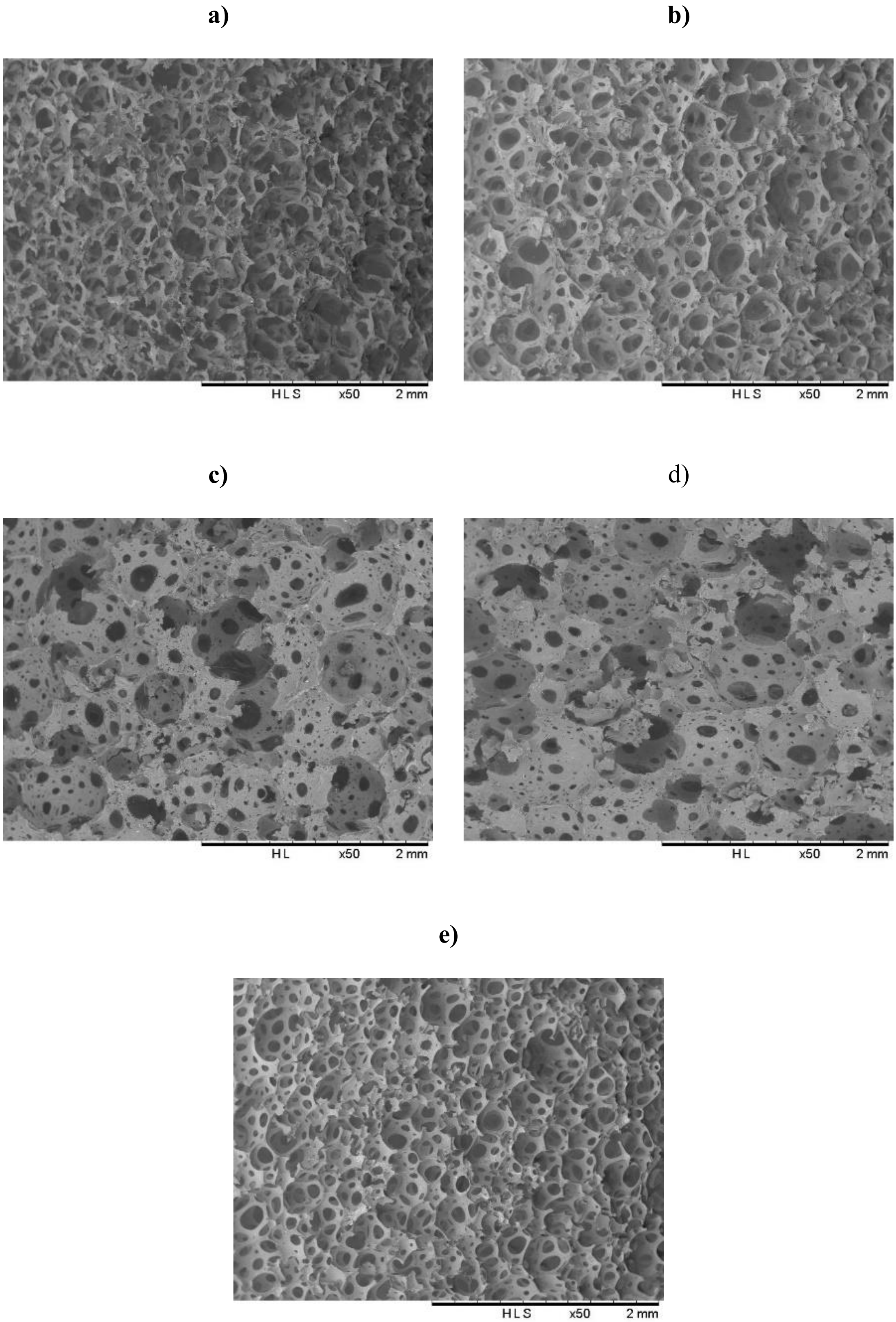

Fig. 7. Scanning electron microscope images at 50× of magnification of rigid foams: (a) NS, (b) NSA3, (c) NSA6 top view, (d) NSA6 side view, and (e) NSO.

Finally, foaming is achieved by mechanical stirring, and not by the release of a blowing agent, so that the structure of the foam appears to be more isotropic and the cells approach a more spherical form than in conventional foams. Fig. 7c and 7d show respectively top (orthogonal to the growth direction) and side views (typically called direction of foam growth) of NSA6. The average cell sizes for these directions are 384 and 432 µm, respectively. The difference of around 50 µm between the two directions shows the difference between the new mechanical foaming process and previous chemical blowing ones for which more than 100 µm of difference between both directions has sometimes been observed (Zhao et al., 2010). The ratio between both diameters gives the degree of anisotropy (Laib et al., 2000) where a value of 1 indicates that the material is fully isotropic. The sample NSA6 has a value of 1.12 indicating its high level of isotropy.

Conclusions

1. The new foaming mechanical method, based on fire-fighting or tunneling foams, has allowed developing quebracho tannin-based foams giving encouraging results.
2. Stable liquid foams with a tannin resin were achieved for a medium period of time and hardening of these foams was carried out at room temperature, without the need to provide any external heat source.
3. The foams are lightweight materials with thermal properties rather similar to those of different tannin foams already published.
4. There is no problem of shrinkage which develops in the foam with this mechanical preparation method.

5. The use of non-ionic ethoxylated amine surfactants in the formulation decreases the cell size and improves the uniformity of the foam, giving more isotropic materials.
6. This work can be considered as a first step to obtain wall-projected tannin-based foams.

Acknowledgements

The authors acknowledge the funding from the BRIIO project financed by the conventions of the French state (FUI) Nr. 1410042V and Nr. 1410043V through Bpifrance financement.

References

Aguilar, R., Ramírez, J.A., Garrote, G., Vázquez, M., 2002. Kinetic study of the acid hydrolysis of sugar cane bagasse. J. Food Eng. 55, 309–318. doi:10.1016/S0260-8774(02)00106-1
Basso, M.C., Giovando, S., Pizzi, A., Celzard, A., Fierro, V., 2013a. Tannin/furanic foams without blowing agents and formaldehyde. Ind. Crops Prod. 49, 17–22. doi:10.1016/j.indcrop.2013.04.043
Basso, M.C., Giovando, S., Pizzi, A., Lagel, M.C., Celzard, A., 2014a. Alkaline Tannin Rigid Foams. J. Renew. Mater. 2, 182–185. doi:10.7569/JRM.2013.634137
Basso, M.C., Lagel, M.C., Pizzi, A., Celzard, A., Abdalla, S., 2015. First Tools for Tannin-Furanic Foams Design. BioResources 10, 5233–5241. doi:10.1537/biores.10.3.5233-5241
Basso, M.C., Li, X., Fierro, V., Pizzi, A., Giovando, S., Celzard, A., 2011. Green, formaldehyde-free, foams for thermal insulation. Adv. Mater. Lett. 2, 378–382. doi:10.5185/amlett.2011.4254
Basso, M.C., Pizzi, A., Al-Marzouki, F., Abdalla, S., 2016. Horticultural/hydroponics and floral natural foams from tannins. Ind. Crops Prod. 87, 177–181. doi:10.1016/j.indcrop.2016.04.033
Basso, M.C., Pizzi, A., Celzard, A., 2013b. Dynamic Monitoring of Tannin-based Foam Preparation: Effects of Surfactant. BioResources 8. doi:10.15376/biores.8.4.5807-5816
Basso, M.C., Pizzi, A., Lacoste, C., Delmotte, L., Al-Marzouki, F., Abdalla, S., Celzard, A., 2014b. MALDI-TOF and 13C NMR Analysis of Tannin–Furanic–Polyurethane Foams Adapted for Industrial Continuous Lines Application. Polymers 6, 2985–3004. doi:10.3390/polym6122985
Celzard, A., Fierro, V., Amaral-Labat, G., Pizzi, A., Torero, J., 2011. Flammability assessment of tannin-based cellular materials. Polym. Degrad. Stab. 96, 477–482. doi:10.1016/j.polymdegradstab.2011.01.014
Celzard, A., Zhao, W., Pizzi, A., Fierro, V., 2010. Mechanical properties of tannin-based rigid foams undergoing compression. Mater. Sci. Eng. A 527, 4438–4446. doi:10.1016/j.msea.2010.03.091
Čop, M., Gospodarič, B., Kemppainen, K., Giovando, S., Laborie, M.-P., Pizzi, A., Sernek, M., 2015. Characterization of the curing process of mixed pine and

spruce tannin-based foams by different methods. Eur. Polym. J. 69, 29–37. doi:10.1016/j.eurpolymj.2015.05.020

Delgado-Sánchez, C., Fierro, V., Li, S., Pasc, A., Pizzi, A., Celzard, A., 2017. Stability analysis of tannin-based foams using multiple light-scattering measurements. Eur. Polym. J. 87, 318–330. doi:10.1016/j.eurpolymj.2016.12.036

Foo, L.Y., Hemingway, R.W., 1985. Condensed Tannins: Reactions of Model Compounds with Furfuryl Alcohol and Furfuraldehyde. J. Wood Chem. Technol. 5, 135–158. doi:10.1080/02773818508085184

Gardziella, A., Pilato, L.A., Knop, A., 2000. Phenolic Resins. Springer Berlin Heidelberg, Berlin, Heidelberg.

Lacoste, C., Basso, M.-C., Pizzi, A., Celzard, A., Ella Ebang, E., Gallon, N., Charrier, B., 2015a. Pine (P. pinaster) and quebracho (S. lorentzii) tannin-based foams as green acoustic absorbers. Ind. Crops Prod. 67, 70–73. doi:10.1016/j.indcrop.2014.12.018

Lacoste, C., Basso, M.C., Pizzi, A., Laborie, M.-P., Celzard, A., Fierro, V., 2013a. Pine tannin-based rigid foams: Mechanical and thermal properties. Ind. Crops Prod. 43, 245–250. doi:10.1016/j.indcrop.2012.07.039

Lacoste, C., Basso, M.C., Pizzi, A., Laborie, M.-P., Garcia, D., Celzard, A., 2013b. Bioresourced pine tannin/furanic foams with glyoxal and glutaraldehyde. Ind. Crops Prod. 45, 401–405. doi:10.1016/j.indcrop.2012.12.032

Lacoste, C., Čop, M., Kemppainen, K., Giovando, S., Pizzi, A., Laborie, M.P., Sernek, M., Celzard, A., 2015b. Biobased foams from condensed tannin extracts from Norway spruce (Picea abies) bark. Ind. Crops Prod. 73, 144–153. doi:10.1016/j.indcrop.2015.03.089

Lacoste, C., Pizzi, A., Laborie, M.-P., Celzard, A., 2014. Pinus pinaster tannin/furanic foams: Part II. Physical properties. Ind. Crops Prod. 61, 531–536. doi:10.1016/j.indcrop.2014.04.034

Laib, A., Barou, O., Vico, L., Lafage-Proust, M.H., Alexandre, C., Rügsegger, P., 2000. 3D micro-computed tomography of trabecular and cortical bone architecture with application to a rat model of immobilisation osteoporosis. Med. Biol. Eng. Comput. 38, 326–332. doi:10.1007/BF02347054

Landrock, A.H., 1995. Handbook of plastic foams: types, properties, manufacture, and applications. Noyes Publications, Park Ridge, N.J., U.S.A.

Li, X, Basso, M.., Fierro, V., Pizzi, A., Celzard, A., 2012. Chemical Modification of Tannin/Furanic Rigid Foams by Isocyanates and Polyurethanes. Maderas Cienc. Tecnol. 0–0. doi:10.4067/S0718-221X2012005000001

Li, X., Basso, M.C., Braghiroli, F.L., Fierro, V., Pizzi, A., Celzard, A., 2012a. Tailoring the structure of cellular vitreous carbon foams. Carbon 50, 2026–2036. doi:10.1016/j.carbon.2012.01.004

Li, X., Basso, M.C., Fierro, V., Pizzi, A., Celzard, A., 2012b. Chemical Modification of Tannin/Furanic Rigid Foams by Isocyanates and Polyurethanes. Maderas-Cienc. Tecnol. 14, 257–265. doi:10.4067/S0718-221X2012005000001

Li, X., Essawy, H.A., Pizzi, A., Delmotte, L., Rode, K., Le Nouen, D., Fierro, V., Celzard, A., 2012c. Modification of tannin based rigid foams using oligomers of a hyperbranched poly(amine-ester). J. Polym. Res. 19. doi:10.1007/s10965-012-0021-4

Li, X., Pizzi, A., Lacoste, C., Fierro, V., Celzard, A., 2013. Physical Properties of Tannin/Furanic Resin Foamed With Different Blowing Agents. Bioresources 8, 743–752.

Lunkenheimer, K., Malysa, K., Wienskol, G., Baranska, M., 2004. Method and procedure for swift characterization of foamability and foam stability. EP1416261 A2.

Martinez de Yuso, A., Lagel, M.C., Pizzi, A., Fierro, V., Celzard, A., 2014. Structure and properties of rigid foams derived from quebracho tannin. Mater. Des. 63, 208–212. doi:10.1016/j.matdes.2014.05.072

Meikleham, N.E., Pizzi, A., 1994. Acid- and alkali-catalyzed tannin-based rigid foams. J. Appl. Polym. Sci. 53, 1547–1556. doi:10.1002/app.1994.070531117

Pizzi, A., 2016. Wood products and green chemistry. Ann. For. Sci. 73, 185–203. doi:10.1007/s13595-014-0448-3

Rafati, R., Haddad, A.S., Hamidi, H., 2016. Experimental study on stability and rheological properties of aqueous foam in the presence of reservoir natural solid particles. Colloids Surf. Physicochem. Eng. Asp. 509, 19–31. doi:10.1016/j.colsurfa.2016.08.087

Szczurek, A., Fierro, V., Pizzi, A., Stauber, M., Celzard, A., 2014. A new method for preparing tannin-based foams. Ind. Crops Prod. 54, 40–53. doi:10.1016/j.indcrop.2014.01.012

Tondi, G., Pizzi, A., Olives, R., 2008. Natural tannin-based rigid foams as insulation for doors and wall panels. Maderas Cienc. Tecnol. 10. doi:10.4067/S0718-221X2008000300005

Tondi, G., Zhao, W., Pizzi, A., Du, G., Fierro, V., Celzard, A., 2009. Tannin-based rigid foams: A survey of chemical and physical properties. Bioresour. Technol. 100, 5162–5169. doi:10.1016/j.biortech.2009.05.055

Zhang, X.., Macosko, C.., Davis, H.., Nikolov, A.., Wasan, D.., 1999. Role of Silicone Surfactant in Flexible Polyurethane Foam. J. Colloid Interface Sci. 215, 270–279. doi:10.1006/jcis.1999.6233

Zhao, W., Pizzi, A., Fierro, V., Du, G., Celzard, A., 2010. Effect of composition and processing parameters on the characteristics of tannin-based rigid foams. Part I: Cell structure. Mater. Chem. Phys. 122, 175–182. doi:10.1016/j.matchemphys.2010.02.062

Zhou, X., Pizzi, A., Sauget, A., Nicollin, A., Li, X., Celzard, A., Rode, K., Pasch, H., 2013. Lightweight tannin foam/composites sandwich panels and the coldset tannin adhesive to assemble them. Ind. Crops Prod. 43, 255–260. doi:10.1016/j.indcrop.2012.07.020

Troisième partie: Conclusions et Perspectives

Conclusions Générales et Perspectives

Différentiation des tanins en fonction des traitements subis lors de l'extraction.

L'utilisation constante de différents types de tanins au début du projet, tous avec la même origine mais montrant des résultats très différents à la même application, ainsi que le manque d'informations techniques pour certains d'entre eux, nous ont amenés à considérer un système permettant d'obtenir clairement les différences physiques et chimiques entre ces tanins.

Ces faits ont promu l'étude susmentionnée sur la différenciation des tanins de même origine. En plus des techniques de caractérisation telles que le spectre de masse MALDI-ToF, le FTIR ou le NMR 13C, la technique qui a mis en évidence de meilleurs résultats dans la différenciation des tanins dans lesquels la seule différence était un degré de sulfitation différent lors de l'extraction est la chromatographie par perméation de gel. Cette technique permet de déduire rapidement la présence ou non, ainsi que s'il existe un degré de sulfitation différent entre plusieurs tanins d'une même origine. Sur la base du fait que la sulfitation réduit généralement la taille des molécules de tanin, réduisant ainsi leur poids moléculaire.

Les réactions avec des tanins et la lignine.

Les différentes techniques utilisées dans la caractérisation du produit obtenu lors de la réaction d'un tanin condensé avec une diamine ont permis de révéler certains points d'intérêt de cette réaction. Même en montrant un résultat inattendu tel que la réaction covalente de l'amine avec la position C3 de la catéchine. Cette réaction a montré qu'elle conduit principalement à la formation de liaisons covalentes entre les groupes amine et les groupes hydroxyle du tanin ou de la catéchine. Ces liaisons sont administrées indistinctement à partir du catalyseur utilisé (acide ou basique) et montrent qu'elles sont de préférence données dans le cycle A, suivies de l'anneau B et finalement dans l'hétérocycle. La présence de ces liens augmente avec la température, puisque, comme prévu, il y a une plus grande avance de la réaction. Mais, d'autre part, il existe aussi la présence de liaisons ioniques entre les groupes hydroxyle et les groupes amine. Puis, bien que le spectre de masse MALDI ToF a joué un rôle déterminant dans la détermination des espèces formées, les essais de RMN ^{13}C ont contribué de manière fondamentale à établir à quels points les molécules de tanins étaient plus facilement liées aux différentes liaisons et au type de liaison elle-même. Aussi, plus le degré de polymérisation du tanin condensé est élevé, plus vite sera un réseau dur en trois dimensions.

Cette réaction peut trouver des applications futures dans des mousses de tanin avec une application pulvérisable ou dans des revêtements par projection en raison de leur rapidité pour former un réseau. Les applications pour lesquelles certains tests ont déjà débuté dans ce même laboratoire, pour obtenir un meilleur « setting time », c'est-à-dire, une fois que la mousse liquide a été projetée, obtenir le temps minimum pour la prise de celle-ci sur le mur où elle est projeté.

Les mêmes types de liaisons, ioniques et covalentes, ont été trouvées lorsqu'une autre substance phénolique, telle que la lignine kraft désulfurée, a réagi avec de l'hexaméthylènediamine comme exemple de diamine. Les différentes techniques utilisées pour la caractérisation (RMN 13C, Maldi Tof et FTIR) ont conclu que des interactions entre des groupes amines et des groupes hydroxyles se produisaient à la fois dans les groupes hydroxyle phénolique et dans les groupes hydroxyle aliphatiques.

Ces réactions pourraient avoir des applications très similaires à celles discutées ci-dessus de la réaction avec l'amine avec le tanin condensé. En outre, il pourrait être intéressant d'effectuer une étude de cette réaction pour la préparation de panneaux de particules.

D'autre part, dans cette thèse, nous avons présenté les résultats obtenus à partir de la préparation d'uréthanes sans utilisation d'isocyanates. Tous deux utilisant du tanin aminé et utilisant de la lignine. Après d'autres études antérieures menées dans ce même groupe de travail dans lequel il a été possible de développer des polyuréthanes exempts d'isocyanates à partir de tanins condensés et de tanins hydrolysables, l'idée était de mener à bien la même réaction, mais cette fois en utilisant un tanin condensé aminé et un tanin condensé carbonaté. Le résultat a été l'obtention d'un polyuréthane exempt d'isocyanate avec au moins 70% des matériaux utilisés dans sa préparation à l'origine naturelle. À partir de ce travail, il a été conclu que non seulement la carbonatation a été produite dans la molécule de tanin propre, mais qu'elle a aussi été produite dans les carbohydrates qu'il contient. Les uréthanes formés à partir de carbohydrates ouvrent ainsi la porte à d'autres recherches futures à explorer.

En suivant les procédures des publications antérieures de ce même groupe de recherche, on a montré les résultats des polyuréthanes fabriqués à partir de lignine kraft désulfurée avec application dans le revêtement de bois obtenant de bons résultats d'hydrophobisation avec des angles de contact allant jusqu'à 96º. Dans sa préparation, diverses alternatives ont été utilisées dans l'application des réactifs sans observer de grandes différences entre eux. En outre, au cours de cette étude, on a observé que dans la lignine se trouvaient des structures plus différentes, le nombre d'espèces d'uréthanes crées est beaucoup plus varié et plus grand que dans le cas des tanins. Aussi, et découlant d'études antérieures de la réaction des diamines avec les tanins condensés et avec la lignine elle-même, l'existence de liaisons covalentes et ioniques dans les nouvelles espèces de polyuréthanes créés a été observée.

Adhésifs de tanins pour panneaux de particules.

Des études antérieures sur l'utilisation d'aldéhydes dérivés de la lignine pour la préparation de résines phénoliques ont permis de réduire ou de remplacer complètement certaines des matières synthétiques couramment utilisées pour la préparation de ces résines. Dans le cadre de cette thèse, on a exposé les résultats obtenus pour la préparation de panneaux de particules non toxiques, respectueux de l'environnement et exclusivement d'origine naturelle. Des aldéhydes dérivés de la lignine telle que la vanilline et un aldéhyde dérivé de celle-ci utilisé comme agent de réticulation, avec un extrait naturel hautement réactif tel qu'un tanin de pin purifié, donnent la possibilité de rendre les résines de très élevées degré de réticulation. D'excellents résultats dans la préparation de panneaux de particules ont été obtenus selon la norme européenne EN319 à partir de vanilline et de tanin sans utilisation de matière synthétique.

À la suite de cette étude, il serait intéressant de vérifier si ce même adhésif provenant de la vanilline pourrait être préparé à l'aide d'une vanille avec un grade non-alimentaire et un test s'il est également valable avec l'utilisation d'autres tanins de pin hautement réactifs mais avec un degré de purification plus faible. Ces deux facteurs pourraient réduire les coûts de préparation si les propriétés de l'adhésif étaient encore acceptables pour la préparation de panneaux particulaires.

Mousses projetables de tanin.

Diverses publications et thèses ont été développées précédemment sur la formulation de mousses à base de tanin. Parce que la mousse résultante, principalement composée de matériaux d'origine naturelle, possède des propriétés auto-extinguibles contre le feu et a une faible densité et conductivité électrique.

Cependant, l'un des problèmes les plus couramment observés dans la formulation de ce type de mousse est la contraction avec la destruction conséquente de la structure cellulaire, si les différentes vitesses impliquées dans la formation d'une mousse ne sont pas bien équilibrées.

Les mousses présentées dans cette thèse font partie du travail réalisé pour le projet BRIIO, dans le but d'obtenir une mousse de tanin qui peut être conçue pour l'isolation thermique des bâtiments. Les mousses développées ont l'avantage de ne montrer aucun signe de contraction lors de leur production, grâce au nouveau système de mousse utilisé, basé sur les mousses utilisées par les pompiers dans la lutte contre le feu. Ce procédé d'expansion des résines de tanin est basé sur la formation d'un matériau cellulaire ou d'une mousse liquide en utilisant un tensioactif avec une grande facilité dans le moussage tels que ceux employés dans l'ouverture de tunnels ou dans les mousses anti-incendie. Cela rend l'optimum qui doit être donné entre la vitesse de polymérisation, la formation de bulles et le durcissement de la matrice, doit maintenant être entre la vitesse de polymérisation et le durcissement de la matrice avec la stabilité des bulles dans la mousse liquide.

En outre, ces mousses continuent à maintenir des propriétés thermiques (moyenne 0,04 W / m ° C) et la faible densité comparables à celles d'autres mousses de base de tanin présentées précédemment. Et comparable à d'autres isolateurs commerciaux tels que la laine de verre ou le liège et les propriétés mécaniques sont meilleurs que ceux de ces exemples commerciaux.

Ce travail présenté sur les mousses de tanin peut être considéré comme une première étape vers l'obtention d'une mousse de tanin projetable. En plus de faire des améliorations pertinentes dans la formulation. Une adaptation de la formulation à un équipement de projection bi- ou tri-composant serait une prochaine étape très intéressante vers une adaptation plus industrielle de ces mousses.

Un autre point de recherche intéressant sur ces mousses peut être une étude biologique de celles-ci. Bien que le tanin puisse jouer un rôle de défense chimique contre les insectes et les champignons dans les plantes et les arbres, ce qui les rend peu assimilables. Comme l'exemple des chênes, qui montrent des doses plus élevées de tanins dans les feuilles pour éviter d'être attaquées par des chenilles, puisque le tanin tue la plupart des larves de celles-ci. Une étude de l'attaque des insectes et/ou des champignons sur les mousses serait intéressante dans la mesure où l'on observerait si le tanin utilisé pour sa fabrication conserve encore les mêmes caractéristiques que dans le cas des plantes.

Liste des publications

- **F.J. Santiago-Medina**, G. Foyer, A. Pizzi, S. Calliol, L. Delmotte. Lignin-derived non-toxic aldehydes for ecofriendly tannin adhesives for wood panels. *International Journal of Adhesion and Adhesives* 2016. Volume 70, Pages 239-248. Published.
- M. Thébault, A. Pizzi, **F.J. Santiago-Medina**, F.M. Al-Marzouki, S. Abdalla. Isocyanate-free polyurethanes by coreaction of condensed tannins with aminated tannins. *Journal of Renewable Materials* 2016. Volume 5, Issue 1, Pages 21-29. Published.
- **F.J. Santiago-Medina**, C. Delgado-Sánchez, A. Pizzi, A. Celzard, V. Fierro, L. Delmotte, C. Vaulot. Understanding and distinguishing condensed tannins with the same origin but influenced by sulfitation. *ProLigno.* Submitted.
- **F.J. Santiago-Medina**, A. Pizzi, M.C. Basso, L. Delmotte, A. Celzard. Polycondensation resins by flavonoid tannins reaction with amines. *Polymers* 2017. Volume 9, Issue 2, Page 37. Published.
- **F.J. Santiago-Medina**, A. Pizzi, M.C. Basso, L. Delmotte, S. Abdalla. Polycondensation resins by lignin reaction with (poly)amines. *Journal of Renewable Materials.* 2017. Volume 5, Number 5, Pages 388-399. Published.
- **F.J. Santiago-Medina**, M.C. Basso, A. Pizzi, L. Delmotte. Polyurethanes from kraft lignin without using isocyanates. *Journal of Renewable Materials*. Accepted.
- **F.J. Santiago-Medina**, C. Delgado-Sánchez, M. C. Basso, A. Pizzi, V. Fierro, A. Celzard. Mechanically blown wall-projected tannin-based foams. *Industrial Crops and Products*. Submitted.

Publications en dehors de la thèse

- **F.J. Santiago-Medina**, A. Pizzi, S. Abdalla. Hydroxymethyl furfural hardening of pine tannin wood adhesives. *Journal of Renewable Materials*. Accepted.
- C. Delgado-Sánchez, **F.J. Santiago-Medina**, V. Fierro, A. Pizzi, A. Celzard. Optimisation of "green" tannin-furanic foams for thermal insulation by experimental design. *Materials and Design*. 2018. Volume 139, Pages 7-15. Published.

Résume

Une alternative aux produits industriels de type phénol ou résorcinol peut être des tanins ou de la lignine. Les deux sont des polyphénols naturels, le tanin est extrait de différentes parties de plantes, tandis que la lignine est habituellement obtenue comme sous-produit dans les industries papetières.

Ces deux produits sont la base principale sur laquelle j'ai travaillé pendant le développement de cette thèse. Dans une première partie, une étude de caractérisation et de différenciation entre différents tannins ayant la même origine mais que présentent un comportement différent lorsqu'ils sont utilisés dans la même application dans les mêmes conditions a été effectuée. Cette étude met en évidence la GPC comme technique fondamentale pour la différenciation des tanins de quebracho sulfités.

D'autre part, les interactions entre différentes substances avec du tanin et de la lignine ont été étudiées. Comme l'étude de la réaction entre les diamines (telles que l'hexaméthylènediamine) avec du tanin et de la lignine pour obtenir des résines polycondensées. En outre, dans cette section ont été obtenus des polyuréthanes avec au moins 70% de substances naturelles dans leur préparation sans utiliser d'isocyanate dans le procédé.

De plus, des aldéhydes dérivés de la lignine, comme la vanilline, ont été utilisés avec le tanin de pin pour la fabrication d'adhésifs dans la préparation de panneaux de particulaires, obtenant des résultats satisfaisants selon les normes européennes et des substances complètement naturelles.

Enfin, dans le cadre d'un projet industriel les étapes initiales pour le développement d'une mousse de tanin rigide applicable par projection pour l'isolation thermique des bâtiments ont été réalisées. Lorsqu'un nouveau système de moussage mécanique a été développé pour des mousses de tanin basées sur des mousses de lutte contre incendie à base de tanin ou dans les mousses des opérations d'ouverture du tunnel, ce nouveau système de moussage évite les problèmes de retrait lors de la formation de la mousse.

Abstract

An alternative to industrial phenol or resorcinol industrial products may be tannins or lignin. Both are natural polyphenols, the tannin is extracted from different parts of plants, while lignin is usually obtained as a secondary product in the pulp and paper mill.

These two products are the main basis on which I have worked during the development of this thesis. In a first part, a study of characterization and differentiation between different tannins with the same origin and that present a different behavior when used in the same application under the same conditions has been done. Highlighting the GPC as a fundamental technique for the differentiation between sulphited quebracho tannins.

On the other hand, the interactions between different substances with tannin and with lignin have been studied. As the study of the reaction between diamines (such as hexamethylenediamine) with tannin and lignin to obtain a polycondensed resins. Also, in this section have been obtained polyurethanes with at least 70% of natural substances in their preparation without using any isocyanate in the process.

In addition, aldehydes derived from lignin, such as vanillin, have been used next to pine tannin for the manufacture of adhesives in the preparation of particleboards, obtaining satisfactory results according to European standards and from completely natural substances.

Finally, within an industrial project the initial steps have been carried out for the development of a rigid tannin foam applicable by projection for the thermal insulation of buildings. Where a new mechanical foaming system has been developed for tannin foams based in fire-fighting foams or in the foams of the tunneling operations, this new system of foaming avoids the problems of shrinkage during the formation of the foam.